NEUROPHYSIOLOGY UNDERLYING NEUROIMAGING OF CORTICAL FUNCTION.

Panagiotis Kovanis

PhD in Psychology

2014

Summary

The aim of this study was to shed light on some of the neurophysiological mechanisms behind visual perception and specifically look into feedback processes that may be taking place during visual processing and also inhibition processes of the visual cortex.

The oblique effect is a preference of the visual system for cardinal orientations rather than oblique ones. A recent MEG study (Koelewijn, et al. 2011) finds in V1 an initial inverse oblique effect (80 msec from stim onset) which however later (120msec from stimulus onset) showed a trend towards the classical oblique effect and feedback processes here are suggested taking place from the extrastriate cortex. We look into this using fMRI and interestingly we do manage to find an inverse oblique effect, which indicates that the initial MEG "inverse" effect in V1 is detectable with fMRI even though fMRI does not have the temporal resolution of MEG. Unfortunately in this fMRI study the extrastiate region was not localized.

In the 3rd experimental chapter (following up on a study by Edden et al.) we look into the relation of behavioral thresholds and gamma activity in the visual cortex. Here we found in the SAM analysis) for the oblique condition, a positive correlation of the oblique main effect in a cortical location in the medial visual cortex (at a frequency range of 30-70 Hz) to behavioral thresholds. However here we did not detected an oblique effect when we compared oblique to cardinal condition.

In the final experimental chapter we look into the relation between GABA and training effects using however two GABA scanning protocols (with and without macromolecule suppression). Here we find that training effects depend on GABA concentration (as found in unpublished findings by Edden et al.). Additionally here we find negative correlations with behavioral thresholds and GABA however these are strongest for the untrained sessions

DECLARATION

This work has not been submitted in substance for any other degree or award at this or any other university or place of learning, nor is being submitted concurrently in candidature for any degree or other award.

Signed …… (candidate) Date ……

STATEMENT 1

This thesis is being submitted in partial fulfillment of the requirements for the degree of ……(insert MCh, MD, MPhil, PhD etc, as appropriate)

Signed …… (candidate) Date ……

STATEMENT 2

This thesis is the result of my own independent work/investigation, except where otherwise stated.
Other sources are acknowledged by explicit references. The views expressed are my own.

Signed …… (candidate) Date ……

STATEMENT 3

I hereby give consent for my thesis, if accepted, to be available online in the University's Open Access repository and for inter-library loan, and for the title and summary to be made available to outside organisations.

Signed …… (candidate) Date ……

STATEMENT 4: PREVIOUSLY APPROVED BAR ON ACCESS

I hereby give consent for my thesis, if accepted, to be available online in the University's Open Access repository and for inter-library loans **after expiry of a bar on access previously approved by the Academic Standards & Quality Committee.**

Signed …… (candidate) Date ……

Acknowledgement

First I would like to thank my supervisor Prof Krish Singh for his guidance, encouragement and continuous support throughout my PhD. He has always been available to answer any questions I may have had and has been a great supervisor.

Also I would like to thank my co-supervisor Prof Frank Sengpiel. Although my cooperation with him was limited to the first year of my thesis mostly, his guidance throughout that time was invaluable.

Additionally I would like to thank Prof. Tom Freeman for helping me during my second experiment with eye tracking, Mark Mikkelsen who has helped with my GABA scans and also with any question I had on GABA. I would like to thank all the people in CUBRIC who have made it a really friendly environment to work in and were always available to help me with any questions I had.

Finally, I would like to thank Cardiff University for providing me the funding to complete this thesis

Contents

1 GENERAL INTRODUCTION.

1.1 Anatomy of the visual cortex.

1.1.1 Basic vision.

Vision is probably the most relied upon of our senses. The eye is a fragile yet sensitive organ that can pick up very small amounts of light. An early study by Hecht, Shlaer and Pirenne (Hecht, Shlaer, & Pirenne, 1943) demonstrated that the minimum energy required for vision was 2.1-5.7 X 10^{-10} erg at the cornea, which they report represents between 54 and 148 quanta of blue-green light. The conditions for maximum retinal sensibility according to Hecht, Shlaer and Pirenne (Hecht, Shlaer, & Pirenne, 1943) involve dark adaptation, peripheral vision, short exposures and selected portions of spectrum. One of the furthest objects visible to the eye, the star Deneb (Cygnus constellation), is located at a distance of 1,500 light years away according to Brittanica online (Deneb) (see Figure **1**), which shows just how far the visual system allows us to see. Olfaction and sound are a lot less sensitive than vision. An overview of the visual system is given in this chapter.

Figure 1: Stars are a good example of how far the visual system allows us to see. The star Deneb (mentioned in the text) is the one in the far left in this image. Human smell compared to vision is a lot more limited. Taken from the ESA/HUBBLE web page **(Wide-field view of the Summer Triangle)**.

The visual system receives information from the environment from the eye. The light,after passing through the cornea and the lens, reaches the retina at the surface at the back of the eye. The retina is covered with more than a hundred million photoreceptors that convert light to neural signals (Palmer, 1999). The amount of light hitting the retina is controlled by the iris and the pupil and high illumination causes a constriction and less light passing through while low illumination causes a dilation of the pupil allowing more light in the eye. Interestingly an increase in the pupil size has been found to also accompany viewing of emotionally interesting stimuli (Hess & Polt, 1960) indicating that psychological state can influence the visual experience at a very early stage (pupil). The light is converted from energy to a neuronal signal in the photoreceptors (Palmer, 1999). The ganglion cell axons leave the eye by the optic nerve which leads to the optic chiasm and, from there, there are two

pathways into the brain on each side (Palmer, 1999), the smaller one (a few percent) goes to the superior colliculus and the larger pathway goes to the Lateral Geniculate Nucleus (LGN) and then to the primary visual cortex or area V1 (Palmer, 1999), which is the largest area in the cortex and receives the majority of ascending projections from the LGN (see Figure **2**). The visual cortex consists of six anatomically defined layers and, in V1, ascending fibres from the LGN mainly synapse in the fourth layer (Palmer, 1999). In non-human primates over half of the neocortex is occupied by areas involved in visual processing and at least 25 visual areas beyond V1 have been identified with the use of microelectrode mapping, tracer injections, histological stains and functional methods (Sereno, et al., 1995).

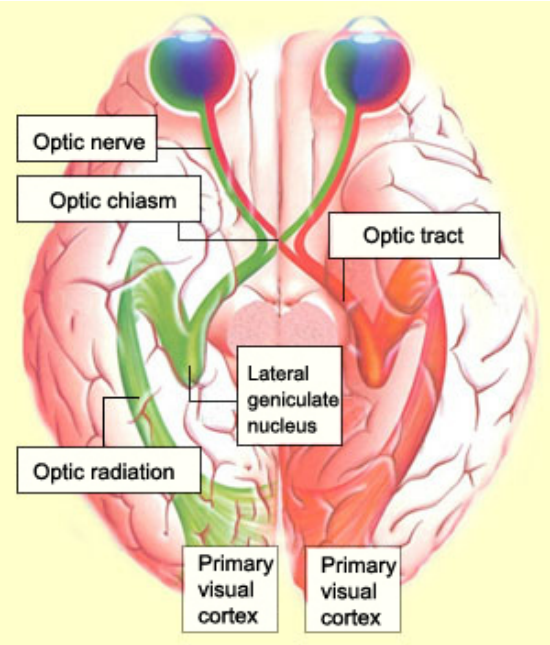

Figure 2: The journey of the visual information from the eye to the primary visual cortex. Image taken from http://thebrain.mcgill.ca

In primate early visual areas, the representation of the visual field on the cortex is retinotopic, which means that neighbouring retinal points project to

neighbouring points on the cortex (Morland, Baseler, Hoffmann, Sharpe, & Wandell, 2001). Retinotopic mapping is a procedure that allows us to get, in detail, information about how the visual field and its cortical representation in the individual subject correspond (Sereno, et al., 1995) (Warnking, et al., 2002) (Engel, et al., 1994). There is variability in the pattern of the folding from one person to another (geographic variability) and also variability in the size and shape of visual areas and their location in relation to geographic landmarks (functional variability) (Van Essen, et al., 2001) therefore it is necessary to generate retinotopic maps individually for every participant. The stimuli used for retinotopic maps stimulate different areas of the visual field at different times. A common approach for estimating retinotopic maps is the traveling wave method (or phase encoded retinotopic mapping) which uses rings and wedges stimuli to slowly and sequentially stimuli specific portions of the visual field (Wandell, Dumoulin, & Brewer, 2007). The traveling wave stimulus consists of contrast patterns at various angles or eccentricities (Wandell, Dumoulin, & Brewer, 2007) and examples are shown in Figure **3**.

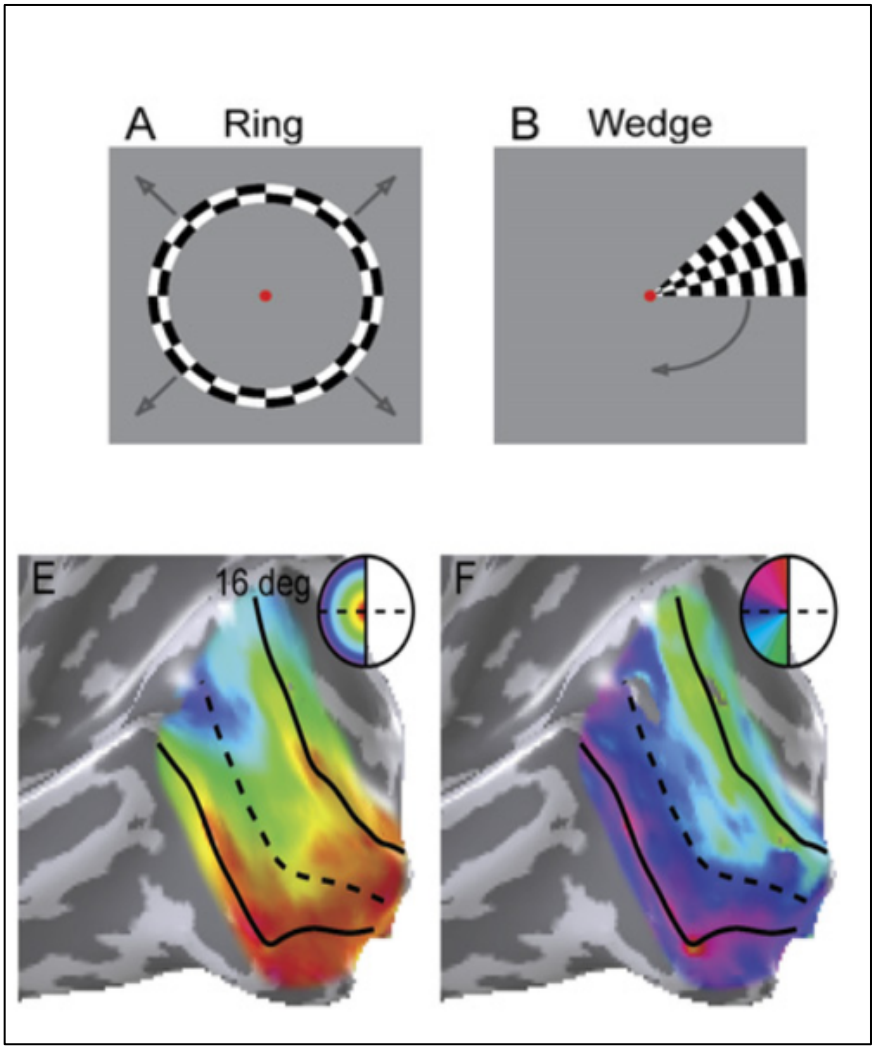

Figure 3 : A figure taken from Wandell et al's paper **(Wandell, Dumoulin, & Brewer, 2007)** showing how the traveling wave stimuli works. The traveling wave stimulus consists of a ring and a wedge stimulus. In the ring stimulus (top left) as the ring expands outwards it stimulates a different part of the retina. As the visual cortex is retinotopically organized, each stimulated retinal point has a corresponding location on the visual cortex. In the bottom left image we can see in the small circle different retinal locations represented with different colors and the same color used to represent its corresponding region in the visual cortex. The wedge stimulus works in a similar manner (shown in the top and bottom right images) however the stimulus rotates clockwise. In both the above stimuli participants fixate at the red point.

Retinal to striate cortex mapping is topographical i.e. nearby regions of the retina project to nearby regions of the striate cortex (Palmer, 1999). This mapping keeps qualitative spatial relations however distorts quantitative relations (Palmer, 1999). The central visual field (area near the fovea) receives

proportionally a larger representation than the periphery on the cortical surface. The disproportion in favor of central to peripheral vision is named cortical magnification and results in more spatial information about objects in centrally presented stimuli compared to peripheral ones (Palmer, 1999).

It is generally believed that each area is specialized for a certain aspect of vision, such as V4 for color and V5 for motion (Snowden, Thompson, & troscianko, 2006). However, in reality, things may be more complicated and for example, Grill-Spector and Malach (Grill-Spector & Malach, 2004) suggest it may be a more productive to talk about a color-processing stream starting from the retina and going through V1, V2 and higher areas such as V4/V8.

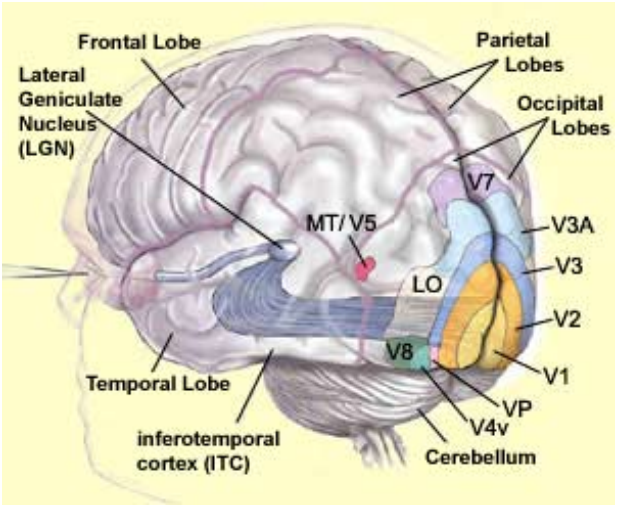

Figure 4 : Position of area V1 and other extrastriate areas of the visual cortex. Image taken from http://thebrain.mcgill.ca

1.1.2 Orientation selectivity

Although ganglion cells and lateral geniculate nucleus cells respond to spot stimuli (Snowden, Thompson, & troscianko, 2006), Hubel and Wiesel found that edge-containing lines most strongly stimulated visual cortex cells (Hubel D. ,

1963). There are a variety of cells in the cortex, however Hubel proposed (Hubel D. , 1963) they can be classified by function into two groups. Firstly, simple cells (Hubel D. , 1963) that respond to line stimuli and edges (straight line boundaries of light and dark areas). The firing rates of individual simple cells depends on both the orientation and position of the shape on the receptive field (Hubel D. , 1963). Complex cells also respond to bars, slits or edges, as long as (Hubel D. , 1963) the shape is suitably oriented for the examined cell. Complex cells, however, are not so sensitive to the exact position (Hubel D. , 1963) of the stimulus, as long as they have the proper orientation. Additionally, contrary to simple cells (Hubel D. , 1963) they respond with sustained firing to lines moving. Additionally to these two categories Hubel and Wiesel identified a third type of cells in the striate, they named hypercomplex cells (Palmer, 1999) that seemed to have an even more selective receptive field than complex cells had. Hypercomplex cells most prominent characteristic is that a line or edge extending beyond a certain length leads to them firing less than they would for shorter lines (Palmer, 1999). It is now believed (Palmer, 1999) that hypercomplex cells are end-stopped simple or complex cells, instead of consisting of a different cell type.

The total retinotopic map is composed of many smaller cortical groups called hypercolumns . Hypercolumns are long, thin cortical columns running perpendicular through the cortical layers. Each hypercolumn has a regular progression across a single dimension representing the tuning of cells for orientation (Palmer, 1999).

1.1.3 The modular visual cortex.

V1 has been of interest to anatomists for many years and its position and size has been estimated a number of times (Dougherty, Koch, Brewer, Fischer, Modersitzki, & Wandell, 2003). The surface of V1 can vary across individuals by a factor of as much as three (Dougherty, Koch, Brewer, Fischer, Modersitzki, & Wandell, 2003).

There are four major criteria for identifying cortical visual areas and for identifying the areas. One or more of the following criteria may be used (Orban, VanEssen, & Vanduffel, 2004): (1) Cyto and myelarchitecture, (2) connectivity, (3) retinotopic organisation or (4) function using single cell, lesion or neuroimaging methods (Orban, VanEssen, & Vanduffel, 2004).

On postmortem brains, cytoarchitectonic mapping of Brodmann's areas can be performed (Amunts, Malikovic, Mohlberg, Schormann, & Zilles, 2000), while on *in-vivo* subjects areas V1, V2, V3 and extrastriate areas can be defined with the use of phase encoded stimulation of the retina and fMRI (Sereno, et al., Borders of Multiple Visual Areas in Humans Revealed by Functional Magnetic Resonance Imaging, 1995).

Whichever method is used there are considerable individual differences in visual areas between subjects (see Figure **5** and Figure **6**). See also Figure **12** in experimental Chapter 1, where I estimate individual V1 areas using a gyral folding algorithm within the Freesurfer software distribution.

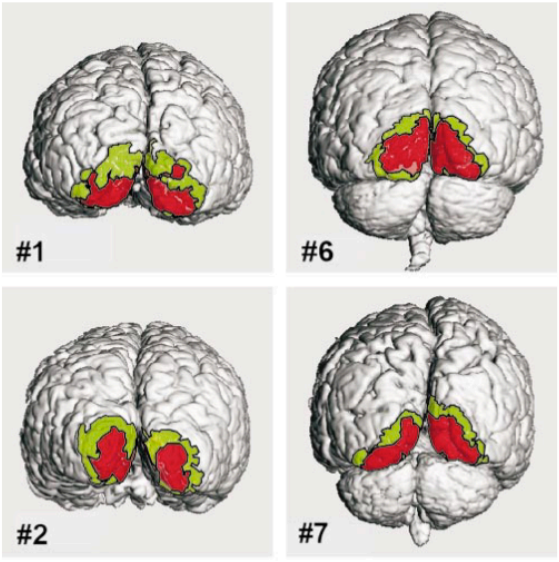

Figure 5: A surface rendering of 4 brains (participant number 1, 6, 2 and 7) and their cytoarchitectonic areas 17 (red color) and 18 (green) as reported by Amunts et al **(Amunts, Malikovic, Mohlberg, Schormann, & Zilles, 2000)**. There are clear differences in the size and shape of these areas as estimated using a cytoarchitectural method.

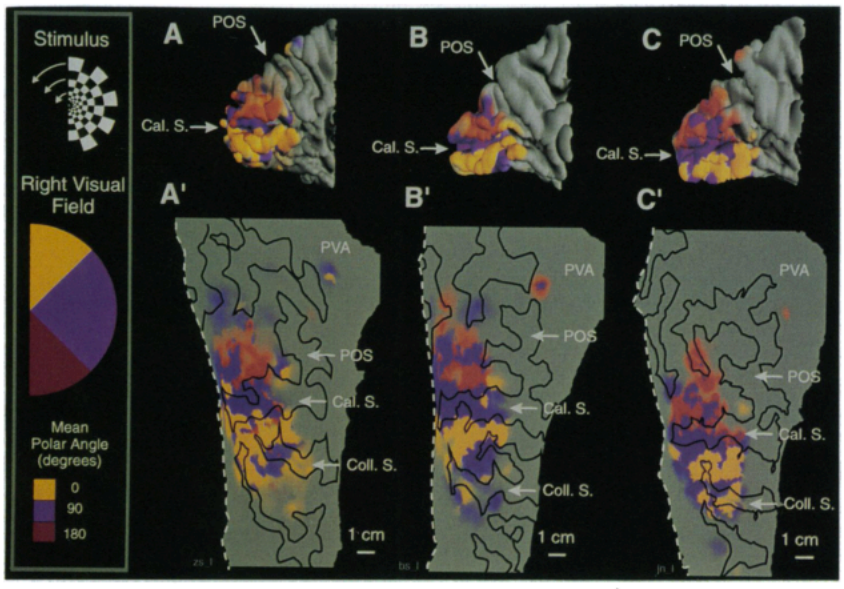

Figure 6: A cortical representation of the visual field quadrants for 3 participants using a checkered hemifield rotating around the circle center of the hemifield. The 3 colored hemifield shows for every part of the visual field the color used to represent the retinotopically corresponding location in the retinotopic maps for 3 participants (A, B, C), as reported by **(DeYoe, et al., 1996)**. Note that each area of the retina has a corresponding cortical area of variable size across participants

1.1.4 The Binding Theory.

The binding problem is often mentioned in studies on vision and consciousness. The "binding problem" according to Revonsuo and Newman (Revonsuo & Newman, 1999) is the question of how the unity of our conscious perception is achieved by the central nervous system's various distributed activities. According to Treisman (Treisman, 1998) our effortless ability to perceive objects with meaning in a scene requires complex visual processes and experiments suggest that attention plays a central part in solving this problem (Treisman, 1998).

Crick and Koch (Crick & Koch, 1990) propose that visual awareness is a form of consciousness and takes 2 forms: A fast one linked to iconic memory and a slow one in which an attentional mechanism binds all the neurons that have activity related to pertinent features of the single visual object (Crick & Koch, 1990). This is achieved (Crick & Koch, 1990) with coherent semisynchronouss oscillations, probably in the gamma range of 40 to 70 Hz. Crick and Koch (Crick & Koch, 1990) propose that since it is hypothesized that the basic mechanism for consciousness is rather similar in different brain parts (Crick & Koch, 1990), they propose using the visual system as a good choice for an experimental approach (Crick & Koch, 1990), as it has several advantages if used to study the neuronal basis of consciousness (Crick & Koch, 1990), particularly as vision in humans and primates is quite similar in contrary to, for example, language (Crick & Koch, 1990). Some early experimental support for this idea comes from the finding of synchronous firing, at gamma frequencies, to the presence of edges in the visual scene, within cat primary visual cortex (Gray & Singer , 1989) (gray, Konig, Engel, & Singer, 1989).

However, despite the popularity of the binding by synchrony hypothesis, Dong et al. (Dong, Mihalas, Qiu, von der Heydt, & Niebur, 2008) failed to find evidence for its support, while a similar report is also made by Thiele and Stoner (Thiele & Stoner, 2003).

1.1.5 Feedback processes in the visual cortex.

Connectivity of areas of the visual cortex has been the object of extensive study (Engel, Kreiter, König, & Singer, 1991) (Bastos, Briggs, Alitto, Mangun, & Usrey, 2014) (Koelewijn, Dumont, Muthukumaraswamy, Rich, & Singh, 2011). The complexity of the connections of the visual areas can be seen in Figure 7.

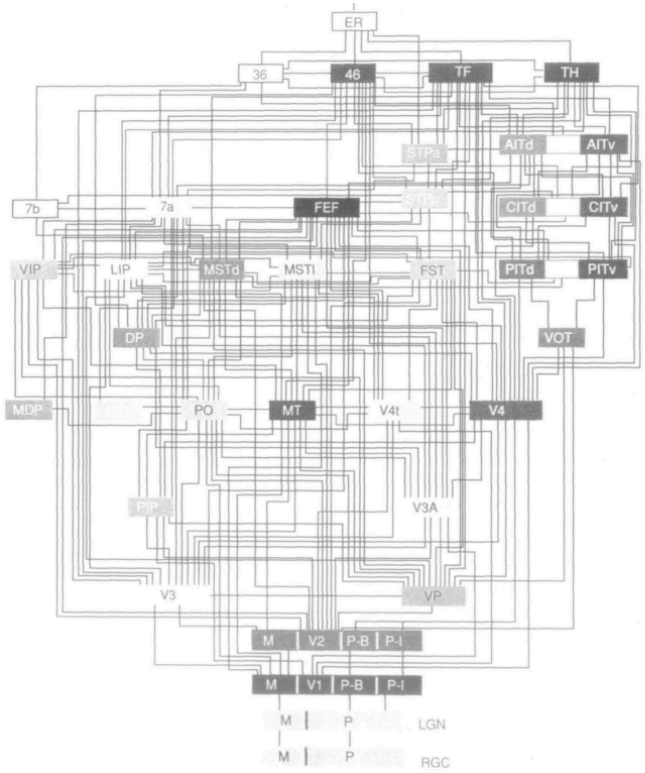

Figure 7: The complexity of the visual areas can be seen in this figure taken from Felleman and van Essen (Felleman & van Essen, 1991).

Areas within visual cortex also connect to areas that are non-visual. A study using retrograde tracers Falchier et al. (Falchier, Clavagnier, Barone, & Kennedy,

2002) showed that peripheral area 17,, representing eccentricities from 10-20 degrees of the visual field, receives projections from the auditory cortex as well as from the poly-sensory area of the temporal lobe (Falchier, Clavagnier, Barone, & Kennedy, 2002). Additionally visual activation in the visual cortex has been found to be affected by tactile stimulation as shown by Malacuso et al. (Macaluso, Frith, & Driver, 2000).

Studies using MEG and EEG (neuroimaging methods with millisecond temporal resolution) have looked into the timings of the communication between visual areas in humans. In a study by Koelewijn et al. (Koelewijn, Dumont, Muthukumaraswamy, Rich, & Singh, 2011) using grating stimuli to examine orientation preference of the visual system (oblique effect), they report finding a feedback process from the extrastiate cortex to the primary visual cortex. Also, although the initial response of the primary visual cortex (80 msec from stimulus onset) was stronger for the oblique stimuli, however later (120 mseconds from stimulus onset) the opposite was found, a preference for cardinal orientations (Koelewijn, Dumont, Muthukumaraswamy, Rich, & Singh, 2011). In another study, using EEG, Wibral et al. (Wibral, Bledowski, Kohler, Singer, & Muckli, 2009) examine the role of feedback processes in visual illusions (apparent motion) and find sensitivity to apparent motion content approximately 90 milliseconds after the start of a sequence of stimuli, most likely originating in hMT/V5+ (Wibral, Bledowski, Kohler, Singer, & Muckli, 2009). The finding of Wibral et al. (Wibral, Bledowski, Kohler, Singer, & Muckli, 2009) is of particular interest, as in the apparent motion visual illusion there is no actual motion (only perceived motion) and the feedback seems to be from hMT/v5+ an area that has been associated with motion.

Feedback processes from the extrastriate areas to the primary visual cortex can be modulated using transcranial magnetic stimulation (TMS) or in animal subjects with chemical interventions. Studies in macaque monkey, using recordings from V1 while deactivating MT/V5, psychophysical research of perceptual integration and TMS intervention studies suggest that feedback to V1 from other visual areas is important for visual awareness (Pascual-Leone & Walsh, 2001). In another study Liang et al. (Liang, Shen, & Shou, 2007) manage to affect the neural oblique effect (enhance it) using a pharmacological intervention in extra-striate cortical area 21a.

As mentioned previously, the majority of projections from the LGN go to V1 (Palmer, 1999). There have been studies showing that the visual input does not necessarily have to pass from V1 but may be received directly from extrastriate areas. In a study with PET, Barbur et al . (Barbur, Watson, Frackowiak, & Zeki, 1993) used a participant blinded by a lesion in area V1 who was able to discriminate direction of motion of a visual stimulus. In this study, it was found that area V5 could respond without activation in V1 which, as they say, shows that the visual input can reach V5 without passing first through V1.

Brain connectivity seems to be influenced by multiple clinical disorders. A dis-ordered brain connectivity and autism are discussed, for example, by Rippon et al. (Rippon, Brock, Brown, & Boucher, 2007) and also Belmont et al. (Belmonte, Allen, Beckel-Mitchener, Boulanger, Carper, & Webb, 2004). Bertone et al. (Bertone, Mottron, Jelenic, & Faubert, 2005), looking into the visual system in autism, found that people with autism were better at identification of orientation of a simple luminance defined grating but were worst when it came to second order gratings (Bertone, Mottron, Jelenic, & Faubert, 2005). Bertone et

al (Bertone, Mottron, Jelenic, & Faubert, 2005) propose that atypical neural connectivity could explain both the enhancement and decrease they found in autism.

1.2 The oblique effect: An overview.

1.2.1 Introduction to the oblique effect

The relative insensitivity of the visual system for oblique orientations relative to cardinal (i.e. horizontal and vertical) orientations is called *the oblique effect* (Baowang, Peterson, & Freeman, 2003) (Furmanski & Engel , 2000) (Appelle S. , 1972) (Emsley, 1925) and forms the core focus for work in this thesis.

This deficiency of the visual system can mean either worst performance at behavioral testing using oblique orientations, or a modified activation profile when using neuroimaging techniques for oblique orientations (Furmanski & Engel , 2000). The term "oblique effect " goes back to at least 1972 (Appelle S. , 1972), however the preference of the visual system for cardinal orientations seems to be known from as early as 1925 (Emsley, 1925). As reported by Fang et al. (Fang, Bauer, Held, & Gwiazda, 1997) in humans the oblique effect varies depending on ethnic origin and in their study Chinese participants had a significantly smaller oblique effect than Caucasians.

At the neuronal level a database study on the oblique effect (using 4,418 cells) of cat's striate cortex (Baowang, Peterson, & Freeman, 2003) find a bias towards neurons dedicated to the detection of horizontal and vertical orientations and also that the cells preferring horizontal orientations have

narrower tuning widths. However other neuro-anatomical studies have revealed only moderate or non-existent firing preferences for the cardinals in normally-reared cats (Senpiel, Stawinski, & Bonhoeffer, 1999).

The opposite phenomenon, namely a preference for obliques over cardinals called *the inverse oblique effect*, has also been observed both behaviorally and in neuroimaging studies of the visual cortex (Koelewijn, Dumont, Muthukumaraswamy, Rich, & Singh, 2011) (Essock, DeFord, Hansen, & Sinai, 2003) (Wilson, Loffler, Wilkinson, & Thistlethwaite, 2001). Using MEG, Koelewijn et al. (Koelewijn, Dumont, Muthukumaraswamy, Rich, & Singh, 2011) report an inverse oblique effect at 80 msec after stimulus onset (in a medial visual location) while the later "classical" oblique effect was found 120 msec (approx.) after stimulus onset in early visual areas but also at a more infero-lateral extrastriate region (Koelewijn, Dumont, Muthukumaraswamy, Rich, & Singh, 2011). According to Koelewijn et al. the early response they find may represent an initial tuning of V1 cells with a higher response to oblique stimuli, whilst at later timepoints the classical oblique effect appears which, they suggest is mediated by areas in extrastriate cortex and could also involve feedback from extrastriate to striate cortex (Koelewijn, Dumont, Muthukumaraswamy, Rich, & Singh, 2011). This inverse oblique effect has also been detected with psychophysical methods (Essock, DeFord, Hansen, & Sinai, 2003) (Wilson, Loffler, Wilkinson, & Thistlethwaite, 2001).

The oblique effect has been studied in relatively few human fMRI studies and has provided a rather confusing and contradictory picture. In a study of three participants, Furmanski and Engel (Furmanski & Engel , 2000) demonstrated a clear classic oblique effect in primary visual cortex that

appeared to match with behavioral performance. In direct contrast however, a more recent fMRI study demonstrated a preference for both oblique and radially-oriented stimuli (see below) over cardinal orientations (Mannion, McDonald, & Clifford, 2010).

1.2.2 Radial Bias

An important feature when studying the oblique effect is its orientation in relation to the centre of the visual field (Mannion, McDonald, & Clifford, 2010). BOLD response in connection to orientation of sinusoidal gratings in visual areas V1, V2, V3 and V3A/B is studied (Mannion, McDonald, & Clifford, 2010). In this study a smaller response is found for cardinal compared to oblique orientations. However, when viewed relative to angular position in the visual field, the anisotropic response distribution in V1, V2, V3, V3A/B, and hV4 has a greater response when the orientation of the pattern is referenced to the visual field meridian (Mannion, McDonald, & Clifford, 2010). This preference for stimuli that are oriented parallel to a line intersecting the centre of fixation is called the radial bias and is well documented (Bennett & Banks, 1991) (Berardi & Fiorentini, 1991) (Fahle, 1986) (Rovamo, Virsu, Laurinen, & Hyvarinen, 1982).

1.2.3 Nature vs. nurture.

A key unanswered question is whether the oblique effect has developed through evolution or that the brain develops this sensitivity through maturation. There have been animal studies assessing if selectivity is developed at an early age or there is a natural bias for cardinal orientations compared to oblique ones (Senpiel, Stawinski, & Bonhoeffer, 1999). One advantage here of using animals is

that researchers have control over the visual environment the animal is reared in but also with small animals we only need to have the animal in a controlled environment for a small time period from its time of birth until it reaches full development. The oblique effect is observed in a variety of species such as rats, ferrets, monkeys and humans, although all these species view the world from a different perspective (Keil & Cristóbal, 2000), which implies that the visual experience constraints the evolution of the visual cortex (Keil & Cristóbal, 2000). Blakemore and Cooper (Blakemore & Cooper, 1970) suggest the visual cortex adjusts during maturation and that cells may alter their preferred orientation towards the visual input that is most common (Blakemore & Cooper, 1970). However in a study by Sengpiel et al. (Senpiel, Stawinski, & Bonhoeffer, 1999) on kittens reared in striped environment, they found over half the cortex was selective to orientations never seen before, which shows that it is not only the visual experience that regulates orientation selectivity (Senpiel, Stawinski, & Bonhoeffer, 1999).

1.2.4 The range of animals demonstrating orientation selectivity

Apelle (Appelle S. , 1972) gave an overview of the large range of species that have been studied for the oblique effect. The oblique effect exists even in species taxonomically far from humans such as the octopus (phylum: mollusca) (Sutherland, 1957). However in the case of the octopus orientation discrimination probably relies on a different physiological mechanism than the one in humans as Wells (Wells, 1959) reports that removal of both statocysts affect the ability of the octopus to detect stimuli of different orientation. In other commonly studied mammalian species (cat, monkey, human) it is assumed that the same neural mechanisms underpin the preference for cardinal orientations.

1.2.5 The Oblique Effect in the retina and LGN.

Throughout this thesis the main interest is orientation preference of the visual cortex. However some elements of orientation anisotropy to the visual system may also be introduced by the eye and LGN. Murray et al. (Murray, Elliott, Pallikaris, Werner, Choi, & Tahir, 2010) find, for example, that the eye 's optics also is a source of variance, as when pupil area is large (6mm), there exists an orientation specific effect for the viewer (some orientations have an advantage to others) when viewing through adapted optics systems. Vidyasagar and Urbas (Vidyasagar & Urbas, 1982) looked into orientation sensitivity in 136 LGN cells in normal cats and 82 LGN cells in cats with lesions in areas 17 and 18 using moving-bar stimuli and found that 32% of cells in normal LGN and 50% of cells in animals with lesions (area 17 and 18) had a optimal response to orientations within ~10 degrees of the vertical and horizontal.

1.2.6 Environmental Effects: Orientation in the natural environment. Gravity and orientation selectivity. Tilting the head and the Oblique Effect. The Oblique Effect in Cosmonauts.

As mentioned previously, the natural environment plays a role on the shaping of our visual experience. Girshick et al. (Girshick, Landy, & Simoncelli, 2011) used a photographic database of natural scenes. They "estimated the local image gradients by convolution" and created histograms of the distribution of visual orientations within these images (Girshick, Landy, & Simoncelli, 2011). As shown inFigure **8**, their analysis demonstrated that cardinal orientations were most prevalent in the images (Girshick, Landy, & Simoncelli, 2011).

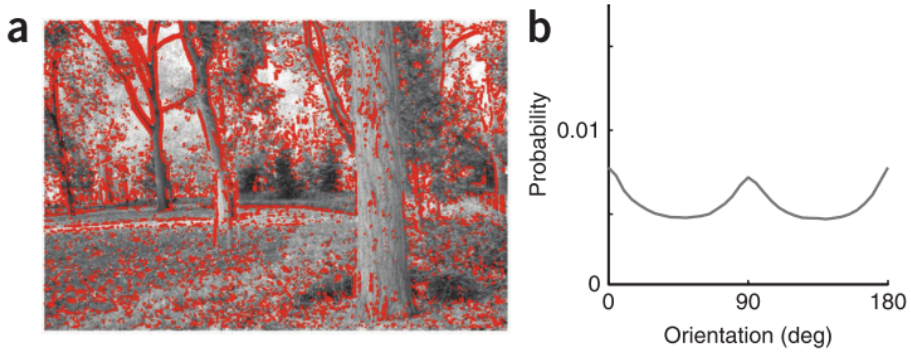

Figure 8: Figure taken from Girshick et al. **(Girshick, Landy, & Simoncelli, 2011)** showing areas with strong orientational representations (red color) and at the right the orientation distribution. It can be seen that cardinal orientations are most prevalent.

In an orientation behavioral task Lipshits and Mclntype (Lipshits & McIntyre, 1999) found better performance for horizontal and vertical oriented stimuli when body and gravitational axis were aligned. This however decreased or disappeared when they tilted the body axis in relation to gravity (Lipshits & McIntyre, 1999) however in tests performed by Cosmonauts in microgravity this orientational preference was maintained (Lipshits & McIntyre, 1999).

1.3 Methods for studying visual cortex function

1.3.1 Invasive methods in animals

One of the possibly most common approaches in measuring neural activity is electrophysiological recordings, with the most popular technique being single unit electrical recording (Purves, et al., 2008), recording action potentials of individual neurons and depending on the electrode's size and placement we can pick up firing from several nearby neurons concurrently, giving information about small populations of neuron cells (Purves, et al., 2008). Although we pick

up the signal from neighboring cells, we can however isolate the response that originates from just one cell, as each cell generates a characteristic signal which is the same for every action potential fired by the cell (Snowden, Thompson, & troscianko, 2006). An advantage with this method is that we can selectively examine simple or complex cell response patterns, including tuning properties for orientation (Li, Peterson, & Freeman, 2003). By using larger electrodes to sample a more extended population of neurons, we can differentially filter the recording to either reveal multi-unit spiking activity (>300Hz) or local-field potentials, including gamma-band responses (<~200Hz).

As mentioned previously animals can be also be used in rearing studies, such as the one by Sengpiel et al. (Senpiel, Stawinski, & Bonhoeffer, 1999) in which animals were reared in a striped environment to test how the visual system‘s orientation selectivity is affected by manipulation of the environment.

With animal studies we can also “knock out” a specific gene in order to learn more about its effect on a specific behavior. Another method using animals is retrograde tracing used to follow neural connections from their synapse to cell body, such as the retrograde transynaptic tracer pseudorabies virus (Luo & Aston-Jones, 2009).

Direct invasive pharmacological intervention is another area in which animal studies have an advantage compared to studies with human subjects. An example of a pharmacological intervention is e.g. Liang et al. (Liang, Shen, & Shou, 2007) where connectivity between area 17 and 21a was examined by injecting glutamate to area 21a (Liang, Shen, & Shou, 2007). A type of research that would not get ethics for human subjects is lesions studies in which case, an area of the brain is impaired and the effects of this lesion is examined on a

specific behavioural measure. For example, Newsome et al. (Newsome, Wurtz, Dürsteler, & Mikami, 1985) examined the effect of a chemical lesion on area MT on viewing moving compared to stationary stimuli..

1.3.2 Non-invasive methods in humans

There are several experimental techniques available that allow the non-invasive study of visual function including orientation tuning properties such as the oblique effect. In this thesis I will use behavioral testing, functional magnetic resonance imaging (fMRI), Magneto encephalography (MEG) and Magnetic Resonance Spectroscopy (MRS).

In previous sections, above, I have already outlined some of the many psychophysical studies that have been used to investigate the oblique effect in both humans (Leibowitz, Myers, & Grant, 1955) but also on a range of animal subjects (Appelle S. , 1972).

In terms of non-invasive neuroimaging, one of the most popular methods is fMRI, which allows the localization of mental processes with a time precision of seconds and a spatial resolution of a few millimeters (Huettel, Song, & McCarthy, 2004). fMRI measures task-related changes in blood oxygenation. fMRI does not directly measure neuronal activation, rather it relies on the metabolic changes that follow the neuronal activity and specifically the fact that blood flow to the region of activation increases following neuronal activity (as active neurons require oxygen and glucose). This blood-flow increase reduces the proportion of de-oxygenated blood in the activated region. As oxygenated and de-oxygenated haemoglobin have different magnetic properties, these differentially affect the relaxation time of the MR signal, resulting in the activated brain region increasing in brightness by a few percent, compared to baseline.

A different imaging method is MEG, which in contrast to fMRI has excellent temporal resolution (approx.. 1msec) (Huettel, Song, & McCarthy, 2004) and is a more direct measure of neural activity than the haemodynamic response of fMRI. However, it's spatial localization properties are not as good as that of fMRI (Snowden, Thompson, & troscianko, 2006). MEG has a better sensitivity to activity in the sulci and is comparatively insensitive to gyral activity (Purves, et al., 2008). As magnetic field strength falls rapidly with distance MEG is thought to be insensitive to deep brain sources (Senior, Russel, & Gazzaniga, Methods in mind, 2006), however activation from the hippocampus (a relatively deep structure) has been demonstrated (Tesche & Karhu, 2000).

GABA spectroscopy is a particularly interesting method, allowing to probe into GABA levels in the cortex of both healthy participants and patients. This allows for the measure of GABA concentration in a small cortical region (e.g. 3x3 cm). One of the most extensively used MRS approaches is the edited MEGA-PRESS technique (Mescher, Tannus, Johnson, & Garwood, 1996) (Mescher, Merkle, Kirsch, Garwood, & Gruetter, 1998). GABA concentration estimates with MRS however are contaminated with macromolecules (MM) which may consist of up to 60% of the signal (Rothman, Petroff, Behar, & Mattson, 1993), it is however an accepted approach to report GABA with macromolecule contamination (GABA+). Recent methods however for removing these co-edited macromolecules have been proposed however (Edden, Puts, & Barker, 2012) allowing for clearer GABA measures.

1.4 The aims of this thesis

The general aim of this thesis is to try and clarify the neural basis of the oblique effect found behaviourally in humans and animals, using fMRI, psychophysics, MEG and MRS estimates of GABA concentration**.**

Although there have been several studies that have attempted to do this with both fMRI and MEG, the results so far have been contradictory and confusing.

In the first chapter I attempt to replicate Koelewijn et al. 's (Koelewijn, Dumont, Muthukumaraswamy, Rich, & Singh, 2011) study however with the use of fMRI instead of MEG. By using as similar an experimental design as possible, I hope to reconcile their MEG findings with previous contradictory fMRI results. In their MEG study they find an inverse oblique effect, a finding that has been reported with naturalistic scenes (Essock, DeFord, Hansen, & Sinai, 2003) (Hansen & Essock, 2004). Also gratings and fMRI have been used like in the study of Mannion et al (Mannion, McDonald, & Clifford, 2010) where the inverse oblique effect was also detected but could have been influenced by a radial bias and possible center surround confounds. In this chapter we also attempt to detect the extrastriate region, reported previously (Koelewijn, Dumont, Muthukumaraswamy, Rich, & Singh, 2011) (Liang, Shen, & Shou, 2007) that feeds back to the primary visual cortex. As the stimulus has the same dimensions as Koelewijn et al. (Koelewijn, Dumont, Muthukumaraswamy, Rich, & Singh, 2011) we check if the inverse oblique effect will be detected with fMRI (controlling though for center surround effects and the radial bias).

In the next chapter, I investigated how stable the behavioral oblique effect is to presentation at non-central locations in the visual field. This is important as

most behavioral studies are centrally fixated, whilst many neuroimaging studies are not. For example, Edden et al. (Edden, Muthukumaraswamy, Freeman, & Singh, 2009) used a centrally presented grating to detect thresholds for an orientation discrimination task. In the second chapter we use the same paradigm as Edden et al ,however the grating patch stimulus is presented in the periphery, allowing an investigation of whether it is the radial bias or the oblique effect that determines performance at the discrimination task. Additionally training effects also reported by Edden et al. (Edden, Muthukumaraswamy, Freeman, & Singh, 2009) will be examined.

In the next Chapter I present results from an MEG experiment in which participants performed an orientation discrimination task in the MEG. Edden et al. (Edden, Muthukumaraswamy, Freeman, & Singh, 2009) previously found that thresholds to an orientation discrimination task were negatively correlated with an individual's visual gamma frequency (the oblique condition gave significant results in their study while not the cardinal). In their study Edden et al. did not measure gamma while performing the behavioral task but instead used the response frequency as a trait measure of the excitation/ inhibition balance of the cortex Gandhi et al. (Gandhi, Heeger, & Boynton, 1999) have previously shown that attending to a stimulus and passively viewing it can lead to differences in neuronal activation, so in this chapter the correlation of gamma and performance will be tested with the behavioral task being performed during the scan itself.

In the final chapter I further investigated some unpublished results from Edden et al. (Edden, Muthukumaraswamy, Freeman, & Singh, 2009). I examined

training effects while performing a orientation discrimination task and look at their relationship to estimates of V1 GABA concentration, using MRS. This is of particular interest because of previous findings that GABAergic inhibition helps determine the orientation tuning properties of cells, but in addition that a release from GABAergic inhibition may also be important for allowing perceptual learning to take place (Vetencourt, et al., 2008).

In this study I used both standard MEGA-PRESS estimates of GABA concentration, which are known to be contaminated with macromolecular contributions, as well as a new MEGA-PRESS sequence implemented here in CUBRIC that is though to suppress macromolecule signals. As no training effects were found for cardinal orientations in Edden et al. I only investigated oblique orientations in this study.

2 Experimental chapter 1

2.1 Introduction.

The oblique effect, the preference of the visual system to cardinal orientations, is a well-established psychophysical phenomenon (Appelle S. , 1972) that has also been studied with imaging procedures such as fMRI (Furmanski & Engel , 2000) (Mannion, McDonald, & Clifford, 2010). In contradiction to the classical oblique effect shown both behaviorally and using fMRI (Furmanski & Engel , 2000), Koelewijn et al. (Koelewijn, Dumont, Muthukumaraswamy, Rich, & Singh, 2011) also report an inverse of the classical oblique effect i.e. a preference for oblique orientations rather that cardinal ones, as revealed by larger MEG response amplitudes. In their study Koelewijn et al. report an early (around 80msec) inverse oblique effect and a later response (around 120msec) showing the classical oblique effect, with the initial response possibly reflecting the initial bottom-up response to orientation in the primary visual cortex. Here we wish to replicate the inverse oblique effect found by Koelewijn et al. (Koelewijn, Dumont, Muthukumaraswamy, Rich, & Singh, 2011) however with the use of functional MRI. Although MEG gives millisecond precision for brain activation, MRI has a much better spatial localization. By replicating Koelewijn et al.'s study with MRI, we wish to probe further the contradictory findings of Furmanski et al. and Koelewijn et al. and also validate the MEG source localization (by using the same paradigm as Koelewijn et al. use). Although fMRI and MEG may show activation in similar spatial locations, they may in fact be tuned to different aspects of neuronal activation (Muthukumaraswamy & Singh, 2008) and it could be that the early evoked

inverse oblique effect found by Koelewijn et al. is not detectable by MRI. A study by Mannion et al. (Mannion, McDonald, & Clifford, 2010) also reports an inverse oblique effect with fMRI, however these results are confounded by a possible 'radial bias' as the oblique orientations were also radial to the fixation point. Additionally, as Koelewijn et al. (Koelewijn, Dumont, Muthukumaraswamy, Rich, & Singh, 2011) report source localizations showing that the initial evoked responses and sustained gamma were found in the medial visual cortex and the later evoked responses were found both in early visual area and a more inferolateral location in extrastriate cortex ,with possible feedback processes taking place from the extrastriate region to the primary visual cortex.

2.1.1 Feedback processes.

One theory regarding the oblique effect is that it is linked to feedback from extrastriate areas of the visual cortex to the striate cortex (Liang, Shen, & Shou, 2007) (Koelewijn, Dumont, Muthukumaraswamy, Rich, & Singh, 2011). In their MEG study Koelewijn et al. showed both an inverse and a 'classical' oblique effect. The inverse oblique effect was detected in primary visual cortex for the early (80 msec from stim onset) evoked response, while for the later response (120 ms) the classical oblique effect was present in both striate and extrastriate cortex. The authors suggested that the early evoked and sustained gamma activity corresponds to the initial tuning of V1 neurons, in which oblique angles give a stronger response, with the later classical oblique effect being mediated by extrastriate cortex via possible feedback to primary visual cortex. This is consistent with a previous study by Liang et al (Liang, Shen, & Shou, 2007) using a combination of pharmacological injections with optical imaging in cats. In their study Liang et al. found that positive feedback from area 21a can alter the

oblique effect observed in area 17 and they suggest a neural mechanism in which feedback from the higher order visual areas enhance the oblique effect in area 17. The presence of feedback processes having an effect on the oblique effect were also reported ,in a study using optical imaging and GABA administration, by Shen et al. (Shen, Liang, & Shou, 2008).

2.1.2 Can fMRI detect an inverse oblique effect?

The initial inverse oblique effect reported by Koelewijn et al. is the initial tunning of the neuronal population in the median visual cortex and was detected with the use of MEG. This inverse oblique effect, which according to Koelewijn et al. may represent the initial orientation tuning of V1 has also been found in a recent fMRI study (Mannion, McDonald, & Clifford, 2010) where they report an anisotropic distribution for the responses found (in areas V1, V2, V3 and V3A/B) with the lowest response for horizontal gratings, a inter-mediate response for vertical and highest response for oblique orientations. They also report, however, that when they consider orientations relative to angular position in the visual field they then find an anisotropic distribution, where the greatest response is found for gratings parallel to the visual field meridian (these findings are shown in Figure **9**). This favouring of orientations radial to the fixation, named the radial bias, has been reported using behavioural methodology by many authors (Bennett & Banks, 1991) (Berardi & Fiorentini, 1991) (Fahle, 1986) (Rovamo, Virsu, laurinen, & Hyvarinen, 1982). However this is not the case in the Koelewijn paper as the only oblique stimulus was tangential to fixation (Koelewijn, Dumont, Muthukumaraswamy, Rich, & Singh, 2011) and thus their inverse oblique effect is a genuine preference of the visual cortex to oblique orientations and cannot be attributed to a “radial bias”. As both the inverse

oblique effect and the later 'classical oblique effect reported by Koelewijn et al. (Koelewijn, Dumont, Muthukumaraswamy, Rich, & Singh, 2011) were detected in the medial visual cortex (at different time points) and the BOLD response does not have the millisecond precision of MEG it could be that the initial inverse oblique effect can not be detected with an fMRI experiment, especially as Mannion et al's (Mannion, McDonald, & Clifford, 2010) inverse oblique effect may in fact be a radial bias. However, the fact that Furmanski et al. (Furmanski & Engel , 2000) report the classical oblique effect using fMRI leaves unanswered questions regarding the true tuning profile of BOLD responses to oriented gratings. Replicating an MEG study, using fMRI, that has previously demonstrated a clear inverse oblique effect, using cardinal, radial and tangential gratings, has the potential to shed light on this rather confusing and contradictory story.

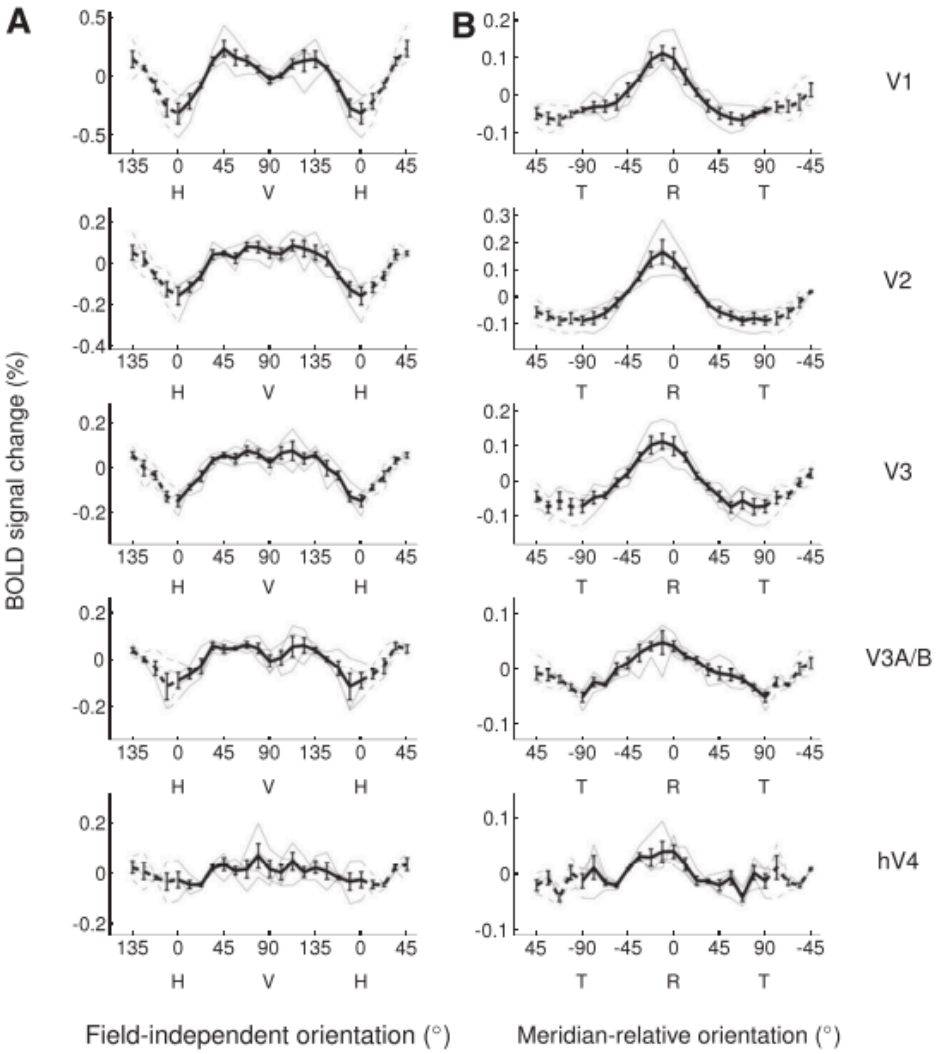

Figure 9: Image taken from the paper of Mannion et al. **(Mannion, McDonald, & Clifford, 2010)** that demonstrates the anisotropic distributions of responses with column A showing the response to a rotating grating in relation to the horizon with 45 and 135 being the oblique angles and 0 and 90 the cardinal orientations. However when these orientations are viewed as meridional-related (gratings parallel to the visual field meridian) then the response to the grating is favored when the grating is radial to the center of fixation. 0 in column B is the radially oriented grating.

An interesting point also to note here is that the stimulus used by Mannion et al. was a grating stimulating the entire visual field and then a region of interest analysis was carried out. This is an efficient design as it allows the orientation preference for the entire visual cortex to be assessed in one experiment.

However, as the entire visual field was stimulated simultaneously, centre surround effects could potentially be affecting the results. In a study by Xing and Heeger (Xing & Heeger, 2000) looking into surround effects on a patch grating it was reported that the presence of a surround stimulus can have an enhancing or suppressing effect on the apparent contrast of the central patch of texture. Relative contrast of central to surround stimuli are important as suppression occurs if the contrast of the surrounding stimulus is higher than the contrast of the central stimulus and enhancement takes place when the surrounding stimulus has a lower contrast compared to the central stimulus (Ejima & Takahashi, 1985) (Cannon & Fullenkamp, 1993). Surrounding stimuli can also have an enhancing or suppressing effect on the central stimulus by altering its size (Cannon & Fullenkamp, 1993). In addition Levitt and Lund (Levitt & Lund, 1997) found that when an optimal high contrast centre stimulus was paired with a surround of similar orientation and drift direction, a profound suppression of the response was elicited (compared to the centre stimulus being presented alone). In contrast, if the surround stimulus was of a different orientation or direction from the central stimulus the response suppression disappeared (Levitt & Lund, 1997). These surround effects may help to explain differences in results between imaging studies that have used relatively small stimuli (The Koelewijn MEG study and the Furmanski fMRI study) and studies using simultaneous whole-field stimulation (Mannion et al.).

2.1.3 Extrastriate areas in the oblique effect.

Koelewijn et al report in their paper that the inverse oblique effect may be due to feedback from an extrastriate area (Koelewijn, Dumont, Muthukumaraswamy, Rich, & Singh, 2011) having an effect on the orientation

preference of V1. One particularly interesting question here is whether fMRI is capable of detecting these extrastriate areas that are involved in the oblique effect. Mannion et al. (Mannion, McDonald, & Clifford, 2010) stated that the orientation preferences they found in V1 were matched in extrastriate regions such as V3 and V3A/B. On the other hand, Furmanski and Engel (Furmanski & Engel , 2000) failed to find a reliable oblique effect outside of area V1 and suggested that as extrastriate responses tended to be weaker than those found in V1 this might make it more difficult to detect orientation preferences in these regions. However, they do not dismiss the possibility that the oblique effect is simply absent in regions outside of V1 (Furmanski & Engel , 2000).

The experiment presented in this Chapter tests whether Koelewijn et al.'s (Koelewijn, Dumont, Muthukumaraswamy, Rich, & Singh, 2011) inverse oblique effect is also detectable with the use of fMRI and also if the extrastriate areas reported by Koelewijn et al. (Koelewijn, Dumont, Muthukumaraswamy, Rich, & Singh, 2011) are also shown using fMRI. To do this a stimulus with the same physical dimensions will be used. As the stimulus we use here is a patch grating and does not stimulate the entire visual field as Mannion et al.'s stimulus did, any inverse oblique effect found here with fMRI will not be cofounded by possible centre-surround effects. Our hypothesis is that fMRI will show the same distribution of brain regions as in the previous MEG study and that extrastriate visual cortex will show a preference for cardinally oriented stimuli (i.e. the classical 'oblique effect'). The results for primary striate cortex is harder to predict as the MEG study found a mixture of cardinal and oblique preferences at different latencies, which will be blurred temporally by fMRI.

A further complication is the unknown dependency of the BOLD response on the underlying mixture of neural activity. For example, using MEG and fMRI, it was shown by Swettenham et al. (Swettenham, Muthukumaraswamy, & Singh, 2013) that the BOLD response does not always show the same stimulus dependencies as MEG measured neural activity. In an experiment using red/green or luminance modulated black/yellow square-wave gratings with spatial frequencies of 0.5, 3, and 6 cycles per degree, they reported that there was weak or no evidence that BOLD amplitude was dependent on spatial frequency or the presence of luminance contrast, compared to colour contrast. However with beamformer analysis of MEG data they managed to find induced and evoked responses that showed strong stimulus dependent modulations of amplitude and latency. Similarly, as Muthukumaraswamy and Singh report (Muthukumaraswamy & Singh, 2008) MEG and fMRI may show activation in similar locations but the dependency of these activations on stimulus properties may be very different and hence may be sensitive to different aspects of neural function. Although imaging techniques pick up a bulk measure it is not possible to know in full the complex neuronal processes in the region under investigation. Distinct neuronal processes cannot be unveiled by imaging techniques, however combining single cell recording and imaging can detect single cell physiology during the oblique effect and with imaging we can inspect larger cell populations.

2.2 Methods.

Fifteen healthy right-handed volunteers (9 male, 5 female) with normal or corrected-to-normal vision were recruited from the CUBRIC database and from researchers within CUBRIC. One participant was rejected due to poor data

quality, leaving 14 volunteers (mean age 31.2; range 20-72; SD=12.7). All participants were screened with CUBRIC standard MRI safety forms and informed consent for the visual experiment) was given. All procedures were approved by the School of Psychology Ethics Committee at Cardiff University.

An MR projector system (Canon SX60 LCOS system), with a Navitar SST300 zoom convertor lens was used. The image was formed on a projection screen that was located behind the participant's head. The pixel resolution was 1024X768 and the system had a 1:1 aspect ratio. The fixation distance was approximately 57cm thus 1cm on the screen is 1 degree of visual angle. A 1024x768 standard image was approximately 25.6 x 19.2 degrees and was presented at a frame-rate of 60Hz. Four stimulus angles were used: 0, 45, 90 and 135 (these can be seen in Figure **10**). The spatial frequency of the stimulus was approximately 3 cycles per degree (3 cycles per degree required 6.667 pixels on the monitor, so it was rounded to 7 pixels thus 2.7 cycles/degree). The stimulus can be seen in Figure **10**. The stimulus was presented for a random time interval from 0.8 to 1.3 seconds and each fMRI trial block lasted 15 seconds (a detailed diagram of the trial timings can be seen in Figure **11**). Each functional scan consisted of 20 blocks (5 minutes). The stimulus timings are similar to that used in the previous MEG study, except a longer baseline period was used to allow the BOLD response to return to baseline. To maintain attention, each time the stimulus disappeared the participant had to press a button as quickly as possible. Participants were instructed to look constantly at a fixation cross during all functional scans. No eye-tracking device was used. Detailed information on the dimensions of the stimulus is given in Figure **10**. The stimulus chosen in this experiment was the same as that used in the study by Koelewijn et. al (Koelewijn,

Dumont, Muthukumaraswamy, Rich, & Singh, 2011) with the difference that here we also used both a tangential and an radial oblique angle in order to assess a possible radial-bias in the response profile.

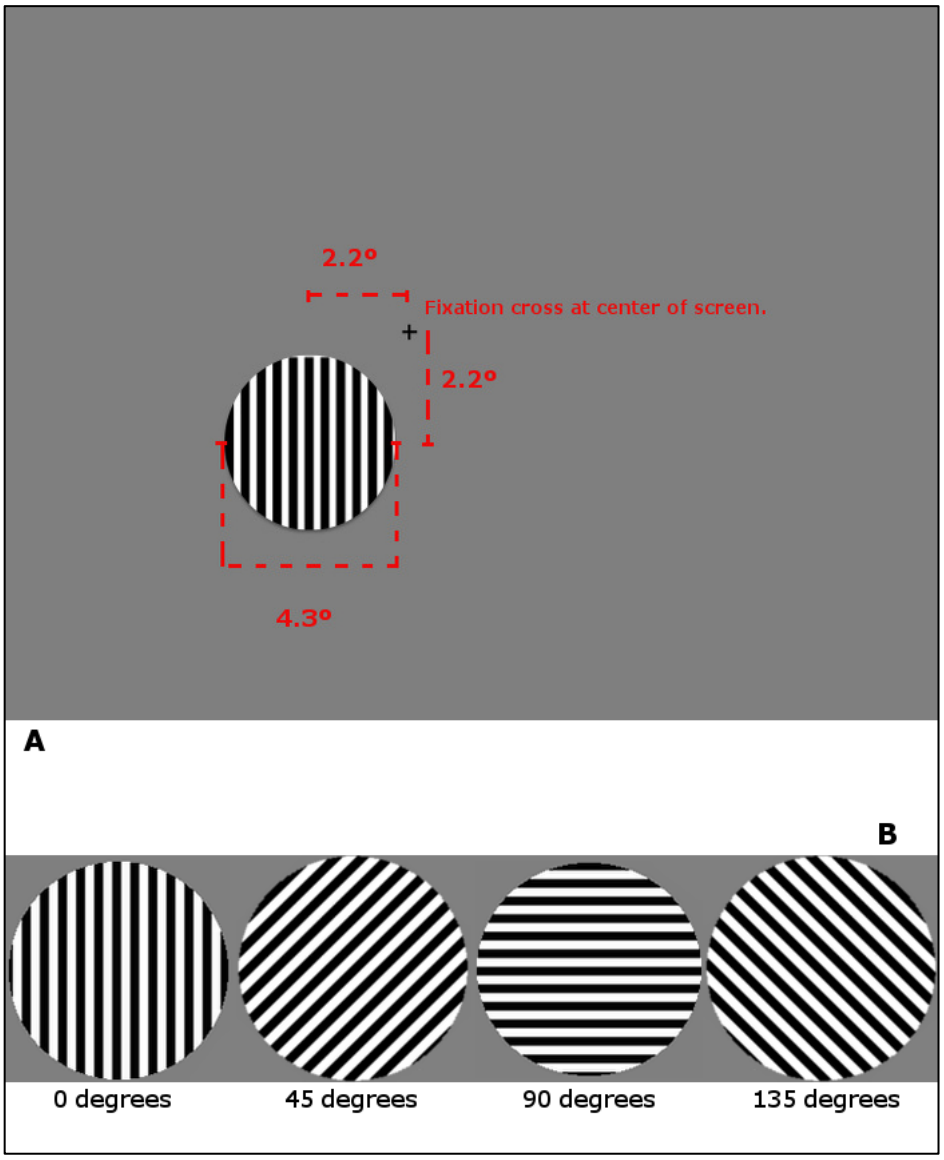

Figure 10: A) screenshot of the stimulus presented with stimulus dimensions shown in red and B) the four different orientations used.

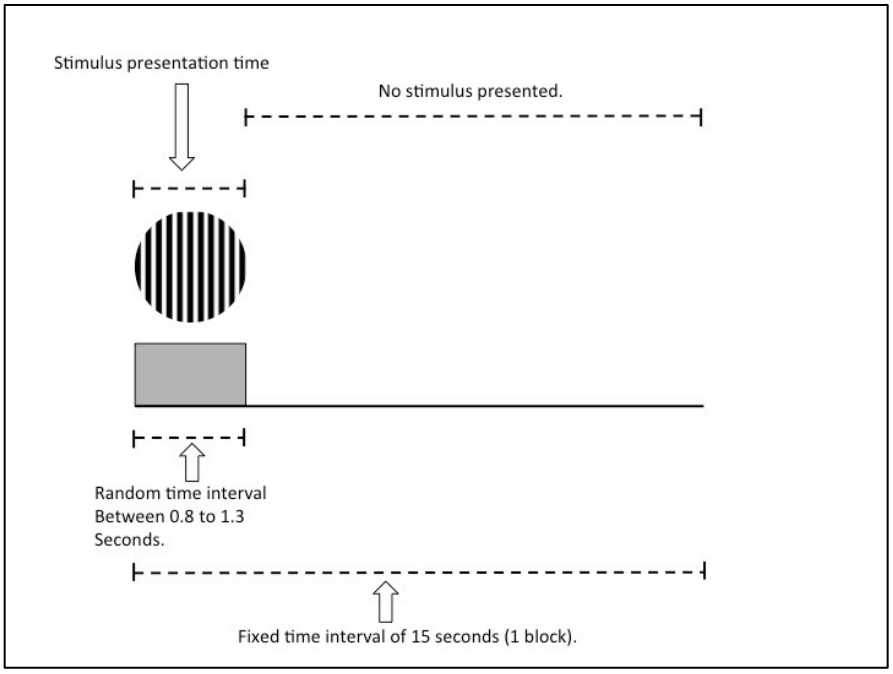

Figure 11: The timing of each stimulus block.

MR data was acquired using a 3 Tesla General Electric Signa HDx scanner (MR software release 14.0-MS_0757.f was installed), with an eight-channel, receive- only head RF coil. For each participant we obtained a 3D FSPGR scan with 1 mm isotropic voxel resolution, matrix size=256*256 and flip angle=20 deg. For the functional images we used TR= 3000 msec, TE=35msec, FOV 192*192 mm, matrix size=64*64, slice thickness 3.00mm, flip angle 90.00 and a 3mm*3mm voxel size. Participants remained in the MRI scanner for approximately 1 hour: 10 minutes were used for acquiring 2 retinotopic maps, 5 minutes for an FSPGR 3D file and a minute for two EPI's (to use with the functional and retinotopic maps). For the stimulus presentation scans approximately 25 minutes were required (5 scans each lasting 5 minutes); during each scan 20 blocks were presented; these 20 blocks consisted of the four grating orientations randomly presented. The stimuli were presented using

Matlab (version 7.7.0.471, R2008b) with the psychophysics Toolbox extensions (Brainard, 1997) (Pelli, 1997).

For the fMRI analysis FSL (FMRIB software library release 4.1© 2008, The University of Oxford) was used while the final statistical analyses were performed using PASW statistics 18 Release 18.0.0 (Jul 30, 2009). Additionally Mri3dX v7.88 (www.jiscmail.ac.uk/lists/mri3dx.html) was used for visualizing the MR and fMRI results.

For the FSL analysis, 100 volumes were used (no volumes deleted). The following were used: A high pass filter cut-off was used at 100 seconds; Mc Flirt motion correction; No slice timing correction; Brain extraction was done with BET. Spatial smoothing was performed using a Gaussian kernel of FWHM 5 mm. For registration, data were initially registered to a whole-brain EPI scan and then to the FSPGR scan.

BOLD magnitudes were extracted from the FSL analyses using two different region-of-interest (ROI) analyses, firstly for the whole occipital lobe (extracted with mri3dX) and secondly for the V1 only. For both of these ROIs, two values were extracted, peak BOLD response and mean BOLD response. The V1 region for each participant was estimated automatically using Freesurfer (version 5.1). After MR segmentation and creation of mesh models of the cortical surface, Freesurfer can construct a model of V1 using an algorithm based both on cortical position and surface folding (Hinds, et al., 2008). The Estimated V1 ROIs are shown for each participant in Figure **12**.

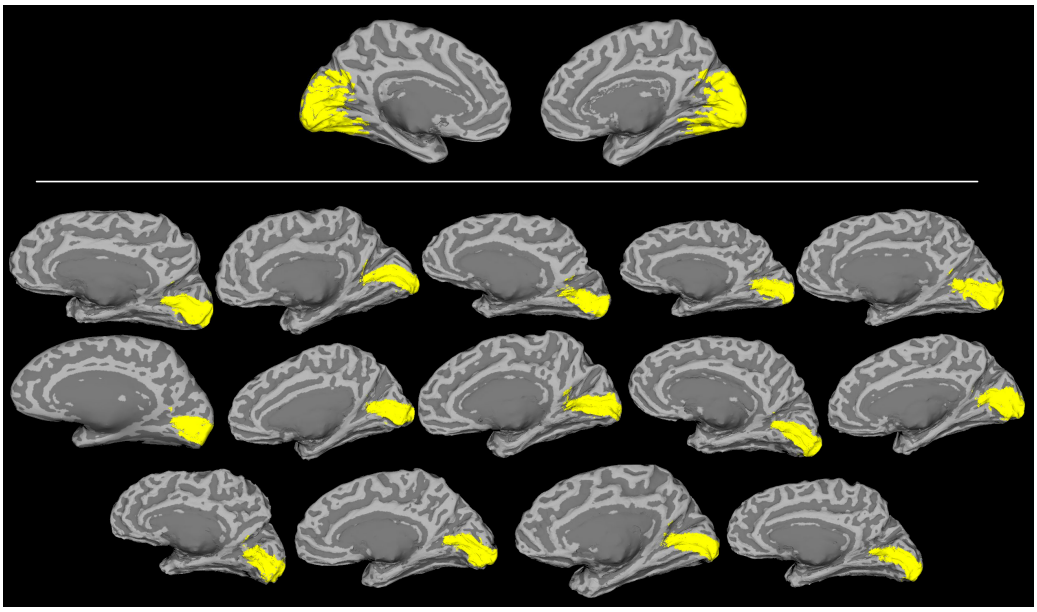

Figure 12: The upper panel shows the whole occipital lobe mask used in the first ROI analysis, overlaid on a template brain. The lower panel shows the individual V1 ROIs, shown on a Freesurfer mesh model of each participant's cortex.

2.3 Results.

In this study we were interested in studying activation during the viewing of four different angles (0, 45, 90, and 135). We wished to reveal locations in the visual cortex demonstrating either an inverse oblique effect (Oblique response > Cardinal response) as in the study by Koelewijn et. al (Koelewijn, Dumont, Muthukumaraswamy, Rich, & Singh, 2011), or cortical regions demonstrating a classic oblique effect profile (Cardinal > Oblique).

2.3.1 Whole-brain analysis.

FSL was used to assess the main effects for each condition separately (angles 0, 45, 90 and 135 contrasted to baseline activation) but also contrasts between angle 0 and 45, 90 and 45, 135 and 45, 90 and 135, 0 and 135 and finally 0 to 90. Unfortunately, FSL analyses using either cluster-based or voxel-level corrected thresholds (both at $p<0.05$) did not reveal any statistically

significant differences between the stimulus orientations. We therefore provide here a simple description of the un-thresholded contrast of parameter estimate (COPE) maps for each of these contrasts respectively are in Figure 13. Here we see that all four stimulus orientations show a strong activation (compared to baseline) in the medial visual cortex (images labeled angle 0, angle 45, angle 90 and angle 135). When contrasting the different orientations angle 0-45 and 90-135 there do not appear to be any strong differences between orientations. However in Figure **14**A it is shown that, for the contrast 90 to 45, there seems to be a small differential activation in the median visual cortex (a possible oblique effect). Also in Figure **14**C we see a negative BOLD response in the contrast of 0 to 135 (a higher activation for 135 degrees compared to 0 degrees gratings therefore perhaps representing an inverse oblique effect). In Figure **14**B we see a greater BOLD response when viewing a 135 oriented grating compared to a 45 one.

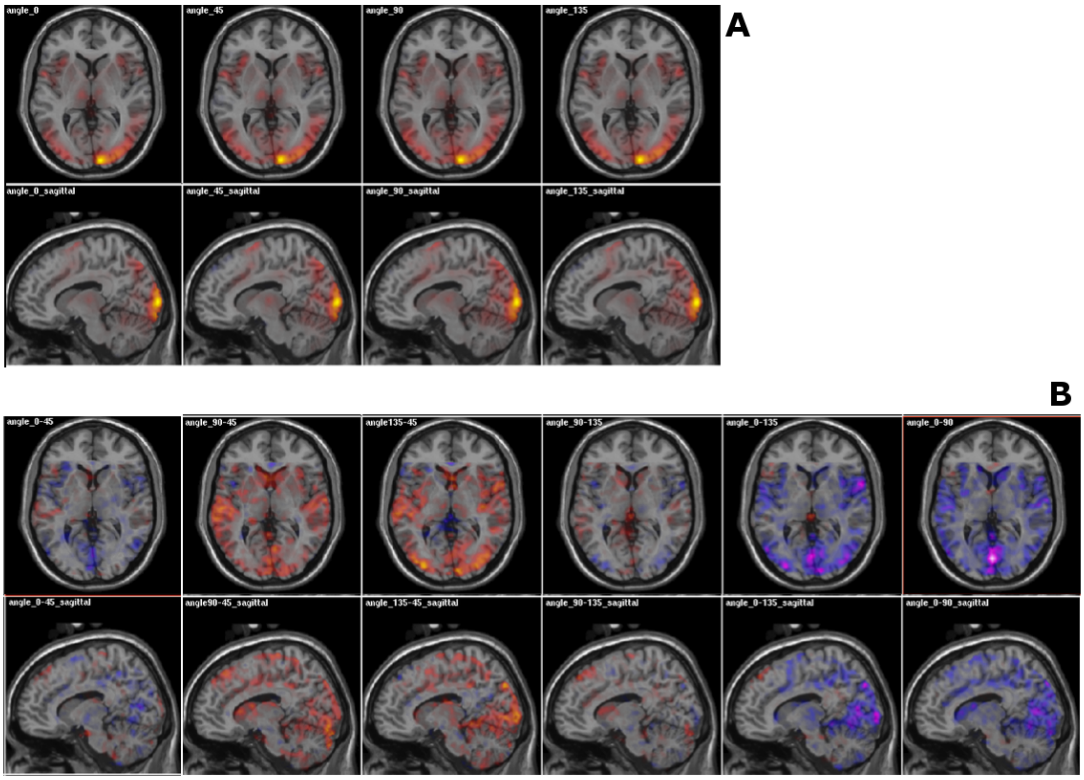

Figure 13: Un-thresholded contrast of Parameter estimate (COPE) maps for the conditions and contrasts between conditions overlaid on a MNI template brain. Figure A shows the main effects (for 0, 45, 90 and 135) and B the contrasts (0-45, 90-45, 135-45, 90-135, 0-135, 0-90). The areas that are yellow/orange are those where there is an increase in the BOLD response while the blue / purple areas are those where there is a relative decrease in the BOLD response.

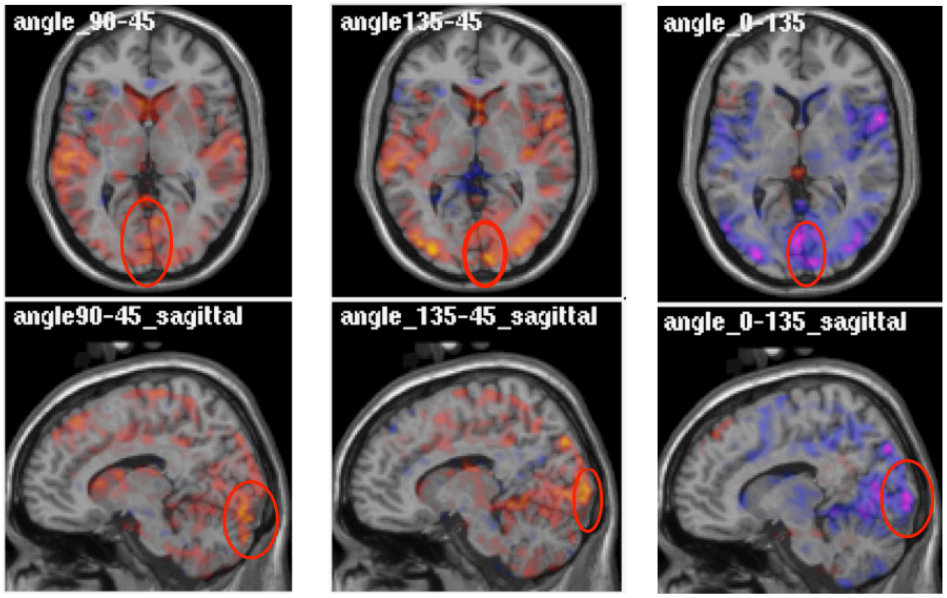

Figure 14. A: the contrast of condition 90 to 45. B: contrast of condition 135 to 45. C: contrast of condition 0 to 135. The red indicates areas where there is an increase in BOLD response (the area with the circle indicates the area with the highest increase in the medial visual cortex) while in purple the area with a decrease in BOLD response (the highest decrease in the medial visual cortex is shown in the circle).

2.3.2 ROI Analysis: Occipital Lobe.

Using mri3dX software, we used an ROI image encompassing the whole area of the occipital lobe (taken from the Talairach Daemon Database) and then for each of the 14 participants 8 values were extracted (4 values for the average activation of the contralateral stimulated brain area when a stimulus of 0, 45, 90 and 135 degrees was presented and 4 for the mean activation for these 4 conditions in the opposite, un-stimulated, occipital lobe). Initially descriptive statistics were examined. For each condition (0, 45, 90 and 135 degree angle stimulus) the mean activations of the participants (only for the stimulated hemisphere) were checked, to determine if there were any outliers among them, but also to determine, if they followed a normal distribution (Shapiro-Wilks test

gave no significant results so the normality assumption was not violated). Figure **15** shows the tuning profile of the BOLD response within the occipital ROI, assessed using both the mean BOLD response and the peak BOLD response within this ROI. Both raw BOLD magnitudes and normalized values are shown. Normalization here refers to dividing each person's BOLD response for each stimulus orientation by the maximum response to any orientation, resulting in a scaled response from 0 to 1.

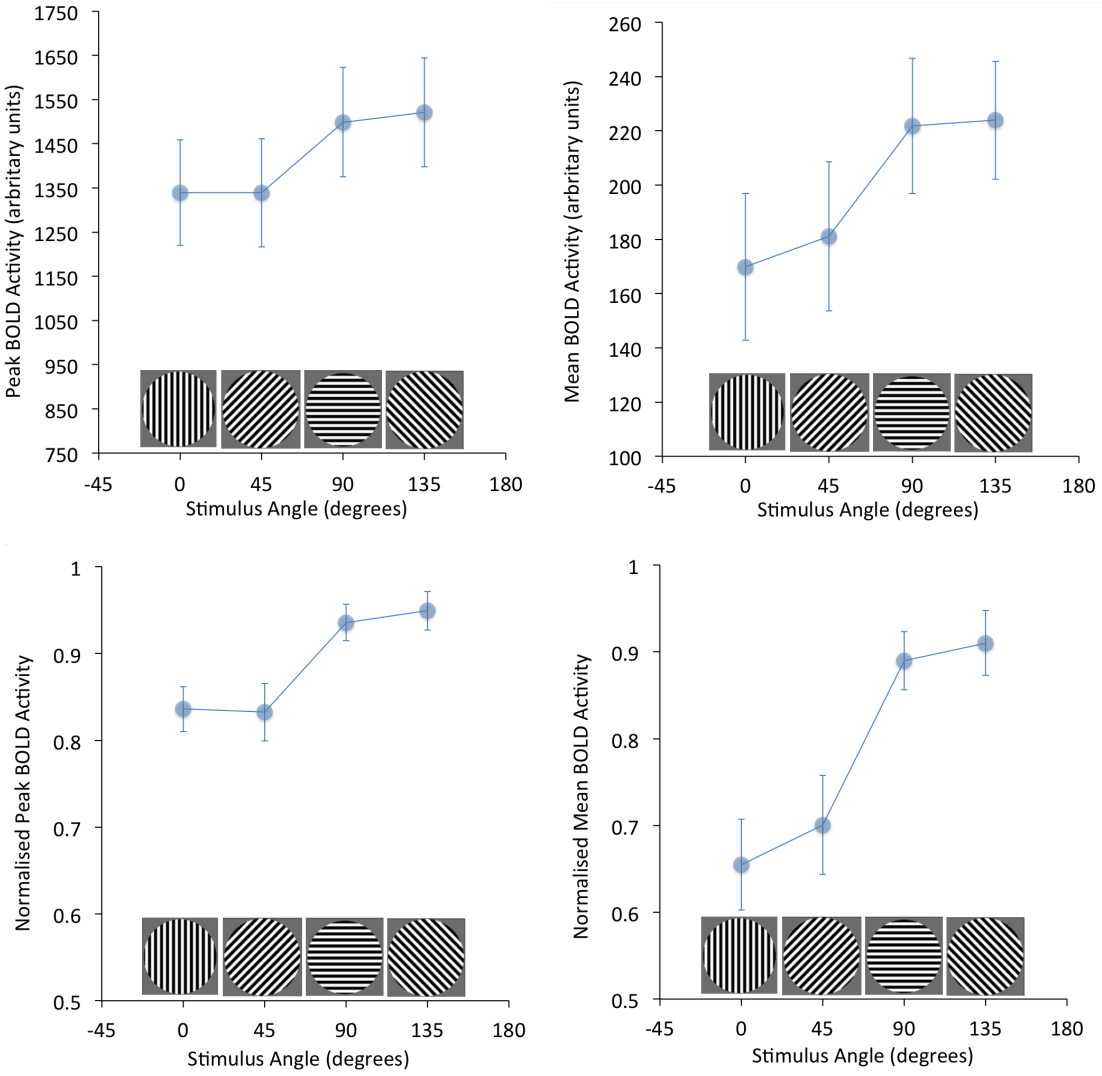

Figure 15: Tuning graphs for the whole occipital ROI, averaged across all participants. Top row is the raw amplitude values, lower row are for normalized

amplitude estimates. Error bars are S.E. on the mean. There is a clear preference for 90 and 135 degrees.

For each condition (0, 45, 90 and 135 degree angle grating) the average activation of the stimulated hemisphere of the 14 participants was contrasted to the opposite hemisphere (which was used as a baseline) using a paired sample t-test. For 0 degrees the activated lobe was significantly different from activation in the opposite (baseline) lobe (t=8.549, a=0,000), as also for 45 degrees (t=7.775, a=0.000), for 90 degrees (t=7.19, a=0.000) and for 135 degrees (t=6.801, a=0.000). T-tests were performed for the averages and maximum values of all participants and also for normalized averages and maximum values (see table below).

Table 1: The p values of all possible contrasts of all participant's peak response, averaged response and normalized peak/averages of the stimulated hemi field (uncorrected for multiple comparisons).

ROI Analysis of occipital lobe. P values of contrasts.

Contrasts / value	0 vs. 45	0 vs. 90	0 vs. 135	45 vs. 90	45 vs. 135	90 vs. 135
Maximum	0.995	0.011	0.003	0.034	0.002	0.711
Norm Max	0.934	0.013	0.002	0.024	0.005	0.730
Mean	0.458	0.005	0.003	0.044	0.012	0.894
Norm mean	0.443	0.003	0.001	0.018	0.006	0.746

2.3.3 ROI Analysis: Individual V1.

Figure 16 shows the same tuning profiles as for Figure **15**, but for an ROI restricted to each person's individual primary visual cortex (V1).

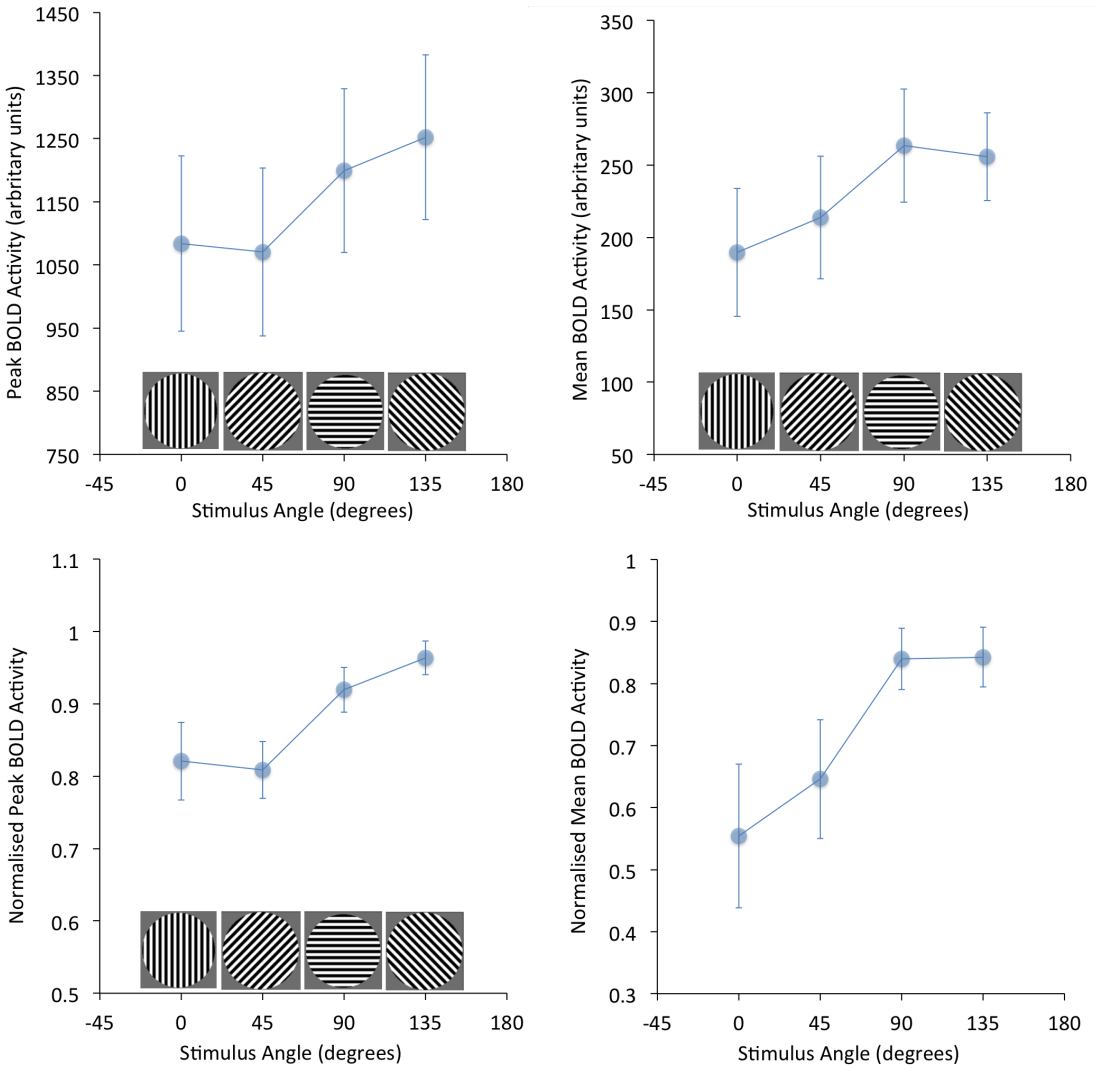

Figure 16: Tuning graphs for the V1 ROI, averaged across all participants. Top row is the raw amplitude values, lower row are for normalized amplitude estimates. Error bars are S.E. on the mean. There is a clear preference for 90 and 135 degrees.

In order to explicitly test for oblique/inverse-oblique effects in the ROI values in the stimulated V1 ROI, a Friedman test was performed separately for the mean

activation values, the maximum values, the sum of the oblique (45 and 135 degrees) maximums, the sum of the cardinal maximums and finally the sum of the oblique averages (in the stimulated lobe V1) and the sum of their cardinal averages. The results of these Friedman tests are displayed in Table 2.

Table 2: The results of the Friedman tests for the average activation for each participant in area V1 (AV right) in each condition, the maximum values for every participant in area V1 for each condition, the sum of the oblique (45 and 135 degrees) maximums for each participant and the sum of cardinal maximums and finally the sum of the oblique averages and the cardinal averages for each participant.

AV right	**X^2 (3) = 6.943, p = 0.074**
Max values	**X^2 (3) = 13.114, p = 0.004**
Max obliques / cardinals	**X^2 (1) = 0.286, p = 0.593**
Averages obliques / cardinals	**X^2 (1) = 0.286, p = 0.593**

As significance was found for the maximum values, a post-hoc analysis was performed for the four contrasts for the max values. As there were 6 contrasts the a-level was set at 0.05/6 = 0.0083. The Wilkcoxon Signed Ranks test results are shown in Table **3**.

Table 3: As the maximum values in area V1 for each condition gave significance in the Friedman test they were later post-hoc analyzed with a Wilcoxon Signed Ranks test to check which conditions had a significant difference (with a Bonferroni correction of 0.05 / 6 = 0.0083.

Wilcoxon Signed Ranks Test

	Max value 45 - 0	Max value 90 - 0	Max value 135 - 0	Max value 90 -45	Max value 135 - 45	Max value 135 - 90
Z	-0.534[a]	-1.475[b]	-2.668[b]	-2.417[b]	-3.233[b]	-1.224[b]
Asympt. Sig (2-tailed).	0.594	0.140	0.008	0.016	0.001	0.221

a: Based on positive ranks.
b: Based on negative ranks.

From the Wilcoxon Signed Ranks test, significant results were found (at a level of significance 0.0083) for the contrasts 135 to 0 and 135 to 45.

So, to summarize, the maximum values in area V1 for each condition had a statistically significant difference $X^2(3) = 13.114$, p= 0.004. Post hoc analysis with a Wilcoxon signed-rank tests was conducted using Bonferroni correction (resulting in a significance level set at $p < 0.0083$). The contrasts 135 to 0 (z = - 2.668, p=0.008) and 135 to 45 (z = - 3.233, p=0.001) were significant. The medians of the max values of each participant were, for the 0 degrees condition 1052.62, for 45 degrees 1002.77, for 90 degrees 1116.73 and for 135 degrees 1148.49.

2.4 Discussion.

The results of this experiment are summarized in the table below:

Table 4: Summary of the results found. The first row shows a description of the effects found with an FSL whole-brain analysis, the second row is for the ROI analysis in which the mean activation for each of the 4 conditions (for every participant) was extracted from the entire occipital lobe (only the stimulated hemisphere was used for the contrasts). The final row shows the results for the analysis performed in area V1 (stimulated lobe) contrasting the maximum values of all four conditions (14 participants).

Stage of Analysis.	Medians or means	Contrasts	
Whole brain analysis.		0-45	Not strong
		0-90	Not strong
		0-135	**Inverse**
		45-90	**Oblique**
		45-135	**Strong**
		90-135	Not strong
Occipital lobe analysis.	Means: 0 < 45 < 90 < 135.	0-45	P=0.458
		0-90	P=0.005
		0-135	P=0.003
		45-90	P=0.044
		45-135	P=0.012
		90-135	P=0.894
V1-region only.	Based on Medians of Maximum values: 45 < 0 < 90 < 135.	0-45	P=0.594
		0-90	P=0.140
		0-135	P=0.008
		45-90	P=0.016
		45-135	P=0.001
		90-135	P=0.221

The prior literature on the oblique effect using fMRI seems to be contradictory as in some cases an oblique effect has been reported (Furmanski & Engel , 2000) however other studies report the inverse oblique effect (Mannion, McDonald, & Clifford, 2010). The study we present here contributes to this debate by demonstrating clear preferences for an inverse oblique effect in the magnitude of the BOLD response (see Figure **15** and **Figure 16**), with the biggest responses being to the tangentially oriented oblique. In the analysis limited to V1 only, we found a statistically significant inverse oblique effect (the 135 degrees

condition median of the max values was greater than the 0 degrees one). An inverse oblique effect with the use of functional MRI has been previously reported by Mannion et al. (Mannion, McDonald, & Clifford, 2010), however in their study Mannion et al report that although the lowest response was found for horizontal gratings, an intermediate response was found for vertical ones and the highest response was found for oblique gratings. However, if orientation was viewed relative to angular position in the visual field then the greatest response was found for gratings parallel to the visual field meridian. The results presented here demonstrate that the median of the 135 degrees grating condition was greater than 0 degrees (vertical grating). The 135 (oblique) orientation is however not radial to fixation but tangential and therefore this inverse oblique effect cannot be attributed to a radial bias. Additionally as a patch grating was used in this study, center surround effects present in the visual stimulus of Mannion et al's (Mannion, McDonald, & Clifford, 2010) experiment would not be present here.

Although it has been reported that MRI and MEG may show activity in reflect different aspects of neuronal activity (Muthukumaraswamy & Singh, 2008) here, using the same stimulus dimensions used n Koelewijn et al.' s MEG study (Koelewijn, Dumont, Muthukumaraswamy, Rich, & Singh, 2011) we demonstrate the same inverse oblique effect using fMRI in V1, including the same strong response to a tangential oblique. Thus we have a somewhat converging story between our fMRI and prior MEG findings.

A question arising from the findings in this study is why the tangential response was greater than the radial one in both the occipital and the V1 region analyses (the 135 degrees condition was greater than the 45 degrees median

with their difference being significant) when there is literature suggesting that it is the radial orientations that are favored (Bennett & Banks, 1991), (Berardi & Fiorentini, 1991), (Fahle, 1986), (Rovamo, Virsu, laurinen, & Hyvarinen, 1982), (Temme, Malcus, & Noell, 1985). In an fMRI study by Mannion et al (Mannion, McDonald, & Clifford, 2010) Glass patterns were used i.e. images composed of randomly positioned pairs of dots (dipoles) with a spatial arrangement to produce the percept of translational or polar global form. In Figure **17** we can see that when orientations were viewed as meridian-relative (orientations specified relative to the local visual field meridian) for translational Glass pattern they found a uni-modal profile of anisotropy in the V1 BOLD response, with a peak response for radial orientations. However when they defined them within a polar glass pattern, V1's profile of anisotropy was bimodal peaking both at the radial and tangential orientations. Additionally in Figure **17** we see that the BOLD response to the tangential orientation is slightly greater than to the radial orientation in V1 (when defined within a polar glass pattern). Rovamo et al report that at eccentricities larger than 20 degrees, the oblique effect was substituted by an effect where the limitation of visual resolution was best for gratings that were meridionally oriented and worst for gratings perpendicular to the visual field meridians (Rovamo, Virsu, laurinen, & Hyvarinen, 1982). It could be that the radial bias has not taken effect for the eccentricity used in our study and that is why we found the tangential response to be greater than the radial one.

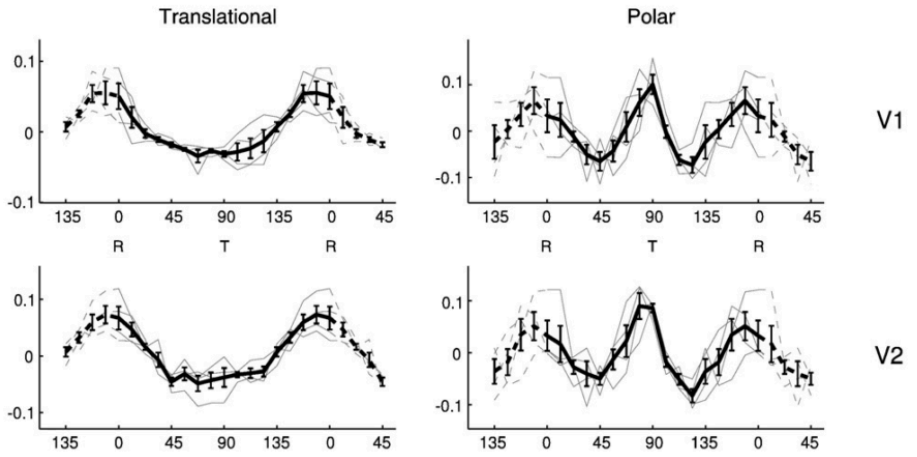

Figure 17: Figure taken from Mannion et al.'s study **(Mannion, McDonald, & Clifford, 2010)** in which they illustrate the modulation of the BOLD response in V1 and V2 to meridian-relative orientations defined within translational (left) and polar (right) Glass patterns, with 0° being radial and 90° being tangential. In the plots the mean over subjects±SEM is the thick black line.

One limitation of this study is that we did not use eye tracking to check participant's fixation. In a study on the oblique effect by Berkley et al (Berkley, Kitterle, & Watkins, 1974) in the periphery of the visual field using gratings at 0 up to 16 and 20 degrees from the fixation point (using stimuli at cardinal or oblique orientations they report (Berkley, Kitterle, & Watkins, 1974) that fixating at eccentric targets could be difficult to accomplish and at eccentricities of 2 to 4 degrees this difficulty is more profound (Berkley, Kitterle, & Watkins, 1974). As our stimulus was placed at a 2.2 degrees distance from fixation the problem mentioned by Berkley et al could potentially affect our study.

Another limitation in this study is the fact that as MRI was used we are unable to investigate the timing of the inverse oblique effect that Koelewijn et al. report (Koelewijn, Dumont, Muthukumaraswamy, Rich, & Singh, 2011). In their study Koelewijn et al report that the "inverse oblique effect" was found in the earliest (80 ms) evoked response, while the later responses (120 ms) showed a "classic", oblique response.

An interesting experiment would be to replicate this study with 2 different stimulus presentation times (one very short and one very long) and then check if both give the same results as this experiment when contrasting (in an analysis limited to V1 region only) the 135 degrees condition to the 0 degrees. Perhaps, as the initial inverse oblique effect reported by Koelewijn et al. was found at 80 msec, it could be that with brief stimulus presentations in fMRI experiments the later classical oblique effect does not have time to build up in the haemodynamic response.

In the Koelewijn et al study the extrastriate cortex was reported playing a role in the oblique effect (Koelewijn, Dumont, Muthukumaraswamy, Rich, & Singh, 2011) as they report that the classic behavioral oblique effect is mediated by the extrastriate cortex and also may involve feedback from the extrastriate to the primary visual cortex. On the other hand Furmanski et al. did not succeed in finding a reliable oblique effect outside of V1 (Furmanski & Engel , 2000). Similarly in the study presented here, no reliable activations were observed in extrastriate cortex. It may be that this reflects a lack of signal-to-noise due to too few trials per condition. This would also explain a lack of statistically significant activations in the whole-brain FSL analysis.

Here we used four conditions and it could be that by focusing on only two conditions, one cardinal and one oblique (selecting the tangential orientation to avoid the confound of the radial bias) we would get more trials for each condition and enhance the statistical power in the FSL analysis, to detect both V1 and extra-striate effects.

The fact that tangential stimuli were favored in our study also provides some evidence that at the eccentricity used in this paper the radial bias was not

yet present as Rovamo et al reports that the oblique effect after a certain eccentricity is replaced by a radial bias (Rovamo, Virsu, laurinen, & Hyvarinen, 1982), although this was not an issue in Koelewijn's paper as the oblique grating they used was tangential (no patch grating in Koelewijn paper was radial to fixation). The reason we used four orientations was to check if the radial orientation was preferred to the tangential one however as the radial bias was not evident at this eccentricity a repetition with only two angles (tangential-cardinal) would represent a reasonable and efficient experimental design..

Finally, one possible explanation for the convergent fMRI and MEG findings of bigger responses to oblique stimuli may relate to the tuning widths of cells. It may be that we are poor at oblique orientations because the orientation tuning widths for oblique cells are wider (Li, Peterson, & Freeman, 2003) and that this would also mean that more cells are stimulated by oblique stimuli, leading to both a higher BOLD response and a stronger visual gamma response as measured with MEG.

3 Experimenal chapter 2

3.1 Introduction.

The oblique effect, the orientation selectivity property of the visual cortex has been studied extensively both psychophysically (Appelle S. , 1972) and with imaging methods (Koelewijn, Dumont, Muthukumaraswamy, Rich, & Singh, 2011) (Mannion, McDonald, & Clifford, 2010). In a recent study by Edden et al. (Edden, Muthukumaraswamy, Freeman, & Singh, 2009) psychophysical and imaging methods were combined to look into the underlying neurophysiological mechanisms of a behavioral oblique effect, the enhanced detection ability of the visual system for orientation differences occurring around a cardinal axis compared to an oblique one. Orientation detection thresholds were found being significantly negatively correlated with visual cortex GABA concentration for obliquely oriented patterns but not for vertically oriented ones (Edden, Muthukumaraswamy, Freeman, & Singh, 2009). Additionally, the thresholds for obliquely oriented stimuli were found negatively correlated with gamma oscillation frequency, however again thresholds for vertical orientations were not correlated to gamma activity. In this study, although a behavioral oblique effect was studied in correlation to GABA and gamma, they did not measure gamma frequency activity while people where performing the orientation discrimination task but instead used the frequency of response to the same grating stimulus as a trait measure of the excitation/inhibition balance in the visual cortex. Edden et al.'s study is of particular interest as it links information about performance at a visual task with GABA and gamma, however in this study behavioral measures were acquired with a centrally presented grating, whilst

the MEG experiment was performed with a non-central stimulus.

Koelewijn et al. (Koelewijn, Dumont, Muthukumaraswamy, Rich, & Singh, 2011) used the high temporal resolution of MEG to detect an early inverse oblique effect (in the medial visual cortex), a finding that can also be found with certain experimental designs with fMRI (as demonstrated in the first experimental chapter of this thesis). As the inverse oblique effects was detected in the periphery it is important to probe further into psychophysical preferences at the eccentricity used by Koelewijn et al. and my first fMRI chapter and establish the oblique effect is present at these eccentricities (especially as the oblique effect may be confounded by a radial bias as discussed later).

Peripheral vision plays an important role in many aspects of our daily experience of the world such as motion perception (Brandt, Dichgans, & Koenig, 1973) and body stabilization (Bessou, Cauquil, Dupui, & Montoya, 1999), consequently the oblique effect has also been studied both in central and peripheral vision. Human lesion studies have shown a retinotopic organization of area V1 of the occipital cortex (Holmes, 1918) and each position of the visual field has a corresponding well-defined region in area V1, forming a retinotopic map where neighborhood relations are kept (Davey & Zanker, 1998). The number of neural elements responsible for one degree of visual field and its corresponding distance in the retinotopic maps varies from the fovea to the periphery ('M-scaling' or 'cortical magnification') (Davey & Zanker, 1998). This cortical magnification has been demonstrated with psychophysical measures that decrease with eccentricity (Rovamo, Virsu, & Nasanen, 1978). A possible neurobiological basis for the preference to oblique orientations has a link to the

finding that in V1 more neural apparatus is allocated to cardinal orientations compared to oblique ones (Xu, Collins, Khaytin, Kaas, & Casagrande, 2006). Additionally, in extrastriate cortex Xu et al. (Xu, Collins, Khaytin, Kaas, & Casagrande, 2006) found that more MT was dedicated to represent cardinal rather than oblique orientations and that the cardinal / oblique anisotropy was more conspicuous in MT parts corresponding to central vision (≤10°). As reported by Koelewijn et al. (Koelewijn, Dumont, Muthukumaraswamy, Rich, & Singh, 2011) feedback processes take place from the extrastriate to the primary visual cortex and (although MEG spatial resolution does not accurate localization of the extrastriate location they found) it could be that feedback from the extrastriate to the striate differs depending on stimulus orientation because of anisotropies in the cortical surface sensitive to each orientation.

The oblique effect in the periphery

The oblique effect has been studied both in the center and the periphery of the visual field. Berkley et al. (Berkley, Kitterle, & Watkins, 1974), report that the limitation of the oblique effect to central vision can be seen in a study by Campbell and Levinson (Cambell, Kulikowski, & Levinson, 1966), in which they studied the visibility of target gratings as a function of orientation. Here it was found that the oblique effect disappeared or nearly disappeared at spatial frequencies below 8 cycles per degree which Berkley et al. (Berkley, Kitterle, & Watkins, 1974) believe suggests that orientation preference is primarily related to neuronal channels dedicated to processing fine details, which are primarily found in the central visual field. To further study the oblique effect in the periphery Berkley et al. used gratings at 0, 2, 4, 6, 8, 12, 16 and 20 degrees from fixation using stimuli at oblique or cardinal orientations. Berkley et al. (Berkley,

Kitterle, & Watkins, 1974) found a better acuity for cardinal gratings than oblique ones, however with eccentric viewing (Berkley, Kitterle, & Watkins, 1974) this difference disappeared (see Figure **18**) and the eccentricity the oblique effect disappeared varied between subjects from 8 to 18 degrees (Berkley, Kitterle, & Watkins, 1974). A methodological problem with studies using peripheral vision is that maintaining fixation when stimuli are presented peripherally can be hard and furthermore at eccentricities of 2 to 4 degrees this difficulty was more profound (Berkley, Kitterle, & Watkins, 1974).

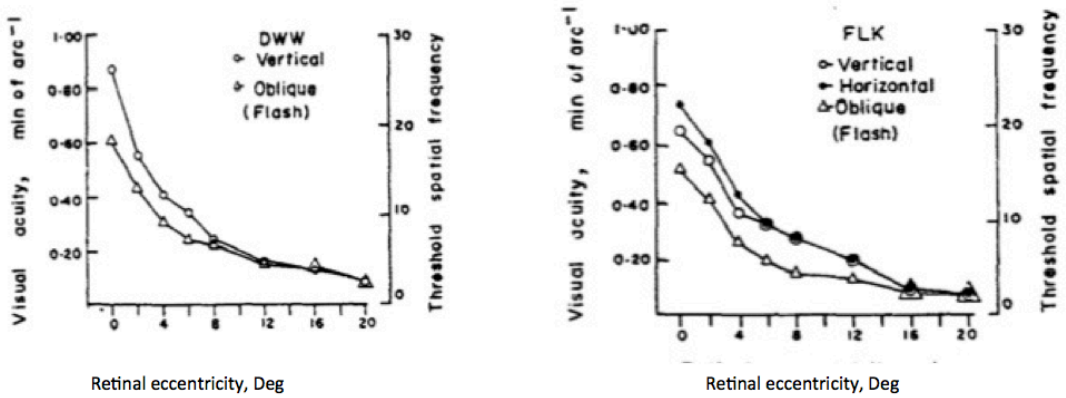

Figure 18: A graph taken from Berkley et al. paper (Berkley, Kitterle, & Watkins, 1974) where we see how visual acuity changes as a function of retinal eccentricity for participant DWW (left) and FLK (right). For DWW the oblique effect disappears at approximately 8 degrees eccentricity while for FLK it disappears at 16 degrees.

Berkley et al.'s findings are supported by Rovamo et al. **(Rovamo, Virsu, laurinen, & Hyvarinen, 1982)** as they report that the oblique effect seems to disappear at eccentricities of 8 to 18 degrees from point of fixation.

The radial bias

In addition to the oblique effect, studies in peripheral vision have also confirmed a radial bias (i.e. a favoring of stimuli oriented collinearly with a line that intersects the center of fixation irrespective of whether it is cardinal or

oblique). This radial bias has been studied extensively in the past with human psychophysics (Bennett & Banks, 1991), (Berardi & Fiorentini, 1991), (Fahle, 1986), (Rovamo, Virsu, laurinen, & Hyvarinen, 1982) (Temme, Malcus, & Noell, 1985). Moving to the periphery, this radial bias may be stronger than the oblique effect as Rovamo et al, report that at eccentricities larger than 20 degrees, the oblique effect was substituted by a meridional effect, where the visual resolution limit was best for gratings that were meridionally oriented and worst for gratings that were perpendicular to the visual field meridians (Rovamo, Virsu, laurinen, & Hyvarinen, 1982).

Edden et al studied the oblique effect by using a central stimulus (Edden, Muthukumaraswamy, Freeman, & Singh, 2009) to find the thresholds for an orientation discrimination task for cardinal and oblique angles. In the current study we will be looking into these discrimination thresholds however by using a peripheral stimulus. As a radial bias is know to occur peripherally, it is interesting to see whether, at a peripheral location, performance in a discrimination task is determined by the oblique effect or a radial bias.

Although we will use modest eccentricities (2.2 degrees above and below foveal fixation) and hence we do not expect the radial bias to dominate, or the oblique effect to be abolished, it is important that we establish whether the 'classic' oblique effect occurs at these eccentricities, as they are commonly used in fMRI and MEG studies, including work presented in this thesis. This will greatly aid in interpreting some surprising findings in the imaging literature, such as the inverse-oblique effects demonstrated in previous MEG (Koelewijn, Dumont, Muthukumaraswamy, Rich, & Singh, 2011) and fMRI (second chapter) studies.

In order to monitor fixation control for these peripheral stimuli, eye tracking was used. A staircase procedure was used as in Edden et al (Edden, Muthukumaraswamy, Freeman, & Singh, 2009). Additionally here we use a patch grating thus avoiding the center surround effects potentially confounding Mannion et al.'s experiment (Mannion, McDonald, & Clifford, 2010). A radial effect (greater BOLD response for gratings radially oriented) was reported by Mannion (Mannion, McDonald, & Clifford, 2010) and in this study we will be presenting 4 grating orientations centered 2.2 degrees horizontally from central fixation (to the left of the screen) and also vertically both in the top and bottom left quadrant. With this design, for oblique orientations, when the upper grating is oriented radial to fixation the lower grating (of the same orientation in relation to the horizon) will be oriented tangentially and vice versa. By contrasting, for example, 135 degrees angles in upper and lower quadrant we can see if they are significantly different and if performance at radial orientations is better (as both top and bottom 135 degree gratings have the same orientation in relation to the horizon but only one of them is radial).

Finally, as Edden et al. (Edden, Muthukumaraswamy, Freeman, & Singh, 2009) reported a significant training effect for the oblique task but not for the cardinal one, we will also test for this training effect using a peripheral stimuli at multiple orientations, using two experimental sessions.

3.2 Methods

Twelve healthy right-handed male and female participants were recruited with normal or corrected to normal vision. One participant's data was excluded

from the analysis as performance in the discrimination tasks in all of the conditions was approximately ten times higher than the rest of the participants while another participant felt nausea from the stimulus and had to stop before completing the experiment.

Additionally, another three participants were excluded as their performance value found was an outliar (they had very bad performace) in at least one of the blocks compared to their other blocks. The final cohort therefore consisted of 7 volunteers. In some of the training effects analysis an additional 3 participants were removed (see results section for details). However poor performance of these participants at the second experimental session was attributed to tiredness and therefore their data was included in the other statistical tests. All people that participated in this study were required to sign informed consent forms. Finally all the procedures were approved by the School of Psychology's Ethics Committee at Cardiff University.

The stimulus consisted of a stationary black/white sine-wave circular grating patch (maximum-contrast, 3 cycle/degree and a diameter 4.3°) displayed in the lower left quadrant of a mean luminance grey background display and was centered 2.2° both horizontally and vertically from a continuously present fixation dot. The stimulus has the same dimensions as the stimulus that was used in the MEG study by Koelewijn et al (Koelewijn, Dumont, Muthukumaraswamy, Rich, & Singh, 2011) and the stimulus used in the first experimental chapter of this thesis (fMRI study). The stimulus orientation was displayed at 0, 45, 90 and 135 degrees. The gray background extended 4.5 degrees from the center of the grating in all directions forming a circle with 9 degrees of visual angle diameter (Figure **19**) while the rest of the screen was black. In the upper left conditions

the grating was displayed in the upper left quadrant of a mean luminance grey background display and was centered 2.2° both up horizontally and vertically from a continuously present fixation dot (with the other stimulus parameters staying the same).

Orientation discrimination thresholds were measured with the use of a two-alternative forced choice procedure. The orientation difference between the gratings was adjusted, using a two interleaved one-up two- down staircases adjusted logarithmically until converging on 71% correct performance (Figure **20**).

The display screen was a Sony Trinitron G400 CRT monitor with ATI RADEONX1600 Pro graphics card. Participants were seated at a 57cm distance from the monitor while a chin rest was used to stabilize the head. The room was completely dark, and a circular aperture was placed over the screen in order to remove all external orientation clues, such as those from the edges of the screen. Neutral density film (3 X 0.6) covered the screen in order to cover the two very thin grey lines (horizontal) visible due to the presence of screen damper wires. An Eyelink 1000 eye tracker recorded eye movements with a sampling rate of 1000 Hz.

On every trial, two circular gratings (contrast 80%; mean luminance 44.5 cd/m2) were displayed sequentially, each for 250 ms, with inter-presentation time chosen randomly from 500–700 ms, while at beginning of each trial fixation alone was presented for 500 ms.

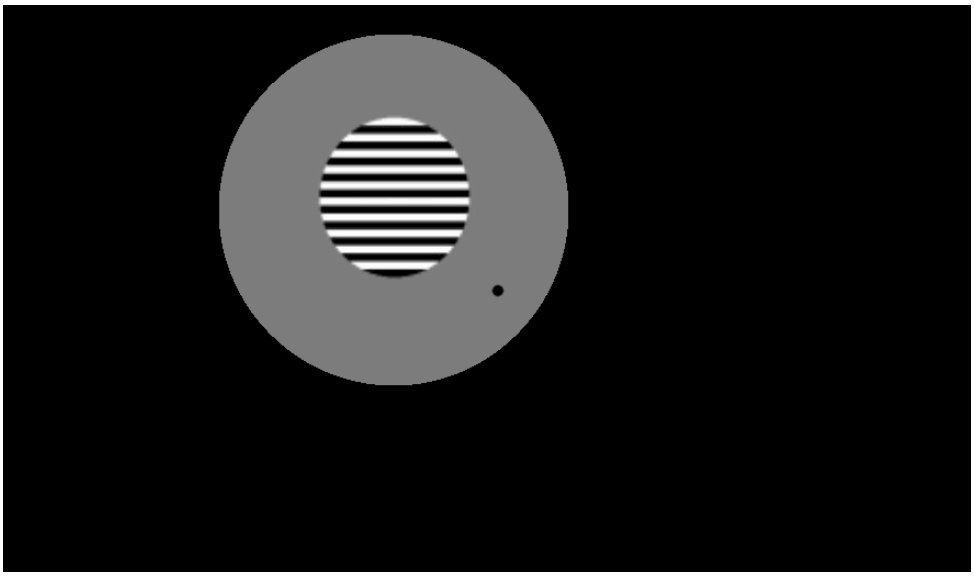

Figure 19: An image of the grating presented at the upper left quadrant of the visual field.

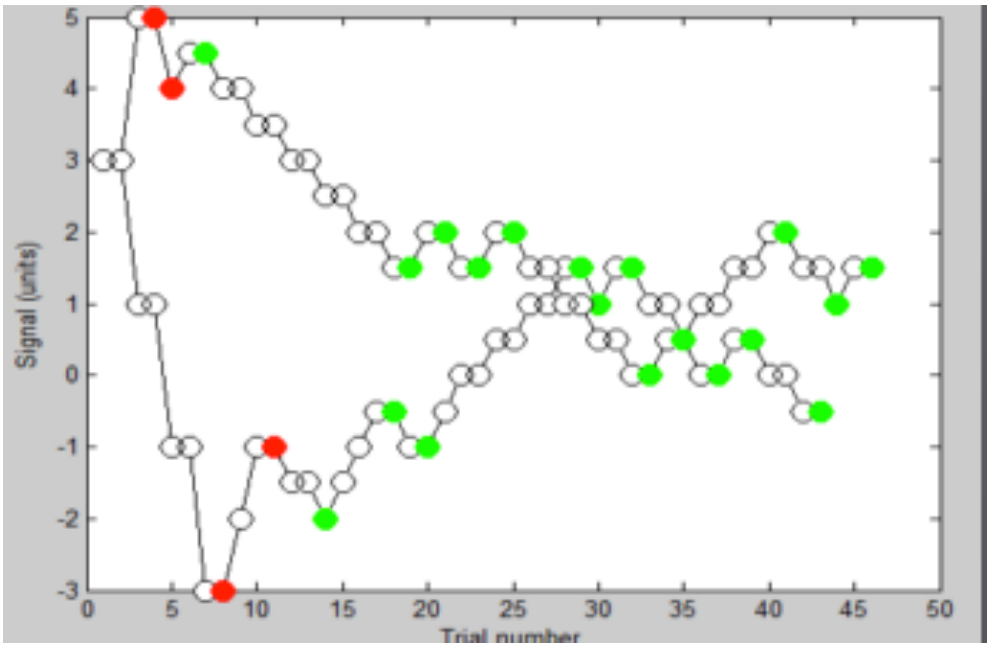

Figure 20: Staircase example for the lower 135 degrees showing the two interleaved staircases. Filed dots represent turning points in the staircase.

Subjects were asked to judge whether the second grating rotated clockwise or counter clockwise in relation to the first. Responses were made using the

buttons on a computer mouse and an auditory tone feedback was given on each trial while also a green fixation after each trial indicated correct response.

Each run consisted of a block of 0, 45, 90 or 135 degrees trials. Each block continued until both staircases completed 12 reversals, usually lasting approximately 4 min. The first two reversals of each staircase were discarded before calculating the threshold in degrees by taking the mean over the last 10 and then averaging the thresholds from the two staircases. Every subject was presented four sets, with four blocks in each set (all four orientations were presented once in a set in a random order). The first two sets were shown in the upper left quadrant and the next two sets in the lower quadrant or the first two sets would be displayed in the lower left quadrant and the next two sets in the upper quadrant. The initial position for each participant was chosen randomly thus the initial position would be either bottom or top. In between every block the subjects had a one-minute break.

In this chapter 0 degrees is vertical, 90 degrees is horizontal, while top 45 and bottom 135 are radial to fixation and top 135 and bottom 45 are tangential to fixation.

3.3 Results.

This experiment was designed to address three main points: 1) is there an oblique effect during the behavioural task (both when the grating is displayed at the lower left quadrant of the visual field and the upper quadrant), 2) is there a radial bias (by contrasting same grating orientations in the upper and the lower quadrant since one would be radial the other tangential) and finally are there

training effects as in the previous study by Edden et al. (Edden, Muthukumaraswamy, Freeman, & Singh, 2009).

All subjects participated in eight different conditions with the grating patch being displayed at orientations of 0, 45, 90 and 135 degrees both in the lower left and the upper left quadrants of the screen. We also wanted to look into the training effect so we repeated every condition a second time therefore each subject was tested for 16 conditions in total. Then, for every subject, the orientation discrimination threshold was calculated from the average of the two staircases used in each of the 16 conditions. These averages can be seen in Figure **21**.

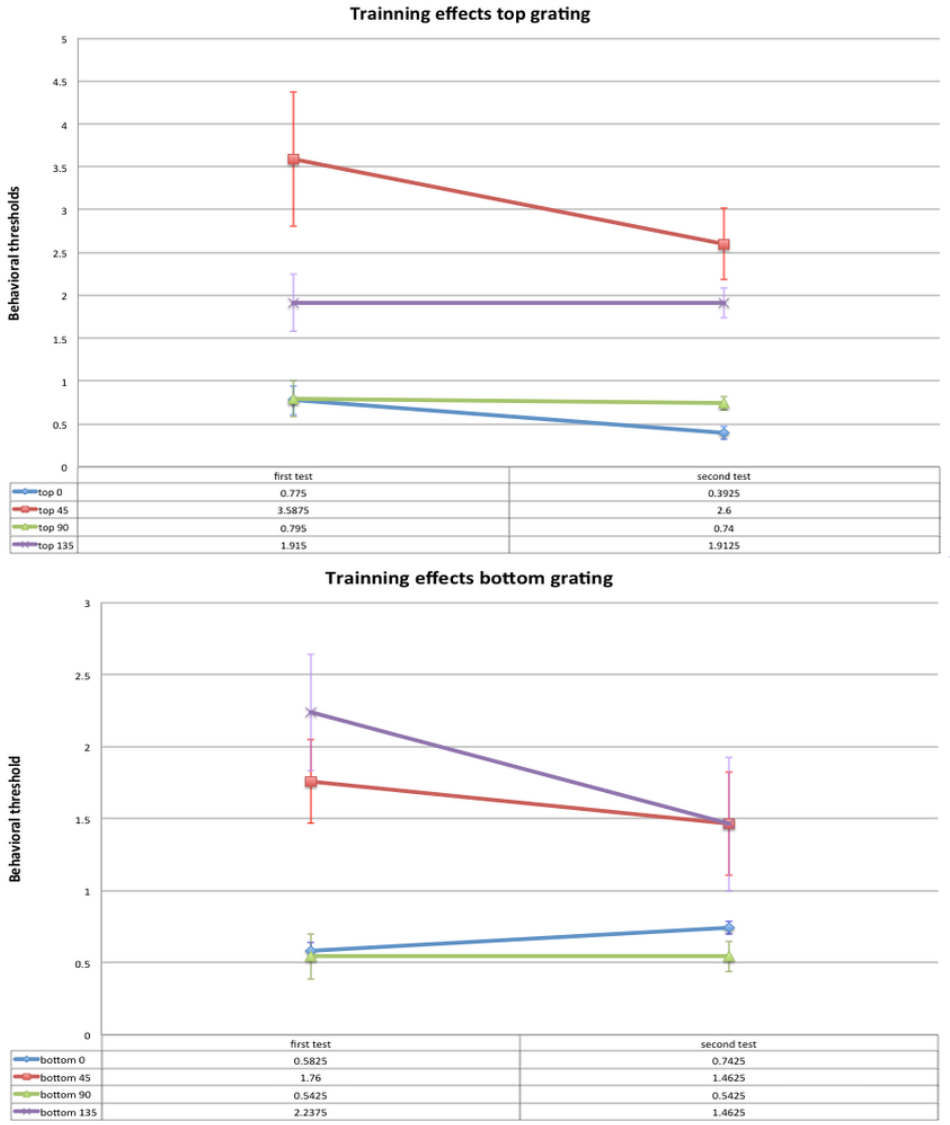

Figure 21: First and second trials of all four tested orientations (blue is 0 degrees, red for 45, green for 90 and purple for 135). Top figure for top presented grating and bottom plot for bottom presented grating. As there were outliers for second bottom grating trials and second top 45, averages are presented after these 3 outlier participants were removed from all trials in these plots (leaving 4 participants in these averages).

In general, Figure **21** demonstrates that the largest thresholds (i.e. poorest discrimination performance) occurs for the oblique stimuli at both top and bottom positions, suggesting that the classic oblique effect dominates.

To test for the oblique effect in both the lower and upper left quadrants of the visual field paired t-tests were performed between pairs of conditions. These t-tests are presented in the table below:

Table 5: Table presenting the t-tests performed to examine the oblique effect.

Tests for oblique effect	
CONTRAST	**Statistical testing**
Bottom 0 - bottom 45	T(6) = -4.237, p=0.05
Bottom 0 - bottom 90	NOT SIGNIFICANT
Bottom 0 - bottom 135	T(6) = -5.428, p=0.002
Bottom 45 - bottom 90	T(6) = 4.626, p = 0.004
Bottom 45 - bottom 135	NOT SIGNIFICANT
Bottom 90 - bottom 135	T(6) = -5.607, p = 0.001
Top 0 – top 45	T(6) = -4.203, p = 0.006
Top 0 – top 90	NOT SIGNIFICANT
Top 0 – top 135	T(6) = -3.913, p = 0.008
Top 45 – top 90	T(6) = 4.435, p = 0.004
Top 45 – top 135	NOT SIGNIFICANT
Top 90 – top 135	T(6) = -4.093, p = 0.006

Also, we tested for training effects at specific orientations (0, 45, 90, 135) and positions (up or down) by comparing the first and second block with same grating patch orientation and position (up or down). Here, as the normality assumption was violated (for all the second bottom trials and the second top 45), non parametric testing was used (Wilcoxon Signed rank test) for first to second trial contrasts (for the cases with second trials with the normality assumption violation). In order to deal with outliers (bad performance) we removed 3 more participants from this part of the analysis (for the non parametric testing) leaving 4 participants. These participants were kept in the other parts of the analysis as bad performance was attributed to tiredness of the participants during the second trials. For the second trials where normality and outlier assumptions were not violated, t-tests were used (with 7 participants) so top 0 to second top 0, top 90 to second top 90 and top 135 to second top 135. The only contrast, however, that gave significant results was for the 0 degrees grating patch in the upper left quadrant with t (6) = 2.808, p=0.031 (the average of the

staircases for the first block being 0.875 degrees and for the second being 0.563 degrees).

Additionally, to examine if there is a preference for radial orientations we also contrasted the bottom 45 condition with the upper 45 condition (the upper 45 being radial), the lower 135 (radial) with the upper 135 (tangential), the lower 45 with the upper 135 and the lower 135 with the upper 45. None of these contrasts, however, were significant.

All pairs of t-tests are included in Appendix 1.

3.4 Discussion.

In this chapter the main goal was to examine the behavioral oblique effect found by Edden et al. (Edden, Muthukumaraswamy, Freeman, & Singh, 2009) but in the periphery of the visual field, to see if we can find evidence for a behavioral radial bias with a patch grating centered 2.2 degrees down or up and 2.2 degrees left from the center of fixation and finally if we can detect any training effects. The findings with $p \leq 0.05$ of this project are summarized in the table below (note however that a total of 24 pairs were tested and a Bonferroni correction is $p = \frac{0.05}{24} = 0.002$).

Table 6: The contrasts of this experiment with a p value 0.05 or lower. The conditions contrasted are 0, 45, 90, 135 degrees with the grating presented in the Bottom or the to quadrant of the screen. In the last row top 0 2nd top 0) are the averages for the 1st and 2nd block with the grating in the top quadrant and at 0 degrees (vertical) orientation. In parenthesis vert = vertical, horiz. = horizontal, Tang. = tangential and rad. = radial.

condition	**Mean values (thresholds in degrees).**	**statistic**	**P value**
Bottom 0-45 (vert.-tang.)	Bottom0 = 0.9 Bottom45 = 2.4	T(6)= - 4.237	0.05
Bottom 0-135 (vert-rad)	Bottom0 = 0.9 Bottom135 = 2.8	T(6)= - 5.428	0.002
Bottom 45-90 (Tang.-horiz.)	Bottom45 = 2.4 Bottom90 = 0.8	T(6)= 4.626	0.004
Bottom 90-135 (horiz.-rad.)	Bottom90 = 0.8 Bottom135 = 2.8	T(6)= - 5.607	0.001
Top 0-45 (vert.-rad.)	Top0 = 0.9 Top45 = 3.4	T(6)= - 4.203	0.006
Top 0-135 (vert.-tang)	Top0 = 0.9 Top135 = 2.8	T(6)= - 3.913	0.008
Top 45-90 (rad.-horiz.)	Top45 = 3.4 Top90 = 0.8	T(6)= 4.435	0.004
Top 90-135 (horiz.-tang.)	Top90 = 0.8 Top135 = 2.8	T(6)= -4.093	0.006
Top 0 2nd top 0 (vert.-vert.)	Top = 0.9 2nd Top = 0.6	T(6)= 2.808	0.031

From the results we see that all the contrasts of cardinal to oblique gratings conditions gave an oblique effect and this peripheral behavioral oblique effect is in accordance with Edden et al. (Edden, Muthukumaraswamy, Freeman, & Singh, 2009) where they also report that their centrally presented grating gave a strong oblique effect (the oblique orientation mean angular discrimination thresholds in their study were reported five times higher than those for vertical oriented gratings). In this experiment we also examined if there is a radial bias by contrasting the conditions bottom 45 to top 45 and top 135 to bottom 135 (with the top 45 degrees and bottom 135 degrees gratings being radial to fixation and the bottom 45 degrees and top 135 degrees gratings being tangential) however none of these contrasts were significant. From the previous table we notice that the radial bottom 135 and the top 45 conditions gave $p \leq 0.05$ results when contrasting bottom 135 to 0 and bottom 135 to 90 and also top 45 to 0 and 45 to 90 degrees. In this case however although 0 and 90 (cardinal) degrees are not radial gratings they have better average discrimination thresholds (lower) from the radial oblique conditions, this however could merely be that the oblique effect is stronger than the radial bias. The last question under investigation was the existence of training effects and here we did find a difference with $p \leq 0.05$ when contrasting the first to second blocks with the grating presented at the top 0 degrees conditions with $T(6) = 2.808$, $p=0.031$ and the average performance showing an improvement in the second block, this test's significance however does not survive the Bonferroni correction ($p=0.002$).

In the first chapter of this thesis a similar patch grating was used as in this experiment's bottom left presented grating and a significant different was found for the tangential to vertical condition. In this chapter we again managed to find

a significant difference between these two conditions when performing a behavioral task, here the p value was 0.05 with no Bonferroni correction used. In the fMRI experiment of this thesis the static patch grating gave a larger BOLD response when contrasting the tangential to vertical grating (with a larger mean for the oblique orientation i.e. an inverse oblique effect) however a similar grating and eccentric presentation in this experiment gave a classic behavioural oblique effect for these two orientations. In examining these two experiments of this thesis we see that an inverse BOLD response is found in V1 while a behavioral task yields a 'classic' oblique effect. Koelewijn et al. (Koelewijn, Dumont, Muthukumaraswamy, Rich, & Singh, 2011) in their study report that, in a medial location, both an inverse oblique effect and a classical oblique effect coexist at different time points, with the later oblique effect being influenced by an extrastriate location. In the fMRI chapter we find an inverse BOLD response while the same patch grating for these same orientations gives a classical behavioral oblique effect in this chapter. In a fMRI experiment by Furmanski and Engel (Furmanski & Engel , 2000) looking at a peripheral stimulus with behavioral measures and fMRI in three participants found a) the classical behavioral oblique effect in a peripheral stimulus b) a similar oblique effect in the BOLD response (while in this thesis an inverse oblique effect was found with fMRI). Koelewijn et al. (Koelewijn, Dumont, Muthukumaraswamy, Rich, & Singh, 2011) discussed Furmanski's findings and explained that the BOLD oblique effect in V1 Furmanski found could be explained by the poor temporal resolution of fMRI which leads to temporal smearing of the early inverse oblique effect with later responses that are bigger for the cardinal orientations, but it is still difficult to reconcile Furmanski's findings with the fMRI results in this thesis. It could be

that certain manipulations of stimulus parameters can reveal the early inverse oblique effect in fMRI. It would be interesting to see if the inverse BOLD signal found for a static patch grating could be replicated if the behavioral task of this study was performed in the MRI scanner, especially since stimulus dimensions in the first experimental chapter (fMRI study) and this chapter (behavioral) were the same. Additionally, replicating this study with fMRI would allow to look further into if there are extrastriate areas present during the behavioral oblique effect as the ones reported by Koelewijn et al. or even extrastriate areas affecting the behavioral oblique effect that are not present when a static grating is presented.

In this chapter a radial effect (better performance at radially oriented stimuli) was not found. To examine for a radial bias we presented the patch grating at two different locations (left bottom and top left) in the visual field. We did not however find a difference when contrasting the bottom 45 degrees condition (tangential) to the top 45 degrees condition (radial) nor the bottom 135 degrees grating (radial) to the top 135 degrees grating (tangential). We did find however that participants performed better for cardinal orientations in the top position than 45 degrees in the same location (oblique being also radial here) and also performance with cardinal orientations in the bottom location was better than the 135 degrees (radial) in the bottom position (with these contrasts again having a p value ≤ 0.05). Although the 45 grating at the top position and the 135 degrees grating in the bottom position were both radial to fixation we see that cardinally oriented gratings were favoured to these two oblique gratings even though these oblique gratings were radial to fixation. Berkley et al (Berkley, Kitterle, & Watkins, 1974) reported that the oblique effect disappears at about 8-

18 degrees (depending on subject) and Rovamo et al (Rovamo, Virsu, laurinen, & Hyvarinen, 1982) similarly find a fading of the oblique effect as we move at the periphery and it is substituted by a radial effect. Therefore, it could simply be that at the eccentricity we used the oblique effect is greater than a radial bias or that the radial bias is not in effect at this eccentricity. This lack of the radial bias at the eccentricity we used (or weaker radial bias than the oblique effect) suggests that at these distances from fixation we do not have to worry about a radial bias confounding any possible inverse oblique effects found with imaging methods.

A weakness with this chapter is the fact that too many questions were tested (we had 24 contrasts tested; see Appendix 1) and thus a Bonferroni corrected level of significant drops to $0.05/24 = 0.002$. At such a strict level of significance the only two contrasts remaining significant are for the grating presented at the lower left quadrant of the visual display for orientations 0 to 135 ($p=0.002$) and 90 to 135 (with $p=0.001$). However, with the grating presented at the lower left quadrant the 45 to 90 degrees conditions contrasted had a $p=0.004$ while in the upper left quadrant the conditions 0 to 45 had a $p=0.006$, condition 0 to 135 had a $p=0.008$, condition 45 to 90 had a $p=0.004$ and conditions 90 to 135 contrasted had a $p=0.006$. These p values although not significant once corrected are quite close to the corrected p value of 0.002. Even so the behavioral oblique effect did give two significant contrasts (for the grating presented al the lower left quadrant of the visual display for orientations 0 to 135 and 90 to 135) at this low Bonferroni corrected level indicating the behavioral effect is quite strong.

In this study we attempted to inspect for training effects during the behavioral oblique effect in a peripheral grating stimulus. None of the test's p values in this study survive a Bonferroni correction however in Edden et al. (Edden, Muthukumaraswamy, Freeman, & Singh, 2009) they report finding a training effect for their discrimination task in oblique orientations (a mean threshold drop from 2.3° to 1.8°) over 3 measurements, however for vertical it was essentially unchanged. In this experiment, the training effect was tested by testing each participant (for all orientations and both in the lower and upper left hemifield). Each orientation was tested however with 2 blocks (each one lasting approximately four minutes) with a cohort of 7 participants in the top 0, 90 and 135 while with top 45 and the bottom grating we removed 3 participants more. One issue here is the fact that the cohort examined was quite small however (probably more importantly) participants should have been tested more times in each condition in order for the training effects to actually take place. As Edden et al. (Edden, Muthukumaraswamy, Freeman, & Singh, 2009) find a significant training effect for the oblique condition (however no for cardinal) it is also probably more efficient to only use one single orientation in experiments looking into training effects as testing less orientations would mean that the single oblique orientation could be tested for longer, thus allowing training effects to surface.

As reported previously, Berkley et al. (Berkley, Kitterle, & Watkins, 1974) find that the oblique effect disappears in the periphery at about 8 to 18 degrees a finding that is supported by Rovamo et al. (Rovamo, Virsu, laurinen, & Hyvarinen, 1982) that also report a declining of the oblique effect as we move to the periphery and is replacement with the radial effect. In Koelewijn et al.'s

experiment (Koelewijn, Dumont, Muthukumaraswamy, Rich, & Singh, 2011), using MEG, find for a patch grating presented peripherally (2.2° both vertically and horizontally from fixation) having an initial tuning for V1 with a strongest response to oblique orientations however later the classical oblique effect appears that is mediated by an extrastriate region and also may involve feedback taking place from extrastriate regions to V1. The classical oblique effect appears after the initial inverse oblique effect in V1 however as the oblique effect disappears when moving to the periphery it would be interesting to replicate Koelewijn et al.'s study (Koelewijn, Dumont, Muthukumaraswamy, Rich, & Singh, 2011) at a greater eccentricity from the centre. As Berkley et al. state (Berkley, Kitterle, & Watkins, 1974) the oblique effect disappears at the periphery; does the initial inverse oblique effect in V1 found by Koelewijn et al. (Koelewijn, Dumont, Muthukumaraswamy, Rich, & Singh, 2011) still appear at such eccentricities? Also if the replication of Koelewijn et al.'s inverse oblique effect is possible in V1 at such eccentricities would we still find a later oblique effect with MEG in V1? Although difficult to ensure similar findings for the Koelewijn et al. experiment at further distances from central vision, the fact that the initial inverse was replace with an oblique effect at 2.2 degrees from fixation and the fact Berkley et al. (Berkley, Kitterle, & Watkins, 1974) report the oblique effect disappears moving further to the periphery, leaves open an interesting prospect of studying the initial inverse oblique effect in V1 either without the feedback processes taking place and affecting the initial tuning of V1 or alternatively different processes taking place (maybe different areas feeding back to V1) and either reducing the strength of the inverse oblique effect or switching it back to the classical stronger MEG response for cardinal orientations. One potential

problem with studying gamma in the periphery is that grating stimuli of 3 cycles per degree has been reported as being non-optimal for generating gamma responses when placed 4 x 4 degrees into the periphery by Swettenham et al. (swettenham, Muthukumaraswamy, & Singh, 2009). This reduction in response may well be ameliorated by using larger stimuli and lower spatial frequencies, in order to better match cortical magnification in the periphery, however such studies have, to date, not been performed either with MEG or behavioural studies of the oblique and inverse oblique effects.

4 Experimental chapter 3: An MEG Study of orientation discrimination and the oblique effect

4.1 Introduction

The oblique effect is a well-studied preference of the visual cortex for cardinally-oriented visual stimuli compared to obliquely-oriented ones (Appelle S. , 1978) (Koelewijn, Dumont, Muthukumaraswamy, Rich, & Singh, 2011) (Furmanski & Engel , 2000) (Mannion, McDonald, & Clifford, 2010). As in this chapter we wish to look into fine temporal aspects of the oblique effect, MEG is used. This chapter reports an experiment in which an orientation discrimination task is performed in the MEG scanner rather than simply correlating offline behavioral performance with gamma induced by a simple grating stimulus, representing a trait measure of the excitation / inhibition balance in the cortex (Edden, Muthukumaraswamy, Freeman, & Singh, 2009). In addition, for the first time, we hope to find a correlation between behavior and the human visual gamma response and we also hope to replicate the findings of Koelewijn et al. (Koelewijn, Dumont, Muthukumaraswamy, Rich, & Singh, 2011) in which an unexpected *inverse* oblique effect was found in the MEG responses.

In this project we found in the SAM analysis (using a permutation approach to control for multiple comparisons) for the oblique condition, a positive correlation of the oblique main effect (first stimulus onset) in areas in the medial visual cortex (at a frequency range of 30-70 Hz) to behavioral thresholds. Unfortunately no oblique effect was detected in this study when we contrasted oblique with the cardinal condition.

4.1.1 Introduction: The Problem to be Addressed.

The oblique effect (the preference of the visual system to vertical or horizontal lines compared to oblique ones) has been studied extensively (Appelle S. , 1978) (Bonds, 1982) (Furmanski & Engel , 2000) (Sutherland, 1957). It involves many structures of the visual system from the eye (see study on radial bias by Schall et al.) (Schall, Perry, & Leventhal, 1986), the lateral geniculate nucleus (Vidyasagar & Urbas, 1982) to the striate and extrastriate cortices. The neurophysiology underpinning the oblique effect is complex and still unknown, but is thought to involve biases in both the striate cortex and feedback processes from extrastriate cortex to the striate cortex (Koelewijn, Dumont, Muthukumaraswamy, Rich, & Singh, 2011). It is also known to be partly innate and partly acquired (shaped by visual experience) (Sengpiel, Stawinski, & Bonhoeffer, 1999) adding to the complexity. All of the above mean that there is still a need for extensive multimodal studies of this problem. In terms of inter-individual variability, Edden et al. (Edden, Muthukumaraswamy, Freeman, & Singh, 2009) showed that orientation detection thresholds negatively correlate with GABA concentration (supporting a key role for GABAergic inhibition) but also negatively correlated with the frequency of induced visual gamma oscillations. These correlations were only significant for obliquely oriented stimuli and not for stimuli that were cardinally-oriented. These results are of particular interest as it was the first study to link human inter-individual performance on a visual task with the concentration of a neurotransmitter and also suggest that GABAergic gamma oscillations play a key role in visual discrimination tasks. However, this experiment did not measure gamma oscillations while subjects were performing the discrimination task but used the

response frequency to the same grating stimulus as a trait measure of excitation/inhibition in the cortex. The study demonstrates, therefore, a tri-partite *correlation* between orientation discrimination, GABA and gamma frequency, but does not confirm any causal relationships. The Authors suggested that people with higher gamma frequency maintain neural synchrony in a more efficient way and therefore enhance stability and accuracy of perceptual grouping leading to better performance at the orientation task, as previously demonstrated in the visual cortex of cat and modeling studies (Samonds & Bonds, 2005) (Samonds, Allison, Brown, & Bonds, 2004).

However, the human MEG study of Edden et al. does not link gamma directly to performance as the task was performed offline in a separate session to the scan. Attending to the grating stimulus while performing a discrimination task may well have a significant effect on MEG responses as previous fMRI studies have demonstrated e.g. (Gandhi, Heeger, & Boynton, 1999). Gandhi et al. (Gandhi, Heeger, & Boynton, 1999) found that the BOLD response was differentially increased in the visual hemisphere contralateral to the side of attention. In addition, in the standard two-alternative-forced-choice (2AFC) procedure used in Edden et al., there is a delay period between the two test stimuli, inducing a significant *working memory* component that will both contribute to the behavioral load and, potentially, generate/modulate MEG measured responses. In order to properly address which oscillatory responses are important for driving both behavioral performance and reflect the neurophysiology underpinning the oblique-effect, it is therefore essential to perform the behavioral task in the MEG scanner itself. This was the aim of the experiment presented in this Chapter.

An oblique effect has been demonstrated both psychophysically (Berkley, Kitterle, & Watkins, 1974) (Rovamo, Virsu, Laurinen, & Hyvarinen, 1982) (Edden, Muthukumaraswamy, Freeman, & Singh, 2009) and with imaging (Furmanski & Engel , 2000) (Mannion, McDonald, & Clifford, 2010) (Koelewijn, Dumont, Muthukumaraswamy, Rich, & Singh, 2011). Behaviorally, the oblique effect has been shown to exist across a number of psychophysical axes, including the resolution frequency (presenting participants with grating of very high spatial frequency and reducing until the participant can view the stimulus) (Rovamo, Virsu, Laurinen, & Hyvarinen, 1982), to measuring acuity with high contrast grating at several retinal eccentricities (from 0 to 20 degrees from fovea fixation) (Berkley, Kitterle, & Watkins, 1974) in which case an oblique effect was found (worst acuity for the oblique orientations). However, this difference disappeared as the eccentricity of the grating increased and the eccentricity at which the oblique effect disappeared varied across participants (Berkley, Kitterle, & Watkins, 1974). The oblique effect has also been demonstrated with imaging experiments having participants passively viewing grating stimuli (no discrimination task to perform). Here an oblique effect has been found (Furmanski & Engel , 2000) however the inverse phenomena, an inverse oblique effect has been found with MRI (Mannion, McDonald, & Clifford, 2010) and MEG (Koelewijn, Dumont, Muthukumaraswamy, Rich, & Singh, 2011). Interestingly, in this MEG study (Koelewijn, Dumont, Muthukumaraswamy, Rich, & Singh, 2011) both the inverse oblique effect and the classical oblique effect were detected, with the inverse oblique effect (for the induced gamma response) appearing for early latencies (about 80 milliseconds) from stimulus onset and the classical

oblique effect appearing at later latencies from stimulus onset. According to Koelewijn et al. the early evoked and sustained gamma response indicated that the initial tuning of V1 with a higher response for obliquely-oriented stimuli and the later classic oblique-effect is mediated by an area in an extrastriate location, implicating feedback to the primary visual cortex (Koelewijn, Dumont, Muthukumaraswamy, Rich, & Singh, 2011). This hypothesis of feedback from extrastriate areas is supported by previous animal research. Using optical imaging and pharmacological injections Liang et al (Liang, Shen, & Shou, 2007) showed positive feedback from area 21a changed the strength of the oblique effect in area 17.

4.1.2 Rationale of study.

In their study Edden et al. found that orientation detection thresholds were negatively correlated to gamma (Edden, Muthukumaraswamy, Freeman, & Singh, 2009) with the oblique condition giving a significant negative correlation ($r = -0.65$, $p < 0.017$) and the test for the cardinal condition not reaching significance ($r = -0.02$, $p = 0.9$).

Here, I replicate this study, however the discrimination task was performed while the participant was in the scanner. I examined if the correlation remained between performance and properties of the induced gamma activation, under test conditions in which working memory and attention were also present during the MEG recording.

In a previous passive-viewing MEG study, (Koelewijn, Dumont, Muthukumaraswamy, Rich, & Singh, 2011) successfully revealed a rich mixture of both early evoked and sustained gamma response, which presumably

represents V1's initial tuning (stronger response for oblique stimuli) and later extrastriate cortical responses, showing a classic preference for cardinal stimuli (i.e. the oblique effect), implicating extrastriate feedback to V1 in mediating the behavioral effect (Koelewijn, Dumont, Muthukumaraswamy, Rich, & Singh, 2011). I therefore decided to use the same stimulus parameters as this previous study, in which the stimulus was centered 2.2 degrees both horizontally and vertically from a fixation point. As Berkley et al (Berkley, Kitterle, & Watkins, 1974) reported that fixating at eccentric targets can be difficult to achieve, particularly at eccentricities of 2 to 4 degrees we chose to monitor eye position using an MEG compatible eye tracker (MEG 250 SMI SensoMotoric instruments GmbH). Additionally as cognitive processes are present during the discrimination task (that may affect visual cortex neuronal activity) in the analysis we added a "working memory" section exploring activities taking place in the period between the two grating presentations of the discrimination task, a period where no actual visual stimulation takes place.

4.2 Methods

4.2.1 Participants.

For this experiment 13 participants took part with mean age m = 27.59 and standard deviation s.d. = 14.53. Male (6) and female volunteers (7) with normal or corrected-to-normal vision were recruited. Before participating all participants gave informed consent. The Ethics Committee, of the School of Psychology at Cardiff University, approved all procedures.

Participants were excluded based on their performance to the behavioral task. Specifically, If the participant's data was too bad and couldn't be modeled

by a Weibull function this participant was excluded. We therefore excluded one participant for the cardinal conditions and 3 participants for the oblique.

Visual stimuli

Two stimulus conditions were used. In the first (*cardinal*) the grating stimulus was vertical to the horizon (90 degrees) while in the second the grating was tilted at an angle of 45 degrees counterclockwise from the horizon. For reasons discussed later in the methods (section 4.2.3) a 2AFC (Two-Alternative Force Choice), method of constant stimuli procedure was adopted. We used 7 separate orientation differences, between the two gratings, which were a logarithmic adjustment around the mean values from the Edden et al. paper (Edden, Muthukumaraswamy, Freeman, & Singh, 2009) i.e. 0.5 degrees for the cardinal orientations and 1.8 degrees for the oblique. The orientation difference values (y) used in our method of constant stimuli was calculated by the formula: $y = mean * 2^x$ where the mean for the cardinal condition was 0.5 degrees and for the oblique condition was 1.8 degrees and *x* was one of seven values chosen from (-1, -0.5, 0, 0.5, 1, 1.5, 2).

The stimulus dimensions were the same as used in the MEG study by Koelewijn et al (Koelewijn, Dumont, Muthukumaraswamy, Rich, & Singh, 2011) and Chapter 2 of this thesis (fMRI study) and are illustrated in Figure **24**.

On every trial, two circular gratings were presented sequentially, each for 250 ms, with an inter-presentation time of 750 ms. The mean orientation for the two gratings was held fixed either at vertical or 45° oblique. Participants had to judge whether the second grating had rotated clockwise or counterclockwise compared to the first. Responses were recorded and visual feedback was given on each trial (green fixation point for correct response).

Stimuli were presented using MATLAB version 7.8.0.347 (32 bit) and the Psychophysics toolbox (Brainard, 1997) (Pelli, 1997). All oblique trials were presented together and so were the cardinal ones. The participant would either be presented with the oblique trials first or the cardinal ones first (counterbalanced across participants). There were 140 oblique and 140 cardinal trials. The cardinal and oblique trial timings and other details are illustrated in the following figure (Figure **22**).

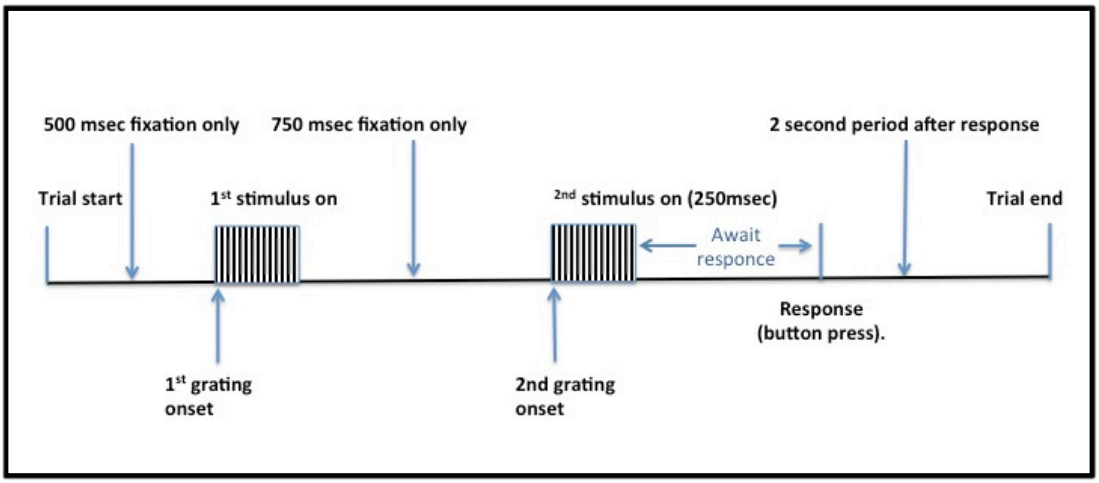

Figure 22:Outline of the trials with triggers. Both stimuli were on for 250 msec. The triggers were for cardinal first onset (trigger 7), second onset (trigger 8), oblique first stimulus onset (trigger 2) and 2nd oblique stimulus onset (trigger 3).

The actual stimulus (at the left the cardinal and at the right the oblique) is seen in the figure below.

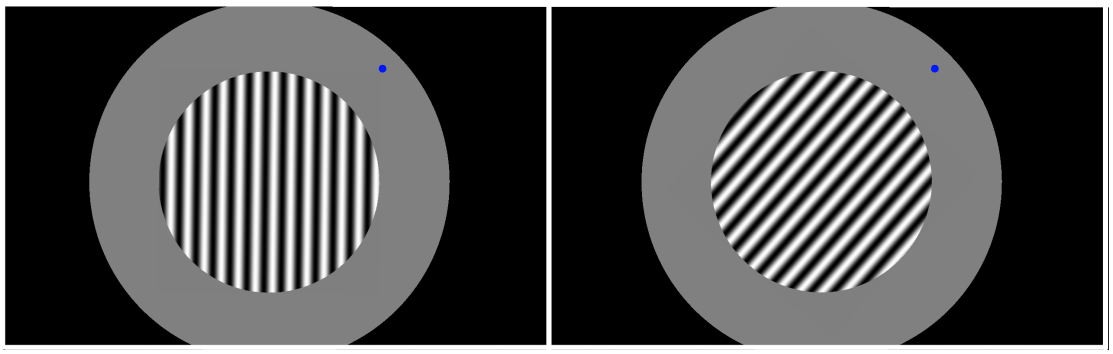

Figure 23: Left image is a picture of the cardinal condition grating and at the right a picture of the oblique grating (grating on). In the inter-stimulus interval, the grating disappeared and only the gray screen, the black aperture and the fixation were seen.

The dimensions of the stimulus can be seen in the following figure:

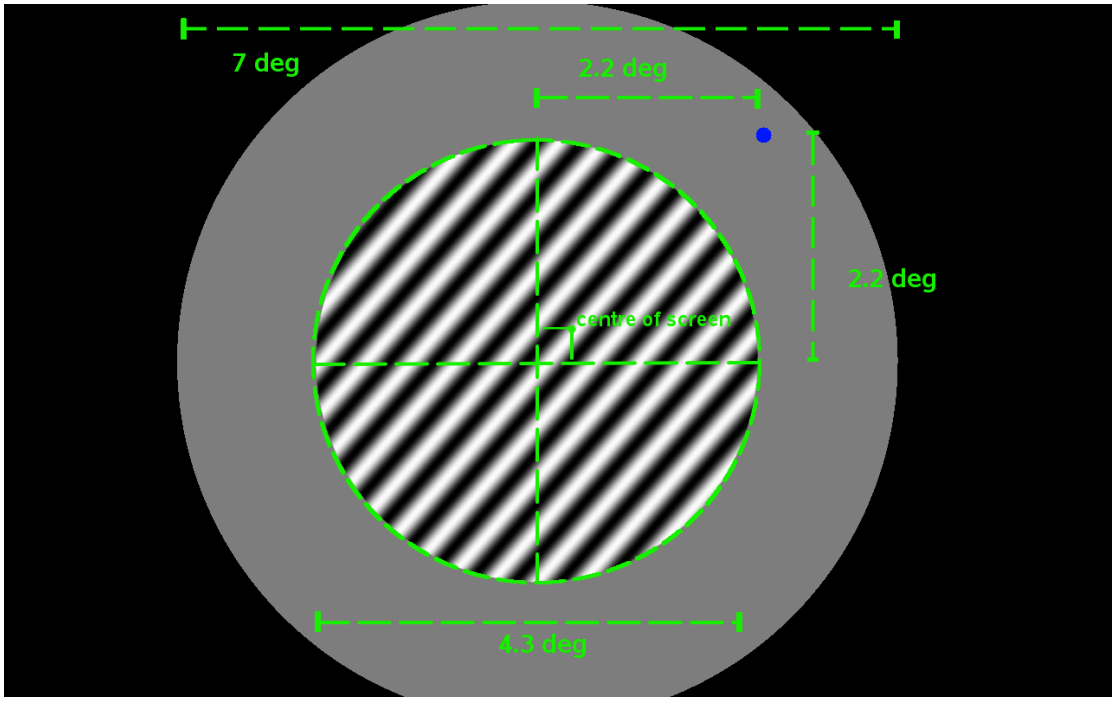

Figure 24: The above figure shows the dimensions of the stimulus used for this experiment. Because of the screen dimensions and distance of the screen to the participant we had to shift the grating center to the left 0.2 degrees from center and down 0.2 degrees from the center in order to get the stimulus with the distances above to fit the screen. The grating spatial frequency was 3 cycles per degree, which is optimal for maximal cortical power in gamma frequencies in V1 **(Adjamian, Holliday, Barnes, Hillebrand, Hatjipapas, & Singh, 2004)**.

4.2.2 Eye tracking

Eye tracking was performed using an infra-red camera system (MEG 250 (MEG 250 SMI SensoMotoric instruments GmbH) with a 250 Hz sampling rate. The eye tracker software was the iViewX 2.6 build 20 by SMI vision (MEG 250 SMI SensoMotoric instruments GmbH). The eye tracker sampled the left eye. The Ksdensity function was used in MATLAB analysis. Ksdensity(*x*) returns a probability density estimate (*f*) for a given sample in the vector *x*, using a normal kernel function (Bowman & Azzalini, 1997) and was used to fit a non-parametric kernel smoothing to the histograms of mean fixation distances for every trial (for each participant individually) as can be seen in the appendix II.

As mentioned previously, fixation at eccentric stimuli is most difficult at 2-4 degrees distance from fixation (Berkley, Kitterle, & Watkins, 1974) and therefore in this project eye tracking was used. Here we wished to get a comparison measure of distance from fixation (measured in degrees of visual angle) before and after stimulus presentation i.e. 250 msec after stimulus appearance and 250 msec before it appeared. A comparison was then made for before after getting the number of trials average fixation shifted towards the stimulus and away (this was done in the X, Y axis separately).

4.2.3 Psychophysics data

To analyze the psychophysics data MATLAB version 8.0.0.783 (R2012b) (MATLAB) was used. Weibull functions were fit using a Matlab toolbox (modelfree 1.1, Zychaluk K., Mathematical Sciences Department , University of Liverpool (Żychaluk).

In the Edden et al. paper (Edden, Muthukumaraswamy, Freeman, & Singh, 2009) a 2AFC design was used, with a staircase procedure to converge to an estimate of discrimination performance. The staircase has certain advantages (Macmillan & Creelman , 2005) compared to a fixed approach (method of constant stimuli) as it requires fewer trials and does not require predefining the difficulty levels. However, the staircase procedure results in varying numbers of trials, at participant-specific difficulty levels, for each participant. This is undesirable in neuroimaging studies (such as MEG) in which it is important to have the same number of trials for each stimulus type (cardinal/oblique) difficulty level and for each participant – in order to match signal-to-noise for each condition. Hence, here, I used a method of constant stimuli approach.

In order to robustly determine discrimination thresholds from potentially noisy data, the raw behavioral data was fitted by a Weibull function, which can be expressed by:

$$P(x) = 1 - exp[-(\frac{x}{a})^b]$$

with a corresponding to the threshold and b being the slope (Macmillan & Creelman , 2005). The Weibull function has many valuable properties (Macmillan & Creelman , 2005) and has been used extensively for studying vision (Nachmias, 1981), (Furmanski & Engel , 2000), (Strasburger, 2001).

For each of the 7 orientation differences that were presented to the participant, and for each of the oblique and cardinal conditions, we plotted the graph of percent correct answers versus orientation difference between the two presented gratings (one for oblique and one for the cardinal condition). Later a Weibull function was used to fit these data points and from this curve the orientation difference was estimated that yielded the 70 percent probability of a

correct answer – this is our measure for the threshold for orientation discrimination. An example is shown in Figure **25**.

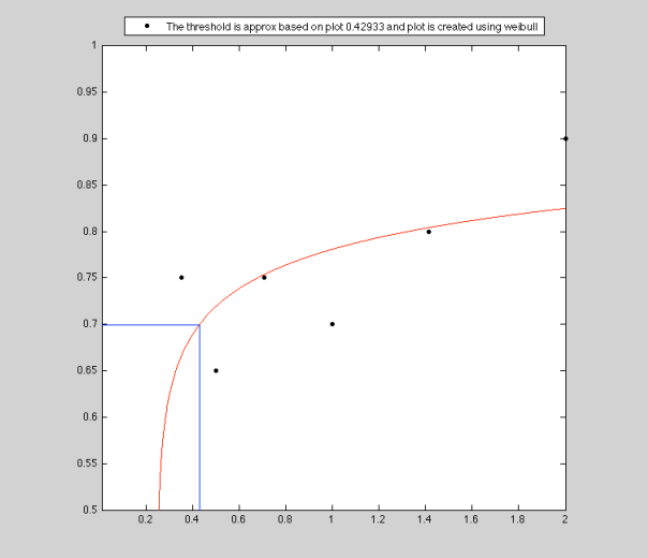

Figure 25: This figure shows the line of best fit (using a Weibull function) for the cardinal orientation discrimination task for the first participant.

4.2.4 MEG acquisition

MEG data was acquired using a 275-channel whole- head system (CTF Systems, a subsidiary of VSM MedTech) in a magnetically shielded room. The sampling rate was 600Hz and the primary sensors were analyzed as synthetic 3rd order gradiometers (Vrba & Robinson, 2001). Line noise was filtered at 50Hz and raw data was inspected for artifacts trial by trial. Head position was recorded using 3 fiduciary markers placed (one 1 cm above the nasion and the others 1 cm anteriorly from the left and right tragi). For the SAM analysis, participants' MEG data were co-registered to structural MRI scans, using the same identifiable landmarks on the structural scans and high-resolution digital pictures of the fiduciary markers.

4.2.5 SAM beamformer analysis

The problem of finding the source location from an externally measured field is known as the "inverse problem". In MEG, using certain *a-priori* assumptions about the nature of dipolar sources, brain shape and conductivity profiles we can get the most likely source estimation generating the magnetic fields measured with the SQUID sensors. A popular source estimation method is beamforming and Synthetic Aperture Magnetometry (SAM) is one of the most popular beamformers used in MEG (VRBA and Robinson 2001). Beamformer models use algorithms that are based on those used in fixed-aperture radars, in which any part of the sky can be scanned using a weighted arrangement of fixed radar detectors. Key assumptions in SAM is that a set of discrete dipolar sources generate MEG data and that the time series of these sources are uncorrelated (Senior, Russell, & Gazzaniga, Methods in mind, 2006). In MEG our interest is discovering the magnitude and time series of the activation at a given point in the cortex, something referred to as a "virtual recording" or "virtual sensor" (Vrba & Robinson, 2001) SAM is a spatial filter allowing us to estimate, for a single location, a set of coefficients (weights) so that the combination of the weighted SQUID sensors provides an estimate of activity at each potential source location. In this project SAM images were built using a 5mm grid throughout the brain for each participant.

In this chapter all images were normalized to a template brain for group analysis. All data was inspected using in-house visualization software, mri3dX.

4.2.5.1 Main effects and contrasts for the cardinal and oblique conditions

Initially the data were epoched, using newDS by VSM MedTech Ltd (CTF MEG Software), at -0.450 to 0.500 seconds around the four onset triggers (First Oblique Onset, Second Oblique Onset, First Cardinal Onset, Second Cardinal Onset: See Figure **22**).

Initially, at a single level analysis, we looked at the main response effects (using the in-house function, makeSAMstatistics) for the first and second presentations of both grating types (oblique and cardinal). For each condition, the main effects were calculated at an individual level by performing a paired t-test contrasting, for all trials, the period from 100-300msec after each stimulus onset (active period) to the period from -200 to 0msec before stimulus onset (baseline period).

A t-test analysis was also performed contrasting the response to oblique and cardinal stimuli, for the active periods (0.10 to 0.30 seconds). This was done for both the first and second grating presentations.

All the main effects and the contrasts were examined in the frequency ranges of 4-8 Hz, 8-12 Hz, 5-15 Hz, 15-25 Hz, 30-70 Hz, 40-60 Hz, 60-80 Hz and 40-80 Hz.

4.2.5.2 Group SAM analysis (permutation testing) for main effects and contrasts.

The significance of all main effects, oblique/cardinal contrasts and correlations between the main effects with the behavioral data was assessed using permutation testing. One participant was excluded from the cardinal analysis and 3 participants from the oblique analysis (due to poor behavioral data i.e the data was not well modeled by a Weibull function). For the analysis of contrasts between cardinal and oblique responses, all participants were included

in the permutation analysis (as we were not interested in determining the correlation with behavioral data). The FSL design file was created as described in the Single-Group Average with Additional Covariate section in the GLM page of the FSL page (FSL wiki/GLM). Randomize v2.5 (a part of FSL, build 414) was run with a cluster based -threshold of 2.3 and a variance smoothing of 10. From the randomize output we took the cluster based p-value maps for all of the above mentioned frequencies and created a mask for all voxels that were above 0.95 (equivalent to $p<0.05$). The mask created for each condition was then multiplied with the uncorrected nifti file of the same condition from the permutation results therefore leaving only the voxels of the uncorrected nifti files that had a significant p-value in the nifti file. Later we used 3dcalc to calculate from the uncorrected t-values for the correlation nifti files the r-values using the formula $r = \sqrt{\frac{t^2}{t^2+DF}}$ where t is the t-value, r is the r correlation value and DF are the degrees of freedom (randomize output gives the t value for correlations not r). For the cardinal condition there were 12 participants (one excluded) so we had 12-2 = 10 degrees of freedom. For the oblique condition there were 10 participants (three excluded) so we had 10-2 = 8 degrees of freedom.

4.2.5.3 Working memory SAM analysis.

In this Chapter, the *working memory* period refers to the time between first and second grating presentations, during which the participant must internally maintain a representation of the first grating, in order to match it to the upcoming second presentation.

For the working memory analysis, the data was initially epoched in periods from -0.500 seconds to 1 second around the onset of the first grating, separately

for Oblique and Cardinal conditions. SAM images were then constructed using 400-850 milliseconds (i.e. the stimulus maintenance phase) as the "active" period and -450 to 0 milliseconds as the baseline period. These images therefore represent oscillatory effects that occur during the working memory, or stimulus maintenance, phase of the trial.

Additionally we contrasted working memory in the oblique condition to the working memory in the cardinal condition in this 400-850 msec period.

Again here 4D files were created using Create4D file from the normalized images of the working memory conditions. Again all the main effects and contrasts were examined at the frequency ranges: 4-8 Hz, 8-12 Hz, 5-15 Hz, 15-25 Hz, 30-70 Hz, 40-60 Hz, 60-80 Hz and 40-80 Hz. A permutation test was run again using *randomize*. The same one participant was excluded as mentioned in the cardinal main effects and for the oblique condition the 3 same participants were excluded (for the same reason i.e. bad psychophysics data). For the contrasts of oblique to cardinal conditions in working memory all thirteen participants were used. Again the FSL design file was created as described in the Single-Group Average with Additional Covariate section in the GLM page of the FSL page (FSL wiki/GLM). Randomize was run again with a cluster based-threshold of 2.3 and a variance smoothing of 10. Again the same procedure as described previously for the analysis of main effects was used, i.e. take the cluster analysis p value image for each condition, make a mask for the significant voxels and then multiply this mask with the equivalent condition uncorrected image. Again, t values were transformed into r-values (with 10 degrees of freedom used for the cardinal condition and 8 for the oblique).

4.2.6 Virtual-sensor analysis.

For the individual level analysis a CUBRIC function was used (newmakeSAMsensors) that uses global data covariance and weights for generation of the beamformer weights. Virtual sensors were place in the medial visual cortex (the exact position for each participant can be seen in the results section (virtual sensor analysis). A high pass filter of 0 and a low pass filter of 100 Hz were used.

Hilbert time-frequency analysis of the single channel was then performed with bert_singlechannel. This function creates time-frequency spectrograms using a Hilbert approach to create, using the Analytic function, the amplitude envelope of each frequency as a function of time. These amplitude envelopes are 'stacked' to give a time x frequency representation see: (Swettenham, Muthukumaraswamy, & Singh, 2009). These time-frequency plots were plotted from 0 to 150 Hz in 0.5 Hz steps with a baseline from -2 to 0 seconds.

These 'bertograms' can be used to create time-frequency representations of oscillatory amplitudes separately for each trial, which are then averaged to form the average time-frequency spectrum. Here we call this an ***AGRAM*** and, importantly it can reveal both induced and evoked oscillatory effects. Alternatively, we can time-average the trials first before calculating the bertrogram from this average. This is known here as an ***EVAGRAM*** and only reveals the oscillatory signatures of phase-locked evoked responses .

4.3 Results

4.3.1 Eye-tracker data.

A patch grating was presented twice per trial and as a sudden grating presentation could cause shift of fixation towards the grating the mean eye fixation was calculated (for every participant) 250 msec after and 250 msec before every stimulus presentation. For each participant there were 280 trials and the grating was presented twice per trial thus 560 cases where a grating patch appeared during a scan. For every stimulus presentation, the mean fixation *before* and *after* were compared (separately for x and y axis) and we determined if the eye had moved towards the patch grating. These results are shown below in **Figure 26**.

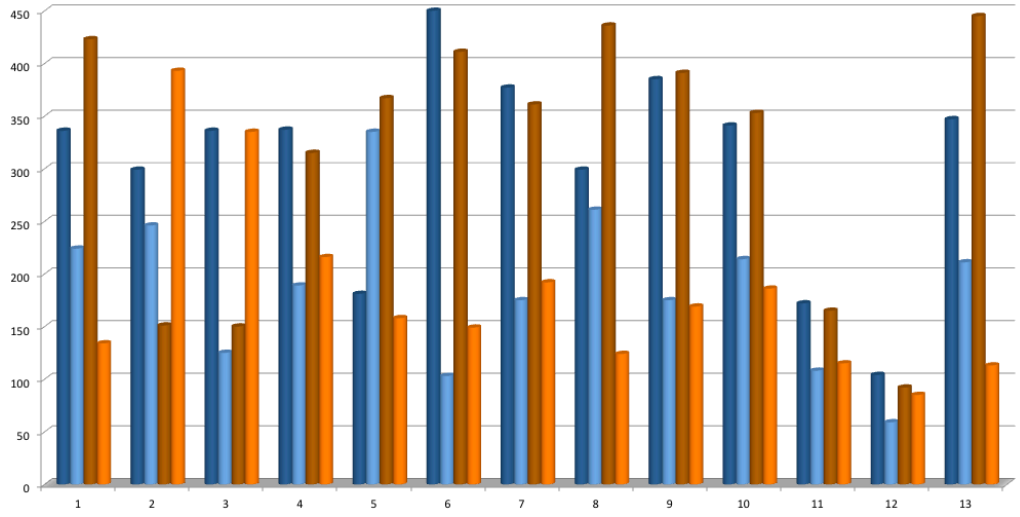

Figure 26: Y –axis shows number of trials and X-axis is participant (total of 13 subjects). There are 4 columns per participant with blue and brown for trials that fixation moved towards the grating (blue in the x-axis and brown in the Y-axis), while cyan and orange is for trials that fixation moved way from the grating (cyan in the x-axis and orange in the Y-axis).

For each participant for every trial we calculated the mean fixation distances when the grating was ON and when the grating was OFF (in the X and Y axis) and then we created two histograms, one for the mean fixation distances for every trial when the grating was ON and one when it was OFF. Then two lines where fit to these two histograms using a non-parametric kernel smoother. The

lines of best fit (using the kernel smoother) are displayed in the figures in Appendix II. In the histograms 0 is the center of fixation.

These plots were used in order to get an overall idea of if average fixation of participants was shifted towards the patch grating compared to a period with no stimulus present.

From figure 26, with a comparison of number of trials that fixation moved towards or away from the patch grating with the sudden appearance of the patch grating, in the x-axis for 12 out of 13 participants gaze shifted from fixation to the grating and in only one away. In the y-axis a shift of gaze towards the grating was found in 11 out of 13 participants (and 2 away). In the appendix II from the the histogram of the mean fixation distances for every trial for individual participants we can observe for every participant (in the x and y axis) that in the x-axis in most cases the most common mean fixation distance for a trial is outside fixation in an opposite direction than the grating while in the y-axis there is just one case where mean fixation distance is 1 degree or above towards the grating.

4.3.2 Psychometric analysis of the data.

The 70% orientation discrimination thresholds for all participants are shown in Figure 27.

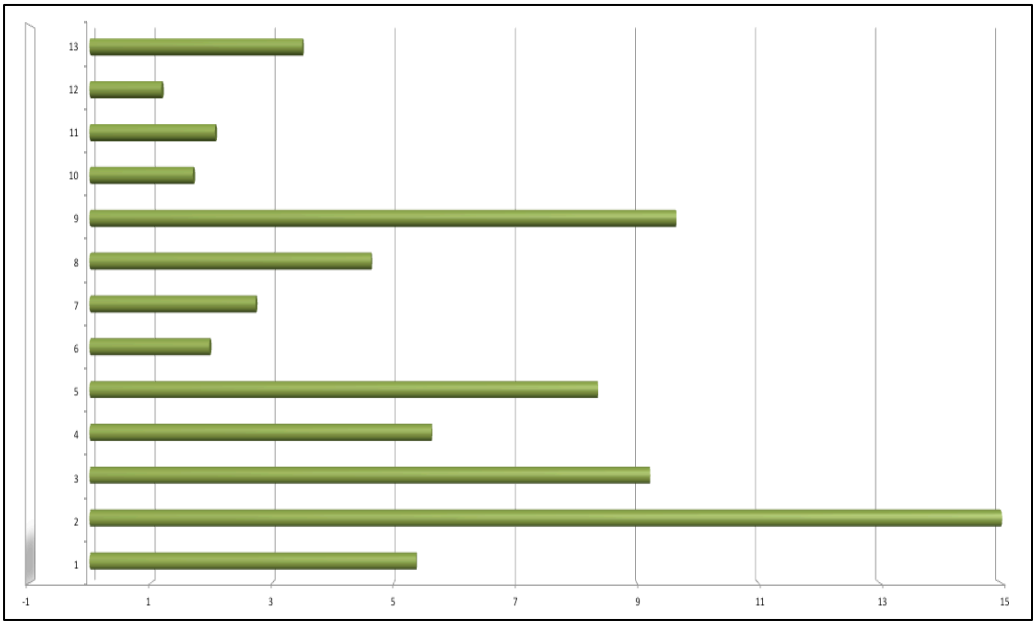

Figure 27: For participants 1 to 13 Cardinal behavioural thresholds were respectively: 0.43, 0.1, 0.78, 0.56, 0.86, 2, 0.52, 1, 0.37, 1.2, 0.79, 0.88, 0.68. For the oblique thresholds in the same order they were: 2.31, 7.19, 7.19, 3.15, 7.19, 3.94, 1.42, 4.63, 3.57, 2.04, 1.63, 1.04, 2.38. In this figure the ratio of oblique to cardinal are shown (X-axis) for participant 1 to 13 (Y axis). For participant 2 (ratio of 71.9) the bar has been cut so the rest of the data would be displayed properly in this figure.

It can be seen that the ratio of oblique to cardinal thresholds was, in all cases, greater than 1, revealing a behavioral oblique effect for all participants.

4.3.3 Group SAM analysis

For the Group SAM analysis (permutation testing) for the main effects and the contrasts of the uncorrected images after selecting the significant voxels (significant voxels in the cluster-based analysis p-values maps) for all of the main effects and contrasts we took the uncorrected images masked to select only the significant (in the cluster based analysis) voxels. The results are presented in the below section (a summary of the findings in appendix III).

Main effects

For the main effects for the first and second grating appearance in the oblique oriented grating we found in the SAM analysis the frequencies that gave

significant results for the main effects were 30-70Hz 40-80 Hz 40-60 Hz and 60-80. For the main effects for the first and second grating appearance in the cardinal oriented grating we again found in the SAM analysis the frequencies that gave significant results for the main effects were 30-70Hz 40-80 Hz 40-60 Hz and 60-80. All these main effects can be seen in Figure **28**.

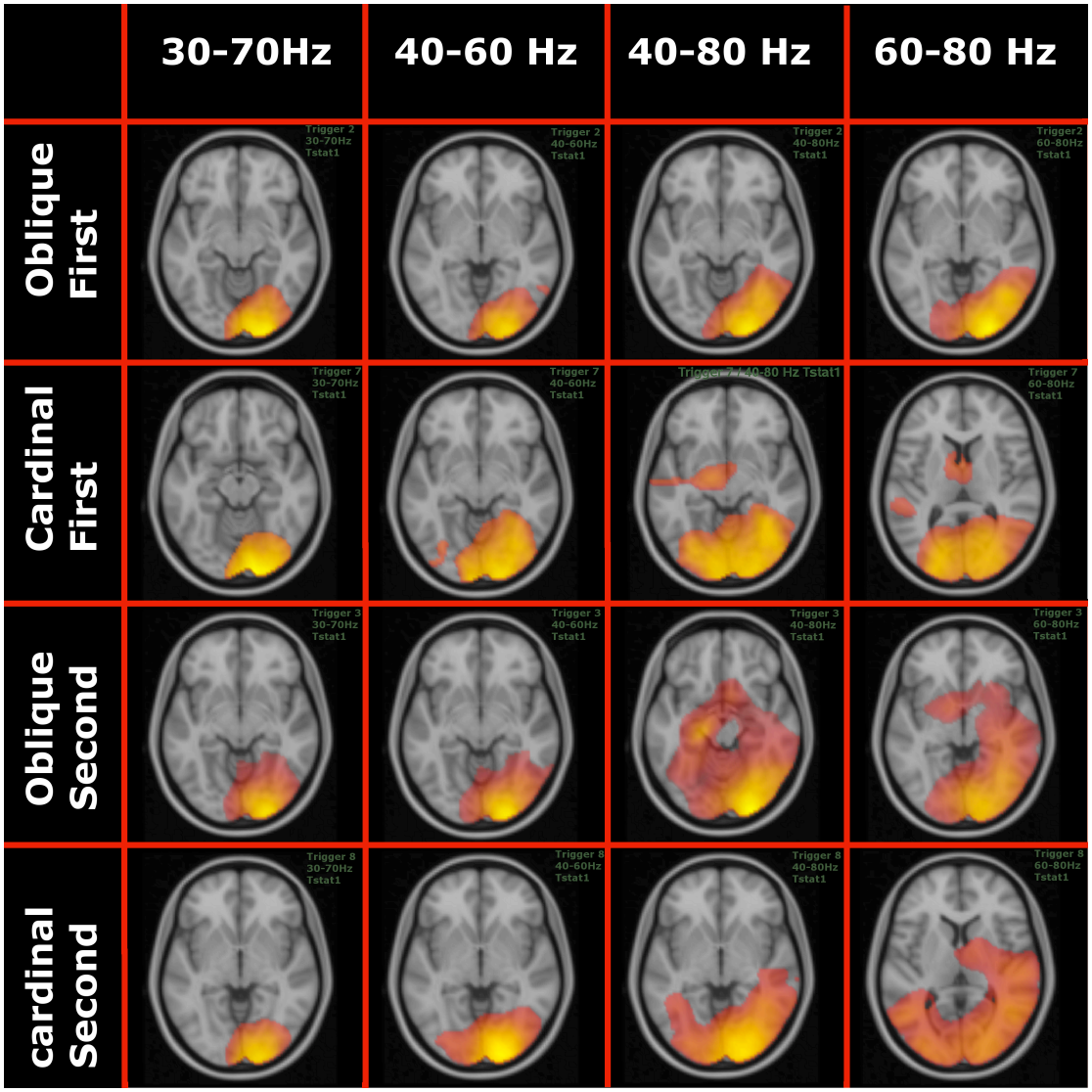

Figure 28: From the SAM analysis the frequencies that gave significant results (p<)0.05 cluster corrected) for the main effects (tstat1) were 30-70 HZ, 40-80 Hz, 40-60 Hz and 60-80 Hz. In this figure the main effects for the first oblique and cardinal grating appearance as also for second oblique and cardinal grating appearance are displayed for these frequencies.

Oblique versus Cardinal Contrasts for both First and Second presentations

Here none of the contrasts gave significant results i.e. we could find no significant oscillatory signatures of either the classic oblique effect or an inverse oblique effect.

Working memory period

Group SAM analysis (permutation testing) for main oscillatory effects during the working memory period revealed significant voxels ($p<0.05$ cluster-based correction) in the 15-25Hz beta band for both cardinal and oblique stimuli. These are shown in Figure **29**.

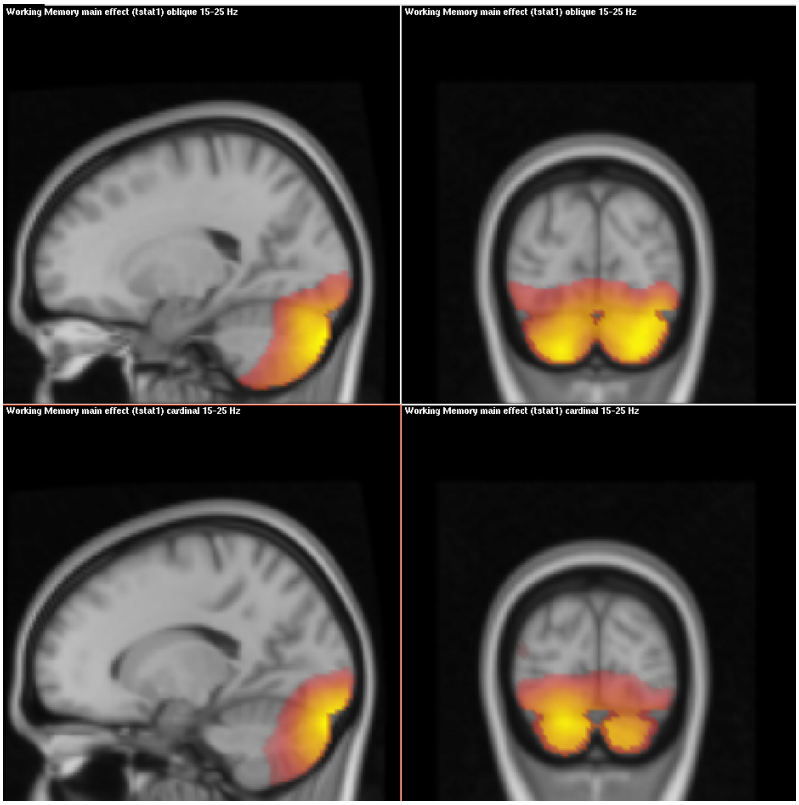

Figure 29: The main effects during the working memory maintenance period were in the 15-25Hz Beta range (Top Panels: Oblique, Bottom Panels: Cardinals)

Contrasting between Cardinal and Obliques revealed no significant differences in this stimulus maintenance period.

Correlations between oscillatory responses and behavioural thresholds

Here, using the SAM images for oscillatory effects related to presentation of the four conditions (FirstCardinal, SecondCardinal, FirstOblique, SecondOblique), we examined whether the amplitude of the oscillatory response across the brain was correlated with behavioral thresholds across individuals. These correlation maps were examined in our standard frequency ranges i.e. 15-25, 30-70, 40-60, 40-80, 4-8, 5-15, 60-80 and 8-12. Here we found significant values when correlating trigger 2 main effect at 30-70 Hz with the behavioral data, trigger 2 at 60-80 Hz and trigger 3 at 5-15 Hz.

For the first presentation of the Oblique stimulus, we found significant results within two gamma ranges (30-70Hz and 60-80Hz), where gamma amplitude was positively correlated with behavioral thresholds i.e. higher gamma is associated with worse performance. These results can be seen in Figure **30** and in Figure **31**.

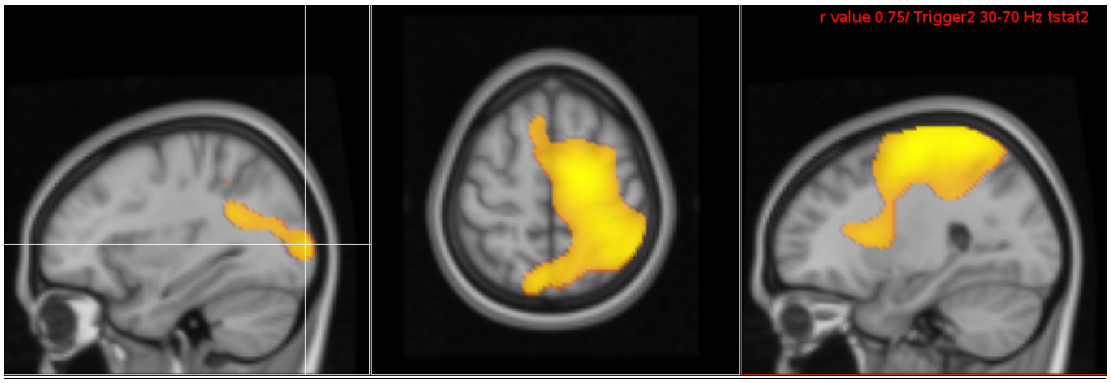

Figure 30: Cortical areas for FirstOblique at 30-70 Hz that gave a significant correlation between amplitude and behavioral data, 100-300msec post-stimulus onset. The maximum value in the visual cortex (indicated in the left picture with crosshair) was r = 0.75, p=0.02.

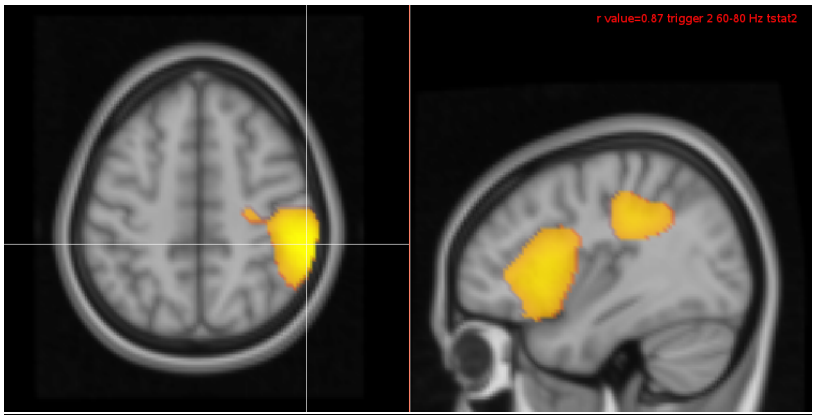

Figure 31: Cortical areas for FirstOblique at 60-80 Hz that gave a significant correlation between amplitude and behavioral data, 100-300msec post-stimulus onset. The peak correlation was in the right parietal cortex (r=0.87, p=0.035). No significant r-values were found in the visual cortex.

Several areas of positive correlation can be seen in the gamma range, including the visual and parietal cortices.

In the Alpha frequency range (5-15Hz) a region of positive correlation was observed deep in the brain, but only for the Second Oblique presentation (Figure **32**). Given the uncertainties of deep source localization with MEG, it is difficult to ascribe a definitive functional localization for this effect.

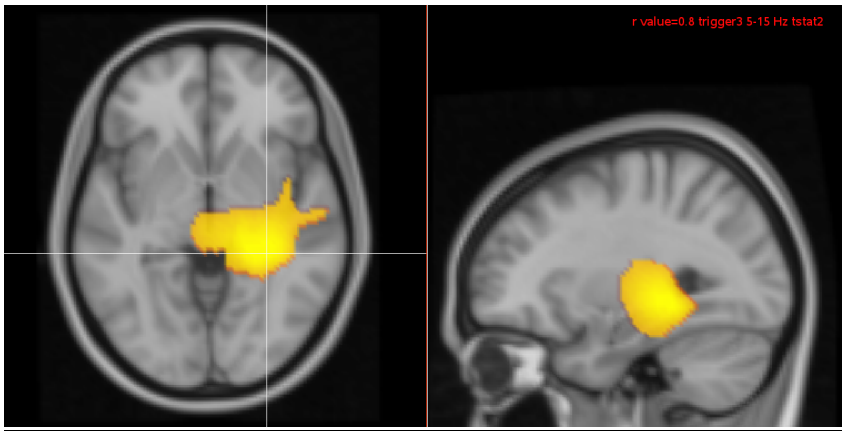

Figure 32: These are the areas for trigger 3 at 5-15 Hz that gave a significant r-value when correlating main effect and behavioral data (r=0.8, p=0.048). No significant areas were found in the visual cortex.

Interestingly, no correlations were found across the brain for the easier Cardinal condition. This mirrors the findings of Edden et al., in which correlations with GABA and gamma frequency were only demonstrated for the more difficult oblique condition. As we shall see in the final experimental chapter, correlations with behavioral orientation thresholds do appear to be stronger for more difficult versions of the task, although it is not clear whether this is due to a true functional difference or just a statistical property of needing more variance across participants.

No significant correlations were found with behavioral thresholds during the working memory maintenance period.

Virtual Sensor analysis

In this section the virtual sensor analysis is presented. Initially peak activation was determined in the visual cortex for each participant separately in order to account for spatial biases arising from inter-subject structural and functional cortical variability. The “medial position” we selected was the peak

activation for the oblique condition main effect (first stimulus onset per trial) at the 30-70Hz frequency. The medial position was selected as in this location in the visual cortex Koelewijn et al. (Koelewijn, Dumont, Muthukumaraswamy, Rich, & Singh, 2011) report an inverse oblique effect. Gamma frequency was selected as these frequency ranges are associated with feedback processes being studied in this chapter. Virtual sensors were generated in these individual locations using beamformer coefficients and later frequency-time plots were generated using the "bertogram" approach described above.

Where were the sensors placed and using what criteria?

Virtual sensors were created for all 13 participants in the medial part of the visual cortex. The points selected are shown in the figures below.

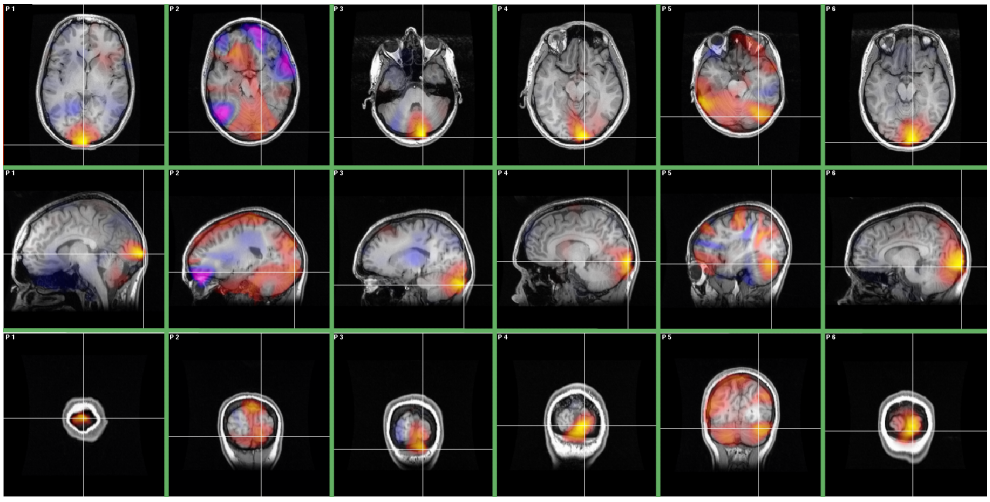

Figure 33: The positions selected for the virtual sensors for participants 1 to 6 (each column is one participant).

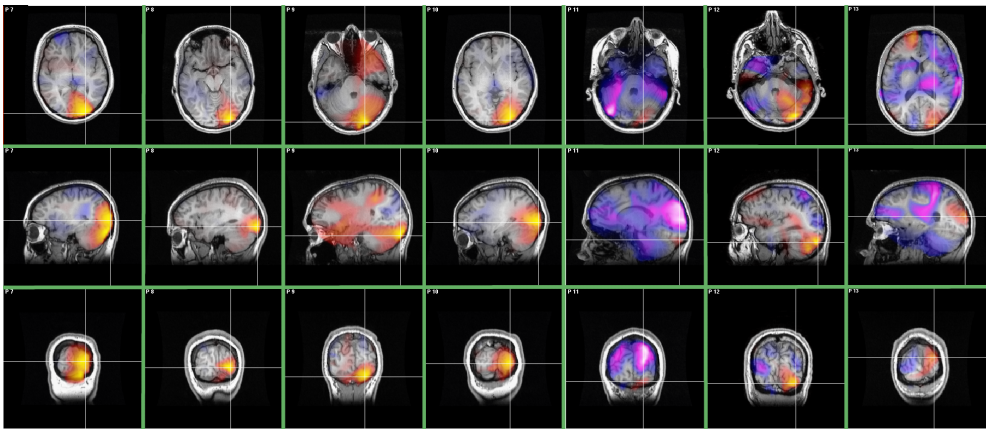

Figure 34: The positions selected for participants 7 to 13. Again images in the same column are of the same participant.

4.3.3.1 Time -Frequency analysis of each individual participant.

The individual AGRAM (induced and evoked) and EVAGRAM (evoked) betrograms, revealing time-frequency effects in each participant are shown in Appendix IV. Some EVAGRAMS have a clear activation (participants 3, 4 and 7) approximately 60-80mseconds after stimulus onset, while other participants did not have such a clear response. The baseline time used to create these plots was the time before the stimulus appears.

4.3.3.2 Time frequency group analysis.

The group analysis for the "medial point" (as described in the virtual sensor analysis part) for all participants is described in this section.

4.3.3.2.1 Averages

For this analysis the individual time frequency plots were used from all 13 participants. Here (for all participants) 4 time frequency average plots were made, one from all individual cardinal EVAGRAMS, one from the individual

AGRAMS and similarly 2 from the oblique EVAGRAMS and AGRAMS. Each pixel in each plot is the average of all the individual plots at that same location.

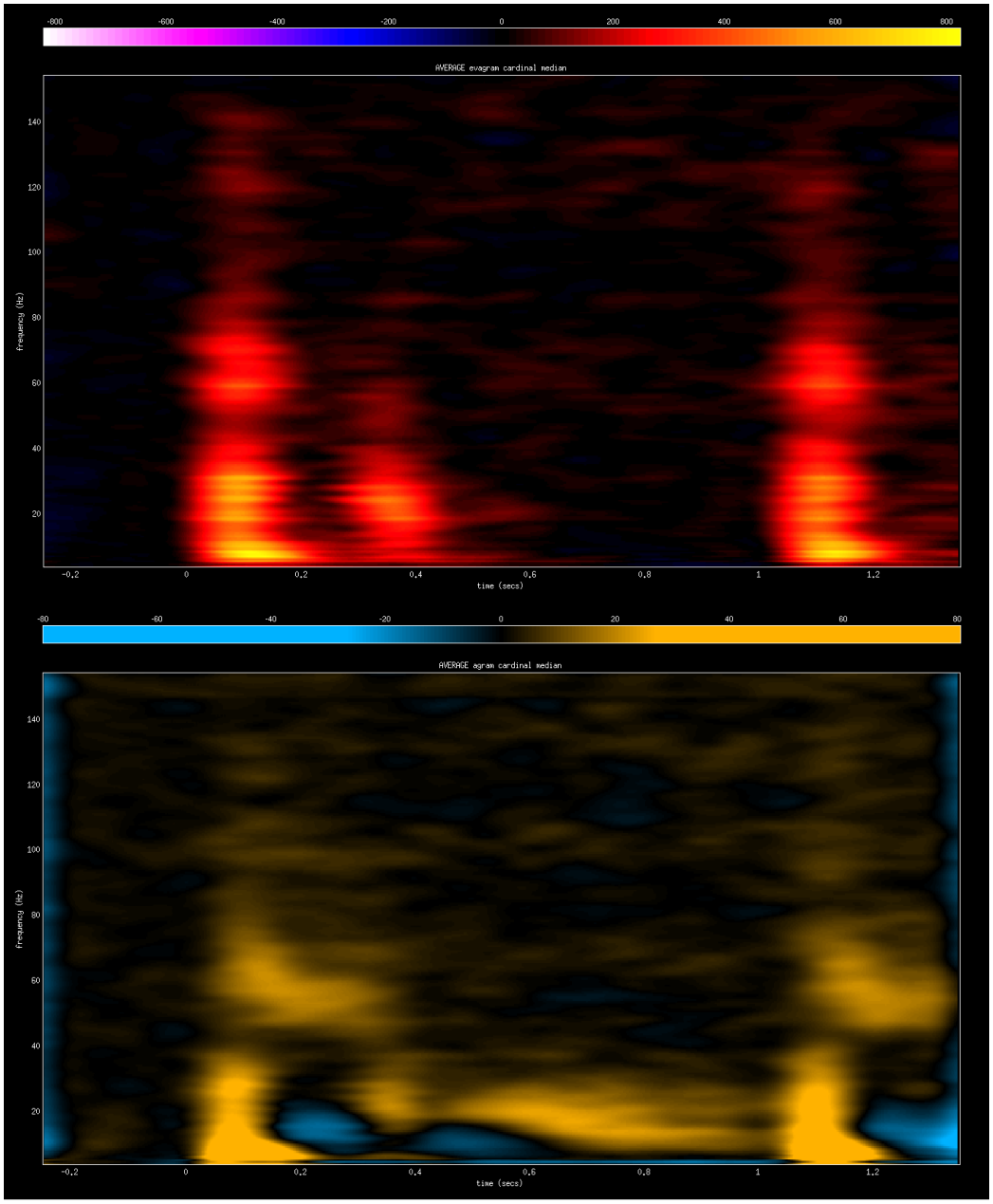

Figure 35: The average bert_singlechannel plot (EVAGRAM at the top and AGRAM at the bottom) for all 13 participants (cardinal condition). The Y axis is frequency (Hz) and the X-axis shows time (seconds).

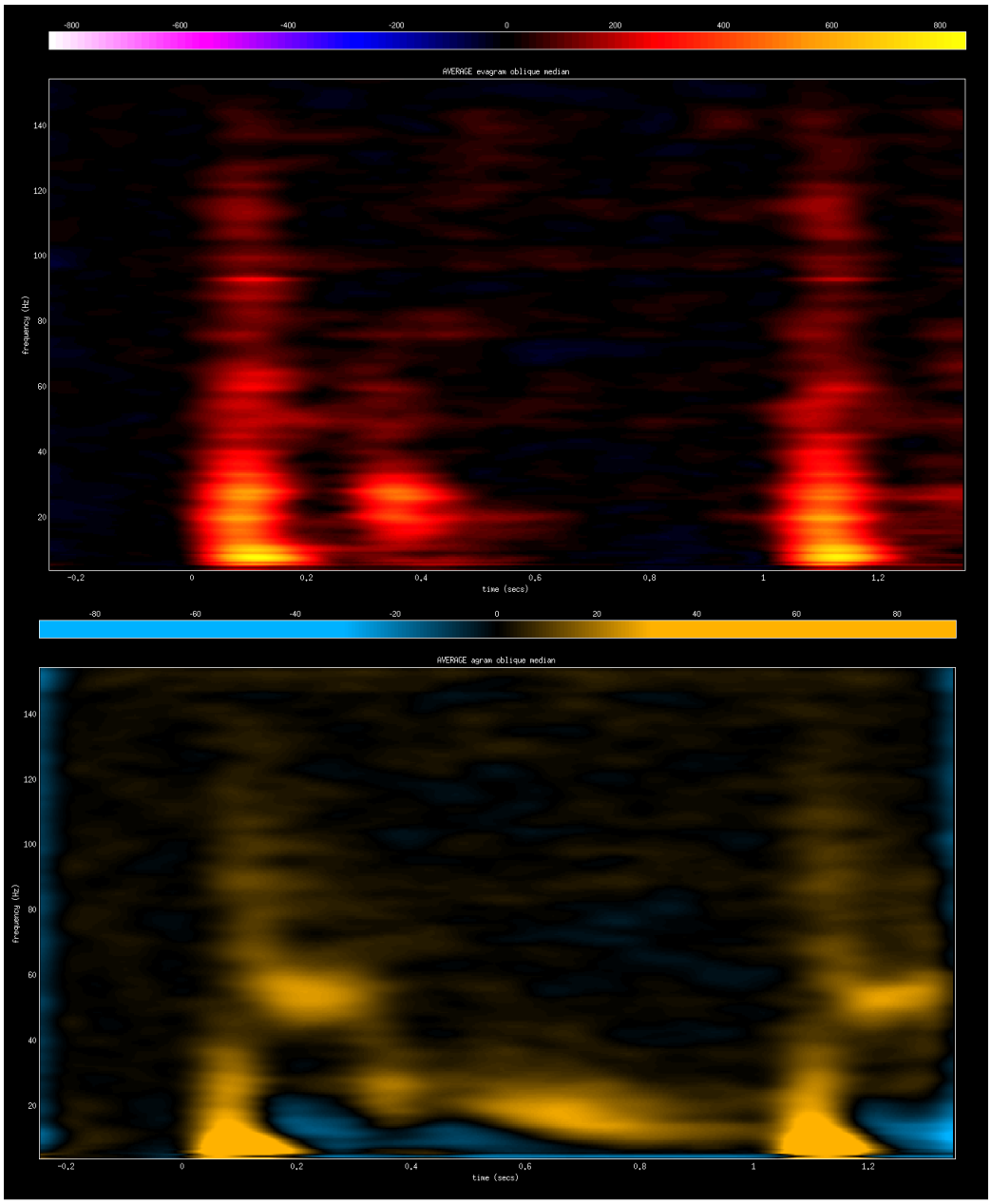

Figure 36: The average bert_singlechannel plot (EVAGRAM at the top and at the bottom the AGRAM) for all 13 participants (oblique condition). The Y axis is frequency (Hz) and the X-axis shows time (seconds).

The plots show clear evidence of low frequency evoked responses at each stimulus onset together with an evoked gamma 'spike' that extends up to around 120 Hz. In the AGRAMs only there is also evidence of a short narrowband burst of sustained gamma at approximately 60Hz, which must be induced rather than evoked, together with evidence of alpha suppression. All of these signals are

consistent with previous studies of evoked and induced responses to grating stimuli (e.g. Swettenham et al., 2009).

4.3.3.2.2 T-tests

After the Hilbert time-frequency analysis of the single channel was performed a paired t test was performed to contrast all the cardinal spectrograms (the spectrograms of every participant) to all the oblique spectrograms. Each location ("pixel") of the result t-test spectrogram is calculated by performing a paired t-test of the cardinal amplitudes of all participants (at the same location in the spectrogram) to the corresponding amplitudes of all participants in the oblique condition.

To control for multiple comparisons we used a permutation method. We performed 1000 permutations and in each permutation an array of random 0's and 1's was created with 13 positions (the total number of participants we had). For each permutation we generated the spectrogram of the paired t-test of the contrast of cardinal to oblique condition value in the specific location however the sign of the difference cardinal minus oblique was changed from + to – or – to + if the randomly generated array had a 1 in the position corresponding to the participant. In each permutation the same array of 0's and 1's was used for all the paired t-tests. For each permutation the maximum absolute value was selected from the generated paired t-test spectrogram (t-max statistic). Then a spectrogram of the paired t test was generated with the contrast of cardinal to oblique condition. The critical threshold is the C+1 largest number of the permutation distribution of the t max statistic with C = a*N rounded downwards ('a' is 95/100 and N is the total number of permutations) and any location with a

t value above this threshold is significant. This was done for EVAGRAM's and AGRAM's however in the spectrograms no significant locations were found.

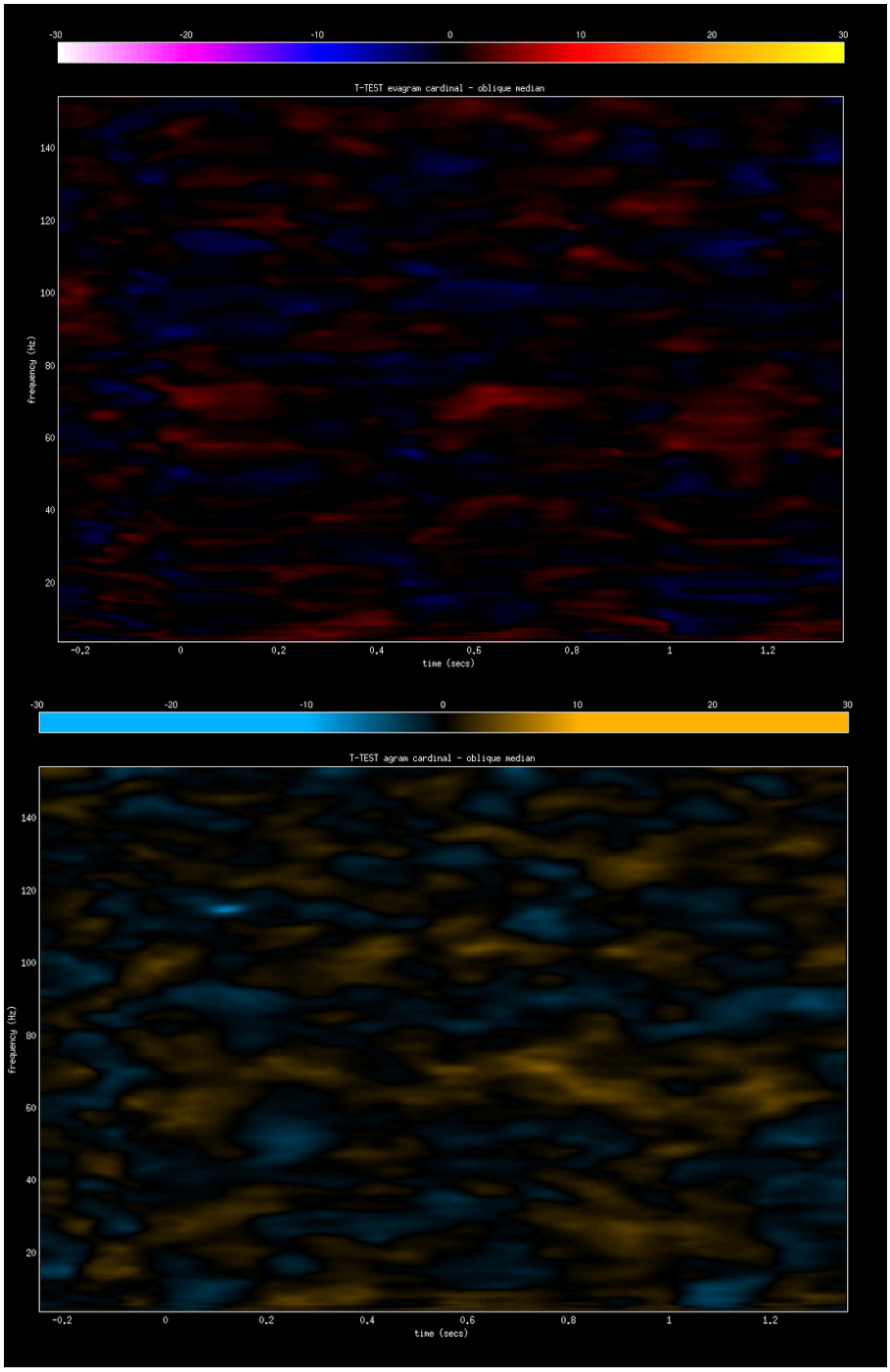

Figure 37: Each location ("pixel") of this t-test spectrogram is calculated by performing a paired t-test of the cardinal amplitudes of each participant (at the same locale in the spectrogram) to the corresponding amplitudes of all participants in the oblique condition. In this figure no account for multiple comparisons is taken.

4.3.3.2.3 Correlation with behavior

Here each element of the time frequency plot for each participant was correlated to individual participants behavioral data and a Bonferroni method was used to control for multiple comparisons (so $a = \frac{0.05}{301*961}$). None of these correlations was significant however. This is obviously a very conservative approach to correction as the individual time-frequency points are not independent. However, inspection of the plots of the correlation coefficient maps did not reveal any suggestions of significant correlation.

4.3.3.3 Power - time and power – frequency plots.

4.3.3.3.1 Power vs. time and power vs. frequency.

Here we plotted (for the sensor in the medial position) power vs. time (the power, averaged across the frequency range from low to high at each time point from starting time to end time) and power vs. frequency (the power, averaged across the time range from start time to end time at each frequency from the lowest to the highest) for a gamma frequency range of 30-70 Hz (for oblique and cardinal conditions). The time-period analyzed was 0-250msec around stimulus onset for all four conditions. The results are displayed in the figures below. In the next four figures the top left plot is the gamma power vs. time plot for the evoked response (EVAGRAM), the top right is the gamma power vs. time plot for the induced response (AGRAM), the bottom left is the power vs. frequency for the evoked response and the bottom right is the power vs. frequency for the induced

response. The mean power value over time was also calculated for each participant (from the Power vs. time plots) and these values were correlated with a Spearman correlation to the participant's behavioral data. These values are referred to as correlation of Average value to Behavioral Thresholds in this subsection (the next 4 figures).

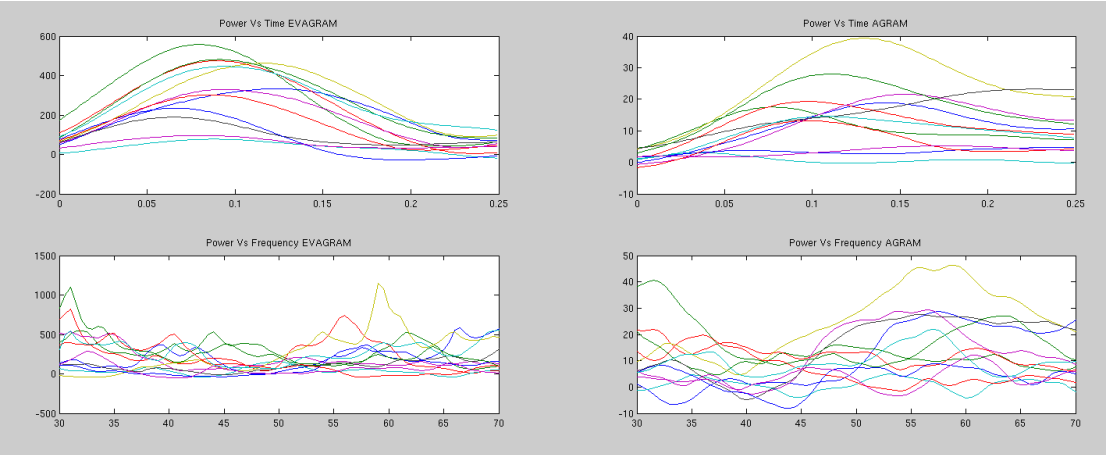

Figure 38: Top row is Y-axis power and X-axis time (seconds) while the second row is power (Y-axis) to frequency (Hz). These plots are for the time period from 0.00 to 0.25 seconds from trial onset (the first grating appearance) and for 30 to 70 Hz for the cardinal condition. The Average value correlated to the Behavioral Thresholds for the EVAGRAM (using a Spearman correlation) was r=0.119 n=12, p=0.716 and for the AGRAM r = 0.266, n=12, p=0.404.

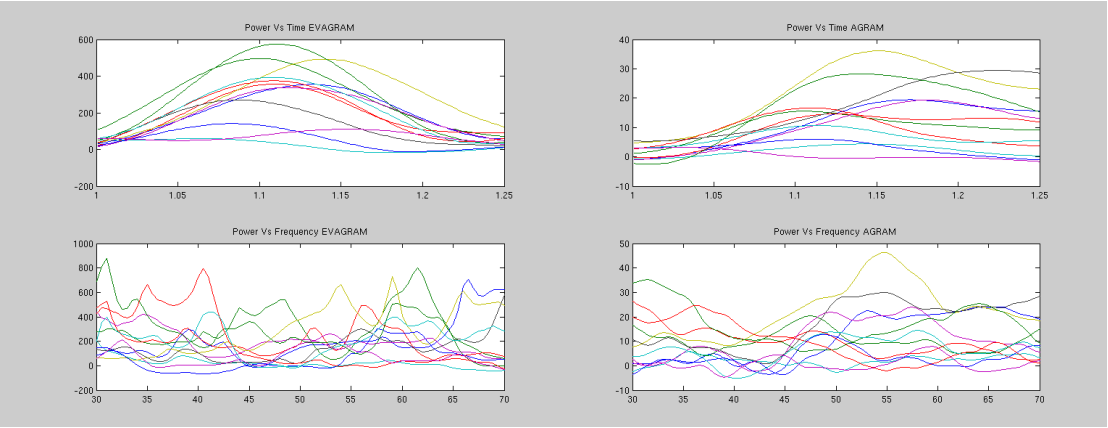

Figure 39: Top row is Y-axis power and X-axis time (seconds) while the second row is power (Y-axis) to frequency (Hz). These plots are for the time period from 1.00 to 1.25 seconds from trial onset (the second grating appearance) and for 30

to 70 Hz for the cardinal condition. The Average value correlated to the Behavioral Thresholds (using a Spearman correlation) for the EVAGRAM was r=0.168, n=12, p=0.604 and for the AGRAM r = 0.168, n=12, p=0.604.

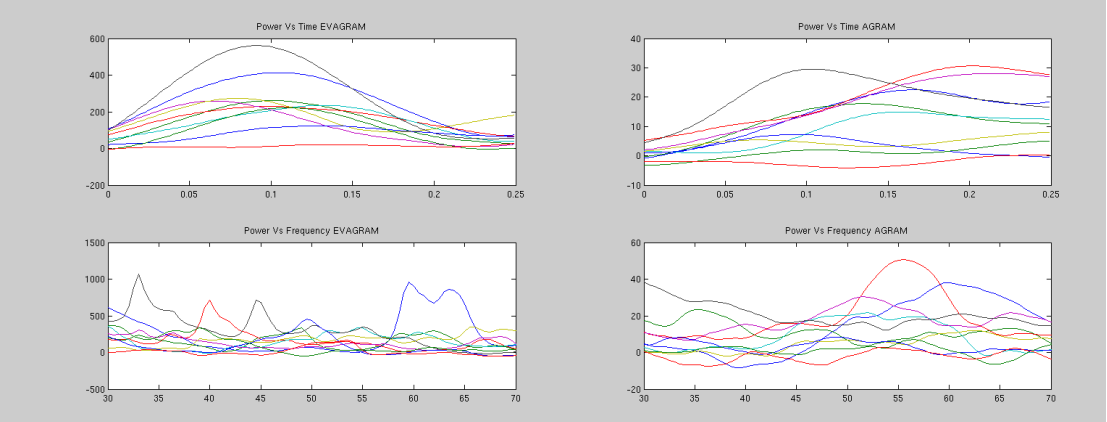

Figure 40: Top row is Y-axis power and X-axis time (seconds) while the second row is power (Y-axis) to frequency (Hz). These plots are for the time period from 0.00 to 0.25 seconds from trial onset (the first grating appearance) and for 30 to 70 Hz for the oblique condition. The Average value when correlated (Spearman correlation) to the Behavioral Thresholds for the EVAGRAM was r=0.2, n=10, p=0.583 and for the AGRAM r = 0.418, n=10, p=0.232.

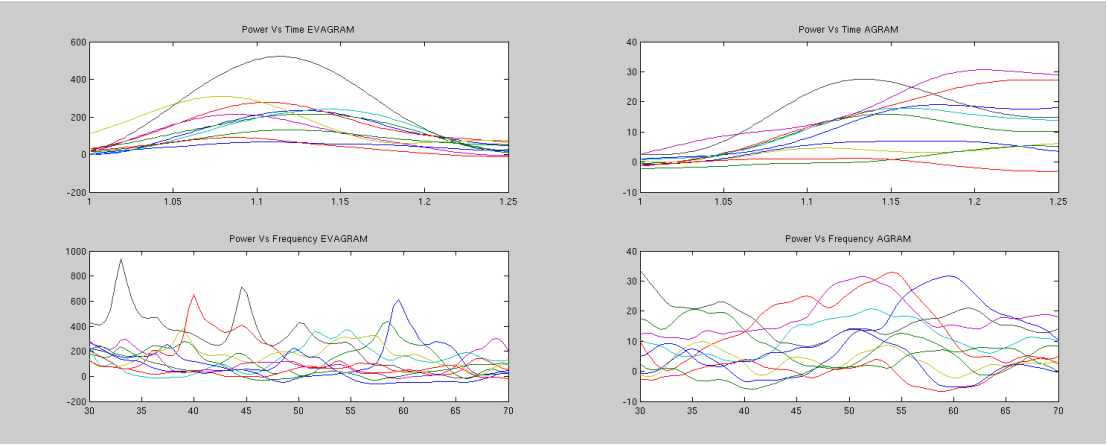

Figure 41: Top row is Y-axis power and X-axis time (seconds) while the second row is power (Y-axis) to frequency (Hz). These plots are for the time period from 1.00 to 1.25 seconds from trial onset (the second grating appearance) and for 30 to 70 Hz for the oblique condition. The Average value correlated (spearman correlation) to the Behavioral Thresholds for the EVAGRAM was r=0.212, n=10, p=0.560 and for the AGRAM r = 0.382, n=10, p=0.279.

4.3.3.3.2 Maximum gamma response amplitude: correlations with behavioral thresholds.

Then, we found the maximum value from the gamma power vs. time plot (plot of the power, averaged across the frequency range from 30-70Hz at each time point from starting time to end time) of each participant both cardinal and oblique condition and correlated them to the results of the behavioral data. These correlations were calculated with a Spearman r-value. This was done over the time period 0 to 250 milliseconds post-stimulus for all four conditions. The results are summarized in Table 1.

Table 7: In the table below we correlated the maximum gamma power (from the Power vs. time plot) of each participant to their behavioral data for both cardinal grating appearances and for both oblique grating appearances (0 to 250 mseconds from each stimulus onset). Then we took the latency at which this maximum power occurred for each participant and correlated this also to the performance to the behavioral task of each participant. For all four columns there are 4 correlations performed so the level of significance is Bonferonni corrected at a = 0.05 / 4 or 0.0125. None of the correlations were found to be significant.

	Max Power EVAGRAM	Max Power AGRAM	Latency of max EVAGRAM	Latency of max AGRAM
1st grating cardinal	r = -0.014 p = 0.974	r = 0.266 p = 0.404	r = 0.007 p = 0.983	r = -0.154 p = 0.635
2nd grating cardinal	r = 0.133 p = 0.683	r = 0.196 p = 0.543	r = -0.126 p = 0.696	r = 0.308 p = 0.331
1st grating	r = 0.2	r = 0.479	r = -0.656	r = 0.264

oblique	p = 0.583	p = 0.166	p = 0.039	p = 0.461
2nd grating	r = 0.224	r = 0.382	r = -0.529	r = 0.188
oblique	p = 0.537	p = 0.279	p = 0.116	p = 0.602

The point of this analysis was to determine if maximum power and latency at which it is reached are correlated with performance at the discrimination task. Although none of the correlations reached corrected significance, there was a trend for the latency of the evoked gamma responses to the first and second oblique conditions to be negatively correlated with behavioral threshold ($p<0.17$ and $p<0.04$).

4.3.3.3.3 Correlations between virtual sensor amplitude and behavioral thresholds at each separate frequency.

Here we correlate the behavioral thresholds for each participant with the amplitude of response at each separate frequency. .As there are multiple correlations performed here we used an omnibus threshold permutation threshold test as described in Nichols and Holmes (Nichols & Holmes, 2001) using 10000 permutations

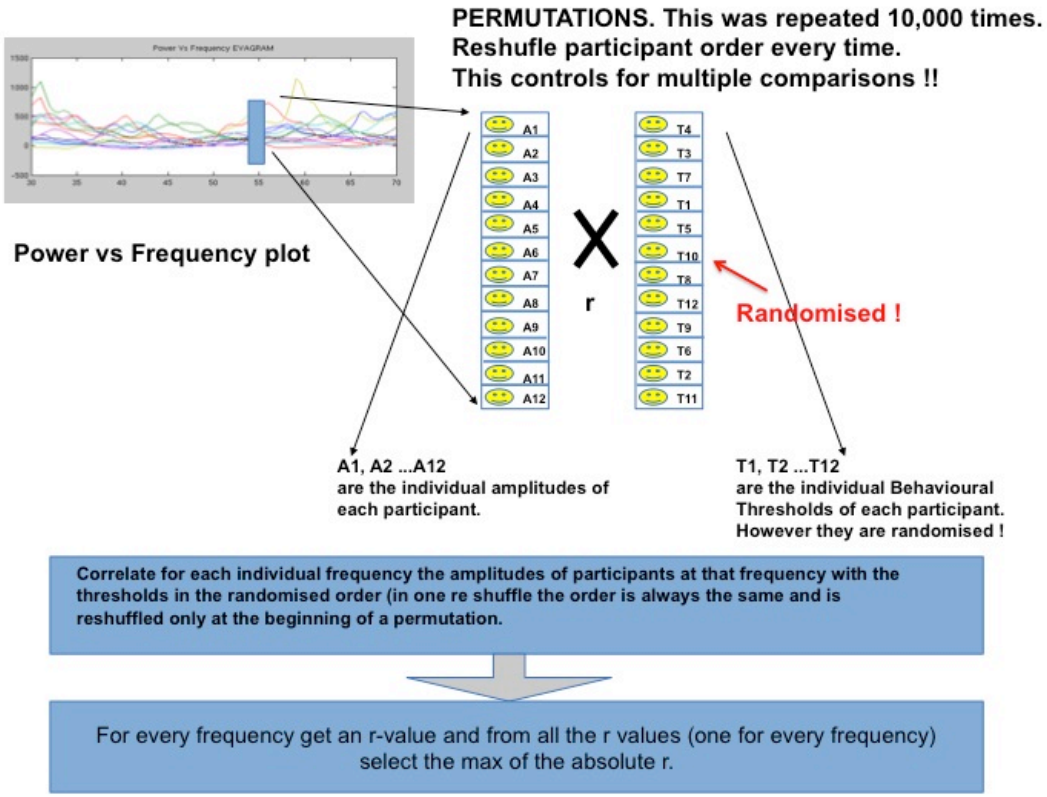

Figure 42: With a permutation method we controled for multiple comparisons. For each of the 10,000 reshufflings the above procedure was used. Initially a random order was created and the behavioural data were put in an array in the randomised participant order. From the Power vs Frequency plot top left for each frequency the amplitudes of all participants were selected (the normal participant order was used here) and they were correlated to the randomised behavioural thresholds of all participants (T1 to T12). Then we got a correlation to frequency plot and from this we took the max absolute r value (maximal statistic). This same procedure was done for all relabelings. From the permutation distribution of the maximal statistics the critical threshold was the c+1 largest member of the permutation distribution with c = a * N (a = 0.95, N = 10000 permutations) rounded down. Specific frequencies with statistics (Pearson's r value) exceeding this threshold (or being lower the negative threshold) exhibit evidence against the null frequency hypothesis. The p value for each voxel is the proportion of the permutation distribution for the maximal statistic that is greater or equal to the voxel statistic.

Using the above procedure the plots below were created. In each plot the r value (blue for EVAGRAM and green for AGRAM) and p value (red line) are ploted. The cyan line is where the +/- thresholds are. All the r values above the +threshold and below the – threshold exibit evidence against the corrected null

hypothesis. Note that For the cardinal condition n=12 (one participant excluded) and for the oblique n=10 (3 participants excluded). The results for this analysis are displayed in the two figures below.

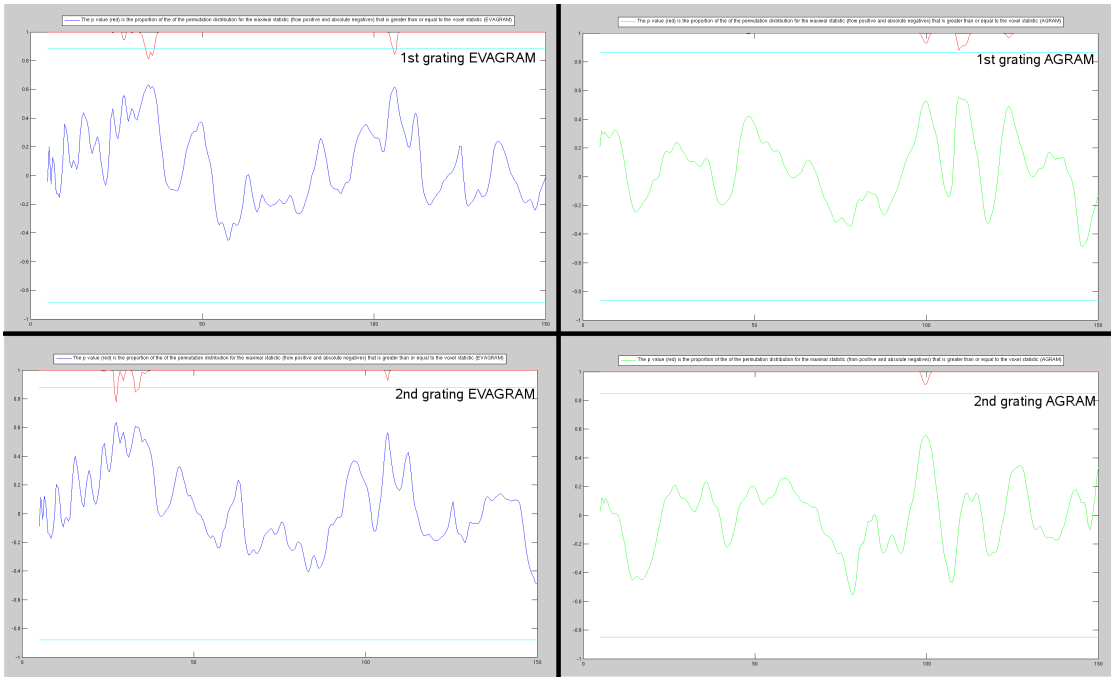

Figure 43:These are the plots created for the cardinal condition. These plots for every frequency show (in blue or green) at every specific frequency how power (from the Power vs. Frequency) correlates with behavioral results. The top left is for the 1st grating evoked response (EVAGRAM), the top right for the 1st gratings induced response (AGRAM); the bottom left is for the 2nd gratings evoked response (EVAGRAM) and the bottom right for the 2nd gratings induced response (AGRAM). For these plots 10,000 permutations were used. In none of the four plots is the r-value above the + threshold or below the – threshold so no r-values exhibit evidence against the null hypothesis. All r-values have an n=12 (1 participant excluded). The p-value is in red.

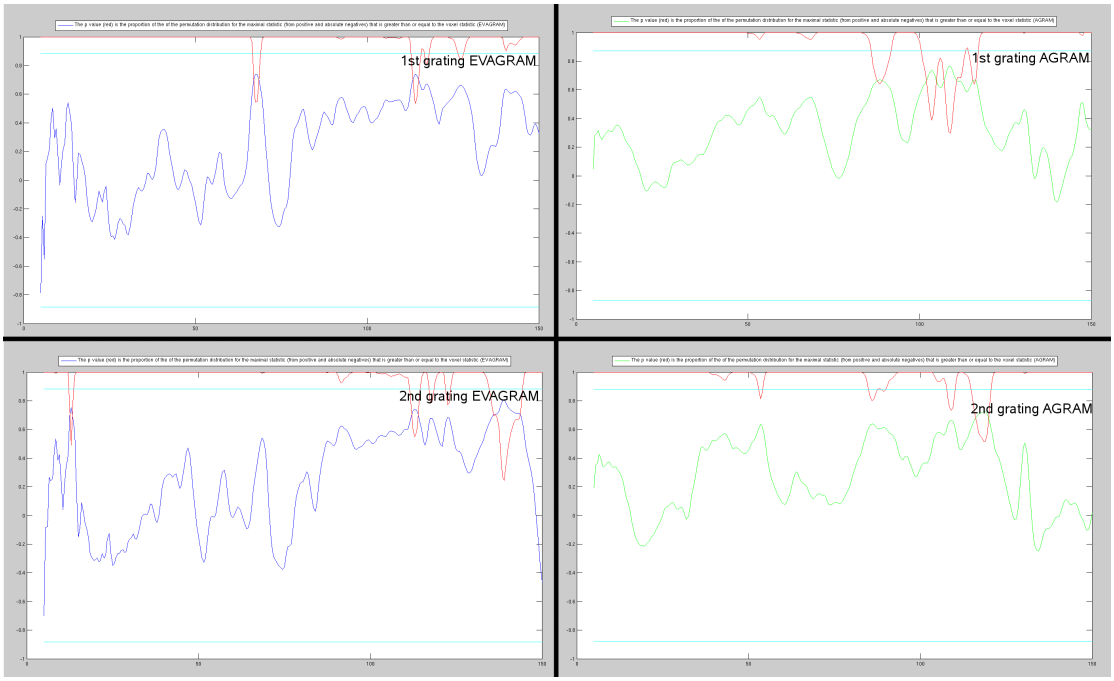

Figure 44: Oblique condition. These are the plots created for the oblique condition. Here the plots for every frequency show (in blue or green) at every specific frequency how power (from the Power vs. Frequency) correlates with behavioral results. The top left is for the 1st gratings evoked response (EVAGRAM), the top right for the 1st gratings induced response (AGRAM); the bottom left is for the 2nd gratings evoked response (EVAGRAM) and the bottom right for the 2nd gratings induced response (AGRAM). For these plots 10,000 permutations were used. In none of the four plots is the r-value is above the + threshold or below the – threshold so no r-values exhibit evidence against the null frequency hypothesis. All r-values have an n=10 (3 participant excluded). The p-value is in red.

4.3.3.3.4 Time-frequency ROI analyses

As the time-frequency analyses shown above did not reveal an oblique effect or any statistically significant correlations with behavior, we sought to improve our statistical power by averaging over time-frequency ROIs.

The logic here is that instead of looking for specific correlations with single time-frequency points, we instead search for the maximum response amplitude within the peri-stimulus time of 0-250 ms (for all 4 conditions) using a 4Hz wide search/averaging window.

This approach presumably will help to control for some of the known individual variability in the maximum response frequency. For example, in a study by Muthukumaraswamy et. Al. (Muthukumaraswamy, Edden, Jones, Swettenham, & Singh, 2009) displaying a grating with similar characteristics as our stimulus (they used a vertical square wave grating presented at the lower left quadrant of the visual display and subtended 4 degrees horizontally and vertically with the upper right corner of the stimulus located at 0.5 degrees horizontally and vertically from a fixation point) they report inter-subject variability of the peak gamma frequency with a standard deviation of 6.6 Hz.

Using a search window 4Hz wide, we scanned from 5-15, 15-30 and 20 -80 Hz to find the position within these frequency ranges that yielded the maximum response in the average EVAGRAM's and AGRAM's for both the cardinal and oblique conditions.

Cardinal results

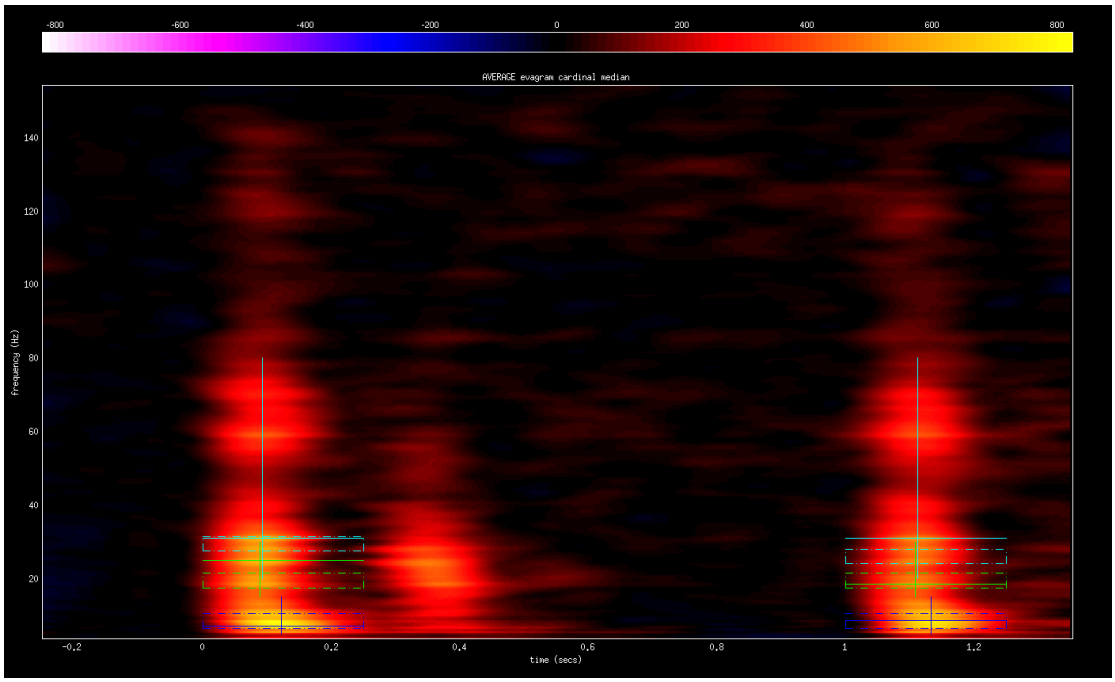

Figure 45: After scanning to find the region with the maximum sum activation (sum of values in an area of 4Hz height and for time periods the grating was on

so an area from 0 to 0.25 mseconds and 4Hz height and an area from 1to 1.25 mseconds and 4Hz height) we found the above maximum sum activation areas (blue is when searching from 5-15 Hz, green when searching from 15-30 Hz and cyan from 20 to 80). The intermittent lines outline the areas and the crosshair indicates the location of the maximum point. This plot is for the cardinal Evoked response.

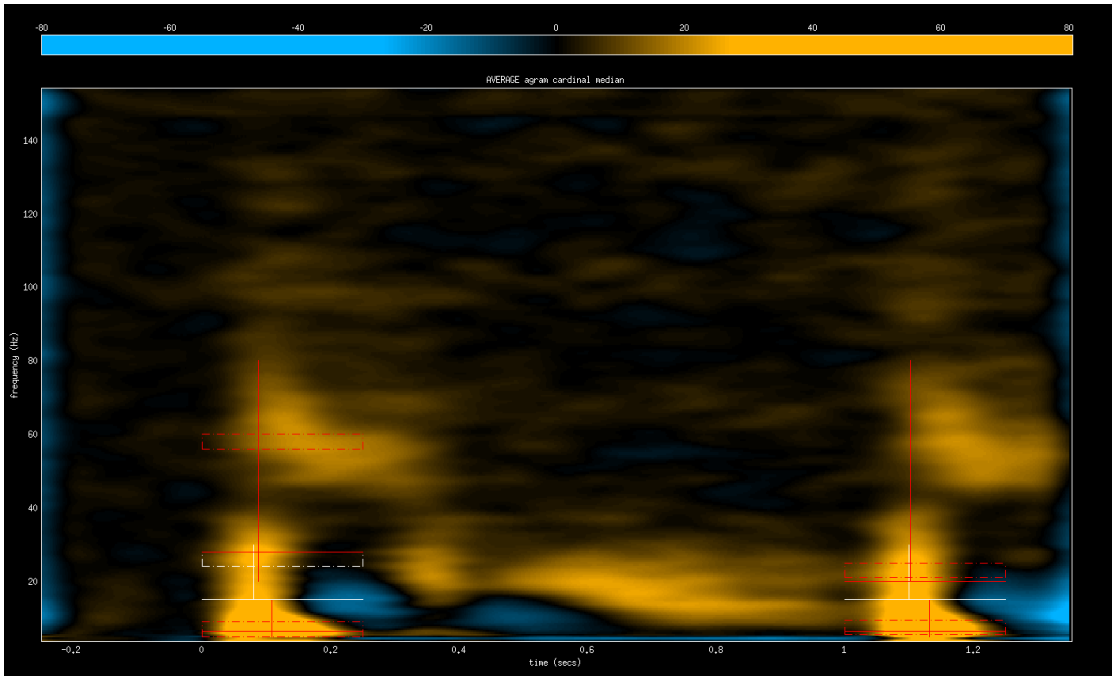

Figure 46: After scanning to find the area with the maximum sum activation (sum of values in an area of 4Hz height and for time periods the grating was on so an area from 0 to 0.25 mseconds and 4Hz height and an area from 1to 1.25 mseconds and 4Hz height) we found the above maximum sum activation areas (blue is when searching from 5-15 Hz, green when searching from 15-30 Hz and cyan from 20 to 80). The intermittent lines outline the areas and the crosshair indicates the location of the maximum location. This plot is for the cardinal induced response.

Oblique results

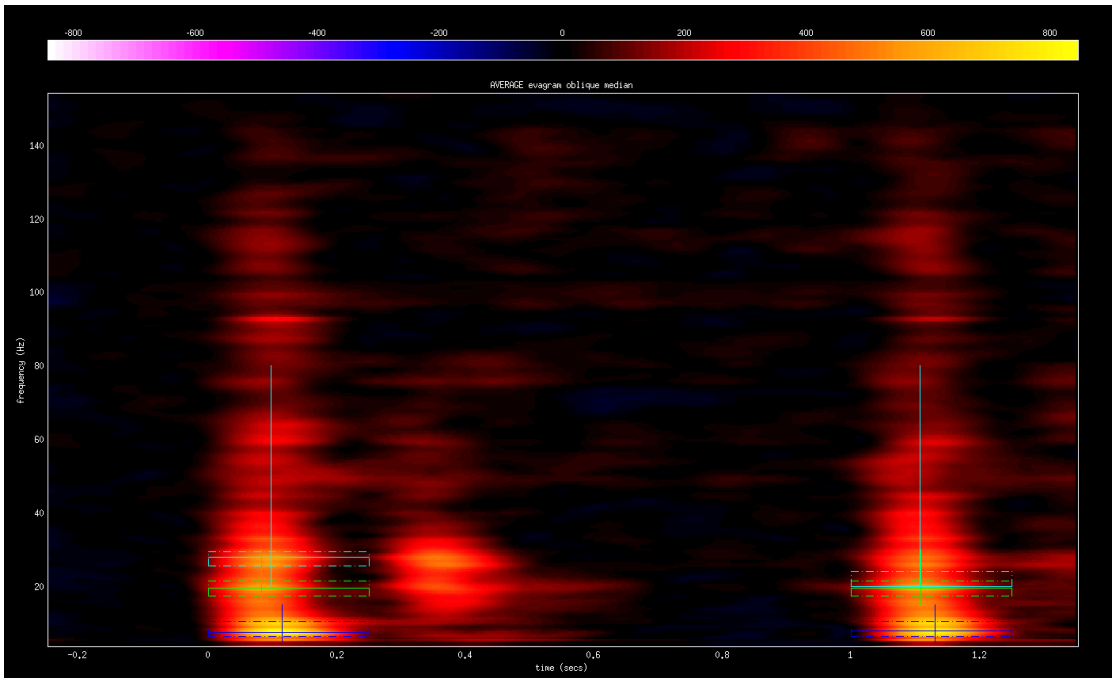

Figure 47: Again after scanning to find the area with the maximum sum activation (sum of values in an area of 4Hz height and for time periods the grating was on so an area from 0 to 0.25 mseconds and 4Hz height and an area from 1to 1.25 mseconds and 4Hz height) we found the above maximum sum activation areas (blue is when searching from 5-15 Hz, green when searching from 15-30 Hz and cyan from 20 to 80). The intermittent lines outline the areas and the crosshair indicates the location of the max. This plot is for the oblique Evoked response.

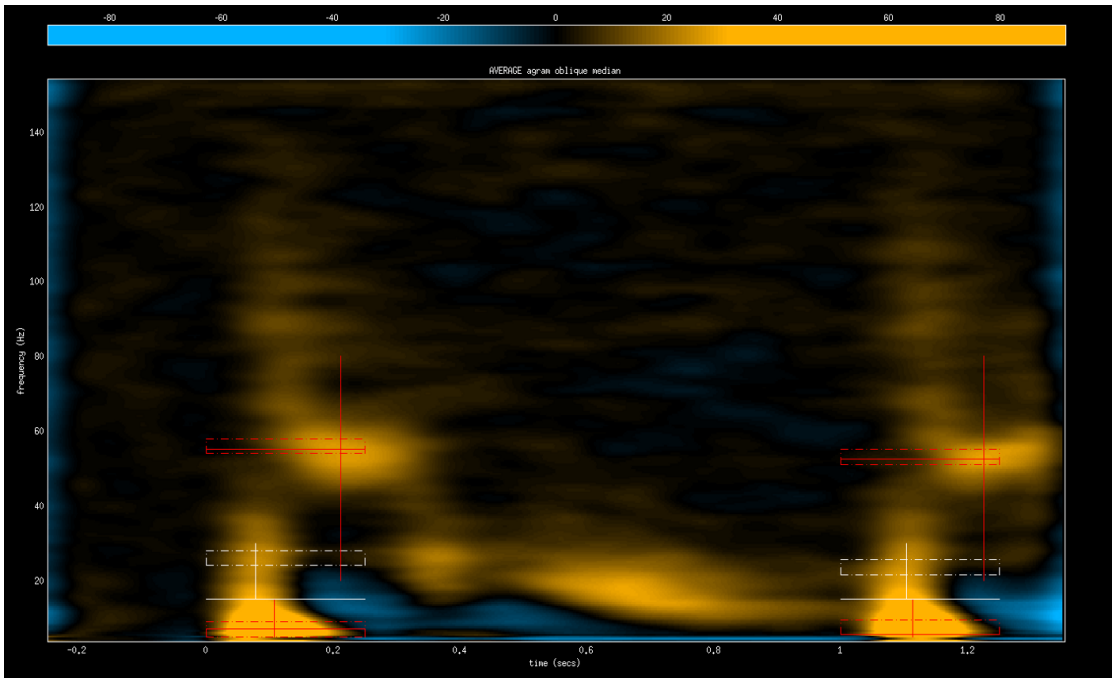

Figure 48: After scanning to find the area with the maximum sum activation (sum of values in an area of 4Hz height and for time periods the grating was on so an area from 0 to 0.25 mseconds and 4Hz height and an area from 1to 1.25 mseconds and 4Hz height) we found the above maximum sum activation areas (blue is when searching from 5-15 Hz, green when searching from 15-30 Hz and cyan from 20 to 80). The intermittent lines outline the areas and the crosshair indicates the location of the max. This plot is for the oblique induced response.

From the above average plots we found a maximum value within the ranges from 5-15, 15-30 and 20 -80 Hz and also the maximum area in these ranges.

The results are summarized in the tables below:

Table 8: In the ranges from 5-15, 15-30 and 20 -80 Hz we found the following values. The time of max and frequency of max relate to a single maximum value in each frequency range and the time and frequency at which they appear. The Max area column shows the 4Hz wide frequency window within which the largest average response was found.

CARDINAL

Range tested	Time of max	Frequency of max	Max area (height 4).
EVAGRAM			
5-15Hz (1st grating)	0.1221	7	6.5-10.5
15-30 Hz (1st grating)	0.0887	25	17.5-21.5
20-80Hz (1st grating)	0.0920	31	27.5-31.5
5-15Hz (2nd grating)	1.1331	8.5	6.5-10.5
15-30 Hz (2nd grating)	1.1081	18.5	17.5-21.5
20-80Hz (2nd grating)	1.1114	31	24-28
AGRAM			
5-15Hz (1st grating)	0.1087	6.5	5-9
15-30 Hz (1st grating)	0.0803	15	24-28
20-80Hz (1st grating)	0.0870	28	56-60
5-15Hz (2nd grating)	1.1314	6.5	5.5-9.5
15-30 Hz (2nd grating)	1.0997	15	21-25
20-80Hz (2nd grating)	1.1014	20	21-25

Table 9: In the ranges from 5-15, 15-30 and 20 -80 Hz we found the following values. The time of max and frequency of max relate to a single maximum value in each frequency range and the time and frequency at which they appear. The Max area column shows the 4Hz wide frequency window within which the largest average response was found.

OBLIQUE

Range tested	Time of max	Frequency of max	Max area (height 4).
EVAGRAM			
5-15Hz (1st grating)	0.1137	7.5	6.5-10.5
15-30 Hz (1st grating)	0.082	19.5	17.5-21.5
20-80Hz (1st grating)	0.0970	28	25.5-29.5
5-15Hz (2nd grating)	1.1298	8	6.5-10.5
15-30 Hz (2nd grating)	1.1081	19.5	17.5-21.5
20-80Hz (2nd grating)	1.1064	20	20-24
AGRAM			
5-15Hz (1st grating)	0.1070	7	5-9
15-30 Hz (1st grating)	0.0770	15	24-28
20-80Hz (1st grating)	0.2121	55	54-58
5-15Hz (2nd grating)	1.1131	5.5	5.5-9.5
15-30 Hz (2nd grating)	1.1031	15	21.5-25.5
20-80Hz (2nd grating)	1.2249	52.5	51-55

Separately, within each of these time-frequency ROIs, we correlated the peak oscillatory response for every participant with their behavioral threshold. as there are two grating presentations and three frequency ranges tested, we Bonferroni corrected the level of significance to $a = \frac{0.05}{6} = 0.0083$.

From the above frequency ranges the only one that was significant (with the Bonferroni correction) was when the latencies of the maximum values (for every participant) were correlated to the individual behavioral data for the

oblique condition trials for a frequency range from 17.5 to 21.5 Hz for the first grating appearance evoked response (EVAGRAM) (r = -0.78, p = 0.008). This is shown in Figure **49**. None of the correlations with amplitude were significant.

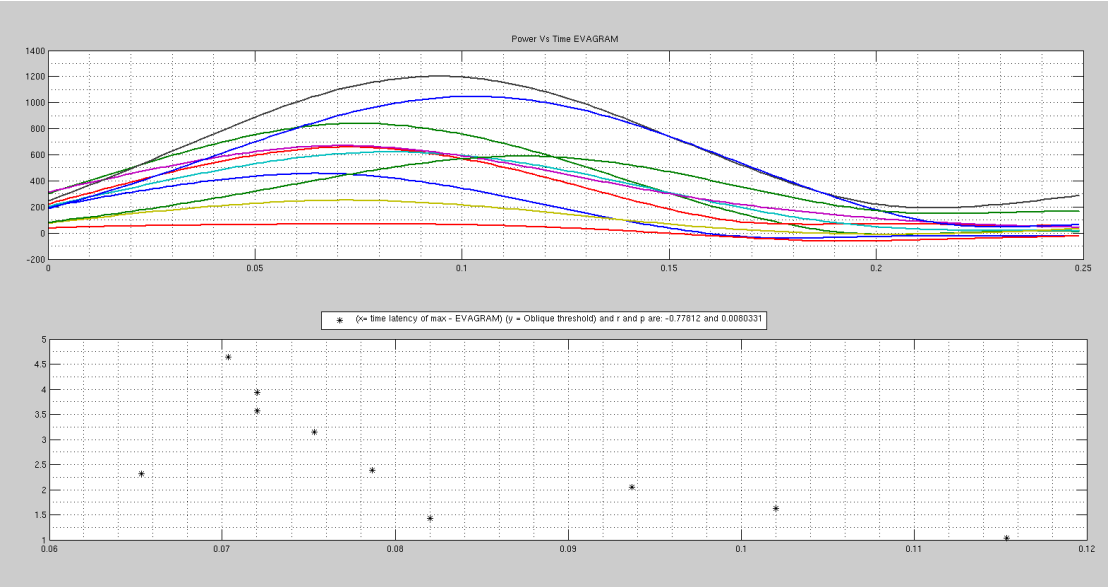

Figure 49: The top plot is the plot of power (EVAGRAM) to time for the first oblique grating appearance from 17.5 to 21.5 Hz (each color is one participant). The points below show for each participant the latency of the max value (x-axis, seconds) and y-axis shows the behavioural orientation discrimination threshold (degrees) for that participant.

4.4 Discussion

4.4.1 Summary of findings.

Eye tracker data

From **Figure 26**, by comparing number of trials gaze moved towards or away from the grating when the patch grating appeared, we see that from 13 participants, in the x-axis in 12 cases eye fixation moved towards the grating and in one case away while in the y-axis for 11 participant fixation moved towards the grating and for 2 participants there were more trials it moved away. From these findings we can see that the sudden appearance of a grating in most cases

resulted in a shift of eye-fixation towards the grating rather than away. From an observation of individual participant eye-tracking data we see that (appendix II) from the histogram of the mean fixation distances for every trial for individual participants, that for the x-axis in most cases the most frequent fixation distance in the histogram is away from fixation point (point 0 in the histogram) but in the opposite direction of where the grating is and in the y-axis there is only one case where most frequent mean trial fixation is positioned 1 degree or more towards fixation (the centre of fixation was 2.2 degrees from the circular grating centre). This indicates that participants were making an attempt to follow the instructions given (i.e. not look at the grating but at fixation), however in some cases in order to avoid looking at the gratings eye-gaze was not at the fixation point but in the opposite direction than the grating (this is more evident in the x-axis with 7 participants most frequent trial mean fixations being in the opposite direction than the grating. This was something we also found to be the case when testing the stimulus as in order to avoid looking at the grating, gaze could shift from fixation in the opposite direction than the grating in some cases. In this project we did not use any criteria for excluding participants based on their eye-tracking data but rather just wanted to have some knowledge of eye fixation and make sure participants did not ignore our instructions and just look at the centre of the grating (as this makes the behavioural task much easier). No explicit exclusion criteria were used with the logic that as fixation in most cases was maintained some bad cases would not have a big effect on the statistical analysis.

SAM analysis

In the group SAM analysis we found a significant main stimulus response effect for the effects of both the cardinal (Table 11) and the oblique conditions

(Table 10) (both the first and the second grating appearance) when performing the analysis at the frequency ranges from 30-70 Hz, 40 – 80 Hz, 40-60 Hz, and 60 to 80 Hz. Unfortunately and unexpectedly, we saw no evidence of differences between cardinal and oblique presentations, either for the first or second presentation.

For the working-memory/stimulus maintenance period, our analyses found significant effects for both cardinal and oblique conditions within the 15-25 Hz frequency range (section 4.3.3). However no significant differences were found when contrasting cardinal to oblique conditions.

When assessing correlations between behavioral thresholds and oscillatory response amplitudes, we found regions with a significant r value in the medial visual cortex for the first oblique grating appearance at 30-70 Hz (see Figure **30**) also again for the first grating appearance at 60-80 Hz (see Figure **31**) (however in this case none of the areas were in the visual cortex) and also for the second grating appearance of the oblique grating at 5-15 Hz (see Figure **32**) (not in the visual cortex however).

No such correlations were found in the working memory period i.e. although significant 15-25Hz power was found in the posterior cortex during this time-period, individual variability in its magnitude did not correlate with behavior.

We believe that it is significant that behavioral correlations are only found for the more difficult oblique condition and not the easier cardinal task. Similar results have previously been found in MEG/MRS/Orientation studies (Edden et

al.) and we also show the same dependencies on task-difficulty in the final experimental Chapter of this thesis.

Within the visual cortex, the only behavioral dependency found was a positive correlation with gamma amplitude in the 30-70Hz range, but only for the first presentation of the oblique grating. This positive correlation i.e. higher amplitude leads to worse performance is hard to explain – a negative correlation would have been expected.

A very speculative explanation might relate to *hyperexcitability* in the visual cortex. Previous work has claimed that strong gamma oscillations may be related to visual disturbances (Adjamian, Holliday, Barnes, Hillebrand, Hatjipapas, & Singh, 2004) and are reflection of the engagement of GABAergic processes to reduce response amplitudes. Failure of GABAergic inhibition may also lead to larger gamma responses. Recently it was shown that large visual gamma oscillations are present in photosensitive epilepsy patients, are particularly strong in drug-naïve patients and are normalized by anti-epileptic drugs [PERRY ET AL., 2014]. It may be, therefore, that participants with larger gamma responses have gain-control mechanisms that are not as well optimized as those with smaller responses and this may lead to poorer performance on this task.

Cortical areas outside visual cortex also appeared to correlate positively with behavioral thresholds i.e. higher gamma amplitude with poorer performance. Some of these may represent down-stream projections from visual cortex and hence also be due to hyperexcitability. Other areas might reflect task irrelevant regions such that people with more activity in these regions may be

less engaged/focused on the orientation discrimination task. Again these interpretations remain highly speculative.

Virtual Sensor analysis results.

For the time frequency analysis individual plots, initially we performed a simple averaging (section 4.3.3.2.1) of all individual plots of all the cardinal condition time frequency plots and for all the oblique time frequency plots (this was done for induced and evoked responses separately). From a simple inspection of these plots we found a peak in activation about 70 ms after stimulus onset.

Later we contrasted for each participant the cardinal to oblique condition (with a t-test and a permutation method to control for multiple comparisons) to look for significant differences (section 4.3.3.2.2). However, this did not reveal any areas on the spectrogram that were significant. Also, we tested to see, for every point in the time frequency spectrograms for every participant, if there were any correlations (4.3.3.2.3) with each participant's behavioral threshold and similarly this did not yield any significant findings.

Then, we took the power vs. time (the power averaged across the frequency range from 30Hz to 70Hz at each time point.. The mean power value from these plots was calculated for each participant (from the Power vs. time plots) and these values were correlated using Spearman rank correlation to the participant's behavioral data. No significant correlations were found. However, there was a trend for the latency of the evoked gamma responses to the first and second oblique conditions to be negatively correlated with behavioral threshold

($p<0.17$ and $p<0.04$) i.e. poorer behavioral performance was associated with faster responses.

Additionally, we correlated the time-average amplitude at each frequency to the behavioral threshold, and assessed significance using permutation testing, however again no significant correlations were found (this was reported in sub-section 4.3.3.3.3).

Finally we sought to improve our ability to detect significant correlations by searching using a moving 4 Hz window over the frequency ranges of interest. In each of the 5-15, 15-30 and 20 – 80 Hz ranges we found the region that yielded the maximum sum of average activation within the window. This analysis gave a significant (with Bonferroni correction) negative correlation with the behavioral data for the latency of the max value of the evoked response (of the oblique condition) from 17.5 to 21.5 Hz.

4.4.2 Interpretation and evaluation

SAM analysis.

Although main effects of stimulation were found, no significant contrasts were found therefore not showing any significant difference between oblique and cardinals in this study. The oblique effect is well documented and the fact that in this case we did not manage to find a significant oblique effect could be because the effect was smeared by feedback because of cognitive processes taking place during the discrimination task. As cognitive processes can have an effect on the visual cortex activation as demonstrated by the attention study of

Gandhi et al. (Gandhi, Heeger, & Boynton, 1999) where they report greater BOLD response when attention was directed to the contralateral hemifield, we wished to test if cognitive processes (working memory in this case) can have an effect on visual activation (keeping in mind however that the behavioral oblique effect is well documented). We contrasted cardinal to oblique for the working memory period (the period between the two grating appearances in every trial) however we did not manage to find any significant results. The lack of a significant result when contrasting cardinal to oblique during the working memory period could indicate that we can possibly rule out the case of working memory having an big effect on visual activation in V1 as there is little difference (as far as working memory processes are concerned) during the oblique and cardinal discrimination task. However, all of the null results demonstrated here could also be due to a lack of statistical power – a replication with more participants would be one way of addressing this problem.

When we tested for areas with activation that correlated with the behavioral thresholds of each participant we did manage to find visual areas that correlated to the behavioral thresholds (in the gamma frequency range, 30-70 Hz). Edden et al. reported that the thresholds for the obliquely oriented stimuli were found to negatively correlate with gamma frequency oscillations at a source location ($r = -0.65$, $p = 0.017$) (Edden, Muthukumaraswamy, Freeman, & Singh, 2009). This study did also manage to find a correlation of behavioral thresholds (this time the behavioral task was performed in the MEG scanner). In our experiment there was a positive correlation of discrimination task thresholds and gamma band amplitude (in a broad-band from 30 to 70 Hz) thus

the higher the discrimination task threshold the higher the gamma activity or higher activity was found for worst performance.

In our study we only found behavioral correlations for the oblique and not cardinal version of the task - this mirrors the findings of Edden et al., in which correlations with GABA and gamma frequency were only demonstrated for the more difficult oblique condition, and the results demonstrated in the final experimental chapter of this thesis.

In the study by Edden et al. (Edden, Muthukumaraswamy, Freeman, & Singh, 2009) GABA and gamma were found correlating with behavioral thresholds (interestingly both gamma and GABA are not significantly correlated with the behavioral thresholds for the cardinal condition). Maybe gamma correlates indirectly with performance, as Edden et al. (Edden, Muthukumaraswamy, Freeman, & Singh, 2009) suggest that gamma frequency is positively correlated with orientation performance through a mutual reliance to GABA and does not affect the task by itself.

We looked into the oblique effect with MEG while performing the task in the scanner and therefore any effects from working memory to the visual activation would show in the results. In the Edden et al. paper they look into the correlations of gamma and GABA with behavioral thresholds, however the participants viewed a static grating in the scanner (the behavioral testing occurred prior to the MEG scanning). By performing the discrimination task we try to see if we can replicate Edden et al. 's (Edden, Muthukumaraswamy, Freeman, & Singh, 2009) findings but having participants perform the task while in the scanner. This on the one hand has an advantage as it gives us insight on how cognitive functions (related to the discrimination task) could affect visual

cortex activation, on the other hand however this could just add complexity to an already complex story. It could be that performing a discrimination task while in the scanner may have some disadvantages and not be the appropriate approach at this point. Koelewijn et al. (Koelewijn, Dumont, Muthukumaraswamy, Rich, & Singh, 2011) report feedback processes taking place from the extrastriate for a static grating and probably the addition of cognitive processes during the task would be appropriate after more is known about these feedback processes.

4.4.3 Methodological criticism and proposed improvements.

In Koelewijn et al. (Koelewijn, Dumont, Muthukumaraswamy, Rich, & Singh, 2011) an inverse oblique effect was found in V1 (medial location). Here this same source location was used for source analysis. Unfortunately no inverse oblique effect was found. Maybe in this case, a possible radial bias (the preference of the visual system to orientations directed towards the center of fixation) was relevant here.

The fact that the inverse oblique effect reported by Koelewijn et al. (Koelewijn, Dumont, Muthukumaraswamy, Rich, & Singh, 2011) was found with the use of an oblique stimulus that was also tangential to the fixation point could indicate that when studying the peripheral oblique effect both cardinal and oblique stimuli must be tangential to fixation to avoid the radial effect confounding the oblique effect.

This is supported by the findings of my fMRI Chapter, in which the BOLD response in V1 to radial (i.e. 45 degree) and vertical (0 degree) stimuli was very similar.Taken together therefore, my fMRI and MEG findings suggest that the

tuning of bulk neural responses to orientation is not a simple oblique, or inverse-oblique effect.

Many of our participants reported that they found it difficult to understand what button to press to report clockwise or counter clockwise (as in their mind they had to first think about the rotation direction and then recall the correct button to press. To make the task easier, and a 'purer' measure of orientation discrimination, the task could be re-designed. Instead of using a sequential 2AFC paradigm, simultaneous presentation of 3 gratings with one of the gratings having a slightly different orientation could be used. Then, participants would simply have to indicate the "odd one out". This would not require stimulus maintenance between presentations and would not require a mental rotation to take place during the trials.

Finally, a key criticism of this study could also be that although thirteen participants did initially seem a sufficient number of participants, as the oblique effect is a well reported deficiency of the visual system for obliquely oriented gratings, it is possible that the increased statistical power of more participants may have allowed us to replicate the inverse oblique effect found by Koelewijn et Al. (Koelewijn, Dumont, Muthukumaraswamy, Rich, & Singh, 2011).

Applications and future directions.

Further analysis that can be done on this dataset.

Earlier it was reported that we tested to see if the behavioral thresholds of the participants correlated to the gamma activation in the visual cortex with the difference from the Edden et al. paper (Edden, Muthukumaraswamy, Freeman, & Singh, 2009) being that the behavioral task was performed while the participant

was in the scanner. This has the advantage that we can further analyze this dataset by labeling each epoch according to how difficult the orientation discrimination task was during that epoch (organize the datasets epochs in seven different levels with 1 being the easiest of the 7 different orientation differences and 7 the hardest) and then for each participant test to see if there is a correlation between how difficult the discrimination task was and gamma activation. This could be done both with the amplitude of gamma frequencies from 30 to 70Hz or alternatively correlate gamma oscillation frequency with performance to the orientation discrimination task and assess both inter-subject and trial-by-trial intra-subject correlations with the behavioral performance as Edden et al. (Edden, Muthukumaraswamy, Freeman, & Singh, 2009) suggest in their paper. Alternatively we could perform a median split (this can be done for cardinal and oblique) and see if the most difficult task trials have significantly different gamma activation. It would be expected that the oblique only would give a significant difference as in the Edden et al. paper it was the oblique trials that gave significant negative correlation between behavioral thresholds and gamma and thresholds / GABA (Edden, Muthukumaraswamy, Freeman, & Singh, 2009) while cardinal correlations did not reach significance. We also found a behavioral correlation only in the oblique condition which could mean that feedback from extrastriate areas are stronger for the oblique and therefore it could be that in studies on feedback processes (how gamma changes with threshold) only using a tangential (to avoid a radial bias) oblique grating would be a more effective way as we would have more trials on the oblique condition and therefore more statistical power to examine for correlations. Edden et al. finally report a training effect during the behavioral discrimination task (Edden,

Muthukumaraswamy, Freeman, & Singh, 2009) however it was only significant for the oblique condition. It could therefore also be interesting to test if the correlation of gamma and behavioral thresholds for the oblique condition remains after an extensive training session at the behavioral task before the scanning. This is the subject of my final experimental chapter.

In this study, eye - tracker data was recorded at a sampling rate of 250 Hz. Hsieh and Tse (Hsieh & Tse, 2009) demonstrated that changes in stimulus visibility were associated with changes in microsaccade rate and also with changes in human V1 BOLD response, as also animal experiments have shown that microsaccades modify V1 neuronal firing (Kagan, Gur, & Snodderly, 2008), (Leopold & Logothetis, 1998). In addition Siegenthalere et al. (Siegenthaler, et al., 2014) found that microsaccade rate decreases and microsaccadic magnitude increases with higher task difficulty. Interestingly Siegenthalere (Siegenthaler, et al., 2014) used a mental arithmetic task without visual stimulation, so the microsaccadic rate cannot be attributed to visual disruption. The sampling rate of our dataset is sufficient to detect microsaccades as we used the same sampling rate as (Hsieh & Tse, 2009), so it would be interesting to see if there is a relation of microsaccade rate with task difficulty and also a difference in microsaccadic rate in the oblique and cardinal condition, especially since as mentioned earlier microsaccade rate can have an effect on activation in V1 area. However, although as reported previously, task difficulty can have an effect on microsaccade rate (Siegenthaler, et al., 2014), to add controversy to the issue in another animal study by Chen et Al. (Chen, Martinez-Conde, Macknik, Bereshpolova, Swadlow, & Alonso, 2008) it was found that microsaccade frequency was not significantly different between easy and hard tasks.

Further directions in studying the oblique effect.

We only found a significant effect in the oblique condition, which could mean either that feedback processes take place only in the oblique condition only or (more likely) are stronger for the oblique stimuli. The fact that there is no significant correlation in the cardinal condition could be (as Edden et al. propose) because of a ceiling effect i.e. because performance was very good, variability was too low in order to give significant results. It would be better when studying changes in gamma in a discrimination task (or generally study feedback processes) to use a simpler paradigm (e.g. only oblique tangential orientations) to increase statistical power.

In a study looking into intra-individual repeatability of induced gamma oscillations and inter-individual variability of gamma oscillations frequency, bandwidth and amplitude, Muthukumaraswamy et al. (Muthukumaraswamy, Singh, Swettenham, & Jones, 2010) showed that both induced and evoked responses were very repeatable across recording session while for the induced gamma oscillations there was a large amount of inter-individual variability existed in frequency, bandwidth and amplitude. They report that (Muthukumaraswamy, Singh, Swettenham, & Jones, 2010) a salient feature of their dataset was that it shows a potential pitfall in grand averaging time-frequency spectrograms when looking at the gamma band as they say that the relative wide range of peak gamma frequencies and bandwidth shows that averaging across participants results in a blurring of the time-frequency plots which in turn can lead to less power when performing statistical tests on individual "pixels". They suggest (Muthukumaraswamy, Singh, Swettenham, & Jones, 2010) that the best approach here is extracting parameters of interest

(from each participant) and then statistically analyze these extracted parameters. Here, this was attempted (sub-section 4.3.3.3.4) however not by extracting individualized parameters of interest but rather selecting the optimal frequency range with a frequency width of 4 Hz under the assumption the 4Hz range with the maximum sum activation would include the most individual peak frequencies. In their paper Muthukumaraswamy et al. (Muthukumaraswamy, Singh, Swettenham, & Jones, 2010) report an individual variability in gamma frequency with a standard deviation 0f 6.6 Hz. By finding the rectangular area between the time intervals the stimulus was on and the frequency range of 4 Hz with the maximum sum activation we were hoping to catch the frequency range of 4Hz that includes the most peak frequencies of the participants. This was done mostly to explore the dataset and is rather exploratory than hypothesis driven. This analysis assumed that the frequency range with the most overall activation would probably include most of the peak frequencies however from a visual inspection of Figure **39** we can see each participant's (different color lines) peak frequency throughout the frequency range of 30 to 70Hz and they seem to be spread out from 30 to 70 Hz. Something we should have done is get from the power to frequency plots from the range of 30 to 70 Hz (Figure **39**) each peak frequency and then correlate each participant's peak frequency with their behavioral thresholds.

Using a set of predefined set of difficulty angles around the thresholds found by Edden et al. (Edden, Muthukumaraswamy, Freeman, & Singh, 2009) could possibly be a mistake as this would mean we would get a ceiling effect for participants that have a high threshold (are very bad at the task), while in cases where the participant had an exceptionally low threshold there would be a floor

effect. It could be that logarithmically adjusting thresholds around individual thresholds instead of the thresholds used in Edden et Al. (pretest each participant with a staircase paradigm and get their thresholds and adjust the orientation differences around individualized thresholds not the thresholds found by Edden et Al. (Edden, Muthukumaraswamy, Freeman, & Singh, 2009) as described in section 4.1.2 would be a better approach.

4.4.4 Conclusion

Neural synchronization has been shown to enhance the steady transmission of information through the cortex (Diesmann, Gewaltig, & Aertsen, 1999). Edden et al suggest that individuals with a higher gamma have a more efficient neural synchrony thus have enhanced stability and accuracy of perceptual grouping and thus have a better performance at the behavioral task. There are a number of studies proposing that there are fewer cells optimized to detect oblique orientations (Mansfield, 1974) (Li, Peterson, & Freeman, 2003) and also less cortical surface is used to represent oblique orientations (Coppola, White, Fitzpatrick, & Purves, 1998) (Wang, Ding, & Yunokuchi, 2003). Edden et al. (Edden, Muthukumaraswamy, Freeman, & Singh, 2009) suggest that these differences in cortical representation and activation are rather modest in analogy to the large differences that are detected in behavioral thresholds. A possibility Edden et al. (Edden, Muthukumaraswamy, Freeman, & Singh, 2009) suggest is that the difference of oblique to cardinal orientations may result from a top-down modulation from higher areas of the visual cortex. This is supported by findings by Liang et al. (Liang, Shen, & Shou, 2007) that suggest a neural mechanism responsible for the enhancement of neural oblique effect in area 17 via feedback processes from the higher order visual cortex. This is also what

Koelewijn et al. (Koelewijn, Dumont, Muthukumaraswamy, Rich, & Singh, 2011) propose as in their study they found both an oblique effect and an inverse oblique effect, with the inverse oblique effect appearing first at around 50 to 98msec (early evoked and sustained gamma) located in a medial location (encompassing V1) and a classical oblique effect (Koelewijn, Dumont, Muthukumaraswamy, Rich, & Singh, 2011) found at a later time (120mseconds) in both a medial location and a also a more inferolateral location. Super (Super, 2003) suggests that the primary visual cortex is involved in cognitive processes such as visual perception and that these neural correlates appear in the late part of the neural response to visual stimulation. It therefore could be that the initial inverse oblique effect found by Koelewijn et al. corresponds to initial "low-level" processing of the visual stimulus (thus at the low-level the oblique stimulus is favored) and the later classical oblique effect of the visual system shows the perceptually favored cardinal orientations.

In this study we did not find any oblique effect (significantly bigger cardinal effect compared to oblique) neither an inverse oblique effect. This is mainly because although the oblique effect is a well documented effect, effects such as the radial bias mentioned in a previous section (especially as the radial i.e. the favored orientation stimulus, in our case is oblique and the cardinal stimulus is tangential -so not the favored orientation according to the radial bias effect) may be blurring the oblique effect thus reducing our data's statistical power. This is precisely what we observed in the fMRI results presented in this thesis, suggesting a concordance between fMRI and MEG measures.

One other point that must be taken into account is that the inverse oblique effect is observed in an early time period according to Koelewijn et al.

(Koelewijn, Dumont, Muthukumaraswamy, Rich, & Singh, 2011) while in our analysis for the SAM analysis we contrasted oblique to cardinal for a time period from 0.10 to 0.30 seconds (the stimulus was on for 250msec) thus including in the analysis time periods for which, according to Koelewijn et al., both the inverse oblique effect and the classic later oblique effect may have taken place. It could therefore be that in the contrast of cardinal oblique the inverse oblique effect was hidden by the classical oblique effect and in order to detect the inverse oblique effect in the SAM analysis we should have limited the time interval of our analysis to the first 100 msec after stimulus onset.

5 Experimental chapter 4.

5.1 Introduction.

In a previous study of orientation discrimination Edden et al. (Edden, Muthukumaraswamy, Freeman, & Singh, 2009) demonstrated that the thresholds for detecting obliquely oriented stimuli were negatively correlated with both gamma oscillation frequency and occipital GABA concentration, but only for obliquely-oriented targets – the responses to vertically oriented targets were not correlated with either. The authors speculated that this might reflect a 'ceiling effect' as thresholds to vertical targets were approximately five times smaller. To date, this relationship between GABA concentration and orientation discrimination performance has not been replicated.

In addition, several studies on the behavioural oblique effect report a training effect that results in improvement of participant's performance at the behavioural task throughout the experiment (Schiltz, et al., 1999) (Schoups, Vogels, & Orban, 1995) (Vogels & Orban, 1985) (Fiorentini & Berardi, 1981) (Edden, Muthukumaraswamy, Freeman, & Singh, 2009). In a study on the training effect during a behavioural discrimination task (Fiorentini & Berardi, 1981), the percentage of correct answers rose progressively for up to 100 to 200 trials before levelling off (Fiorentini & Berardi, 1981). From this point, performance remained constant for weeks after testing, in the tasks that involved discrimination of complex gratings (Fiorentini & Berardi, 1981). This long-lasting effect of training effects on the sensitivity to grating orientation was also reported by Schoups et al. (Schoups, Vogels, & Orban, 1995) as they report

that the improvement in performance lasted for several months and also that improvement was more evident between daily sessions rather than within sessions (Schoups, Vogels, & Orban, 1995), possibly because fatigue would interfere with the learning effect.

This training effect has also been studied with imaging methods (Rauch, et al., 1997). Interestingly, Rauch et al. found that all seven subjects who manifested robust learning effects also showed significant activation in the putamen and additionally they found a pattern in which participants with the most robust reaction time advantage showed activation in the putamen while participants with a marginal time advantage displayed striatal activation restricted to the caudate nucleus (Rauch, et al., 1997). Additionally Schilts et al. (Schiltz, et al., 1999) have proposed that neuronal mechanisms playing a part in perceptual learning might rely on the nature of the feature in use in the discrimination task (Schiltz, et al., 1999). Training in tasks that require traits represented in topographic maps like e.g. sound frequency in the auditory cortex may result in map expansion (Schiltz, et al., 1999). However perceptual learning in tasks utilising higher-order features that are represented in ways other than topographic maps, such as orientation in the visual cortex, may rely on different mechanisms and therefore show a decrease of activation (Schiltz, et al., 1999). Schilts et al. in their PET study (Schiltz, et al., 1999) found extensive training to lead to decreased activity in the early visual cortex.

One more point of interest with the training effect is that it is not transferable to other orientations. Fiorentini and Berardi (Fiorentini & Berardi, 1981) found that when they used gratings perpendicular to the gratings used in the training session, or the grating spatial frequency was changed by one octave,

the perceptual learning was lost (Fiorentini & Berardi, 1981). For more subtle changes, however, such as orientation changes of 30 degrees or changes of the grating spatial frequency of ½ octave, Fiorentini and Berardi report that the training effect remained (Fiorentini & Berardi, 1981).

As shown a training effect has been reported during the study of the behavioural oblique effect. This training effect however seems to be limited to the obliquely oriented gratings as in a study by Edden et al. study (Edden, Muthukumaraswamy, Freeman, & Singh, 2009) a significant training effect was found during behavioural testing however only for an oblique angle. Edden et al. (Edden, Muthukumaraswamy, Freeman, & Singh, 2009) found that for a behavioural oblique discrimination task mean discrimination threshold for the rotation discrimination task fell from 2.3 to 1.8 degrees over three measurement sessions for the oblique orientation, however for the vertical grating the mean discrimination threshold remained essentially unchanged (0.55 to 0.54 degrees). This is in agreement with Vogels et al. (Vogels & Orban, 1985) as they report that orientation discrimination improves with practice for oblique orientations but not for principal ones (Vogels & Orban, 1985).

GABA spectroscopy offers the ability for in-vivo probing into neuroinhibition processes taking place in the cortex of both healthy participants and patients. The edited MEGA-PRESS technique (Mescher, Tannus, Johnson, & Garwood, 1996) (Mescher, Merkle, Kirsch, Garwood, & Gruetter, 1998) has developed into one of the most extensively used MRS approaches for estimating GABA, as it is easy to implement within already existing PRESS sequences (Mullins, et al., 2014) and allows for the suppression of overlapping molecules at much greater concentration, such as those from Creatine (Mullins, et al., 2014).

This leads to reasonable estimates of GABA concentration, but it is still known that the estimated concentration is contaminated by macromolecules (MM), which may contribute up to 60% of the signal (Rothman, Petroff, Behar, & Mattson, 1993). One widely accepted approach when reporting GABA is to therefore report GABA with macromolecule contamination as GABA+.

However, recently two approaches have been suggested for removing these co-edited macromolecules, the "pre-inversion" and the symmetrical suppression" methods (Edden, Puts, & Barker, 2012) with the pre-inversion method comprising of acquiring an extra MM-only acquisition obtained with pre-inversion which is then followed by excitation of metabolite T1 recovery at the null point (Edden, Puts, & Barker, 2012). The symmetric suppression method on the other hand takes advantage of the fact that the coedited at 3ppm MM signal is paired to spins at 1.7ppm, so that for the ON scans the editing pulses are applied at 1.9ppm and for off scans at 1.5 ppm. This way the editing pulses (for ON and OFF scans) are 0.2 ppm away from the macromolecule signal, which is inverted at the same amount in both scans, therefore the macromolecule signal in the difference spectrum is suppressed (Edden, Puts, & Barker, 2012). The symmetric approach is an approach that is gaining popularity which can be applied at 3 Tesla with the use of a slightly increased echo time (above the 68msec typical MEGA PRESS echo time) (Edden, Puts, & Barker, 2012) . This study suggested that an echo time of 80 msec allows more selective editing pulses to be used, allowing suppression of coedited macromolecule signal without significant reduction in the GABA signal. This ability to measure GABA without macromolecule contamination offers an interesting opportunity to examine if

behavioural findings with standard GABA+ protocols can be replicated with the macromolecule (mm) suppression protocols.

Both animal and modelling studies have demonstrated that GABAergic inhibition plays a key role in determining the orientation tuning of cells within visual cortex and it was this that motivated the original Edden et al. study in humans. However, it has also been recently suggested that GABA in the visual system may play a key role in perceptual learning.

For example, some interesting animal work has suggested that plasticity in the visual cortex of rats can be enhanced by a reduction of GABAergic inhibition (Vetencourt, et al., 2008) and that long-term potentiation (LTP) in the visual cortex of rats can be enhanced/promoted by the blocking of GABAergic inhibition (Artola & Singer, 1987). As plasticity and LTP should play a key role in learning across the brain, including perceptual learning within the visual cortex (Aberg & Herzog, 2012), this raises the possibility that people with lower GABA concentration in the visual cortex may show larger increases in performance over time, compared to people with higher GABA concentration.

Some support for this can actually be found in the original data from the Edden et al. paper. They found that visual cortex GABA and gamma oscillation frequency significantly negatively correlated with behavioural thresholds. These correlations however were not found for the much easier vertical oriented stimuli (Edden, Muthukumaraswamy, Freeman, & Singh, 2009)**.** A significant effect of training for the behavioural oblique condition was also reported however again this did not reach significance on the cardinal condition (Edden, Muthukumaraswamy, Freeman, & Singh, 2009). This was also the case for (as seen in Figure **50**) unreported results from the Edden et al. paper that show a

relation of GABA and training effect however only in obliquely oriented gratings. As the condition that gave a significantly negative correlation of gamma and GABA to behavioural thresholds (Edden, Muthukumaraswamy, Freeman, & Singh, 2009), was also the only condition in the Edden et al. study to give a significant training effect it is interesting to see if there is a relation between GABA and training (performance improvement at a discrimination task).

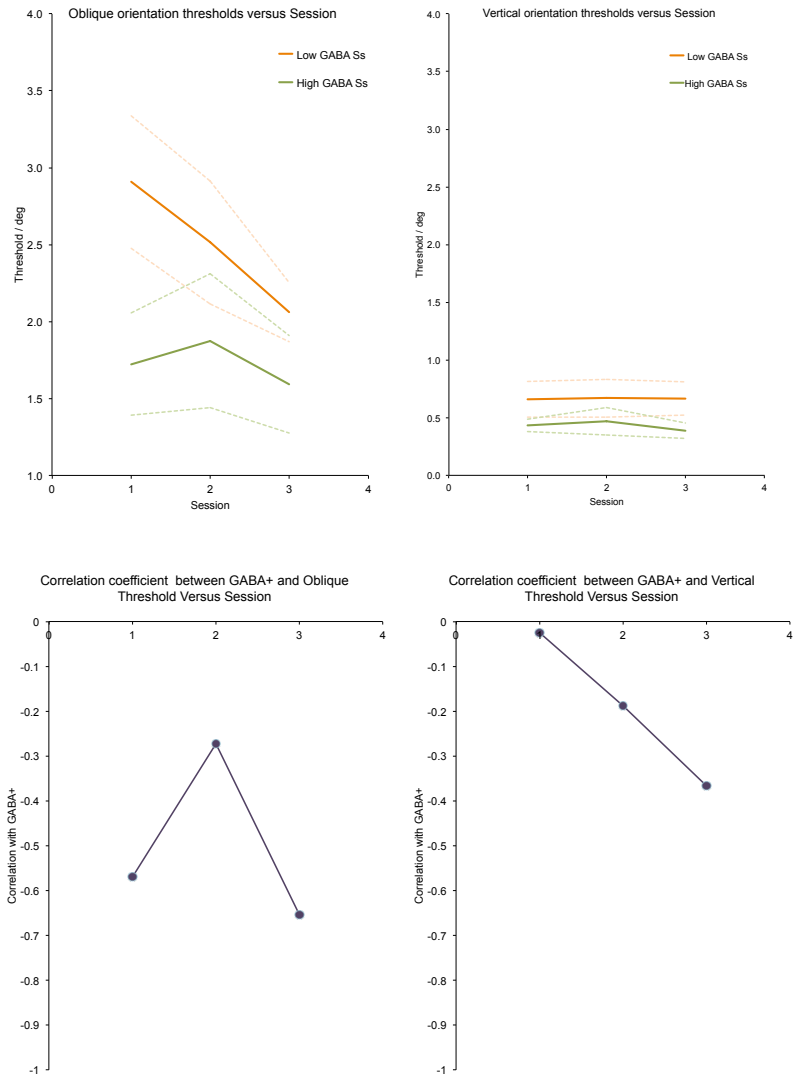

Figure 50: Unpublished new analyses of the data from the Edden et al. paper. A training effect was observed for the oblique condition while in the cardinal condition no significant training effect was found. When performing a median-split for participants based on GABA+, this training effect only appeared to be present for participants with low GABA+ concentration (upper panels). Across sessions, all thresholds showed a negative correlation with GABA+, but the

strength of the correlation varied and was stronger for the more difficult oblique condition (lower panels)

The work in this chapter therefore has several aims:

- Can we replicate the relationship between GABA concentration and orientation discrimination?
- Does this relationship hold when a macromolecular suppressed sequence is used?
- Can we observe training effects that are dependent on GABA+/GABAmm?
- If the grating orientation changes, does the training effect transfer to another orientation?

To do this we will use the same orientation discrimination threshold procedure used in the Edden et al. study. However, as no training effect was found for cardinal gratings in that study, here we only used oblique gratings thus increasing statistical power of the results. Schoups et al. (Schoups, Vogels, & Orban, 1995) report that improvement was more evident between daily sessions rather than within sessions. This according to Schoups et al. (Schoups, Vogels, & Orban, 1995) was in part a result of fatigue interfering with the learning effect, but there is a large amount of literature suggesting that sleep consolidation is important for perceptual learning (Maquet, 2001) (Fenn, Nusbaum, & Margoliash, 2003). It was therefore decided in this study to spread our experimental sessions across two tasks.

5.2 Method.

Spectroscopy: For GABA+, GABA-edited MR spectra were acquired using a 3 × 3 × 3 cm^3 voxel located medially in the occipital lobe with the MEGA-PRESS method (Mescher, Merkle, Kirsch, Garwood, & Gruetter, 1998) (Edden & Barker, 2007) . The lower area of the voxel was aligned with the cerebellar tentorium and placed so as to avoid containing the sagittal sinus while remaining inside the occipital lobe (see Figure **51**). For the scans we used: TE = 68 ms; TR = 1.8 sec; 512 transients of 2048 data points were attained in 15 min; a Gaussian editing pulse of 16 ms was applied in alternating scans at 1.9 ppm. We applied three hertz exponential line broadening and a high-pass water filter, and we generated the MEGA-PRESS difference spectrum. The unsuppressed PRESS water signal and the edited GABA signal at 3 ppm and were combined. By taking into account the editing efficiency and also the T1 and T2 relaxation times of GABA and water we found a concentration measure in institutional units. With the use of a linear fit of the baseline and a Gaussian fit to the peak (Marshall, et al., 2000) the integral of the GABA peak was automatically calculated. For GABA MM-suppressed (GABAmm) we used a similar MEGA-PRESS acquisition but with TE = 80 ms and editing pulses are 20 ms at 7.5 ppm. Two 15 min measurements were taken, one for GABAmm and one for GABA+. All the GABA spectra are displayed in Figure **52**. The GABAmm and GABA+ scan order was randomised. For the analysis of GABA, internally developed software was used and also the GANNET toolbox for MATLAB (Edden, Puts, Harris, Barker, & Evans , 2013). As GABA levels in female participants vary according to menstrual cycle (Epperson, et al., 2002) female behavioural testing took place either the day of GABA scan and the next day or the day before the GABA scan and day of GABA scan.

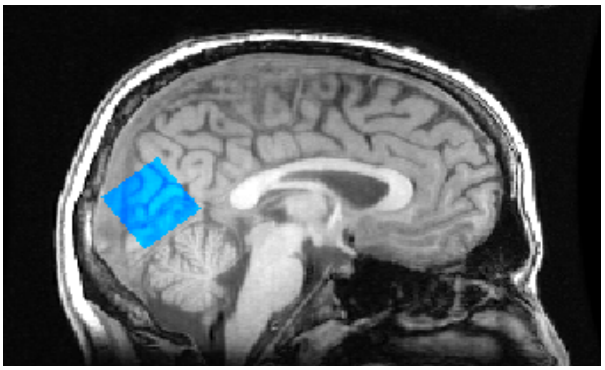

Figure 51: Demonstration of the voxel position used to measure GABA (participant 2).

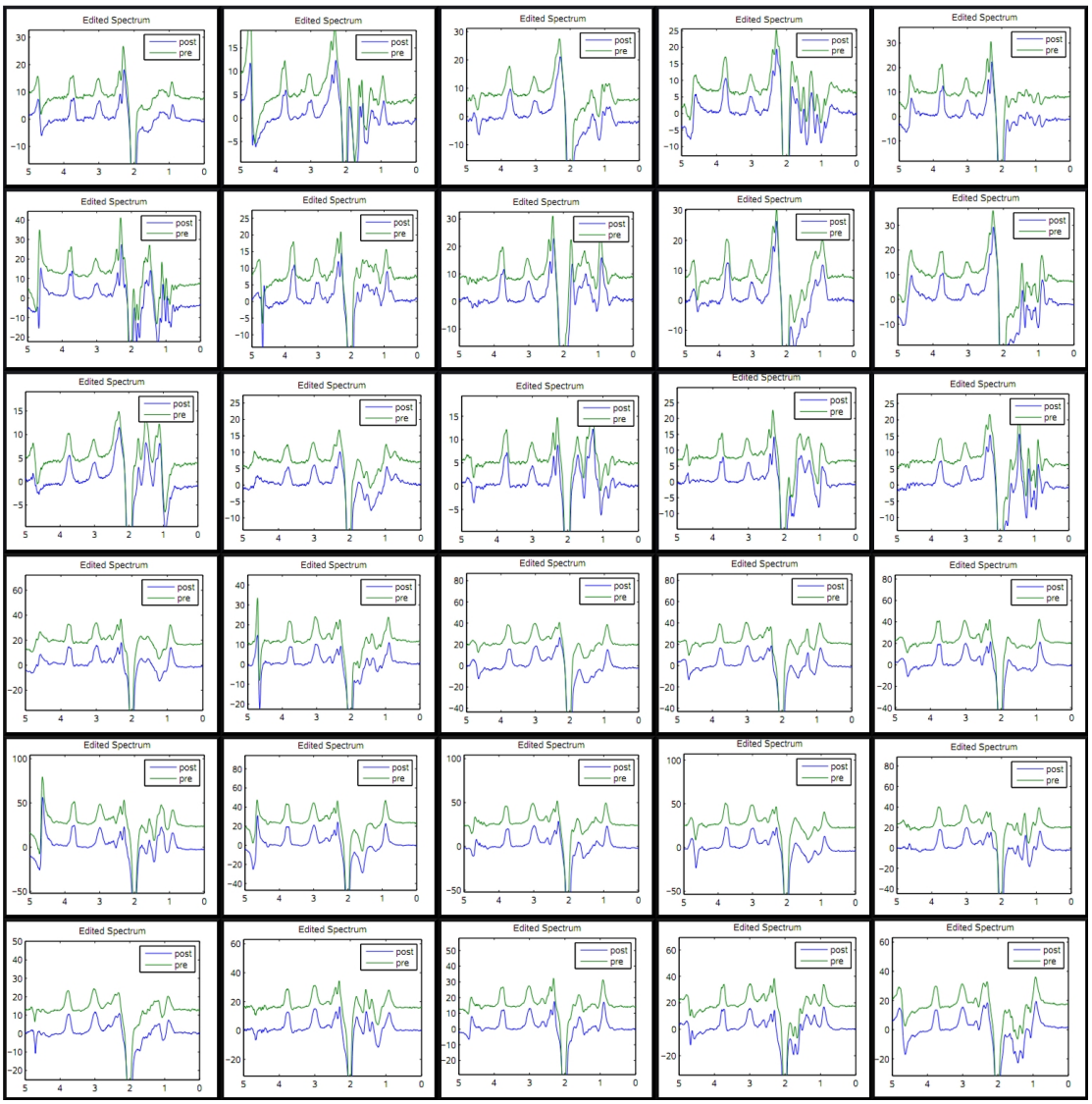

Figure 52: The GABA spectra for all participants. From left to right are participants 1 to 15 starting from the top row (and 4th from start for GABA-Plus). The top three rows are for the MMS-GABA and the bottom three for GABA-Plus.

Stimulus:

Here seven different orientation differences were used that were a logarithmic adjustment around the mean discrimination threshold found in the Edden et al paper (Edden, Muthukumaraswamy, Freeman, & Singh, 2009) for oblique orientations (1.8 degrees). This was done by taking 7 values of x from -1 to 2 in steps of 0.5 [so x =-1, -0.5, 0, 0.5, 1, 1.5, 2]. The orientation difference values (y) used for the method of constant stimuli was calculated by the formula: $y = 1.8 * 2^x$ (where x=0 the orientation difference was the mean found by Edden et al.). The grating (Figure **53**) was centrally presented with a diameter of 4 degrees and a spatial frequency of 3 cycles per degree. Also, a black frame with a 7 degree wide aperture was used and a central fixation for the grating off periods. After the participants response, the fixation changed color to green (for correct answers) or to red (wrong answers). For each discrimination examination there was a 500msec fixation only period followed by two 350 mseconds grating presentations separated by a random inter-presentation period (fixation-only) from 400 to 600 milliseconds and after, the stimulus froze while waiting for a response while finally there was a 2 seconds period after the response of only fixation. Each session consisted of 140 trials and after the 70 first trials the participant was given a small rest break. In each discrimination session the grating stimuli had a mean orientation of either 45 or 135 degrees (orientation was held constant across a trial).

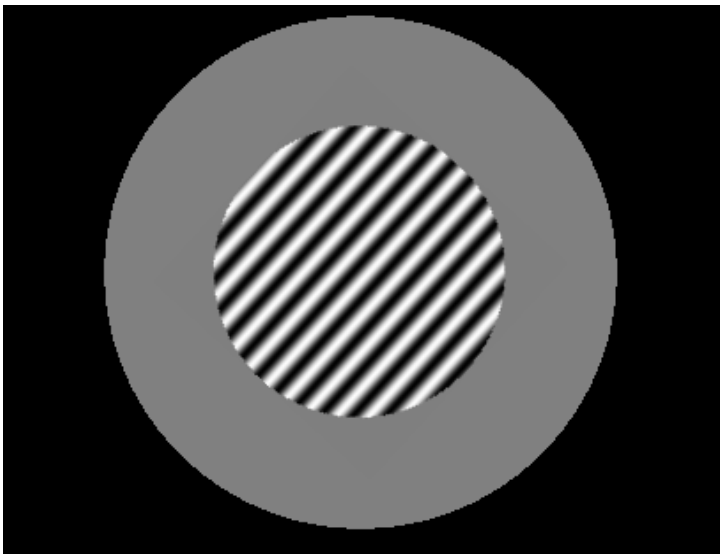

Figure 53: The centrally presented grating.

Each participant was examined for a total of 8 sessions. As we were interested to probe into sleep effects we had two experiments; a sleep consolidation experiment and a behavioral testing without a sleep interval in between first and last trial. As mentioned earlier in the introduction training effects are specific to orientation, therefore we had participants perform 3 trials on the first day at an oblique orientation (45 or 135 degrees) and the next day perform the last sleep consolidation trial at 45 or 135 degrees and for the no sleep trials (the remaining four trials) the grating orientation was switched to 135 or 45 degrees. The assumption is here that training effects (for a specific grating orientation) would transfer to the next day, however by switching the grating orientation, the last four trials would be unaffected by any training effects from the previous day (this is supported by literature in the introduction and inspected further in the results section). The sleep consolidation sessions were at 45 or 135 degrees while for the trials with no consolidation gratings were at 135 or 45 (the initial session's orientation was randomly chosen with

half participants getting the 45 degrees grating first). The design of the experiment can be seen in Figure **54**.

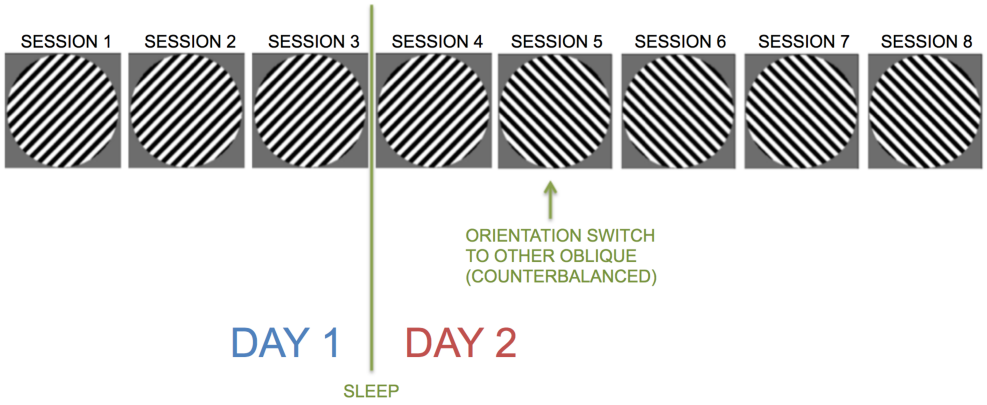

Figure 54: The order of sessions can be seen in this figure. Session 4 would potentially benefit from sleep consolidation, while Sessions 5-8 would not.

The stimulus was presented with MATLAB (7.8.0.347; 32-bit) using the psychophysics toolbox extension (Brainard, 1997) (Pelli, 1997). Analysis of statistics on the behavioral results was done with SPSS version 20. For each separate session, each participants' the percentage correct performance was calculated at each orientation difference. This data was fitted using a Weibull function and based on this fitted curve, the orientation difference needed to yield 70% correct performance was estimated. Weibull plots were fit using the modelfree toolbox 1.1, Zychaluk K., Mathematical sciences department, University of Liverpool (Żychaluk).

Participants: 15 participants with normal or corrected to normal vision were tested (9 male and 6 female) with age mean = 30.07, sd = 5.28. All people that participated in this study were required to sign informed consent forms and

the procedures were approved by the Ethics Committee of the School of Psychology , Cardiff University.

5.3 Results.

5.3.1 A comparison of GABAmm and GABA+

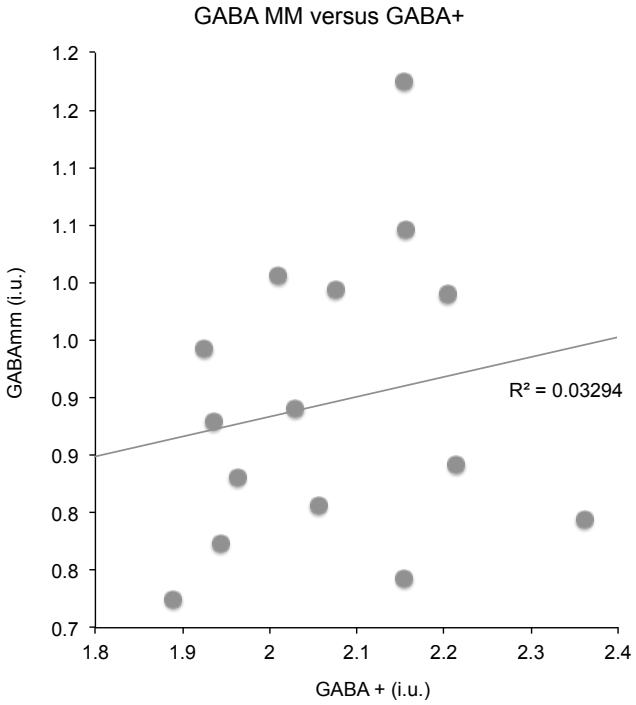

Figure 55: The relationship between GABA+ and GABAmm for each participant.

On average, GABAmm concentration was 43% of the GABA+ concentration (standard error 2%) for each participant, which is line with previous findings (Rothman, Petroff, Behar, & Mattson, 1993).

Surprisingly, no correlation was found between the GABA+ and GABAmm measurement (Figure **55**). This indicates that the two measures are providing independent measures, one of which, presumably is more related to GABA than

the other. For this reason, we will present results separately using both measures.

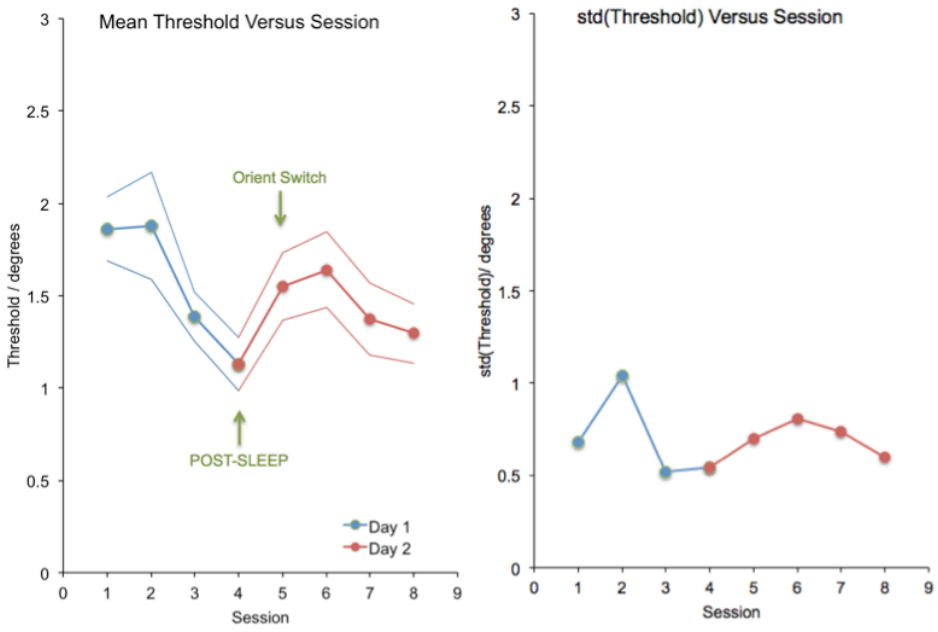

Figure 56: mean behavioural thresholds plotted versus session (left panel) and the standard deviation of this mean across participants versus session (right panel). Thin lines indicated the standard error on the mean.

5.3.2 Analysis of psychophysics data.

Five psychophysics sessions (out of a total of 120: 15 participants x 8 sessions) had to be discarded due to a poor Weibull function fit to the data. All analyses shown here are therefore from a total of 115 sessions. An analysis of behavioural performance versus threshold is shown in Figure **56**. In these figures larger thresholds mean poorer performance. There is a clear improvement in performance over Day 1 and this is preserved after sleep. There is also a clear 'switch cost' when performance worsens after the switch to the second orientation before performance appears to improve again. The variance across

the group also seems to follow a similar pattern i.e. when group performance is poor, the variance across the group is larger.

5.3.3 Dependency on GABA+ and GABAmm.

We examined how these thresholds depended on GABA+ and GABAmm and this is shown in Figure **57**.

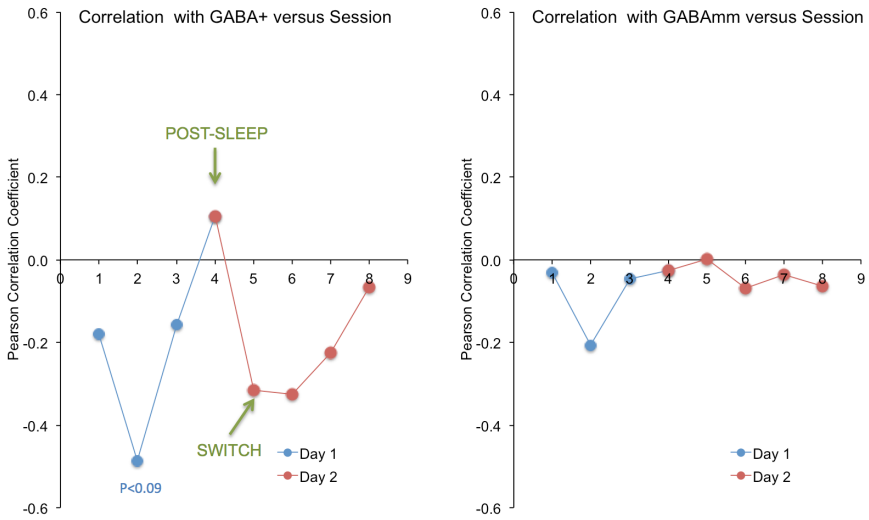

Figure 57: Correlation between GABA+ and behavioral threshold, plotted against session (left panel). The right panel shows the same plot, but for the correlation between GABAmm and behavioral threshold.

The results indicate that there is a tendency for correlations with GABA+ to be negative i.e. the higher the GABA+ concentration, the better the performance. This is true for Sessions 1,2,3, 5, 6, 7 and 8. None of these individual pairwise correlations reach statistical significance, but session 2 shows an uncorrected trend of $p<0.09$. Note that the key result for the previous Edden et al. paper was a negative correlation between GABA+ and oblique orientation discrimination performance, so this study provides some support for a replication of this finding.

Interestingly, the only correlation which was not negative for GABA+ was from the first session after sleep.

In contrast, GABAmm showed no apparent correlations with behavioural performance, although all the correlations found were slightly negative.

One thing that can be observed in Figure **57** is that, for GABA+, the correlations appear to follow the shape shown for the thresholds themselves in Figure **56** i.e. when average performance is poor for the group, negative correlations with GABA+ are the strongest. This can be explored further by plotting the threshold-GABA correlations against the threshold for all eight sessions – this is shown in Figure **58**.

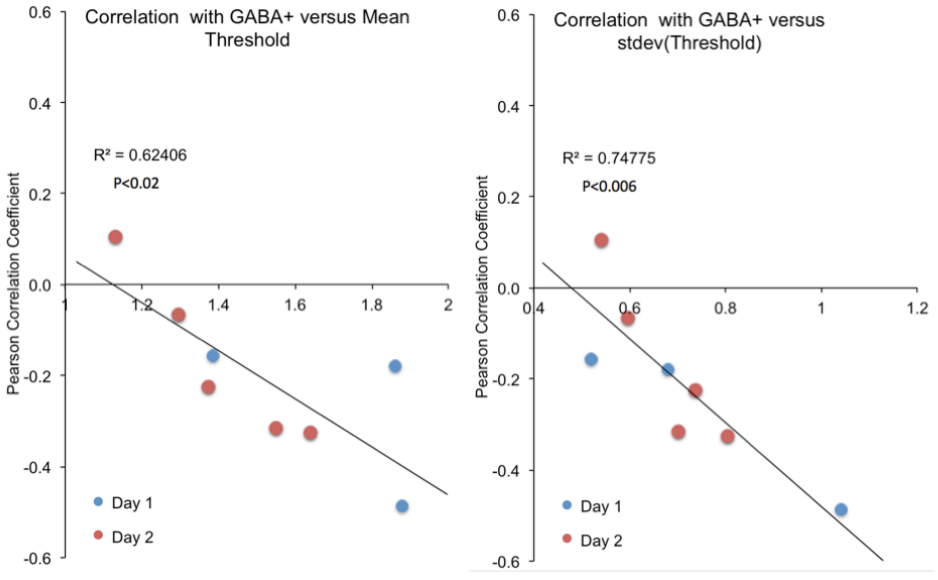

Figure 58: Plots of the correlation between behavioural threshold and GABA+ versus mean threshold across the group (left panel) and the standard deviation on this mean threshold (right panel). Each dot represents one of the eight experimental sessions, colour coded for Day.

Figure **58** demonstrates strong correlations between the GABA+ correlations and both the mean threshold and standard deviations on this mean. This indicates that the strongest negative correlations are for sessions in which mean performance is worst (high mean threshold) and when there is most variability across the group. This again fits with the previous Edden et al. finding in which correlations between GABA+ and performance were not found for the easiest version of the task i.e. when the target was vertical rather than oblique. Interestingly, in this study, we found similar dependencies for the GABAmm correlations even though these correlations are very much weaker than for GABA+ (Figure **59**).

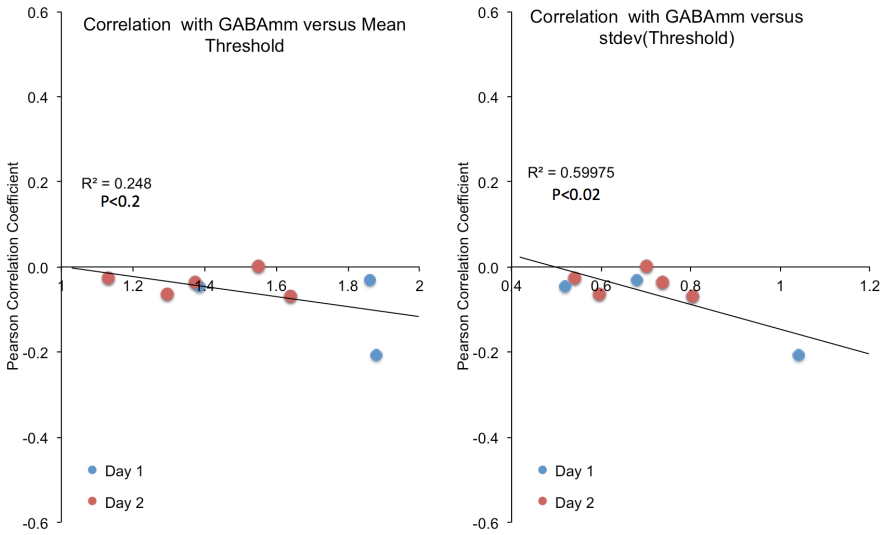

Figure 59: Plots of the correlation between behavioral threshold and GABAmm versus mean threshold across the group (left panel) and the standard deviation on this mean threshold (right panel). Each dot represents one of the eight experimental sessions, color coded for Day.

5.3.4 Training Effects: Dependency on Sleep, Orientation and GABA.

To quantify training effects we used the percentage change in threshold for each participant, referenced to the very first session. As there is a 'switch cost'

we treated each orientation separately – Orientation 1 will be the first orientation each participant was trained on. Orientation 2 will be the second, on Day 2. Figure **60** shows these percentage difference scores plotted as a function of Session.

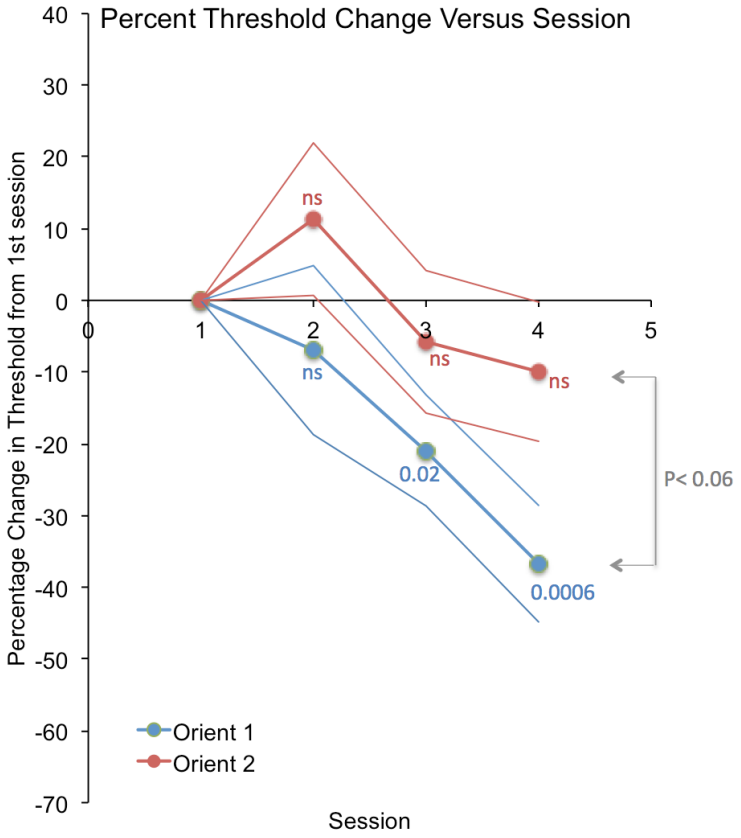

Figure 60: Training effects, plotted as mean percentage change over sessions. Thin lines are the standard error on the mean. Labels next to each data point show the p-value for the training effect.

There is clear evidence of improving performance over sessions and this is most pronounced for the first grating orientation (blue). None of the effects for the second orientation (red) were significant. Interestingly, the strongest training effect ($p<0.0006$, uncorrected) was for the first session after sleep, which was the last session for the first grating orientation. This suggests that sleep at least preserves, if not deepens, performance improvements on this task.

We can estimate the effect of sleep consolidation by pairwise comparing the difference in performance, just for Orientation 1, between Sessions 2 and 3 with the difference between Sessions 3 and 4, which spans a period of sleep. A paired-t test revealed no significant difference in the magnitude of these differences. However this is not a strong test of sleep consolidation as it assumes that the overall rate of performance improvement would have been constant if sleep had not occurred, which we simply do not know. An alternative test is to compare the performance improvement in the very last sessions of Orientation 1 with that of the very last session of Orientation 2. These are the end-points of the blue and red curves in Figure **60**. This is of interest because only Orientation 1 had a period of sleep. Here, a paired T-test revealed a trend towards increased performance improvement for Orientation 1 ($p<0.06$ uncorrected). Again, this is not a strong test of sleep effects as it is possible that participants had simply received all the available benefit of training from earlier in the experiments, irrespective of whether sleep occurred or not. In fact, looking at Figure **60** this appears to be the case. The only training effects that were significantly different from zero were the third session for Orientation 1 ($p<0.02$, uncorrected) and the third session for Orientation 1 ($p<0.0006$, uncorrected), suggesting that most of the training effects were gained from this first grating orientation.

5.3.5 The relationship between training effects and GABA concentration.

Initially we performed a median-split of participants (8 and 8) based on the GABA+ measure. The training effects are plotted in Figure **61**.

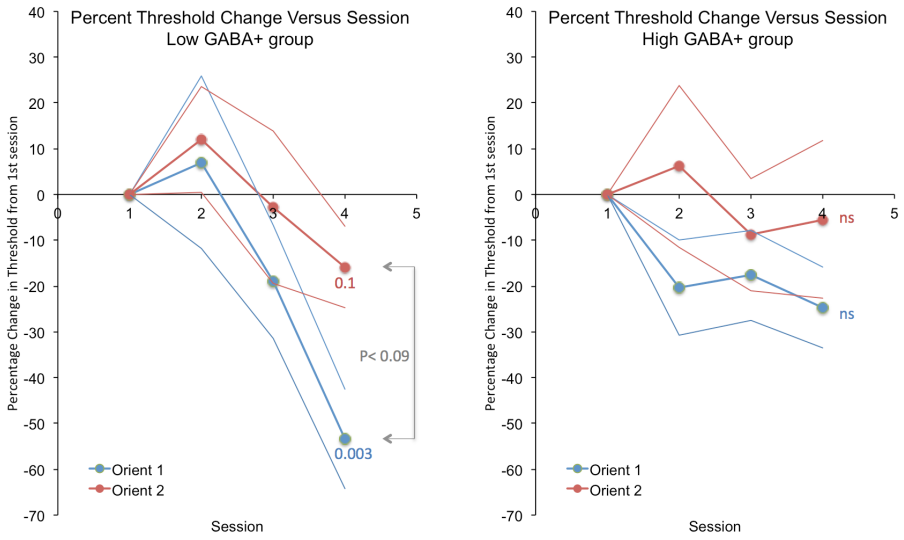

Figure 61: Training effects, plotted as mean percentage change over sessions, using a median-split in low-GABA+ and high-GABA+ groups. Thin lines are the standard error on the mean. Labels next to each data point show the p-value for the training effect (non-significant if not present).

Figure **61** indicates that there is a difference between the two groups with only the low GABA+ group demonstrating a clear training effect for Orientation 1 ($p<0.003$, uncorrected) and a trend for Orientation 2 ($p<0.1$, uncorrected). No significant training effects were observed for the high GABA+ group.

This can further be explored by examining the correlation between GABA+ and training effects, measured as the percentage change difference in threshold between the last and the first session for each orientation (Figure **62**).

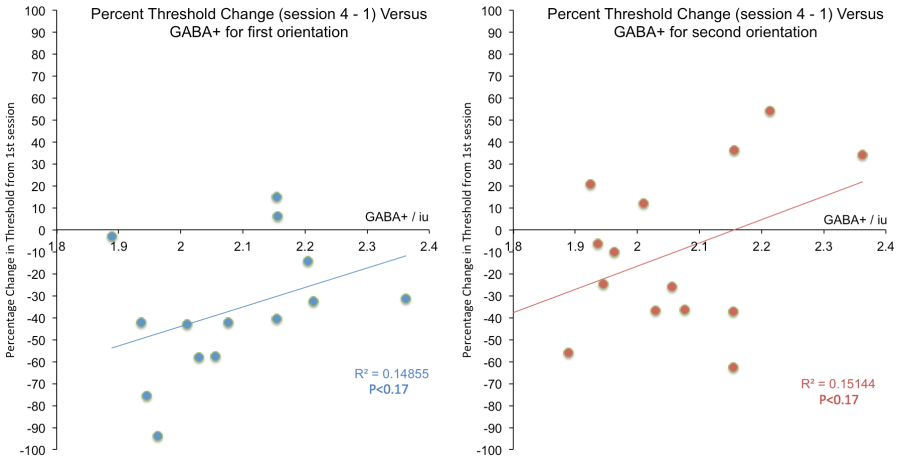

Figure 62: Correlations between training effects and GABA+ concentration for the first grating orientation (left panel) and the second orientation (right panel).

For both orientations, there is an apparent trend to positive correlation between the change in threshold over the experiment and GABA+ such that people who have higher GABA concentrations demonstrate less of a training effect (both $p<0.17$, uncorrected). No such dependency was observed for the GABAmm measure.

5.4 Discussion.

GABA+ and GABAmm are both used for the quantification of GABA in a specified voxel area, the difference being that GABA+ has an additional "contamination" of other macromolecules e.g. Creatine. The fact that GABA+ and GABAmm do not correlate indicates that GABAmm (GABA with macromolecule suppression) concentration in an individual and GABA+ are to some extent unrelated measures (although both contain GABA). Edden et al. found that GABA+ is negatively correlated to orientation discrimination (oblique) and in this study we find a similar result for GABA+ but surprisingly this is not the case with GABAmm. Ende et al. (Ende, et al., 2012) report decreased GABAmm in

females with borderline personality disorder (BPD) in relation to healthy females however this would have been missed if only GABA+ sequences were acquired. So, in Edden et al. and this Chapter, GABA+ "predicts" performance while in Ende et al. it is GABAmm that has the more predictive power. The obvious implication is that in the Edden et al. study and the work presented here it may be the macromolecules themselves that are linked to orientation discrimination performance, although why that may be the case is unclear as we simply do not know what the precise make-up is of these macromolecules. It is of course possible that individual variability in these macromolecules is functionally relevant for behaviour. Alternatively, because the GABAmm sequences are relatively new, and have not been used in many studies linking behaviour to GABA, our null findings may reflect a problem with this experimental approach.

The increased training effects for low GABA+ appear consistent with Edden et al.'s unpublished results (Edden, Muthukumaraswamy, Freeman, & Singh, 2009) that found a training effect for low GABA+ but not high GABA+ participants using a similar protocol to the one used here (see Figure **50**). The fact that the stronger training effect for low GABA+ participants can not be replicated when the median split is based on GABAmm protocols could again be an indication that the strength of the training effects could be affected not only by GABA but rather from the combination of GABA and macromolecules contaminating the GABA measures in GABA+ protocols.

Plasticity in the visual cortex is enhanced by the reduction of GABA inhibition (Vetencourt, et al., 2008), which perhaps would lead us to predict that lower GABA+ participants would show a stronger training effect, which is

consistent with both the Edden et al. result and the work in this Chapter. It therefore could be that participants with lower GABA+ have a better ability (better plasticity) to improve behaviourally. However, as shown in Figure **58**, there are negative correlations between threshold and GABA+ in the very first experimental sessions i.e. before training. This means that it is important for future studies to disentangle the effect of GABA on baseline performance at behavioural tasks from its effect on the ability to improve at a behavioural task.

The fact that the standard deviation throughout training reduces indicates that individual differences decrease through the training sessions and it could be that inhibition has an advantage in cognition and high GABA means that best performance is reached without training and as low GABA participants train they eventually compensate for the disadvantage they initially have (therefore the standard deviation drops).

Stated differently, it could be that each individual has an optimal performance level on this task, however low GABA participants need more training to reach this optimal performance (this is why variance reduces with training i.e. once optimal performance is reached by all participants).

Although interesting we still must address the fact that this effect is not found using GABAmm. Is it GABA or an additional co-edited macromolecule responsible for the fact that low GABA+ participants show stronger training?

Here we found that for low GABA+ participants there was a stronger increase in behavioral performance after sleep – perhaps suggesting a role for sleep consolidation, particularly for this group. However, this cannot be demonstrated unambiguously here as the task design was identical for all participants. So the pattern in threshold improvement that we saw may have

happened even if no sleep had occurred. The only way to have clearly demonstrated a sleep effect would be to have a design in which all eight sessions took place in some participants with sleep, and some participants without sleep.

What we can say is, however, that performance is preserved after sleep and training seems to transfer overnight. In addition there appears to be a switch cost when the grating orientation switches to the other oblique. Looking at Figure **56**, this "switch cost" does not return the mean threshold to the same level as for the first orientation, suggesting that some training is preserved/transferred by an orientation switch and some is not.

The behavioral training to the orientation discrimination task involves a range of behavioral skills and neuronal processes and it could be that some of these skills survive the 90 degree switch of the grating. The case is that, however some of the training seems to be present in the first trial of orientation 2 (in Figure **56** the point of orientation switch). An stated above, an improved design would examine behavioural training effects either with a sleep consolidation period or without. It could be that either when the grating switches orientation (at the 5th trial) part of the training effect survives, or more likely, amelioration in the behavioral discrimination task is dependent on a mixture of cognitive (neuronal) processes and it is that some of them survive the 90 degrees switch of the grating stimulus i.e. skills that are relevant to the discrimination of oblique gratings but not dependent on a specific orientation.

GABA measures rely on a bulk estimate of GABA concentration from a 3 cm x 3 cm x 3 cm voxel in the occipital cortex, which is measured over a period of 15 minutes approximately. This allows us a bulk measure of GABA concentration in the visual cortex however this does not allow one to measure any time

fluctuations of GABA in the visual cortex and to quantify with any precision GABA / coedited macromolecules in areas of possible interest. Conclusions can be made for individuals regarding the overall GABA concentration in the visual cortex, however no precise effects of GABA can be seen. As a number of cognitive processes take place in the human visual area, and we only take a measure of GABA at a specific time, it is difficult to link GABA levels to specific training effects during the task.

As both MEG-measured gamma oscillations and GABA negatively correlate with behavioral measures and also resting GABA concentration is a predictor of gamma oscillations (Muthukumaraswamy, Edden, Jones, Swettenham, & Singh, 2009) it would be interesting to examine if the relation of GABA and gamma activation can be replicated with GABAmm measures. This is especially interesting because a recent study has cast doubt on the GABA+ to gamma frequency relationship (Cousijn, et al., 2014). Using GABAmm measures may help to shed some light on this controversy, either confirming or refuting the relationship between bulk GABA estimates and electrophysiological signals.

Finally, there are several other neurally-relevant chemicals that we could investigate using MRS. One of these is Creatine (Mullins, et al., 2014) which plays a role in the homeostasis of brain energy (Rae, Digney, McEwan, & Bates, 2003). An oral supplementation of Creatine has been shown to have a significant positive effect on working memory and intelligence (Raven's Advanced Progressive Matrices) (Rae, Digney, McEwan, & Bates, 2003) which shows that brain energy capacity can have an effect on brain performance (Rae, Digney,

McEwan, & Bates, 2003). Interestingly for our task, Creatine can act as a partial GABAA agonist affecting GABAergic neurotransmission (Neu, et al., 2002).

An interesting replication of the study we performed, therefore, would be to have participants perform the same behavioural task we had in this experiment with one group taking a Creatine supplement to see if Creatine can enhance performance on this visual discrimination task. At the same time we would be able to see if baseline Creatine concentration (as assessed with MRS) was predictive of performance and/or training effects and how this baseline concentration interacted with Creatine supplementation.

6 General Discussion

Introduction

Throughout this thesis I have used multiple experimental techniques in humans, to try and reveal the neurophysiological basis of the oblique effect, the comparative deficiency of the visual system to gratings at oblique orientations compared to cardinal ones.

This oblique effect is well studied on a range of species (Appelle S. , 1972) and has been demonstrated as a behavioural advantage for cardinal contours (Emsley, 1925) and also as a higher BOLD response for cardinal orientations (Furmanski & Engel , 2000). Recently an inverse oblique effect has also been reported with fMRI (Mannion, McDonald, & Clifford, 2010) and also MEG (Koelewijn, Dumont, Muthukumaraswamy, Rich, & Singh, 2011).

Background

The inverse oblique effect and modulations of visual activation in V1

In this thesis the goal was to probe further into the oblique effect and its underlying neurophysiology with imaging techniques. The oblique effect as one can see throughout this thesis has been studied extensively with a range of imaging techniques both on human subjects and animals.

Recent findings of Koelewijn et al. (Koelewijn, Dumont, Muthukumaraswamy, Rich, & Singh, 2011) have demonstrated an opposite effect (an inverse oblique effect) and the point that is of particular interest in this study is that they find an early inverse oblique effect (in a medial location in the visual

cortex) however later in the same medial location and a more infero-lateral location they report a classical oblique effect. This is interesting because, as they suggest, the initial response could represent the initial tuning of V1, with a stronger response for the oblique stimuli possibly reflecting the broader tuning widths of these orientations. They also found a later 'classic' oblique effect which is probably mediated from the extrastriate cortex and may implicate feedback processes from the extrastriate cortex. This study is of interest as for one it finds the opposite of the classical oblique effect (the inverse oblique effect) and also shows that the later oblique effect may in fact be a result of an extrastriate modulation.

An inverse oblique effect has been reported in the past with behavioural studies using dot patterns (Wilson, Loffler, Wilkinson, & Thistlethwaite, 2001) or even naturalistic stimuli (Essock, DeFord, Hansen, & Sinai, 2003) and recently with sinusoidal gratings (Mannion, McDonald, & Clifford, 2010) using fMRI (although with Mannion et al.' s study the radial bias could have explained the inverse oblique effect found).

The role of inhibition in the oblique effect.

The oblique effect has been studied both with behavioural paradigms (Cambell, Kulikowski, & Levinson, 1966) (Emsley, 1925) and also imaging methods (Mannion, McDonald, & Clifford, 2010). Recently Edden et al. (Edden, Muthukumaraswamy, Freeman, & Singh, 2009) look into the role of GABA in orientation selectivity and find a significant negative correlation of visual GABA concentration with orientation detection thresholds for oblique gratings and also thresholds of obliquely oriented stimuli were negatively correlated with gamma frequency oscillations (for cardinal stimuli these correlations were not

significant). These results demonstrate an important role of GABA inhibition in orientation selectivity and also show, for the first time, a link between inter-individual performance on a behavioural task is linked to GABA concentration.

Summary of findings

Chapter one:

In this chapter a patch grating similar to Koelewijn et al. (Koelewijn, Dumont, Muthukumaraswamy, Rich, & Singh, 2011) is used in order to replicate the inverse oblique effect found by Koelewijn et al. (Koelewijn, Dumont, Muthukumaraswamy, Rich, & Singh, 2011). However, here, I used fMRI both in order to try and reconcile contradictory findings between fMRI and MEG and also to localise the extrastriate regions reported by Koelewijn et al. feeding back to V1. The expectation was that the any extrastriate regions found would demonstrate the classical oblique effect.

In the analysis limited to area V1, a statistically significant inverse oblique effect was found (the 135 degrees condition median of the max values was greater than the 0 degrees one). Also, interestingly, we found that the response to tangential patch gratings was greater than the response to radial gratings.

No robust reponses were detected in extrastriate cortical regions, so we were unable to investigate the role of extrastriate feedback in mediating the oblique effect in the BOLD response

Chapter 2

In this chapter I wished to examine a variety of points:

1) Establish the oblique effect with a behavioural paradigm.

2) Test for a radial bias at these eccentricities.

3) Look for training effects at these orientations.

Using the same stimulus properties as the previous fMRI study, as expected a classic behavioural oblique effect was found, which is in contrast to the tangential preference revealed by the BOLD study.

No radial bias was found at these stimulus eccentricities, confirming the stability of the behavioural oblique effect

When examining training effects it was only the top left vertical patch grating that showed a significant training effect.

The point here is that too many questions were asked (especialy as we tested for training effect and there were a total of 16 blocks here) which means participants may have got tired and also each condition (4 of them) was not tested enough.

Chapter 3

In this chapter we replicate Edden et al. (Edden, Muthukumaraswamy, Freeman, & Singh, 2009) testing the negative correlations they found with behavioural performance and gamma however here participants perform the discrimination task during scanning rather than get tested behaviourally before going in the scanner and in the scanner viewing a static grating. I examined here if gamma oscillations and behavioural thresholds remained while working memory and attention would also be present during the scan.

Here, when examining the SAM results, we did not manage to find an oblique effect, which is somewhat disappointing as the oblique effect is well documented and has been reported in the past with MEG (Koelewijn, Dumont, Muthukumaraswamy, Rich, & Singh, 2011). However, when looking for

correlations between behavioural thresholds and oscillatory response amplitude, we found areas in the medial visual cortex with significant r values (when examining a frequency range of 30-70Hz for the oblique grating (first grating onset) as also for the first oblique grating appearance at 60-80Hz and also for the second grating appearance (oblique condition) at 5-15 Hz (however not in the visual cortex in these latter two cases).

Later, using a "bertogram" approach we plotted (for a medially located point) individual frequency-time plots and then proceeded with a group analysis. However, when contrasting cardinal to oblique for all participants (using t-tests with permutations) no significant differences were found here. Also we tested every point on the time-frequency spectrogram for correlations with behavioural thresholds, however no significant correlations were found. We also took the power vs time (power averaged across a frequency range 30-70 Hz at each time point). The average power value from these plots, for each participant, was calculated and these values were later correlated using a Spearman rank correlation to the behavioural data, however again this analysis did not show any significant results. In this analysis however we did however find a trend for the latencies of the evoked gamma responses (first and second oblique grating presentation) to negatively correlate with behavioural thresholds so poorer behavioural performance was associated with faster visual cortex responses.

Chapter 4

Here we are looking further into the relationship between GABA and orientation discrimination reported by Edden et al. (Edden, Muthukumaraswamy, Freeman, & Singh, 2009). We test if this relationship holds

if macromolecule suppressed sequences are used (instead of the GABA with macromolecule contamination), can we find training effects dependent on GABA with macromolecules and GABA with suppressed sequences and finally if training effects transfer if the tested orientation changes.

In this chapter we found, when examining individual GABA+ and GABAmm concentrations, that there was no correlation between these two GABA measures. Also in this experiment we did manage to find training effects and also higher variance was found for the more untrained sessions. Finally as in Edden et al. (Edden, Muthukumaraswamy, Freeman, & Singh, 2009) we found the training effects for the low GABA+ participants, however for high GABA+ we did not find any significant training effects.

Additionally, here we correlated for every session the behavioural thresholds to GABA+ and GABAmm measures and what is interesting here is that we find that the strongest negative correlations for sessions where the session average performance is worst and also the group has the higher variability. This agrees with previous findings by Edden et al. (Edden, Muthukumaraswamy, Freeman, & Singh, 2009) where correlations between GABA+ and behavioural data were not found for the easiest version of the task (for a cardinal targert). This was also the case for the GABAmm however these correlations were not so strong.

In this chapter we discussed further issues such as what are the merits of GABA+ and also GABAmm protocols, also the advantages of low GABA to plasticity in the brain and also we discuss the role of a sleep interval between training sessions (however this experiment did not allow to really probe into the effect of sleep in training effects).

Contribution of findings

The inverse oblique effect reported by Koelewijn et al. with MEG may represent an initial tuning of the oscilatory activation in the primary visual cortex, which is later modulated by an extrastriate region and switches to the classical oblique effect. In the first experimental chapter of this thesis we managed to detect an inverse oblique effect with the used of fMRI using the same stimulus dimensions as Koelewijn et al. demonstrating that under certain manipulations of the stimulus we can probe into the initial tuning of primary cortex cells.

In the second chapter we managed to look further into the radial bias and confirm that at the eccentricities used in both our fMRI experiment and Koelewijn et al.'s MEG experiment were not confounded by a radial bias.

The MEG experiment (3rd experimental chapter) looks further into Edden et al.' s findings of the negative correlations of behavioural thresholds to properties of the gamma response(for oblique stimuli). Whilst, in Edden et al. the behavioural testing took place outside of the scanner, here we performed the behavioural testing during the MEG scan itself, providing a potentially opportunity to directly link gamma to individual variability in behavioural performance. In this chapter we find, for example ,a correlation between behavioural thresholds and gamma (30-70Hz) amplitude, however only for the first grating onset of the discrimination task, not the second, showing that correlations between performance and gamma frequency amplitude do exist however cognitive processes taking place between the two gratings of the orientation discrimination task could have a modulating effect on them.

In the last experimental chapter we examined the relationship between GABA+ and GABAmm protocols in the measurement of GABA concentration and also examine the effect of GABA on training effects. The findings here were quite promising as for one we managed to confirm some unreported findings of Edden et al. showing that low GABA participants demonstrate a clear training effect. Additionally, we find when examining throughout the training sessions that the strongest negative correlations between GABA and session average thresholds are for the worst performance training sessions (where additionally the variance of the mean is largest) indicating that the negative correlations weaken as training effects take place.

Future research

In the initial fMRI experiment we managed to find an inverse oblique effect with fMRI using a stimulus similar to that used by Koelewijn et al. (Koelewijn, Dumont, Muthukumaraswamy, Rich, & Singh, 2011). Although an inverse oblique effect has been reported previously by Mannion et al. (Mannion, McDonald, & Clifford, 2010), the fact their inverse oblique effect could in fact had been a radial bias makes our fMRI experiment (first experimental chapter) particularly interesting as it shows that fMRI can also detect the inverse oblique effect with the same stimulus as Koelewijn et al. As in Koelewijn et al. state the inverse oblique effect could in fact (in the medial location of the visual cortex) show the initial tuning of the primary visual cortex which later is mediated by an extrastriate location switching the response in the medial location to the classical oblique effect. In our fMRI experiment we did not manage to detect this extrastriate location with fMRI probably because we used four different

orientations (so too many conditions leading to a lack of statistical power) and also the retinotopic maps we collected where not of sufficient quality to allow the localisation of extrastriate regions for a region of interest analysis. Although it could be that the parameters of Koelewijn et al.'s stimulus were optimal for detecting an inverse oblique effect it could be that also the fact that the stimulus on our fMRI experiment was too brief (0.8 to 1.3 seconds) and therefore did not provide enough time for the classical oblique effect to appear. It would therefore be interesting to see if replicating our fMRI experiment with longer stimulation times would give a classical oblique effect. A way to probe into the extrastriate region feeding back to V1 would be to focus on only two orientations in the paradigm (improving therefore the statistical power of the analysis) and also dedicate more time in retinotopic mapping in order to locate the extrastriate regions allowing to limit the BOLD response analysis to a region of interest. This way we would be able to know also the area involved so if, for example, we find an oblique effect in area V5, knowing what this area is associated with (e.g. perception of motion) would possibly allow us to speculate further on what triggers these feedback processes.

7 References.

(n.d.). Retrieved 01 06, 2014, from MEG 250 SMI SensoMotoric instruments GmbH: http://www.smivision.com/en.html
Żychaluk, K. (n.d.). *Model-free estimation of a psychometric function*. Retrieved from http://www.modelfree.liv.ac.uk/index.html
Aberg, K., & Herzog, M. (2012). About similar characteristics of visual perceptual learning and LTP. *Vision research , 61*, 100-6.
Adjamian, P., Holliday, I., Barnes, G., Hillebrand, A., Hatjipapas, A., & Singh, K. (2004). Induced visual illusions and gamma oscillations in human primary visual cortex. *The European journal of neuroscience* , 587-92.
Amunts, K., Malikovic, A., Mohlberg, H., Schormann, T., & Zilles, K. (2000). Brodmann's areas 17 and 18 brought into stereotaxic space-where and how variable? *NeuroImage* , 66-84.
Appelle, S. (1972). Perception and discrimination as a function of stimulus orientation: the "oblique effect" in man and animals. *Psychological bulletin* , 266-78.
Appelle, S. (1978). PERCEPTION AND DISCRIMINATION AS A FUNCTION OF STIMULUS ORIENTATION:THE "OBLIQUE EFFECT" IN MAN AND ANIMALS. *Psychological Bulletin* , 266-278.
Artola, A., & Singer, W. (1987). Long-term potentiation and NMDA receptors in rat visual cortex. *Nature , 330*, 649-652.
Baowang, L., Peterson, M. R., & Freeman, R. D. (2003). Oblique effect: a neural basis in the visual cortex. *Journal of neurophysiology* , 204217.
Barbur, J., Watson, J., Frackowiak, R., & Zeki, S. (1993). Conscious visual perception without V1. *Brain , 116*, 1293-302.
Bastos, A., Briggs, F., Alitto, H., Mangun, G., & Usrey, W. (2014). Simultaneous Recordings from the Primary Visual Cortex and Lateral Geniculate Nucleus Reveal Rhythmic Interactions and a Cortical Source for Gamma-Band Oscillations. *The Journal of neuroscience* , 7639-7644.
Belmonte, M., Allen, G., Beckel-Mitchener, A., Boulanger, L., Carper, R., & Webb, S. (2004). Autism and abnormal development of brain connectivity. *The Journal of neuroscience.* , 9228-31.
Bennett, P., & Banks, M. (1991). The effects of contrast, spatial scale, and orintation on foveal and peripheral phase discrimination. *Vision Research.* (31), 1759-1786.
Berardi, N., & Fiorentini, A. (1991). Visual field asymmetries in pattern discrimination: a sign of asymetry in cortical visual field representation? *Vision Research* (31), 1831-1836.
Berkley, M. A., Kitterle, F., & Watkins, D. W. (1974). Grating visibility as a function of orientation and retinal eccentricity. *Vision , 15*, 239-244.
Bertone, A., Mottron, L., Jelenic, P., & Faubert, J. (2005). Enhanced and diminished visuo-spatial information processing in autism depends on stimulus complexity. *Brain* , 2430-41.
Bessou, M., Cauquil, A., Dupui, P., & Montoya, R. (1999). Specificity of the monocular crescents of the visual field in postural control. *C. R Acad. Sci.* , 749-757.

Blakemore, G., & Cooper, C. (1970). Development of the brain depends on the visual environment. *Nature* , 477-478.
Bonds, A. (1982). An "Oblique Effect" in the Visual Evoked Potential of the Cat. *Experimental Brain Research* (46), 151-154.
Bowman, A., & Azzalini, A. (1997). *Applied Smoothing Techniques for Data Analysis : The Kernel Approach with S-plus illustrations.* Oxford: Oxford University press.
Brainard, D. (1997). The psychophysics toolbox. *Spatial Vision* , 433-436.
Brandt, T., Dichgans, J., & Koenig, E. (1973). Differential Effects of Central Versus Peripheral Vision on Egocentric and Exocentric Motion Perception*. *Experimental Brain Research* , 476-491.
Cambell, J., Kulikowski, J., & Levinson, J. (1966). The Effect Of Orientation on the visual resolution of grating. *Journal of Physiology* , 427-436.
Cannon, M., & Fullenkamp, S. (1993). spatial interactions in apparent contrast: indivisual differences in enhansement and suppresion effects. *Vision Research* (3), 1685-1695.
Chapman, B., & Bonhoeffer, T. (1998). Overrepresentation of horizontal and vertical orientation preferences in developing ferret area 17. *Experimental Brain Research , 95*, 2609-14.
Chen, Y., Martinez-Conde, S., Macknik, S., Bereshpolova, Y., Swadlow, H., & Alonso, J. (2008). Task difficulty modulates the activity of specific neuronal populations in primary visual cortex. *nature Neuroscience* , 974-982.
Coppola, D., White, L., Fitzpatrick, D., & Purves, D. (1998). Unequal representation of cardinal and oblique contours in ferret visual cortex. *Proceedings of the National Academy of Sciences of the United States of America* , 2621-2623.
Cousijn, H., Haegens, S., Wallis, G., Near, J., Stokes, M., Harrison, P., et al. (2014). Resting GABA and glutamate concentrations do not predict visual gamma frequency or amplitude. *Proceedings of the National Academy of Sciences of the United States of America* , 9301-6.
Crick, F., & Koch, C. (1990). Towards a neurobiological theory of consciousness. *Seminars in the Neurosciences* , 263-275.
CTF MEG Software. (n.d.). (VSM MedTech.Ltd) Retrieved from http://www.ctf.com/software.html
Davey, M., & Zanker, J. (1998). Detecting the orientation of short lines in the periphery. *Australian and New Zealand Journal of Ophthalmology. , 26*, 104-107.
Deneb. (n.d.). Retrieved July 22, 2014, from Encyclopaedia Britannica. Encyclopaedia Britannica Online. Encyclopædia Britannica Inc.: http://www.britannica.com/EBchecked/topic/157635/Deneb
DeYoe, E., Carmant, G., Bandettini, P., Glickman, S., Wieser, J., Cox, R., et al. (1996). Mapping striate and extrastriate visual areas in human cerebral cortex. *Neurobiology* , 2382-2386.
Di Stasi, L., McCamy, M., Catena, A., Macknik, S., Cañas, J., & Martinez-Conde, S. (2013). Microsaccade and drift dynamics reflect mental fatigue. *The European journal of neuroscience* , 2389-2398.
Diesmann, M., Gewaltig, M., & Aertsen, A. (1999). Stable propagation of synchronous spiking in cortical neural networks. *Nature* , 529-33.
Dong, Y., Mihalas, S., Qiu, F., von der Heydt, R., & Niebur, E. (2008). Synchrony and the binding problem in macaque visual cortex. *Journal of Vision , 8*, 1-16.

Dougherty, R., Koch, V., Brewer, A., Fischer, B., Modersitzki, J., & Wandell, B. (2003). Visual field representations and locations of visual areas V1 / 2 / 3 in human visual cortex. *Journal of Vision* , 586-598.
Edden, R., & Barker, P. (2007). Spatial effects in the detection of gamma-aminobutyric acid: improved sensitivity at high fields using inner volume saturation. *Magnetic resonance in medicine* , 1276-1282.
Edden, R., Muthukumaraswamy, S., Freeman, T., & Singh, K. (2009). Orientation discrimination performance is predicted by GABA concentration and gamma oscillation frequency in human primary visual cortex. *The Journal of neuroscience* , 15721-6.
Edden, R., Muthukumaraswamy, S., Freeman, T., & Singh, K. (2009). Orientation discrimination performance is predicted by GABA concentration and gamma oscillation frequency in human primary visual cortex. *The Journal of neuroscience , 29* (50), 15721-6.
Edden, R., Muthukumaraswamy, S., Freeman, T., & Singh, K. (2009). Orientation discrimination performance is predicted by GABA concentration and gamma oscillation frequency in human primary visual cortex. *The Journal of Neuroscience* , 15721–15726.
Edden, R., Puts, N., & Barker, P. (2012). Macromolecule-suppressed GABA-edited magnetic resonance spectroscopy at 3T. *Magnetic resonance in medicine , 68*, 657-61.
Edden, R., Puts, N., Harris, A., Barker, P., & Evans , J. (2013). Gannet: A batch-processing tool for the quantitative analysis of gamma-aminobutyric acid-edited MR spectroscopy spectra. *Journal of Magnetic Resonance Imaging* , 1-8.
Ejima, Y., & Takahashi, S. (1985). Apparent contrast of a sinusoidal grating in the simultaneous presence of peripheral grating. *Vision research* (25), 1223-1232.
Emsley, H. (1925). Irregular astigmatism of the eye : effect of correcting lenses. *Transactions of the Optical Society* , 28-42.
Ende, G., Sack, M., Tunc-skarka, N., Weber-fahr, W., Hoerst, M., Krause-utz, A., et al. (2012). Decreased GABA in the anterior cingulate cortex of female borderline personality disorder patients Proc. *Proc. Intl. Soc. Mag. Reson. Med* , 130.
Engel, A., Kreiter, A., König, P., & Singer, W. (1991). Synchronization of oscillatory neuronal responses between striate and extrastriate visual cortical areas of the cat. *Proceedings of the National Academy of Sciences of the United States of America.* , 6048-52.
Engel, S., Rumelhart, D., Wandell, B., Lee, A., Glover, G., Chichilnisky, E., et al. (1994). fMRI of human visual cortex. *Nature* , 525.
Epperson, C., Haga, K., Mason, G., Sellers, E., Gueorguieva, R., Zhang, W., et al. (2002). Cortical -Aminobutyric Acid Levels Across the Menstrual Cycle in Healthy Women and Those With Premenstrual Dysphoric Disorder. *Archives general Psychiatry , 59*, 851-858.
Essock, E., DeFord, K., Hansen, B., & Sinai, M. (2003). Oblique stimuli are seen best (not worst!) in naturalistic broad-band stimuli: a horizontal effect. *Vision Research* , 1329-1335.
Fahle, M. (1986). Curvature detection in the visual field and a possible physiological correlate. *Brain Research.* (63), 113-124.
Falchier, A., Clavagnier, S., Barone, P., & Kennedy, H. (2002). Anatomical evidence of multimodal integration in primate striate cortex. *The Journal of neuroscience* , 5749-59.

Fang, L., Bauer, J., Held, R., & Gwiazda, J. (1997). The oblique effect in Chinese infants and Adults. *Optometry and Vision Science* , 816-821.
Felleman, D., & van Essen, D. (1991). Distributed Hierarchical Processing in the Primate Cerebral Cortex. *Cerebral Cortex* , 1-47.
Fenn, K., Nusbaum, H., & Margoliash, D. (2003). Consolidation during sleep of perceptual learning of spoken language. *Nature* , 614-6.
Fiorentini, A., & Berardi, N. (1981). Learning in grating waveform discrimination : specificity for orientation and spatial frequency. *Vision Research* , 1149-1158.
FSL wiki/GLM. (n.d.). Retrieved 2013, from FMRIB Software library v5.0 September 2012: http://fsl.fmrib.ox.ac.uk/fsl/fslwiki/GLM#Single-Group_Average_with_Additional_Covariate
Furmanski, C., & Engel , S. (2000). An oblique effect in human primary visual cortex. *Nature* , 535-6.
Gandhi, S., Heeger, D., & Boynton, G. (1999). Spatial attention affects brain activity in human primary visua cortex. *Biological sciences. , 96*, 3314-3319.
Gandhi, S., Heeger, D., & Boynton, G. (1999). Spatial attention affects brain activity in human primary visual cortex. *Proceedings of the National Academy of Sciences , 96*, 3314-3319.
Girshick, A., Landy, M., & Simoncelli, E. (2011). Cardinal rules: visual orientation perception reflects knowledge of environmental statistics. *Nature neuroscience* , 926-32.
Gray, C., & Singer , W. (1989). Stimulus-specific neuronal oscillations in orientation columns of cat visual cortex. *Proceedings of the National Academy of Sciences of the United States of America , 86*, 1698-1702.
gray, C., Konig, P., Engel, A., & Singer, W. (1989). Oscilatory responses in cat visual cortex exhibit inter-columnar synchronization which reflects gloabal stimulus properties. *Nature , 338*, 334-337.
Grill-Spector, K., & Malach, R. (2004). The human visual cortex. *Annual review of neuroscience* , 649-77.
Hansen, B., & Essock, E. (2004). A horizontal bias in human visual processing of orientation and its correspondence to the structural components of natural scenes. *Journal of Vision* , 1044-1060.
Hecht, S., Shlaer, S., & Pirenne, M. (1943). Energy, quanta and vision. *The Journal of general physiology.* , 819-840.
Hess, E., & Polt, J. (1960). Pupil Size as related to Interest Value of Visual Stimuli. *Science* , 349-350.
Hinds, O., Rajendran, N., Polimeni, J., Augustinack, J., Wiggins, G., Wald, L., et al. (2008). Accurate prediction of V1 location from cortical folds in a surface coordinate system. *NeuroImage* , 1585-99.
Holmes, G. (1918). Disturbances of vision by cerebral lesions. *The british journal of ophthalmology.* , 353-383.
Hsieh, P., & Tse, P. (2009). Microsaccade Rate Varies with Subjective Visibility during Motion-Induced Blindness. *PLOS One , 4* (4), 1-9.
Hubel, D. H., & Wiesel, T. N. (1959). RECEPTIVE FIELDS OF SINGLE NEURONES IN THE CAT ' S STRIATE CORTEX. *Journal of Physiology* .
Hubel, D. (1963). The visual cortex of the brain. *Scientific American , 209*, 54-63.
Huettel, S. A., Song, A. W., & McCarthy, G. (2004). *Functional Magnetic Resonance.* Massachusetts: SinauerAssosiates, Inc.

Jensen, O., Kaiser, J., & Lachaux, J. (2007). Human gamma-frequency oscillations associated with attention and memory. *Trends in neurosciences* , 317-324.
Kagan, I., Gur, M., & Snodderly, D. (2008). Saccades and drifts differentially modulate neuronal activity in V1 : Effects of retinal image motion , position , and extraretinal influences. *Journal of Vision* , 1-25.
Kastner, S., Pinsk, M. A., De Weeder, P., Desimone, R., & Ungerleider, L. G. (1999). Increased activity in human visual cortex during directed attention in the absence of visual stimulation. *Neuron , 22*, 751-761.
Keil, M., & Cristóbal, G. (2000). Separating the chaff from the wheat: possible origins of the oblique effect. *Journal of the Optical Society of America.* , 697-710.
Koelewijn, L., Dumont, J., Muthukumaraswamy, S., Rich, A., & Singh, K. (2011). Induced and evoked neural correlates of orientation selectivity in human visual cortex. *Neuroimage* , 29832993.
Leibowitz, H., Myers, N., & Grant, D. (1955). Radial Localization of a Single Stimulus as a Function of Luminance and Duration of Exposure. *JOURNAL OF THE OPTICAL SOCIETY OF AMERICA VOLUME* , 76-78.
Leopold, D., & Logothetis, N. (1998). Microsaccades differentially modulate neural activity in the striate and extrastriate visual cortex. *Experimental brain research , 123* (3), 341-345.
Leopold, D., & Logothetis, N. (1998). Microsaccades differentially modulate neural activity in the striate and extrastriate visual cortex. *Experimental brain research , 123* (3), 341-5.
Leventhal, A., & Schall, J. (1983). Structural basis of orientation sensitivity of cat retinal ganglion cells. *The journal of comparative neurology* (220), 465-475.
Levick, W., & Thibos, L. (1982). Analysis of orientation bias in cat retina. *Journal of Physiology* (329), 243-261.
Levitt, J., & Lund, J. (1997). Contrast dependence of contextual effects in primate visual cortex. *Nature , 387*, 73-76.
Levitt, J., & Lund, J. (1997). Contrast dependence of contextual effects in primte visual cortex. *Nature , 387*, 73-76.
Li, B., Peterson, M., & Freeman, R. (2003). Oblique effect: a neural basis in the visual cortex. *Journal of neurophysiology* , 204-217.
Li, G., Yang, Y., Liang, Z., Xia, J., & Zhou, Y. (2008). GABA-mediated inhibition correlates with orientation selectivity in primary visual cortex of cat. *Neuroscience , 155*, 914-22.
Liang, Z., Shen, W., & Shou, T. (2007). Enhancement of oblique effect in the cat's primary visual cortex via orientation preference shifting induced by excitatory feedback from higher-order cortical area 21a. *Neuroscience* , 377-383.
Liang, Z., Shen, W., & Shou, T. (2007). Enhancement of oblique effect in the cat's primary visual cortex via orientation preference shifting induced by excitatory feedback from higher-order cortical area 21a. *Neuroscience* , 377-83.
Lipshits, M., & McIntyre, J. (1999). Gravity affects the preferred vertical and horizontal in visual perception of orientation. *Neuroreport* , 1085-9.
Luo, A., & Aston-Jones, G. (2009). Circuit projection from suprachiasmatic nucleus to ventral tegmental area: a novel circadian output pathway. *The European journal of neuroscience* , 748-60.
Macaluso, E., Frith, C., & Driver, J. (2000). Modulation of Human Visual Cortex by Crossmodal Spatial Attention. *Science* , 1206-1208.

Macmillan, N., & Creelman , C. (2005). *Detection Theory: A users guide.* London: LAWRENCE ERLBAUM ASSOCIATES, PUBLISHERS.
Maffei, L., & Campbell, F. (1970). Neurophysiological localization of the vertical and horizontal visual coordinates in man. *Science* , 386-387.
Mannion, D. J., McDonald, S., & Clifford, C. W. (2010). Orientation anisotropies in human visual cortex. *Journal of neurophysiology* , 3465-3471.
Mannion, D., McDonald, J., & Clifford, C. (2010). The influence of global form on local orientation anisotropies in human visual cortex. *NeuroImage , 52* (2), 600-5.
Mannion, D., McDonald, S., & Clifford, C. (2010). Orientation anisotropies in human visual cortex. *Journal of Neurophysiology* , 3465–3471.
Mansfield, R. (1974). Neural Basis of Orientation Perception in Primate Vision. *Science , 186*, 1133-1135.
Mansfield, R., & Ronner, S. (1978). Orientation anisotropy in monkey visual cortex. *Brain Research.* (149), 229-234.
Maquet, P. (2001). The role of sleep in learning and memory. *Science (New York, N.Y.)* , 1048-52.
Marshall, I., Bruce, S., Higinbotham, J., MacLullich, A., Wardlaw, J., Ferguson, K., et al. (2000). Choice of spectroscopic lineshape model affects metabolite peak areas and area ratios. *Magnetic resonance in medicine.* , 646-649.
MATLAB. (n.d.). Retrieved from http://www.mathworks.co.uk/products/matlab/
Mescher, M., Merkle, H., Kirsch, J., Garwood, M., & Gruetter, R. (1998). Simultaneous in vivo spectral editing and water suppression. *NMR in biomedicine , 11*, 266-272.
Mescher, M., Tannus, A., Johnson, M., & Garwood, M. (1996). Solvent Suppression Using Selective Echo Dephasing. *NMR in biomedicine* , 226-229.
Morland, A., Baseler, H., Hoffmann, M., Sharpe, L., & Wandell, B. (2001). Abnormal retinotopic representations in human visual cortex revealed by fMRI. *Acta Psychologica* , 229-247.
Mullins, P., McGonigle, D., Gorman, R., Puts, N., Vidyasagar, R., Evans, J., et al. (2014). Current practice in the use of MEGA-PRESS spectroscopy for the detection of GABA. *NeuroImage* , 43-52.
Murray, I., Elliott, S., Pallikaris, A., Werner, J., Choi, S., & Tahir, H. (2010). The oblique effect has an optical component: Orientation-specific contrast thresholds after correction of high-order aberrations. *Journal of Vision* , 1-12.
Muthukumaraswamy, S., & Singh, K. (2008). Spatiotemporal frequency tuning of BOLD and gamma band MEG responses compared in primary visual cortex. *NeuroImage , 40*, 1552-60.
Muthukumaraswamy, S., Edden, R., Jones, D., Swettenham, J., & Singh, K. (2009). Resting GABA concentration predicts peak gamma frequency and fMRI amplitude in response to visual stimulation in humans. *Proceedings of the National Academy of Sciences of the United States of America* , 8356-8361.
Muthukumaraswamy, S., Singh, K., Swettenham, J., & Jones, D. (2010). Visual gamma oscillations and evoked responses: Variability, repeatability and structural MRI correlates. *Neuroimage* , 3349-3357.
Nachmias, J. (1981). On The Psychometric function for contrast detection. *Vision Research* , 215-223.

Neu, A., Neuhoff, H., Trube, G., Fehr, S., Ullrich, K., Roeper, J., et al. (2002). Activation of GABAA Receptors by Guanidinoacetate: A Novel Pathophysiological Mechanism. *Neurobiology of disease , 11*, 298-307.
Newsome, W., Wurtz, R., Dürsteler, M., & Mikami, A. (1985). Deficits in visual motion processing following ibotenic acid lesions of the middle temporal visual area of the macaque monkey. *The Journal of neuroscience* , 825-40.
Nichols, T. E., & Holmes, A. P. (2001). Nonparametric Permutation Tests For Functional Neuroimaging: A primer with Examples. *Human Brain Mapping* (15), 1-25.
Orban, G., VanEssen, D., & Vanduffel, W. (2004). Comparative mapping of higher visual areas in monkeys and humans. *Trends in cognitive sciences* , 315-324.
Palmer, S. (1999). *Vision Science. Photons to Phenomenology.* Massachusetts: The MIT Press.
Pascual-Leone, A., & Walsh, V. (2001). Fast backprojections from the motion to the primary visual area necessary for visual awareness. *Science , 292*, 510-2.
Pelli, D. (1997). The Video Toolbox software for visual psychophysics: Transforming numbers into movies. *Spatial Vision* , 437-442.
Pettigrew, J., Nikara, T., & Bishop, P. (1968). Responses to Moving Slits by Single Units in Cat Striate Cortex. *Experimental brain research* (6), 373-390.
Purves, D., Brannon, E. M., Cabeza, R., Huettel, S. A., LaBar, K. S., Platt, M. L., et al. (2008). *Principles of Cognitive Neuroscience.* Massachusetts: SinauerAssociates, Inc.
Rae, C., Digney, A., McEwan, S., & Bates, T. (2003). Oral creatine monohydrate supplementation improves brain performance: a double-blind, placebo-controlled, cross-over trial. *Proceedings. Biological sciences / The Royal Society , 270*, 2147-50.
Rauch, S., Whalen, P., Savage, C., Curran, T., Kendrick, A., Brown, H., et al. (1997). Striatal recruitment during an implicit sequence learning task as measured by functional magnetic resonance imaging. *Human brain mapping , 5*, 124-32.
Revonsuo, A., & Newman, J. (1999). Binding and consciousness. *Consciousness and cognition* , 123-7.
Rippon, G., Brock, J., Brown, C., & Boucher, J. (2007). Disordered connectivity in the autistic brain: challenges for the "new psychophysiology". *International journal of psychophysiology.* , 164-72.
Rothman, D., Petroff, O., Behar, K., & Mattson, R. (1993). Localized 1H NMR measurements of gamma-aminobutyric acid in human brain in vivo. *Proceedings of the National Academy of Sciences of the United States of America , 90*, 5662-6.
Rovamo, J., Virsu, V., & Nasanen, R. (1978). Cortical magnification factor predicts the photopic contrast sensitivity of peripheral vision. *Nature* , 54-56.
Rovamo, J., Virsu, V., laurinen, P., & Hyvarinen, L. (1982). Resolution of gratings orientated along and across meridians in peripheral vision. *Ophthalmol.Vis.Sci.* (23), 666-670.
Rovamo, J., Virsu, V., Laurinen, P., & Hyvarinen, L. (1982). Resolution of gratings oriented along and across meridians in peripheral vision. *Invest. Ophthalmol. Vis. Sci* (23), 666-670.
Samonds, J., & Bonds, A. (2005). Gamma oscillation maintains stimulus structure-dependent synchronization in cat visual cortex. *Journal of neurophysiology* , 223-36.

Samonds, J., Allison, J., Brown, H., & Bonds, A. (2004). Cooperative synchronized assemblies enhance orientation discrimination. *Proceedings of the National Academy of Sciences of the United States of America , 101*, 6722-7.
Sasaki, Y., Rajimehr, R., Byoung , W. K., ekstrom, L. B., Vanduffel, W., & Tootell, R. (2006). The radial bias: A different slant on visual orientation sensitivity in human and non-human primates. *Neuron* (51), 661-670.
Schall, D., Perry, V., & Leventhal, A. (1986). Retinal Ganglion cell dentritic fields in old world monkeys are oriented radially. *Brain Research* , 18-23.
Schall, J., & Leventhal, A. (1986). Retinal ganglion cell dentritic fields in old-world monkeys are oriented radialy. *Brain Research* (368), 18-23.
Schiltz, C., Bodart, J., Dubois, S., Dejardin, S., Michel, C., Roucoux, A., et al. (1999). Neuronal mechanisms of perceptual learning: changes in human brain activity with training in orientation discrimination. *NeuroImage* , 46-62.
Schoups, A., Vogels, R., & Orban, G. (1995). Human perceptual learning in identifying the oblique orientation: retinotopy, orientation specificity and monocularity. *The Journal of physiology , 483.3*, 797-810.
Schwartz, S. H. (2010). *Visual Perception. A Clinical Orientation.* New York: Mc Graw Hill.
Sengpiel, F., Stawinski, P., & Bonhoeffer, T. (1999). Influence of experience on orientation maps in cat visual cortex. *Nature neuroscience* , 727-732.
Senior, C., Russel, T., & Gazzaniga, M. (Eds.). (2006). *Methods in mind.* Massachusetts: The MIT press.
Senior, C., Russell, T., & Gazzaniga, M. (2006). *Methods in mind.* Massachusetts: The MIT press.
Senpiel, F., Stawinski, P., & Bonhoeffer, T. (1999). Influence of experience on orientation maps in cat visual cortex. *Nature neuroscience* , 727-732.
Sereno, M., Dale, A., Reppas, J., Kwong, K., Belliveau, J., Brady, T., et al. (1995). Borders of Multiple Visual Areas in Humans Revealed by Functional Magnetic Resonance Imaging. *Science , 268*, 889-893.
Sereno, M., Dale, A., Reppas, J., Kwong, K., Belliveau, J., Brady, T., et al. (1995). Borders of Multiple Visual Areas in Humans Revealed by Functional Magnetic Resonance Imaging. *Science , 268*, 889-893.
Shen, W., Liang, Z., & Shou, T. (2008). Weakened feedback abolishes neural oblique effect evoked by pseudo-natural visual stimuli in area 17 of the cat. *Neuroscience letters* , 65-70.
Siegenthaler, E., Costela, M., McCamy, McCamy, B., Di Stasi, L., Otero-Millan, J., et al. (2014). Task difficulty in mental arithmetic affects microsaccadic rates and magnitudes. *The European journal of neuroscience* , 287-94.
Singh, K. (2009). *mri3dX*. Retrieved from http://cubric.psych.cf.ac.uk/Documentation/mri3dX/features.
Snowden, R., Thompson, P., & troscianko, T. (2006). *Basic Vision. An Introduction to Visual Perception.* Oxford: Oxford University Press.
Strasburger, H. (2001). Invariance of the psychometric function for character recognition across the visual field. *Perception and psychophysics* , 1356-1376.
Super, H. (2003). Working memory in the primary visual cortex. *Archives of neurology* , 809-812.
Sutherland, N. (1957). Visual discrimination of orientation by octopus. *British Journal of Psychology* , 55-71.

Swettenham, J., Muthukumaraswamy, S., & Singh, K. (2013). BOLD Responses in Human Primary Visual Cortex are Insensitive to Substantial Changes in Neural Activity. *Frontiers in human neuroscience , 7*, 1-11.
swettenham, J., Muthukumaraswamy, S., & Singh, K. (2009). Spectral properties of induced and evoked gamma oscilations in human early visual cortex to moving and stationary stimuli. *Journal of Neurophysiology* , 1241-1253.
Swettenham, J., Muthukumaraswamy, S., & Singh, K. (2009). Spectral properties of induced and evoked gamma oscillations in human early visual cortex to moving and stationary stimuli. *Journal of neurophysiology , 102*, 1241-53.
Tallon-Baudry and, C., & Bertrand, O. (1999). Oscillatory gamma activity in humans and its role in object representation. *Trends in cognitive sciences* , 151-162.
Temme, L., Malcus, L., & Noell, W. (1985). Peripheral visual field is radialy organised. *Am. J. Optom. Physiol.* (62), 545-554.
Tesche, C., & Karhu, J. (2000). Theta oscillations index human hippocampal activation during a working memory task. *Proceedings of the National Academy of Sciences of the United States of America* , 919-24.
Thiele, A., & Stoner, G. (2003). Neuronal synchrony does not correlate with motion coherence in cortical area MT. *Nature* , 366-370.
Treisman, A. (1998). Feature binding, attention and object perception. *Philosophical transactions of the Royal Society of London.* , 1295-306.
Van Essen, D., Lewis, J., Drury, H., Hadjikhani, N., Tootell, R., Bakircioglu, M., et al. (2001). Mapping visual cortex in monkeys and humans using surface-based atlases. *Vision research* , 1359-78.
Vetencourt, J., Sale, A., Viegi, A., Baroncelli, L., De Pasquale, R., O'Leary, O., et al. (2008). The antidepressant fluoxetine restores plasticity in the adult visual cortex. *Science* , 385-8.
Vidyasagar, T., & Urbas, J. (1982). Orientation sensitivity of cat LGN neurones with and without inputs from visual cortical areas 17 and 18. *Experimental brain research* , 157-169.
Vogels, R., & Orban, G. (1985). The effect of practice on the oblique effect in line orientation judgment. *Vision Research , 25*.
Vrba, J., & Robinson, S. (2001). Signal processing in magnetoencephalography. *Methods (San Diego, Calif.) , 25*, 249-271.
Wandell, B., Dumoulin, S., & Brewer, A. (2007). Visual field maps in human cortex. *Neuron* , 366-83.
Wang, G., Ding, S., & Yunokuchi, K. (2003). Difference in the representation of cardinal and oblique contours in cat visual cortex. *Neuroscience letters , 338*, 77-81.
Warnking, J., Dojat, M., Guerin-Dugue, A., Delon-Martin, C., Olympieff, S., Richard, N., et al. (2002). fMRI Retinotopic Mapping—Step by Step. *NeuroImage* , 1665-1683.
Wells, M. (1959). Proprioception and Visual Discrimination of Orientation in Octopus. *Journal of Experimental Biology* , 489-499.
Weymouth , F. W. (1960). Stimulus orientation and threshold: an optical analysis. *American journal of Ophthalmology* (50), 569-571.
Wibral, M., Bledowski, C., Kohler, A., Singer, W., & Muckli, L. (2009). The timing of feedback to early visual cortex in the perception of long-range apparent motion. *Cerebral Cortex* , 1567-82.

Wide-field view of the Summer Triangle. (n.d.). Retrieved July 22, 2014, from ESA/HUBBLE: http://www.spacetelescope.org/images/heic0807c/
Wilson, H., Loffler, G., Wilkinson, F., & Thistlethwaite, W. (2001). An inverse oblique effect in human vision. *Vision Research* , 1749-1753.
Xing, J., & Heeger, D. (2000). Measurement and modeling of center-surround suppression and enhancement. *Vision Research. , 41*, 571-583.
Xu, X., Collins, C., Khaytin, I., Kaas, J., & Casagrande, V. (2006). Unequal representation of cardinal vs. oblique orientations in the middle temporal visual area. *Proceedings of the National Academy of Sciences of the United States of America , 103*, 17490-5.
Zhan, X., & Shou, T. (2002). Anatomical evidence of subcortical contributions to the orientation selectivity and columns of the cat ' s primary visual cortex. *Neuroscience Letters* , 247-251.

8 Appendix I

The SPSS statistics are presented in this appendix.

A. Normality testing.

Tests of Normality

	Kolmogorov-Smirnov[a]			Shapiro-Wilk		
	Statistic	df	Sig.	Statistic	df	Sig.
Bottom_0	.247	7	.200*	.845	7	.111
Bottom_45	.234	7	.200*	.898	7	.320
Bottom_90	.259	7	.169	.816	7	.059
Bottom_135	.176	7	.200*	.923	7	.496
Top_0	.132	7	.200*	.978	7	.947
Top_45	.223	7	.200*	.923	7	.490
Top_90	.204	7	.200*	.890	7	.273
Top_135	.146	7	.200*	.979	7	.957
SecondBottom_0	.336	7	.017	.779	7	.025
SecondBottom_45	.479	7	.000	.502	7	.000
SecondBottom_90	.281	7	.099	.685	7	.003
SecondBottom_135	.278	7	.109	.761	7	.017
SecondTop_0	.209	7	.200*	.908	7	.384
SecondTop_45	.418	7	.001	.557	7	.000
SecondTop_90	.180	7	.200*	.957	7	.794
SecondTop_135	.225	7	.200*	.896	7	.306

*. This is a lower bound of the true significance.

a. Lilliefors Significance Correction

B. T-tests for contrasts with t-test assumptions not violated.

Paired Samples Test

		t	df	Sig. (2-tailed)
Pair 1	**Bottom_0 - Bottom_45**	**-4.237**	**6**	**.005**
Pair 2	**Bottom_0 - Bottom_90**	**.292**	**6**	**.780**
Pair 3	**Bottom_0 - Bottom_135**	**-5.428**	**6**	**.002**
Pair 4	**Bottom_45 - Bottom_90**	**4.626**	**6**	**.004**
Pair 5	Bottom_45 - Bottom_135	**-2.404**	**6**	**.053**
Pair 6	Bottom_90 - Bottom_135	**-5.607**	**6**	**.001**
Pair 7	**Top_0 - Top_45**	**-4.203**	**6**	**.006**
Pair 8	**Top_0 - Top_90**	**.740**	**6**	**.487**
Pair 9	**Top_0 - Top_135**	**-3.913**	**6**	**.008**
Pair 10	**Top_45 - Top_90**	**4.435**	**6**	**.004**
Pair 11	**Top_45 - Top_135**	**.864**	**6**	**.421**
Pair 12	**Top_90 - Top_135**	**-4.093**	**6**	**.006**
Pair 13	**Bottom_45 - Top_45**	**-1.177**	**6**	**.284**
Pair 14	**Bottom_135 - Top_135**	**.080**	**6**	**.939**
Pair 15	**Bottom_45 - Top_135**	**-.817**	**6**	**.445**
Pair 16	**Bottom_135 - Top_45**	**-.727**	**6**	**.495**
Pair 17	**Top_0 - SecondTop_0**	**2.808**	**6**	**.031**
Pair 18	Top_90 - SecondTop_90	**1.390**	**6**	**.214**
Pair 19	Top_135 - SecondTop_135	**1.256**	**6**	**.256**

C. The non parametric tests used in the training contrasts where t-test assumptions were violated.

Test Statistics[a]

	SecondBottom_0 - Bottom_0	SecondBottom_45 - Bottom_45	SecondBottom_90 - Bottom_90	SecondBottom_135 - Bottom_135	SecondTop_45 - Top_45
Z	**-1.826[b]**	**-.730[c]**	**.000[d]**	**-.730[c]**	**-.730[c]**
Asymp. Sig. (2-tailed)	**.068**	**.465**	**1.000**	**.465**	**.465**

a. Wilcoxon Signed Ranks Test

b. Based on negative ranks.

c. Based on positive ranks.

d. The sum of negative ranks equals the sum of positive ranks.

9 Appendix II

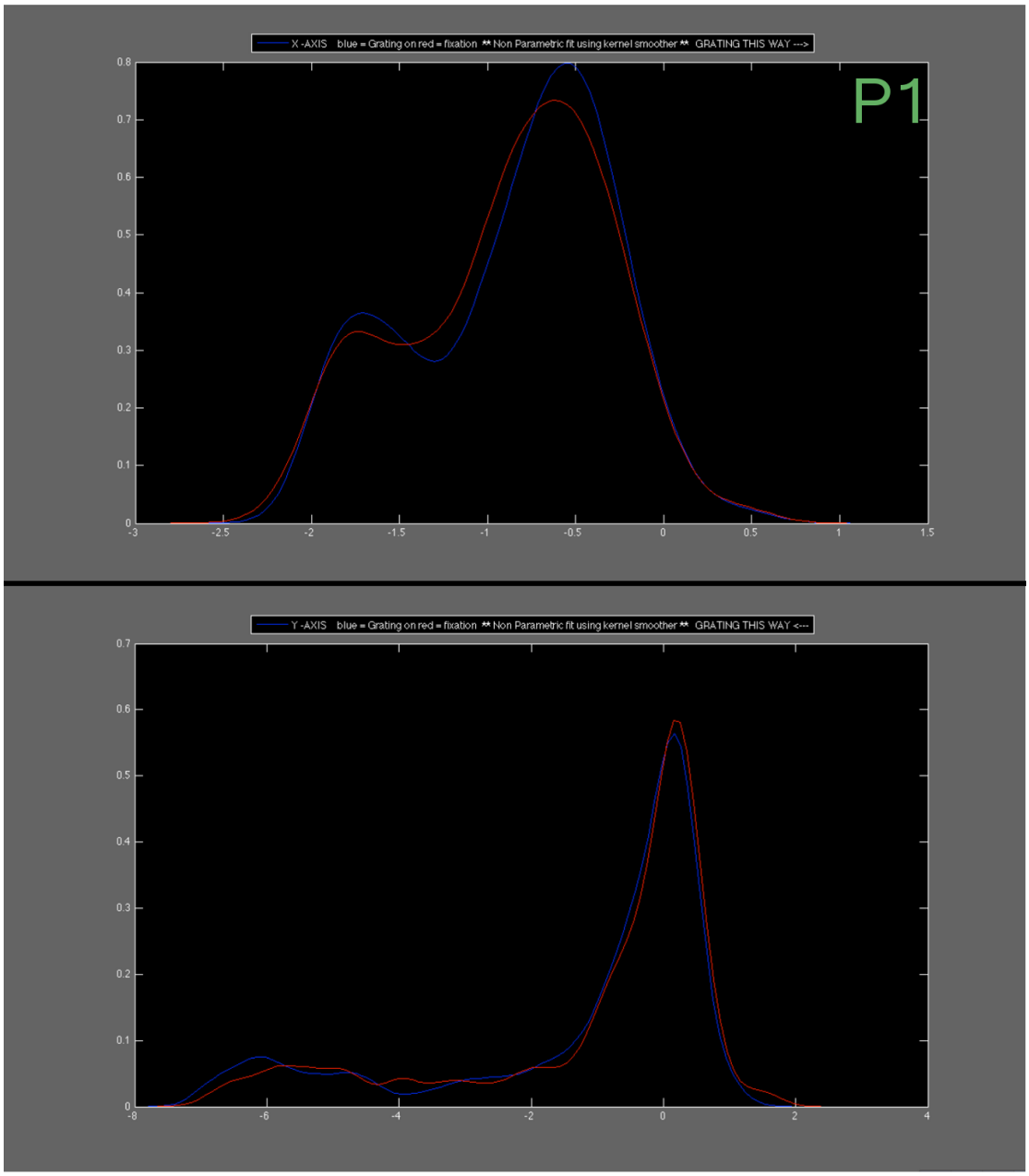

Figure 63: This figure displays the lines of best fit using a non-parametric kernel smoothing to the histograms of the mean fixation distances for every trial for participant 1 when the grating was ON (blue line) and when it was OFF (red line). Distance is how far fixation is from fixation in the x and y dimensions. At the top plot the grating is to the right from point 0 (point of fixation) on the x-axis, while on the bottom plot the grating is to the left from point 0 (fixation). Values on the x-axis are in degrees of visual angle distance from fixation while the y-axis shows how frequent each trial mean fixation was.

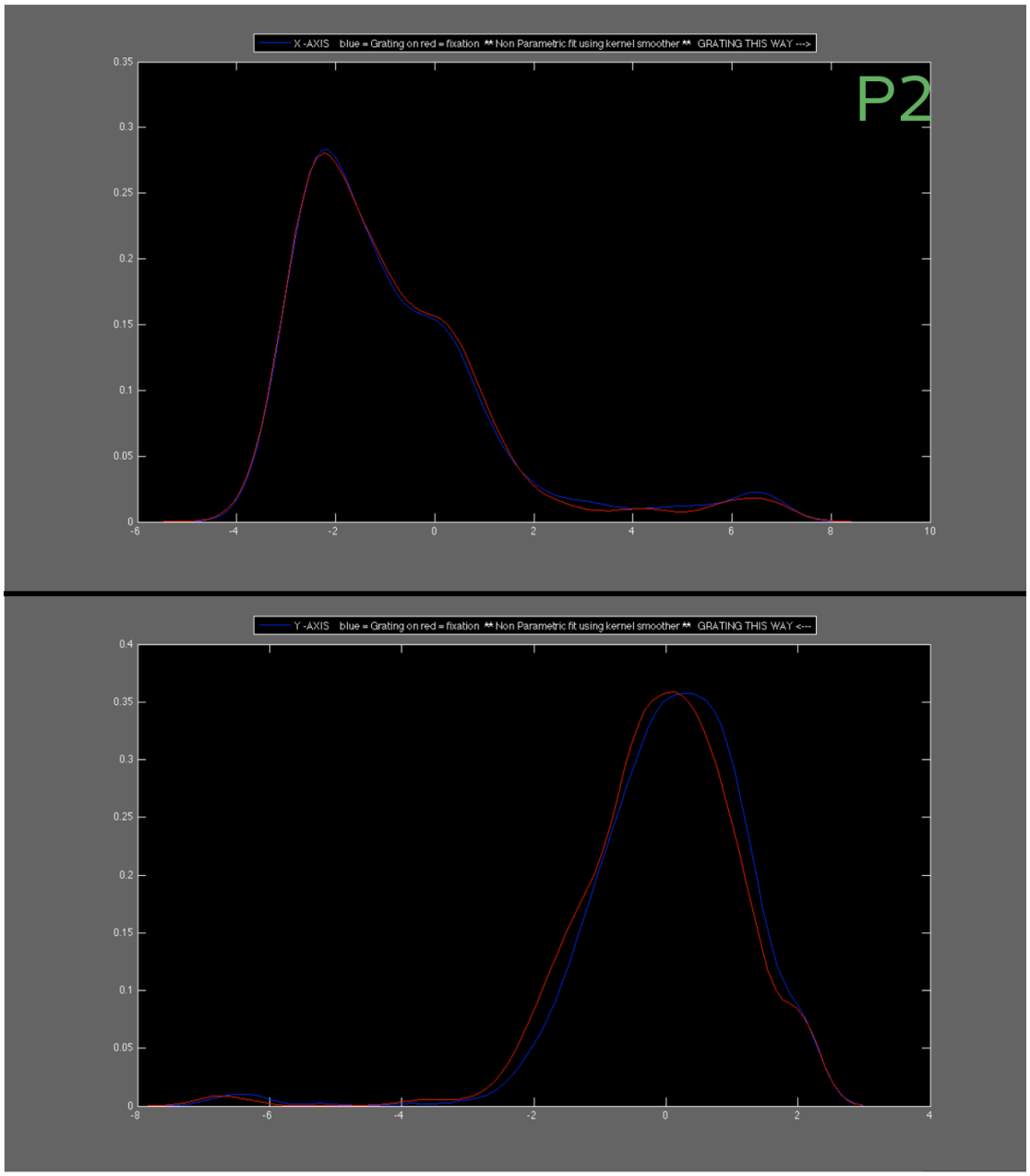

Figure 64: This figure displays the lines of best fit using a non-parametric kernel smoothing to the histograms of the mean fixation distances for every trial for participant 2 when the grating was ON (blue line) and when it was OFF (red line). Distance is how far fixation is from fixation in the x and y dimensions. At the top plot the grating is to the right from point 0 (point of fixation) on the x-axis, while on the bottom plot the grating is to the left from point 0 (fixation). Values on the x-axis are in degrees of visual angle distance from fixation while the y-axis shows how frequent each trial mean fixation was.

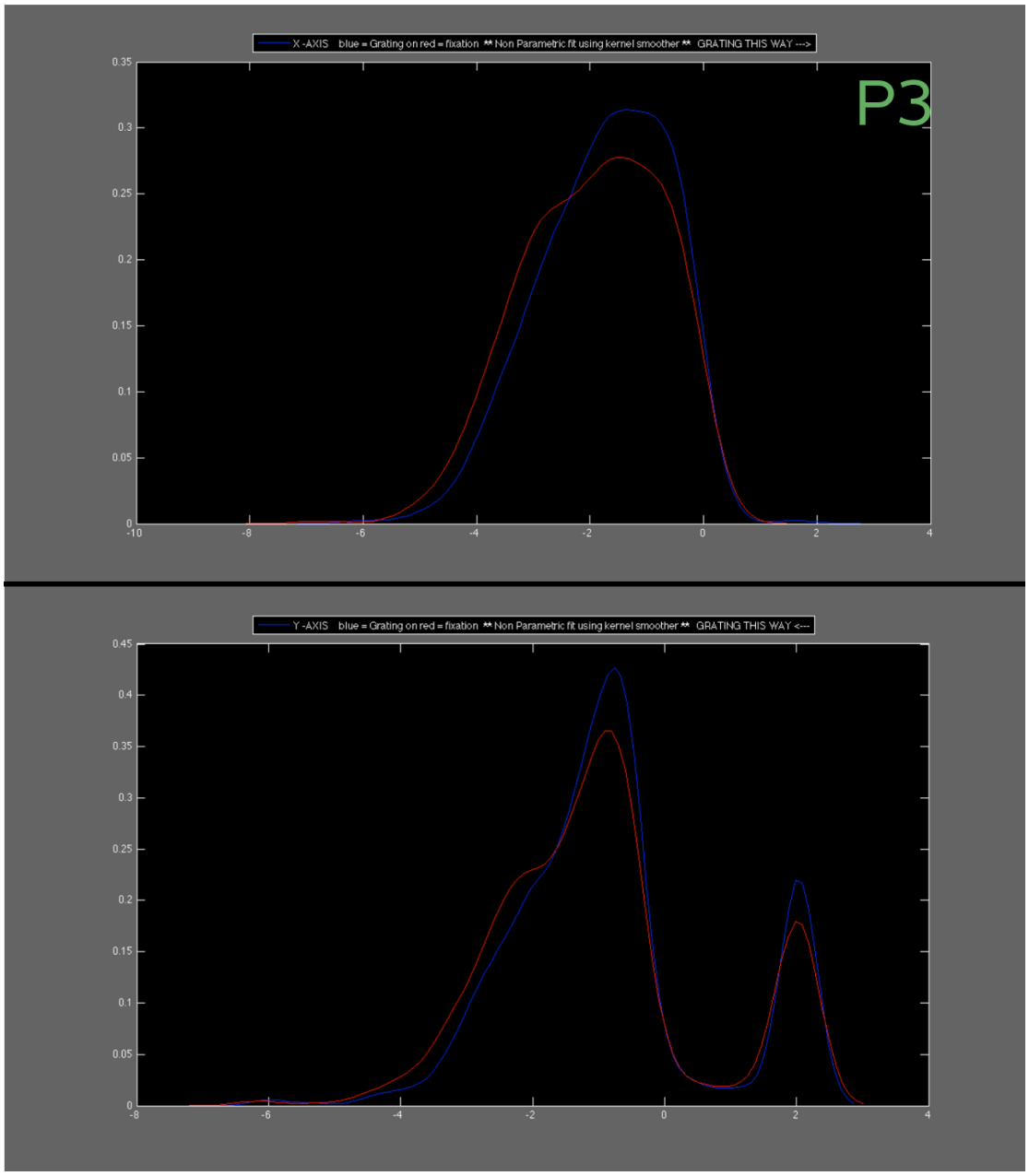

Figure 65 This figure displays the lines of best fit using a non-parametric kernel smoothing to the histograms of the mean fixation distances for every trial for participant 3 when the grating was ON (blue line) and when it was OFF (red line). Distance is how far fixation is from fixation in the x and y dimensions. At the top plot the grating is to the right from point 0 (point of fixation) on the x-axis, while on the bottom plot the grating is to the left from point 0 (fixation). Values on the x-axis are in degrees of visual angle distance from fixation while the y-axis shows how frequent each trial mean fixation was.

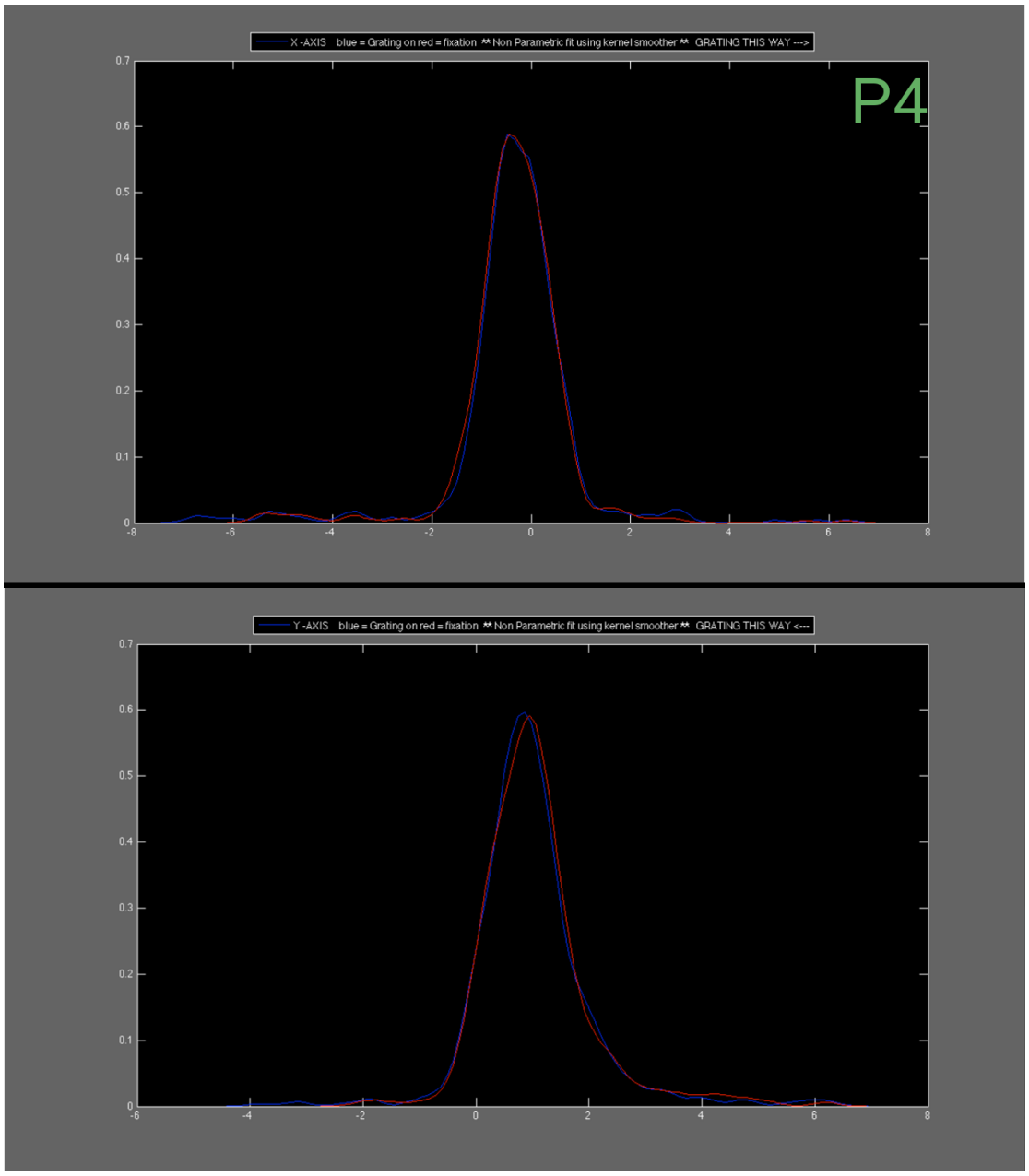

Figure 66: This figure displays the lines of best fit using a non-parametric kernel smoothing to the histograms of the mean fixation distances for every trial for participant 4 when the grating was ON (blue line) and when it was OFF (red line). Distance is how far fixation is from fixation in the x and y dimensions. At the top plot the grating is to the right from point 0 (point of fixation) on the x-axis, while on the bottom plot the grating is to the left from point 0 (fixation). Values on the x-axis are in degrees of visual angle distance from fixation while the y-axis shows how frequent each trial mean fixation was.

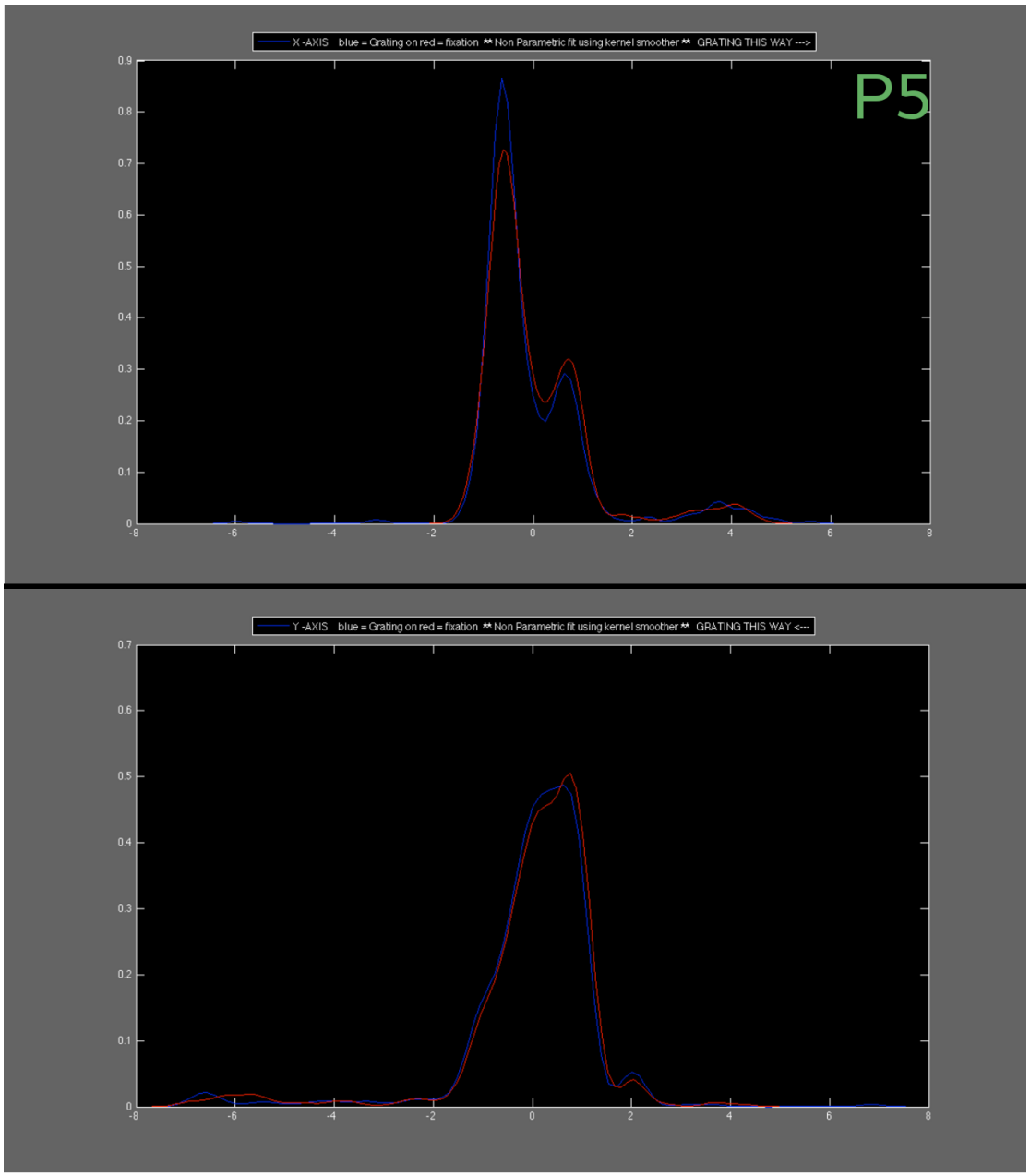

Figure 67: This figure displays the lines of best fit using a non-parametric kernel smoothing to the histograms of the mean fixation distances for every trial for participant 5 when the grating was ON (blue line) and when it was OFF (red line). Distance is how far fixation is from fixation in the x and y dimensions. At the top plot the grating is to the right from point 0 (point of fixation) on the x-axis, while on the bottom plot the grating is to the left from point 0 (fixation). Values on the x-axis are in degrees of visual angle distance from fixation while the y-axis shows how frequent each trial mean fixation was.

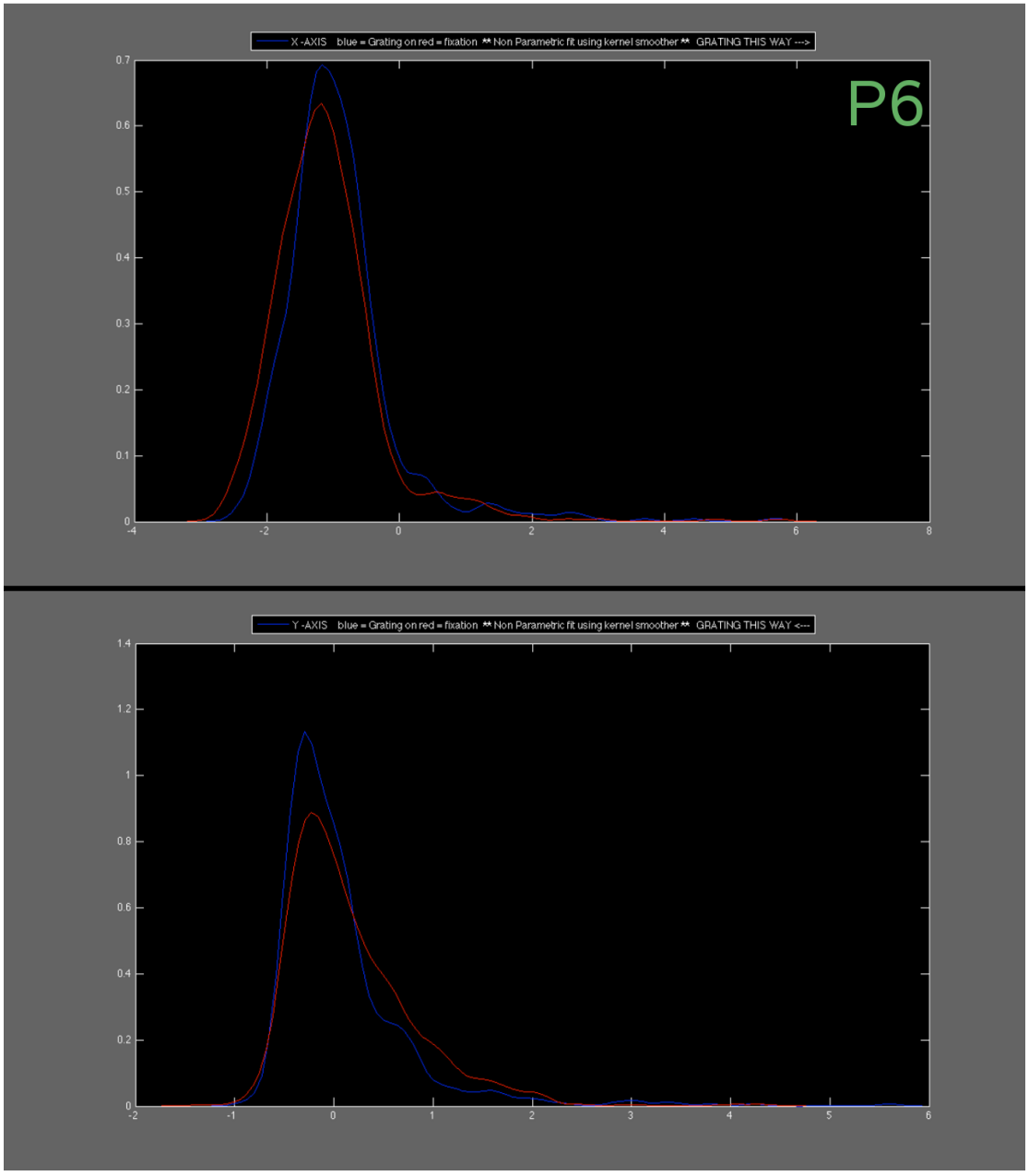

Figure 68 This figure displays the lines of best fit using a non-parametric kernel smoothing to the histograms of the mean fixation distances for every trial for participant 6 when the grating was ON (blue line) and when it was OFF (red line). Distance is how far fixation is from fixation in the x and y dimensions. At the top plot the grating is to the right from point 0 (point of fixation) on the x-axis, while on the bottom plot the grating is to the left from point 0 (fixation). Values on the x-axis are in degrees of visual angle distance from fixation while the y-axis shows how frequent each trial mean fixation was.

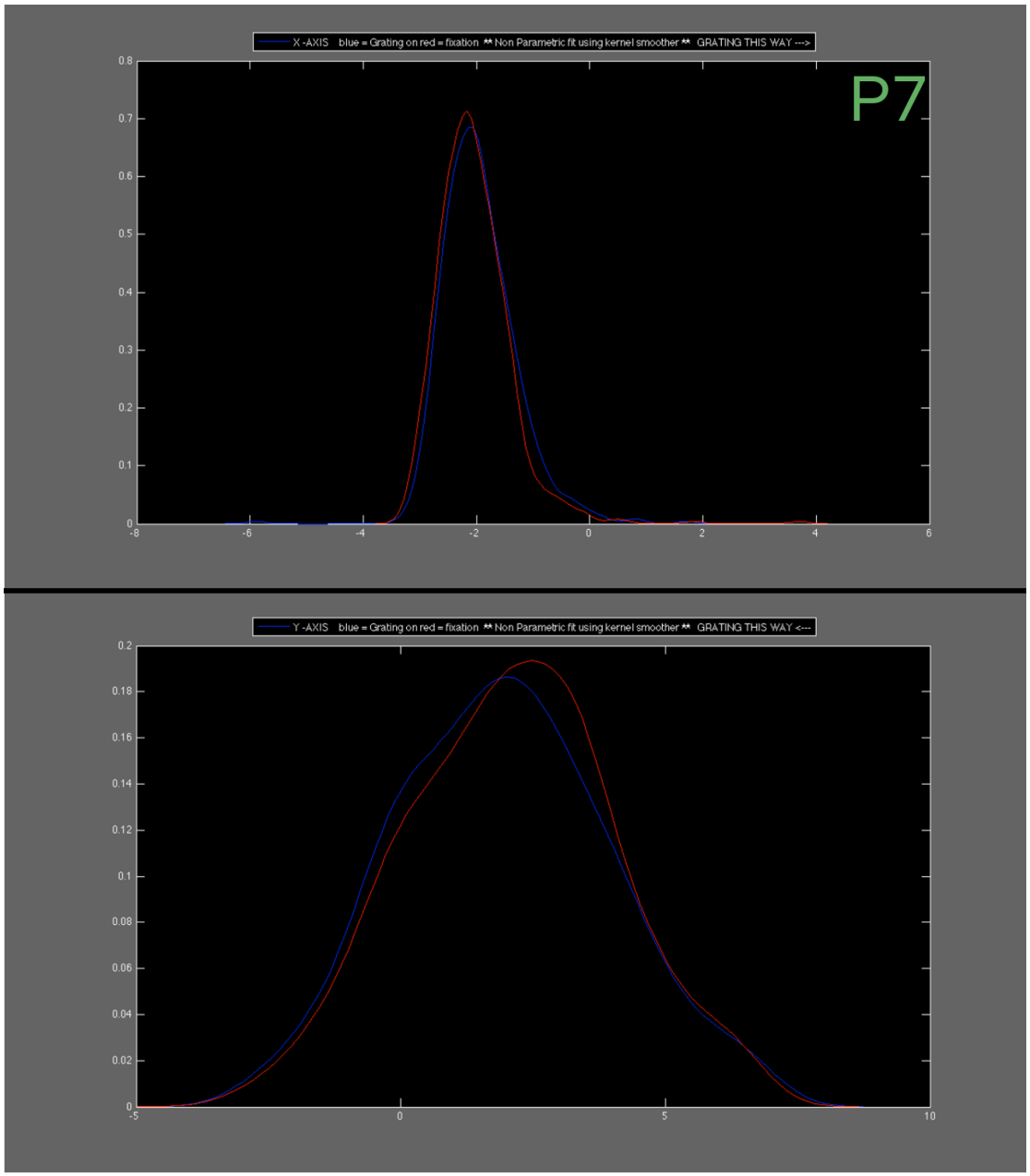

Figure 69: This figure displays the lines of best fit using a non-parametric kernel smoothing to the histograms of the mean fixation distances for every trial for participant 7 when the grating was ON (blue line) and when it was OFF (red line). Distance is how far fixation is from fixation in the x and y dimensions. At the top plot the grating is to the right from point 0 (point of fixation) on the x-axis, while on the bottom plot the grating is to the left from point 0 (fixation). Values on the x-axis are in degrees of visual angle distance from fixation while the y-axis shows how frequent each trial mean fixation was.

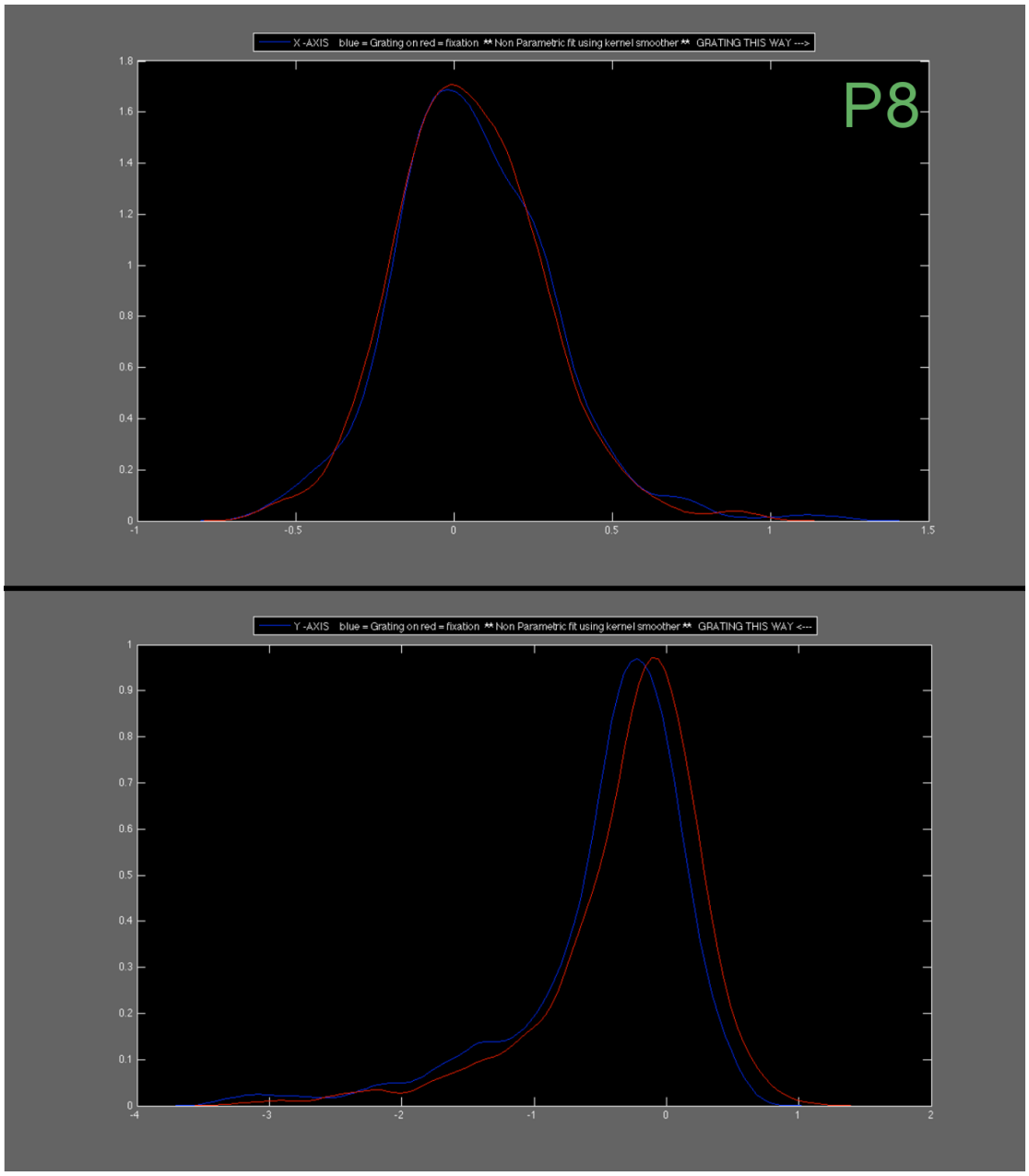

Figure 70: This figure displays the lines of best fit using a non-parametric kernel smoothing to the histograms of the mean fixation distances for every trial for participant 8 when the grating was ON (blue line) and when it was OFF (red line). Distance is how far fixation is from fixation in the x and y dimensions. At the top plot the grating is to the right from point 0 (point of fixation) on the x-axis, while on the bottom plot the grating is to the left from point 0 (fixation). Values on the x-axis are in degrees of visual angle distance from fixation while the y-axis shows how frequent each trial mean fixation was.

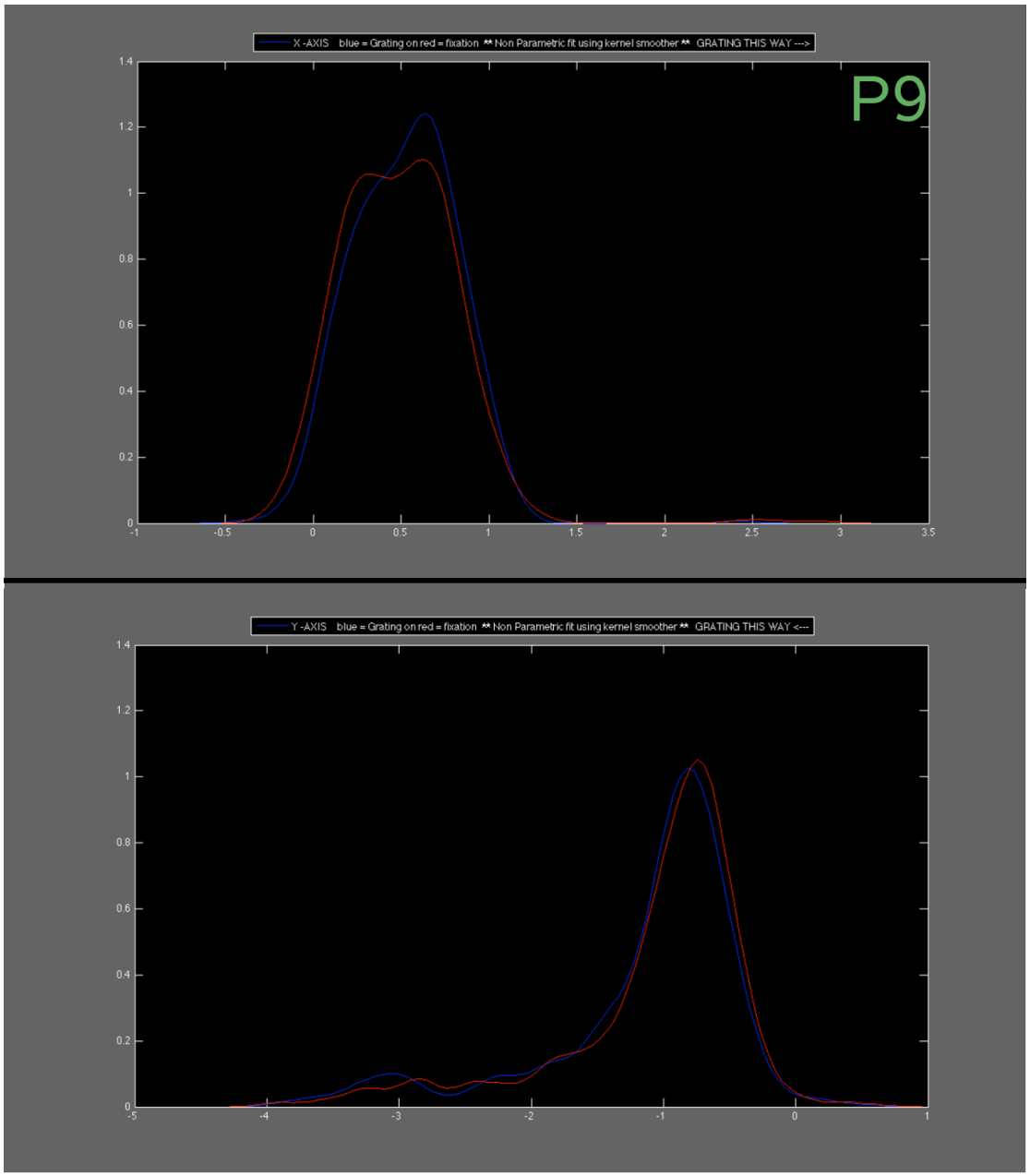

Figure 71: This figure displays the lines of best fit using a non-parametric kernel smoothing to the histograms of the mean fixation distances for every trial for participant 9 when the grating was ON (blue line) and when it was OFF (red line). Distance is how far fixation is from fixation in the x and y dimensions. At the top plot the grating is to the right from point 0 (point of fixation) on the x-axis, while on the bottom plot the grating is to the left from point 0 (fixation). Values on the x-axis are in degrees of visual angle distance from fixation while the y-axis shows how frequent each trial mean fixation was.

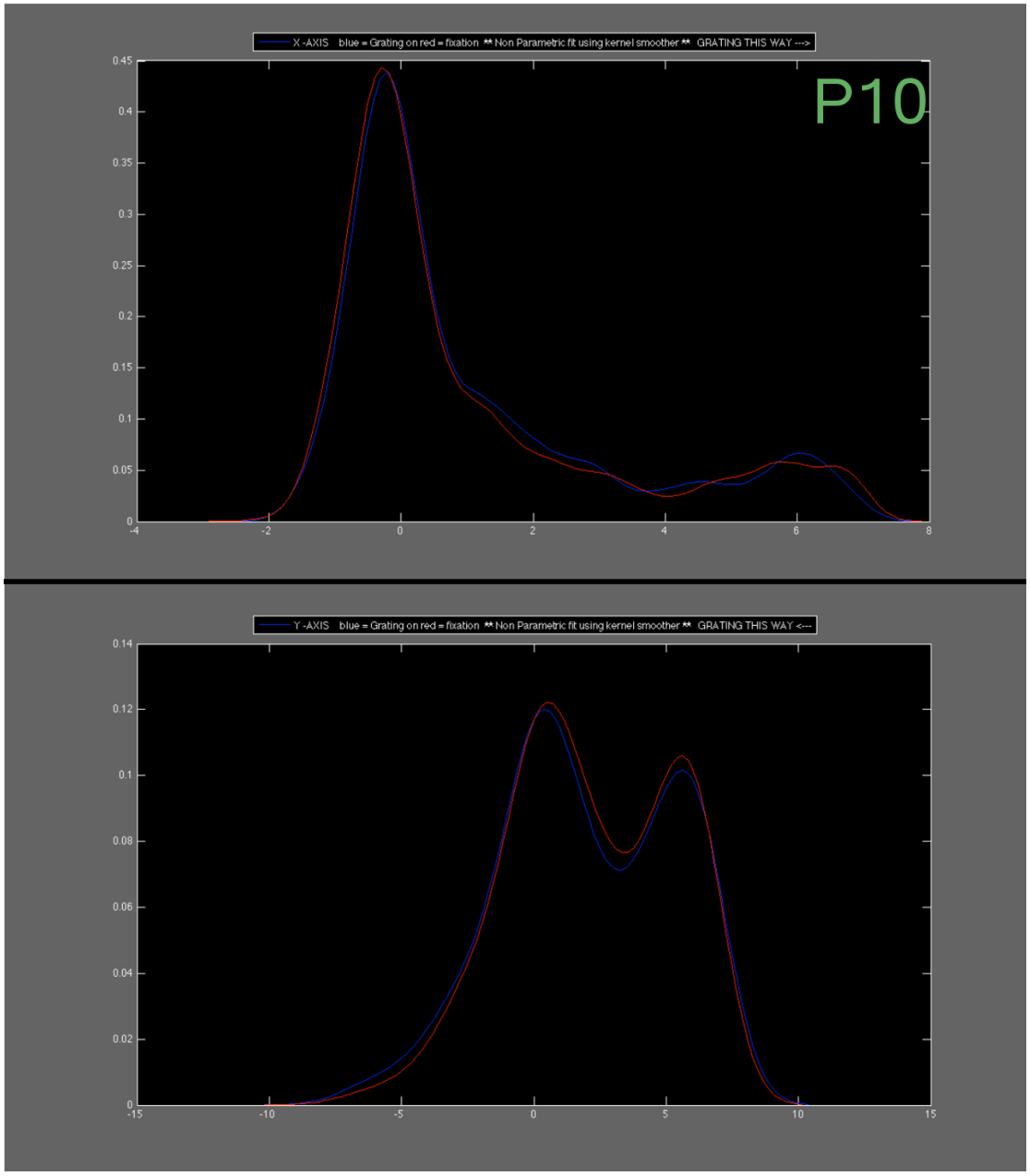

Figure 72: This figure displays the lines of best fit using a non-parametric kernel smoothing to the histograms of the mean fixation distances for every trial for participant 10 when the grating was ON (blue line) and when it was OFF (red line). Distance is how far fixation is from fixation in the x and y dimensions. At the top plot the grating is to the right from point 0 (point of fixation) on the x-axis, while on the bottom plot the grating is to the left from point 0 (fixation). Values on the x-axis are in degrees of visual angle distance from fixation while the y-axis shows how frequent each trial mean fixation was.

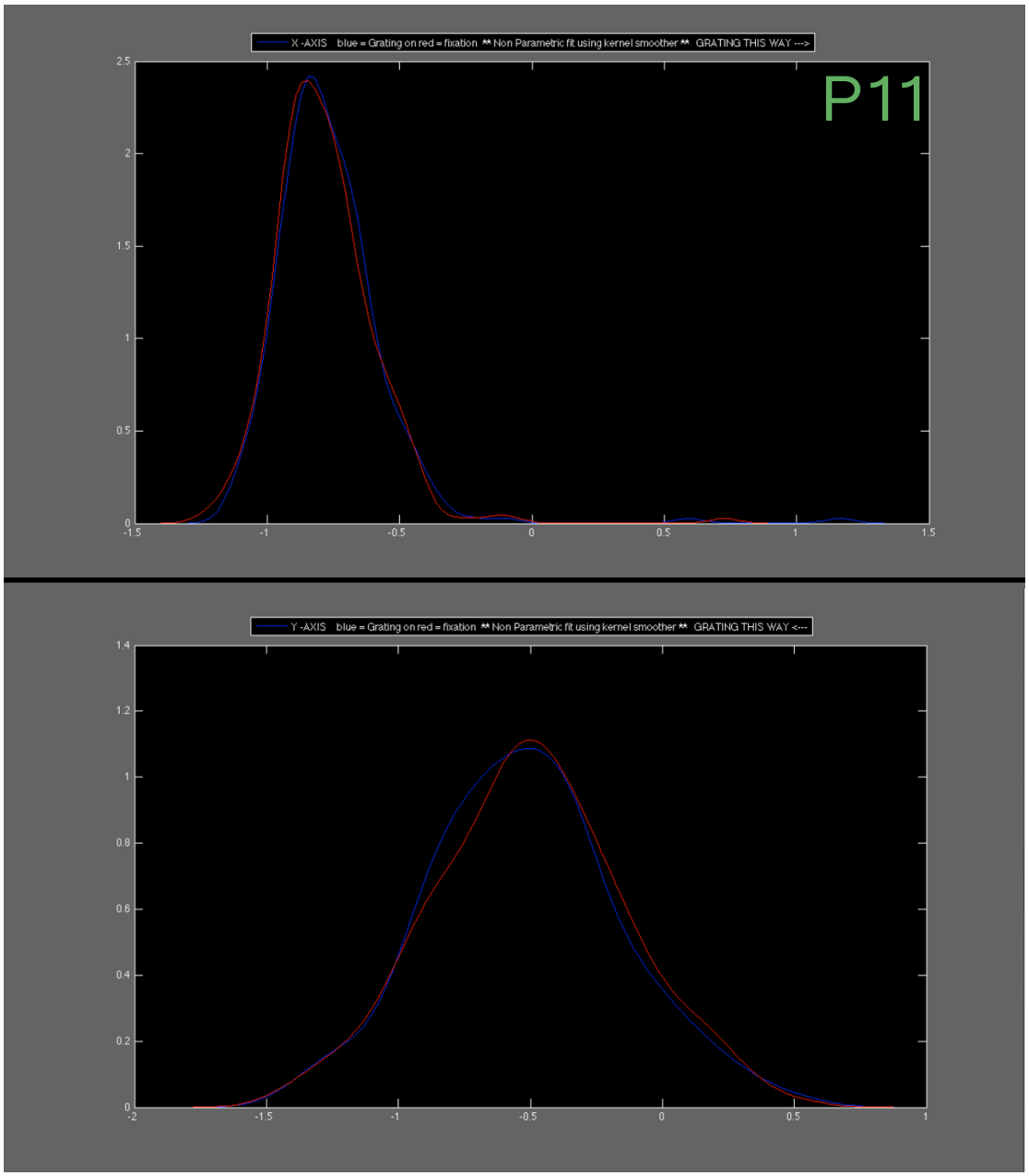

Figure 73: This figure displays the lines of best fit using a non-parametric kernel smoothing to the histograms of the mean fixation distances for every trial for participant 11 when the grating was ON (blue line) and when it was OFF (red line). Distance is how far fixation is from fixation in the x and y dimensions. At the top plot the grating is to the right from point 0 (point of fixation) on the x-axis, while on the bottom plot the grating is to the left from point 0 (fixation). Values on the x-axis are in degrees of visual angle distance from fixation while the y-axis shows how frequent each trial mean fixation was.

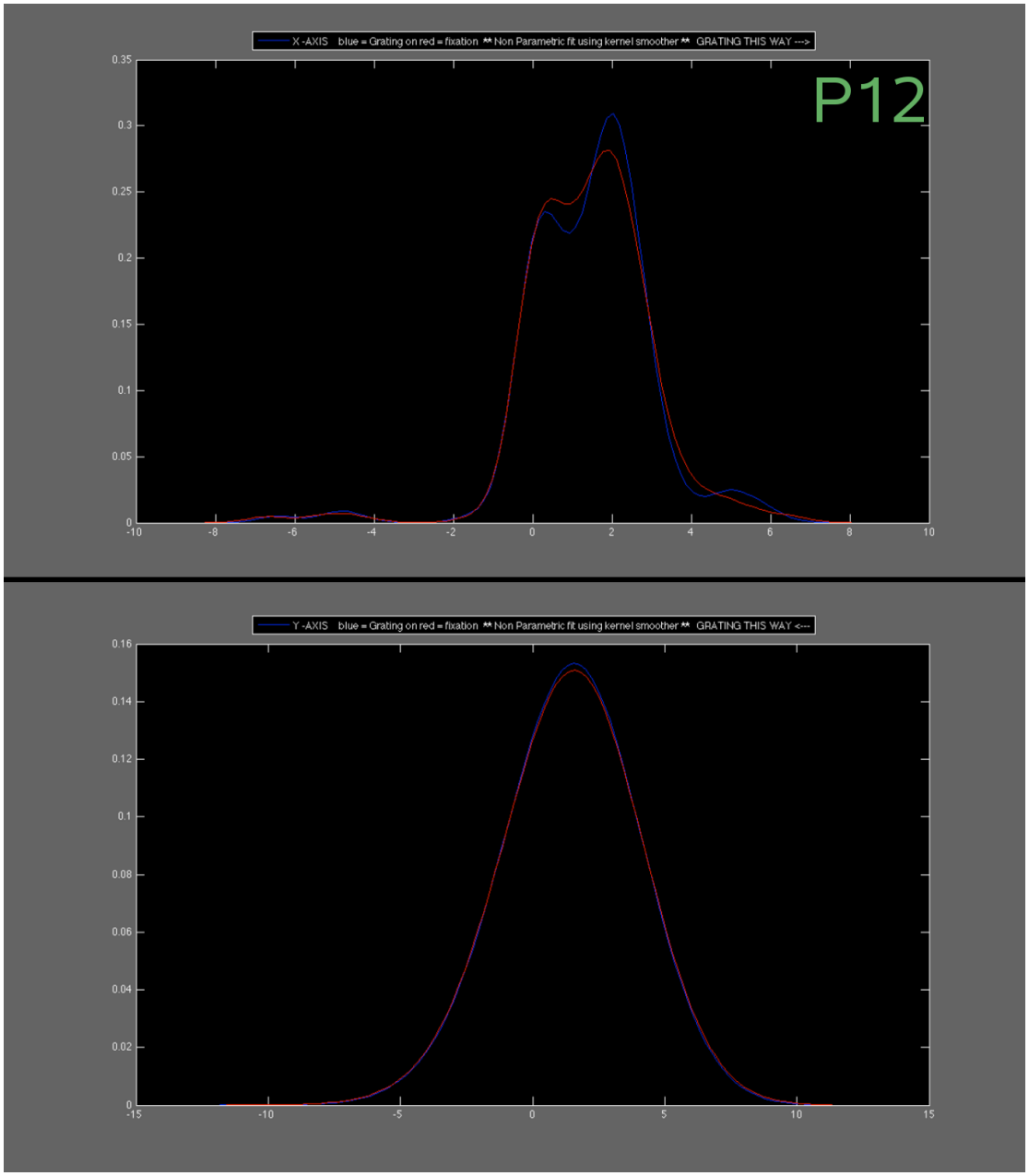

Figure 74: This figure displays the lines of best fit using a non-parametric kernel smoothing to the histograms of the mean fixation distances for every trial for participant 12 when the grating was ON (blue line) and when it was OFF (red line). Distance is how far fixation is from fixation in the x and y dimensions. At the top plot the grating is to the right from point 0 (point of fixation) on the x-axis, while on the bottom plot the grating is to the left from point 0 (fixation). Values on the x-axis are in degrees of visual angle distance from fixation while the y-axis shows how frequent each trial mean fixation was.

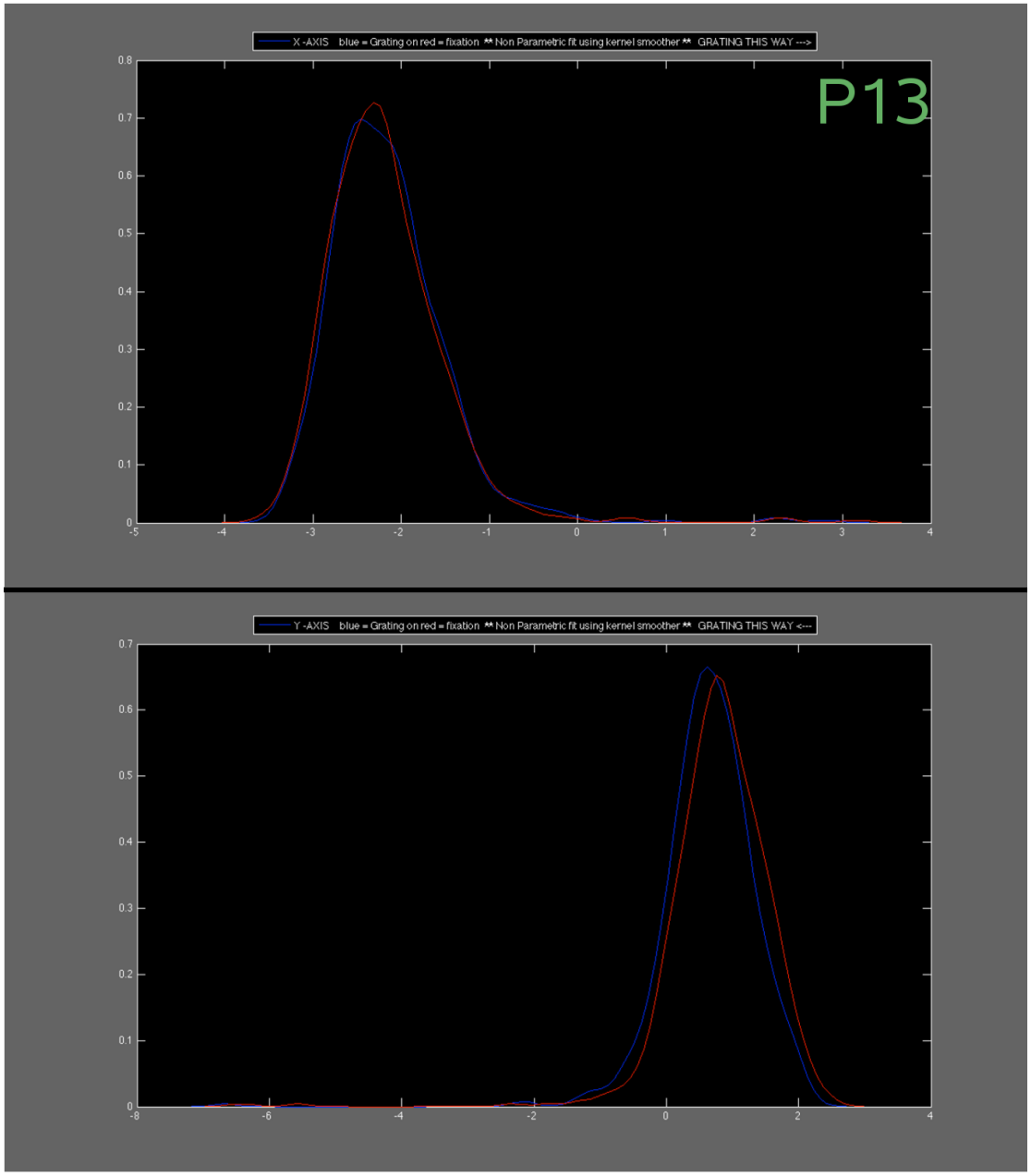

Figure 75: This figure displays the lines of best fit using a non-parametric kernel smoothing to the histograms of the mean fixation distances for every trial for participant 13 when the grating was ON (blue line) and when it was OFF (red line). Distance is how far fixation is from fixation in the x and y dimensions. At the top plot the grating is to the right from point 0 (point of fixation) on the x-axis, while on the bottom plot the grating is to the left from point 0 (fixation). Values on the x-axis are in degrees of visual angle distance from fixation while the y-axis shows how frequent each trial mean fixation was.

10 Appendix III

TABLES WITH THE SUMARY OF THE GROUP SAM ANALYSIS:

Table 10: Trigger 2 is the main effect of trigger 2 and trigger 3 of 3. Tstat 1 is the main effect while tstat2 is the results for positive correlations of MEG activation to behavioral thresholds and tstat3 for negative correlations. Yes means there was significant activation in the visual cortex, * means no (significant) visual activation found while NO means that there was no significant activation whatsoever found).

Trigger2	Tstat1	Tstat2	Tstat3	Trigger3	Tstat1	Tstat2	Tstat3
15-25 Hz	No	No	No		No	No	No
30 -70 Hz	Yes	Yes	No		Yes	No	No
40-60 Hz	Yes	No	No		Yes	No	No
40-80 Hz	Yes	No	No		Yes	No	No
4-8 Hz	No	No	No		No	No	No
5-15 Hz	No	No	No		No	Yes*	No
60-80 Hz	Yes	Yes*	No		Yes	No	No
8-12 Hz	No	No	No		No	No	No

Table 11: Trigger 7 is the main effect of trigger 7 and trigger 8 of 8. Tstat 1 is the main effect while tstat2 is the results for positive correlations of MEG activation to behavioral thresholds and tstat3 for negative correlations. Yes means there was significant activation in the visual cortex, * means no significant visual activation found while NO means that there was no significant activation found).

Trigger7	Tstat1	Tstat2	Tstat3	Trigger8	Tstat1	Tstat2	Tstat3
15-25 Hz	No	No	No		No	No	No
30 -70 Hz	Yes	No	No		Yes	No	No
40-60 Hz	Yes	No	No		Yes	No	No
40-80 Hz	Yes	No	No		Yes	No	No
4-8 Hz	No	No	No		No	No	No
5-15 Hz	No	No	No		No	No	No
60-80 Hz	Yes	No	No		Yes	No	No
8-12 Hz	No	No	No		No	No	No

11 Appendix IV

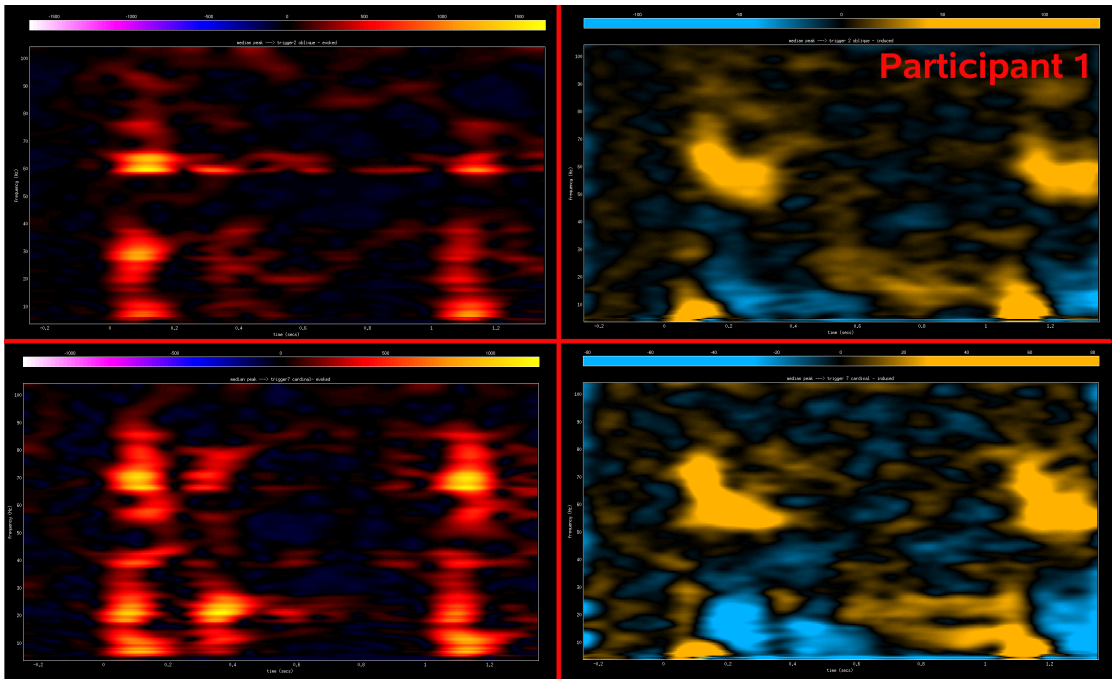

Figure 76: This figure shows for the medial placed sensor for participant 1 the oblique evoked response (top left image), the oblique induced response (top right), the cardinal evoked response (bottom left) and the cardinal induced response (bottom right). Y-axis is frequency and x-axis time.

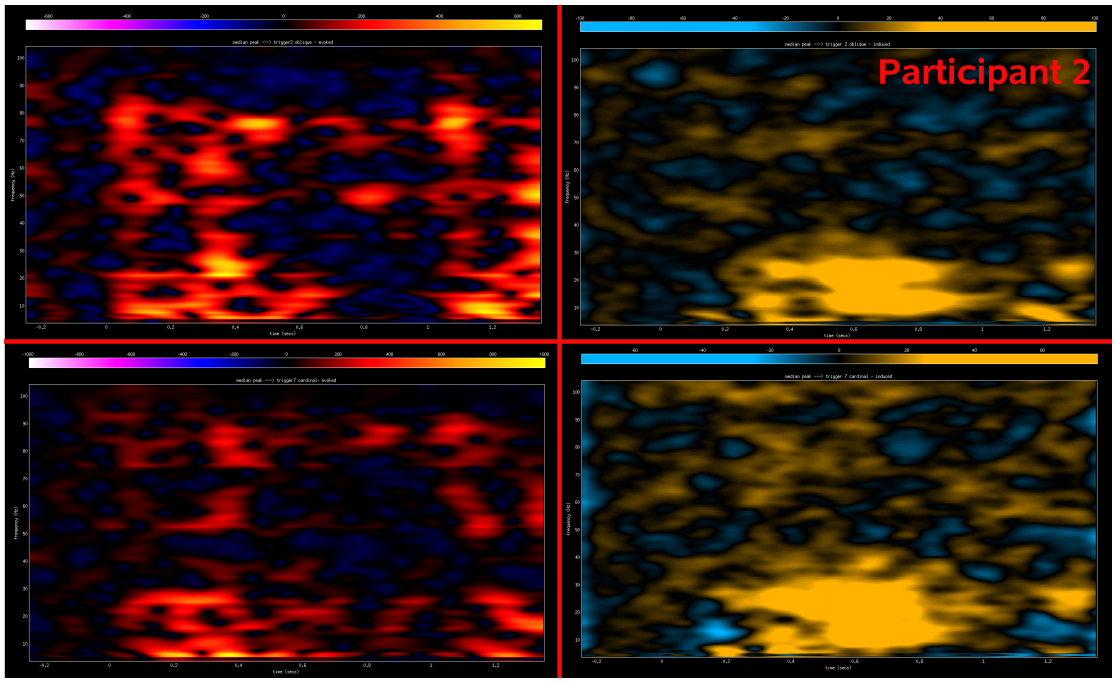

Figure 77: This figure shows for the medial placed sensor for participant 2 the oblique evoked response (top left image), the oblique induced response (top

right), the cardinal evoked response (bottom left) and the cardinal induced response (bottom right). Y-axis is frequency and x-axis time.

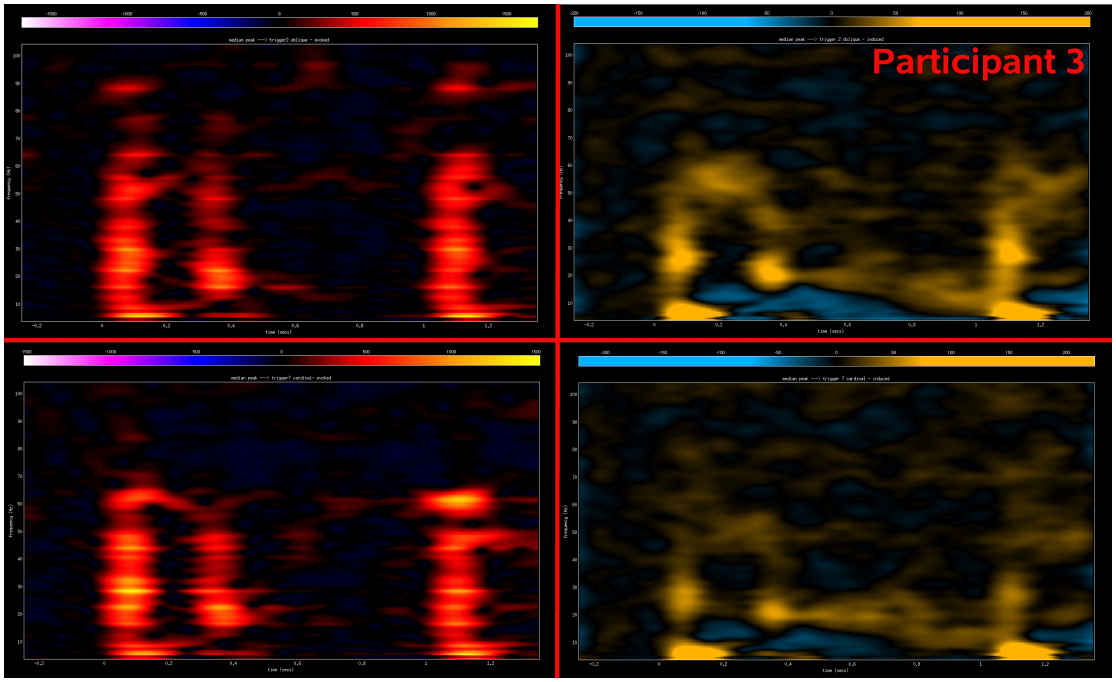

Figure 78: This figure shows for the medial placed sensor for participant 3 the oblique evoked response (top left image), the oblique induced response (top right), the cardinal evoked response (bottom left) and the cardinal induced response (bottom right). Y-axis is frequency and x-axis time.

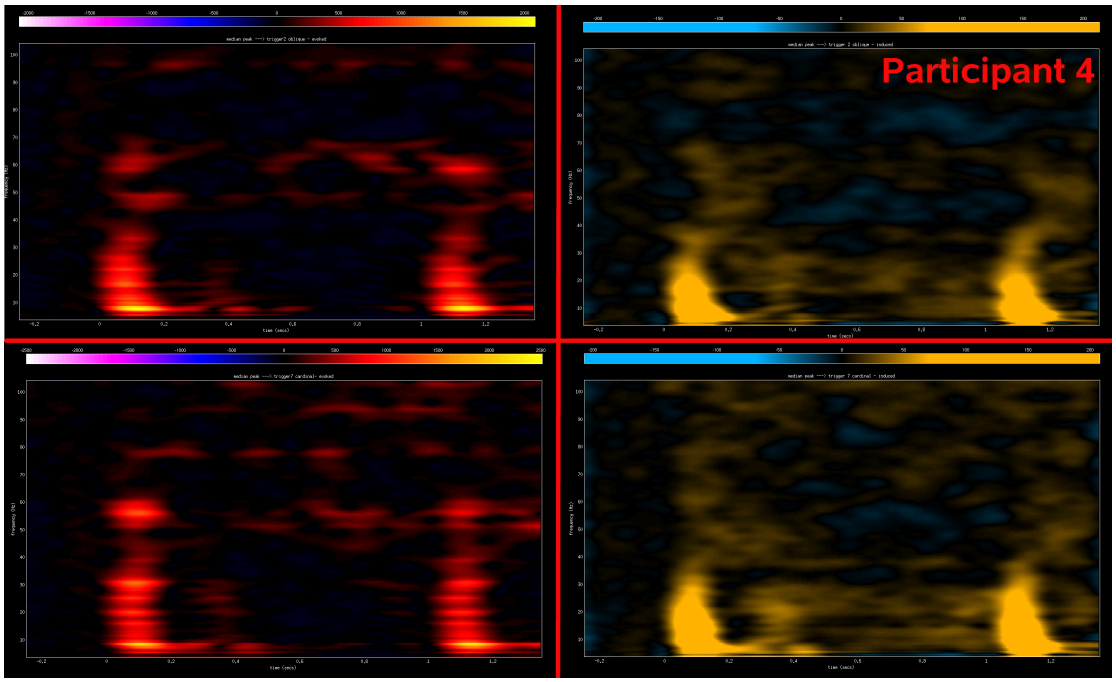

Figure 79: This figure shows for the medial placed sensor for participant 4 the oblique evoked response (top left image), the oblique induced response (top right), the cardinal evoked response (bottom left) and the cardinal induced response (bottom right). Y-axis is frequency and x-axis time.

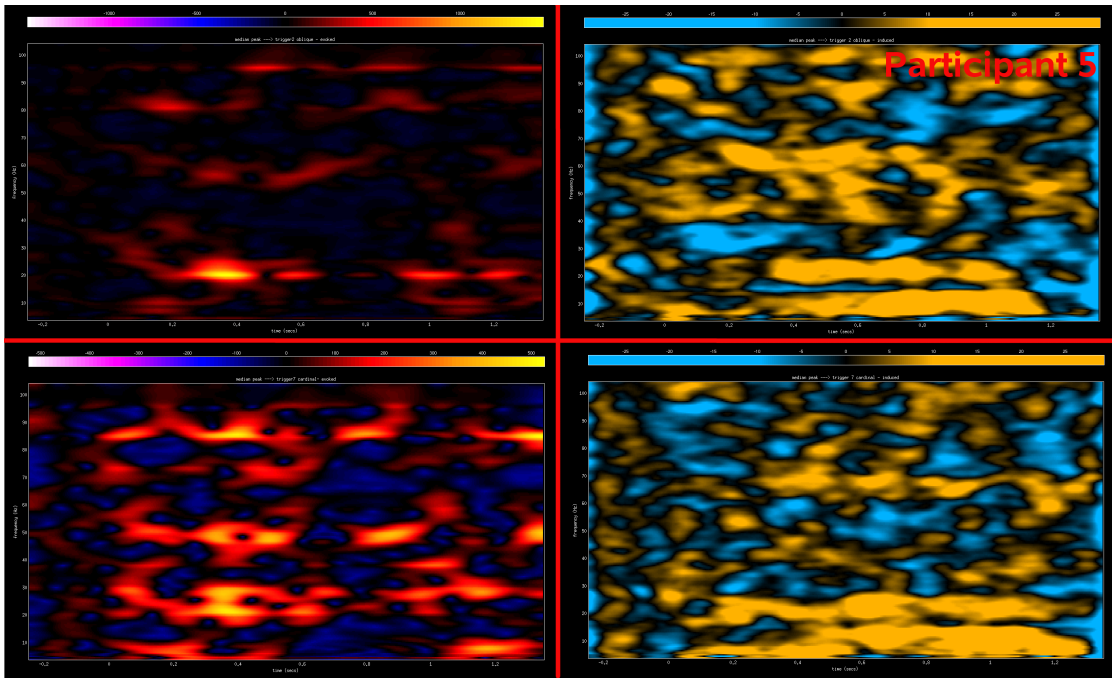

Figure 80: This figure shows for the medial placed sensor for participant 5 the oblique evoked response (top left image), the oblique induced response (top right), the cardinal evoked response (bottom left) and the cardinal induced response (bottom right). Y-axis is frequency and x-axis time.

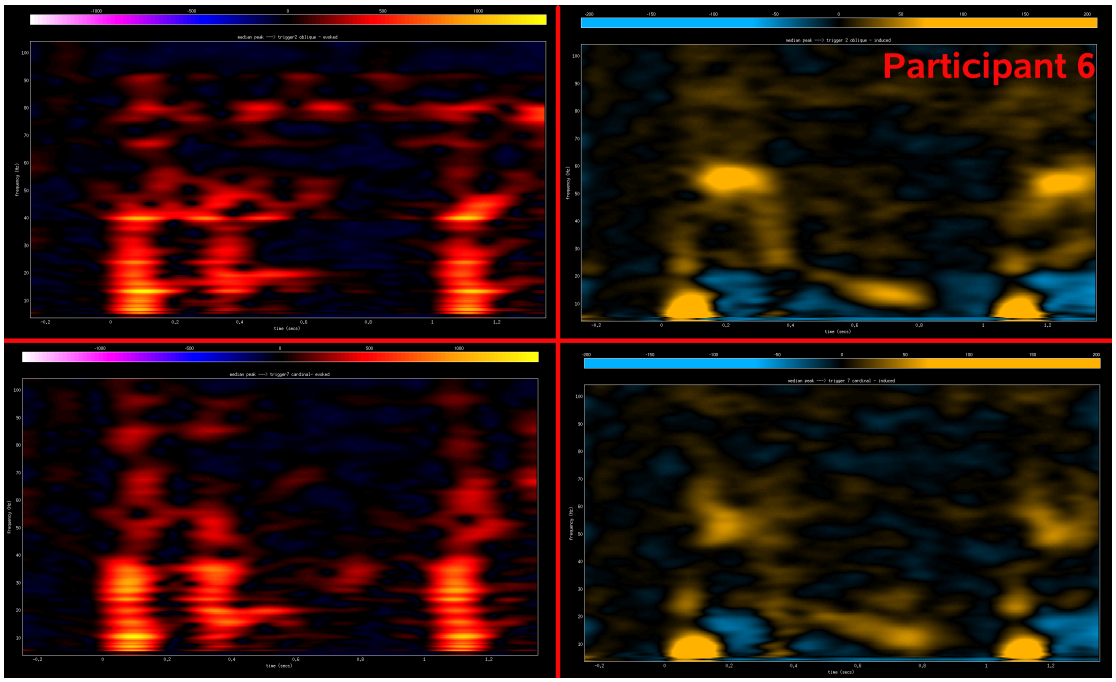

Figure 81: This figure shows for the medial placed sensor for participant 6 the oblique evoked response (top left image), the oblique induced response (top

right), the cardinal evoked response (bottom left) and the cardinal induced response (bottom right). Y-axis is frequency and x-axis time.

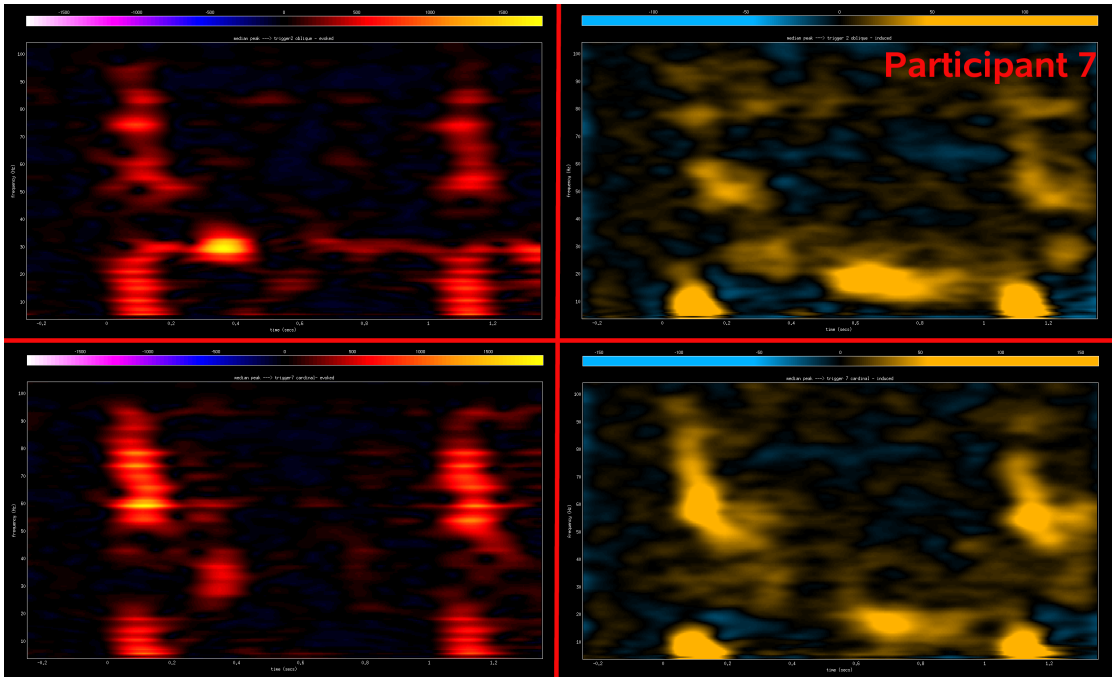

Figure 82: This figure shows for the medial placed sensor for participant 7 the oblique evoked response (top left image), the oblique induced response (top right), the cardinal evoked response (bottom left) and the cardinal induced response (bottom right). Y-axis is frequency and x-axis time.

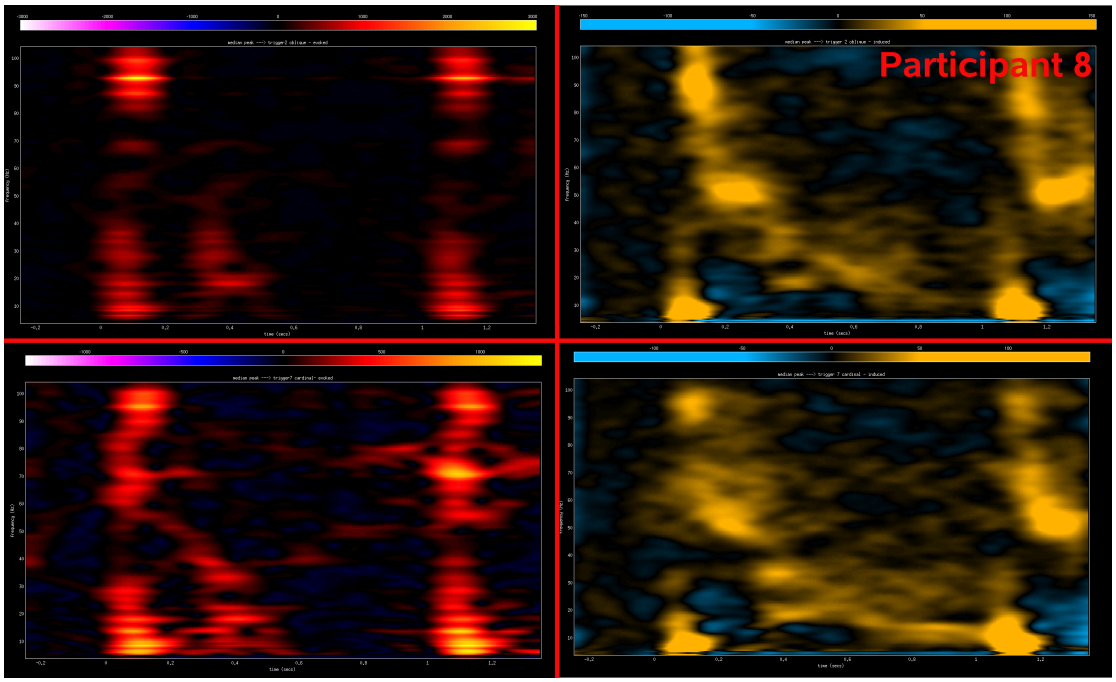

Figure 83: This figure shows for the medial placed sensor for participant 8 the oblique evoked response (top left image), the oblique induced response (top right), the cardinal evoked response (bottom left) and the cardinal induced response (bottom right). Y-axis is frequency and x-axis time.

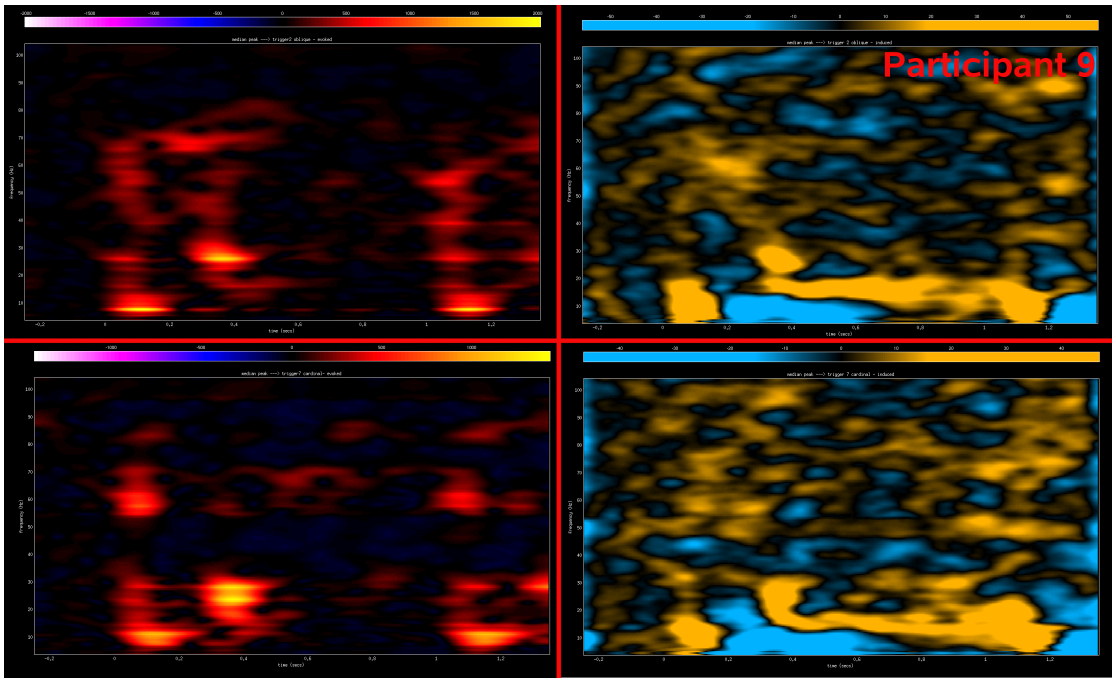

Figure 84: This figure shows for the medial placed sensor for participant 9 the oblique evoked response (top left image), the oblique induced response (top right), the cardinal evoked response (bottom left) and the cardinal induced response (bottom right). Y-axis is frequency and x-axis time.

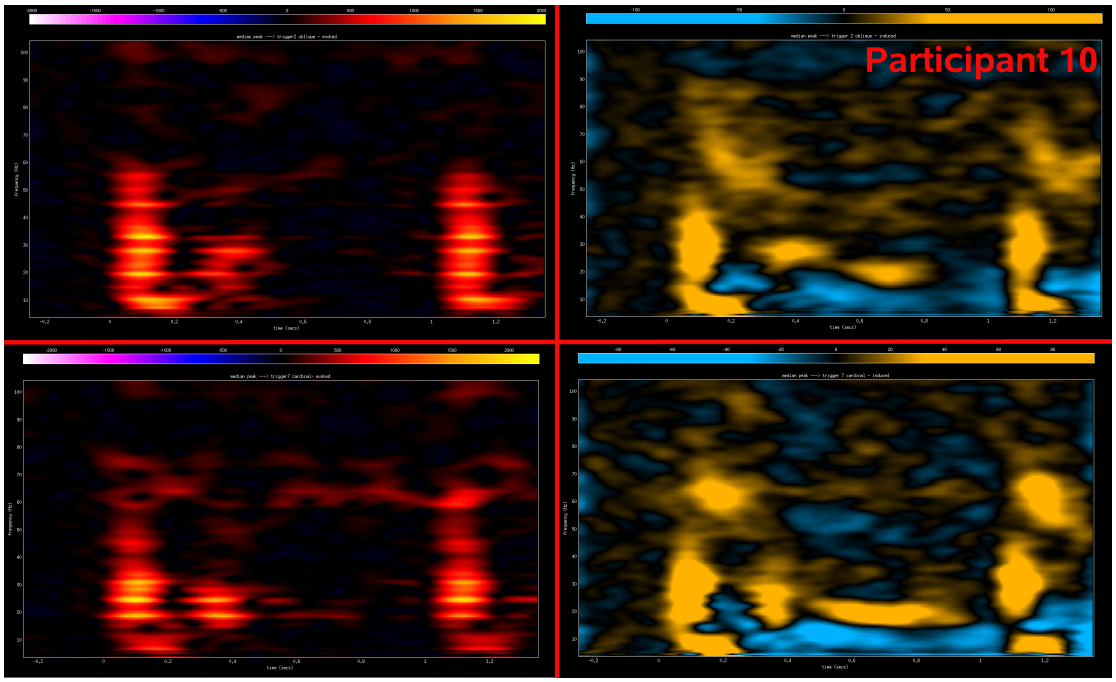

Figure 85: This figure shows for the medial placed sensor for participant 10 the oblique evoked response (top left image), the oblique induced response (top

right), the cardinal evoked response (bottom left) and the cardinal induced response (bottom right). Y-axis is frequency and-x axis time.

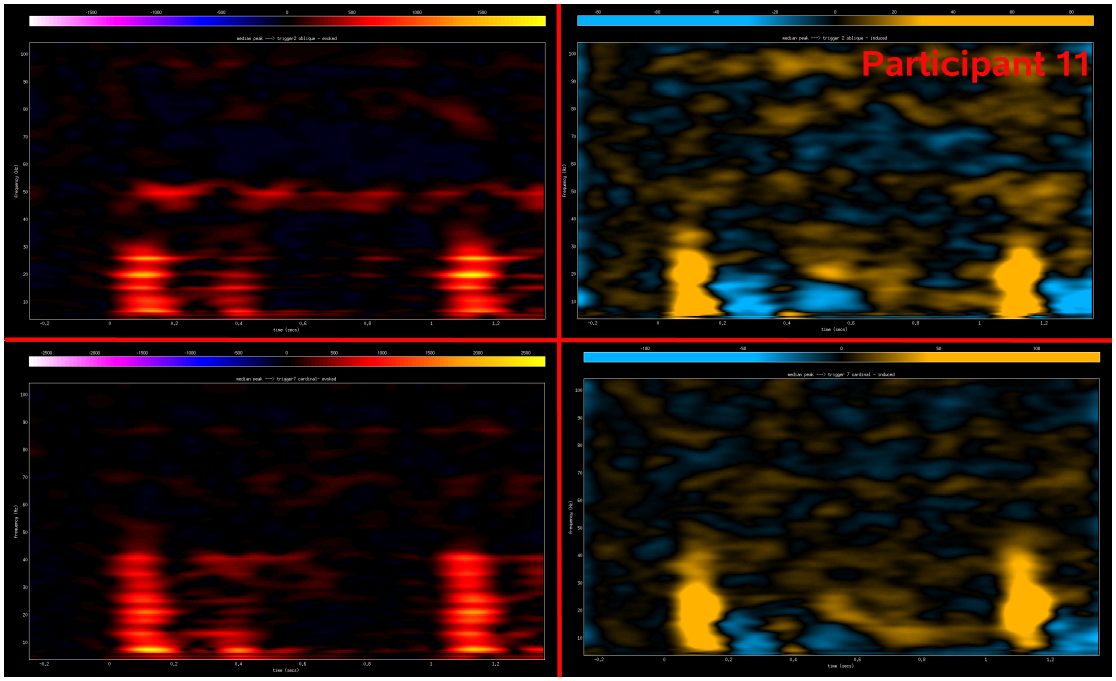

Figure 86: This figure shows for the medial placed sensor for participant 11 the oblique evoked response (top left image), the oblique induced response (top right), the cardinal evoked response (bottom left) and the cardinal induced response (bottom right). Y-axis is frequency and x-axis time.

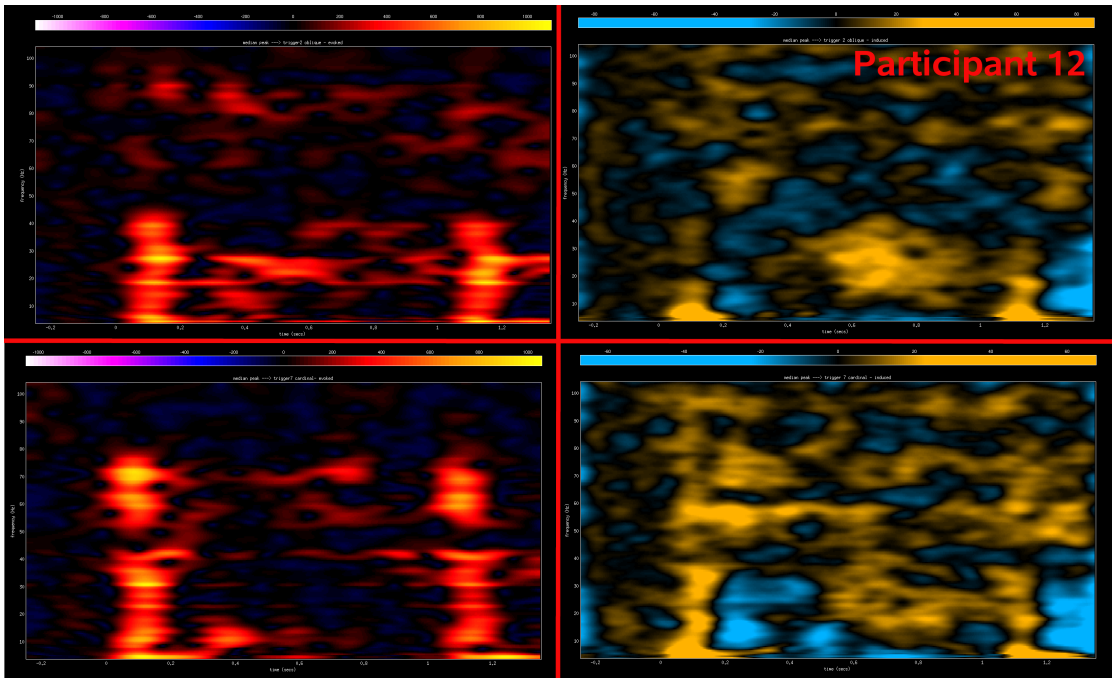

Figure 87: This figure shows for the medial placed sensor for participant 12 the oblique evoked response (top left image), the oblique induced response (top right), the cardinal evoked response (bottom left) and the cardinal induced response (bottom right). Y-axis is frequency and x-axis time.

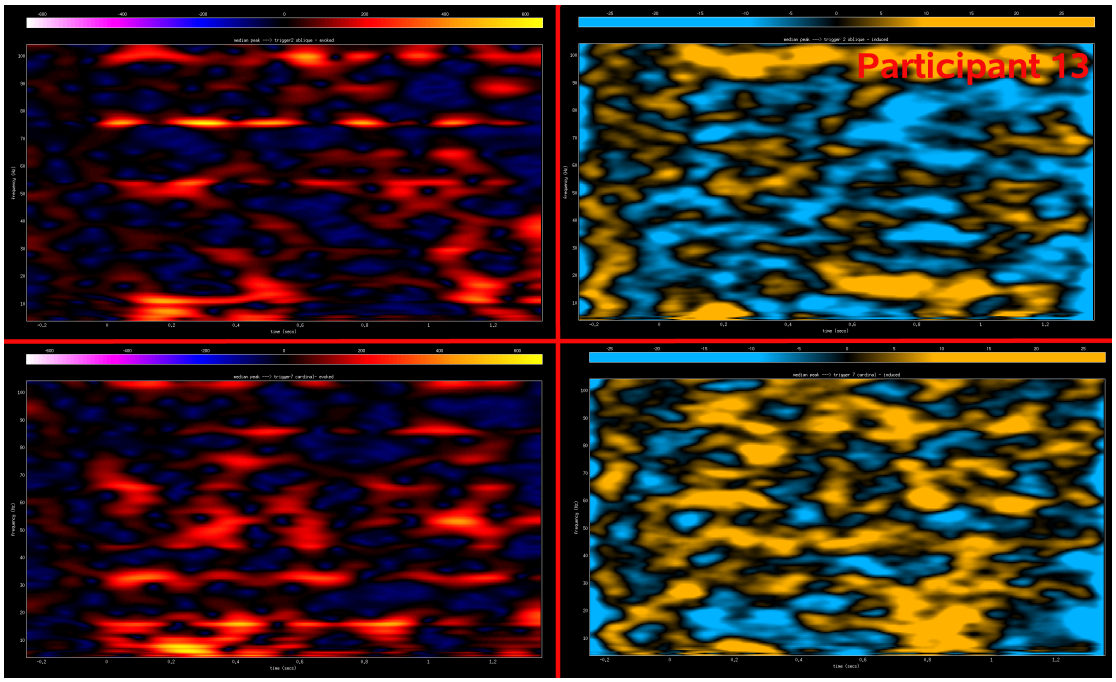

Figure 88: This figure shows for the medial placed sensor for participant 13 the oblique evoked response (top left image), the oblique induced response (top

right), the cardinal evoked response (bottom left) and the cardinal induced response (bottom right). Y-axis is frequency and x-axis time.